

Supporting Information

Multi-targeted Imidazoles: Potential Therapeutic Leads for Alzheimer's and Other Neurodegenerative Diseases

Anne-Sophie Cor nec,^a Ludovica Monti,^b Jane Kovalevich,^c Vishruti Makani,^c Michael J. James,^c Krishna G. Vijayendran,^a Killian Oukoloff,^b Yuemang Yao,^c Virginia M.-Y. Lee,^c John Q. Trojanowski,^c Amos B. Smith III,^a Kurt R. Brunden,^{c,*} and Carlo Ballatore^{b,*}

^a*Department of Chemistry, School of Arts and Sciences, University of Pennsylvania, 231 South 34th St., Philadelphia, PA 19104-6323;* ^b*Skaggs School of Pharmacy and Pharmaceutical Sciences, University of California, San Diego, 9500 Gilman Drive, La Jolla, CA 92093 ;* ^c*Center for Neurodegenerative Disease Research, Institute on Aging, University of Pennsylvania, 3600 Spruce Street, Philadelphia, PA 19104-6323*

S2. Details about docking studies.

S3–8. X-ray report for compound **98**.

S9–150. NMR spectra of test compounds.

S151. Supplemental Figure 1: Analysis of Table 2 compounds for their ability to reduce multiple COX and 5-LOX products.

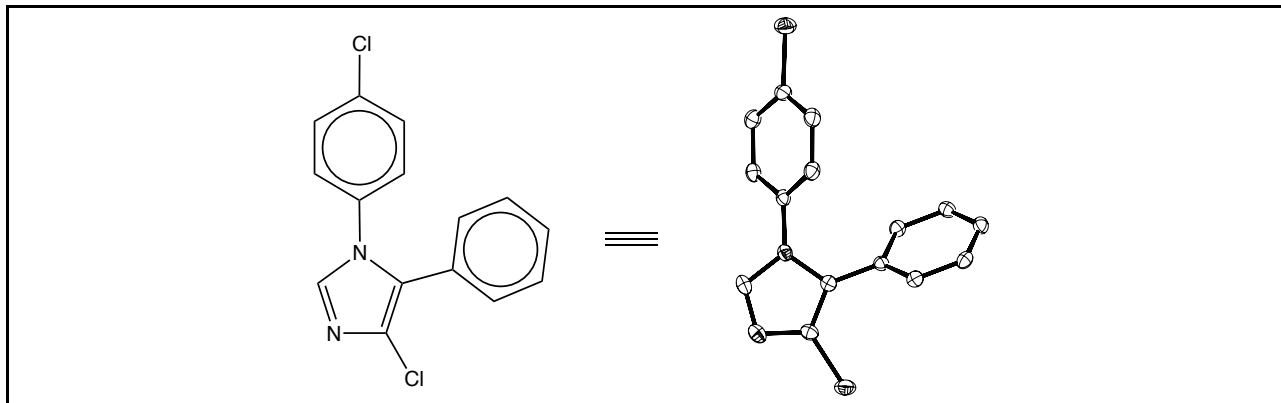
S152. Supplemental Figure 2: Concentration-response relationship of compounds **64** and **70** in the HEK293 acetylated α -tubulin assay.

The structure of COX-1 was prepared from the X-ray structure available in the Protein Data Bank database (PDB code: 3KK6). Using Autodock 4.2, water molecules, ligand and hydrogens were removed, while polar hydrogens and Gasteiger charges were added. The structure was converted in .pdbqt format.

Compounds were built and minimized with the MMFF94 force field using Chem3D (CambridgeSoft), saved in .mol2 format and converted in .pdbqt format using Autodock 4.2. Autodock Vina software was used for docking calculation.¹ In the configuration files we set a grid of 20 (x), 30 (y), 35 (z) and centered at -32.085 (x), 43.871 (y) and -5.222 (z) corresponding to the active site. Docking results were analyzed and docking poses were selected following the conformation and binding affinity results.

¹ Improving the speed and accuracy of docking with a new scoring function, efficient optimization, and multithreading Trott, Oleg; Olson, Arthur J. *Journal of Computational Chemistry*, 31(2), 455-461

X-ray Structure Determination of 1436 (compound 98) - CCDC 1529316



Compound 1436x, $C_{15}H_{10}Cl_2N_2$, crystallizes in the orthorhombic space group $P2_12_12_1$ (systematic absences $h00$: $h=$ odd, $0k0$: $k=$ odd and $00l$: $l=$ odd) with $a=8.0987(4)\text{\AA}$, $b=9.6131(4)\text{\AA}$, $c=17.2587(8)\text{\AA}$, $V=1343.65(11)\text{\AA}^3$, $Z=4$, and $d_{\text{calc}}=1.429 \text{ g/cm}^3$. X-ray intensity data were collected on a Bruker APEXII [1] CCD area detector employing graphite-monochromated Mo-K α radiation ($\lambda=0.71073\text{\AA}$) at a temperature of 100K. Preliminary indexing was performed from a series of thirty-six 0.5° rotation frames with exposures of 10 seconds. A total of 4191 frames were collected with a crystal to detector distance of 59.9 mm, rotation widths of 0.5° and exposures of 10 seconds:

scan type	2θ	ω	ϕ	χ	Frames
ϕ	32.00	44.52	349.55	-24.38	739
ϕ	-28.00	348.53	335.02	-55.24	669
ω	37.00	1.45	201.14	-31.86	308
ω	37.00	335.50	316.23	-20.60	350
ϕ	39.50	166.34	331.87	-58.65	739
ϕ	-35.50	197.88	22.47	48.96	739
ω	39.50	123.67	224.27	-99.82	184
ω	39.50	359.79	317.07	99.72	72
ω	-30.50	311.87	203.97	-93.68	124
ω	37.00	324.24	181.66	91.29	139
ω	-38.00	306.44	63.99	-90.90	128

Rotation frames were integrated using SAINT [2], producing a listing of unaveraged F^2 and $\sigma(F^2)$ values. A total of 34619 reflections were measured over the ranges $4.72 \leq 2\theta \leq 54.956^\circ$, $-10 \leq h \leq 10$, $-12 \leq k \leq 12$, $-22 \leq l \leq 22$ yielding 3093 unique reflections ($R_{\text{int}} = 0.0167$). The intensity data were corrected for

Lorentz and polarization effects and for absorption using SADABS [3] (minimum and maximum transmission 0.7019, 0.7456). The structure was solved by direct methods - SHELXS-97 [4]. Refinement was by full-matrix least squares based on F^2 using SHELXL-2014 [5]. All reflections were used during refinement. The weighting scheme used was $w=1/[\sigma^2(F_o^2) + (0.0288P)^2 + 0.3254P]$ where $P = (F_o^2 + 2F_c^2)/3$. Non-hydrogen atoms were refined anisotropically and hydrogen atoms were refined using a riding model. Refinement converged to $R_1=0.0197$ and $wR_2=0.0539$ for 3020 observed reflections for which $F > 4\sigma(F)$ and $R_1=0.0204$ and $wR_2=0.0546$ and $GOF = 1.072$ for all 3093 unique, non-zero reflections and 172 variables. The maximum Δ/σ in the final cycle of least squares was 0.001 and the two most prominent peaks in the final difference Fourier were +0.21 and -0.15 e/ \AA^3 .

Table 1. lists cell information, data collection parameters, and refinement data. Final positional and equivalent isotropic thermal parameters are given in Tables 2. and 3. Anisotropic thermal parameters are in Table 4. Tables 5. and 6. list bond distances and bond angles. Figure 1. is an ORTEP representation of the molecule with 50% probability thermal ellipsoids displayed.

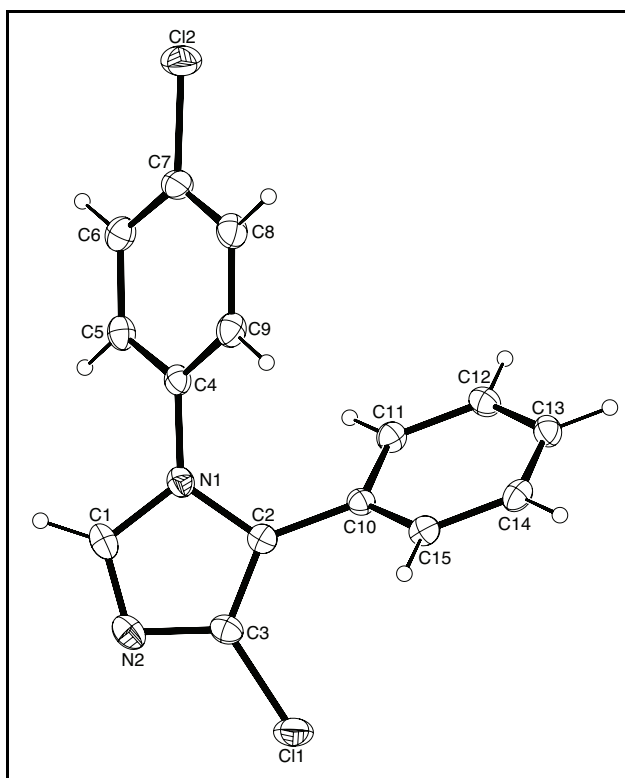


Figure 1. ORTEP drawing of the title compound with 50% thermal ellipsoids.

Table 1. Summary of Structure Determination of Compound 1436

Empirical formula	C ₁₅ H ₁₀ Cl ₂ N ₂
Formula weight	289.15
Temperature/K	100
Crystal system	orthorhombic
Space group	P2 ₁ 2 ₁ 2 ₁
a	8.0987(4) Å
b	9.6131(4) Å
c	17.2587(8) Å
Volume	1343.65(11) Å ³
Z	4
d _{calc}	1.429 g/cm ³
μ	0.469 mm ⁻¹
F(000)	592.0
Crystal size, mm	0.38 × 0.25 × 0.13
2θ range for data collection	4.72 - 54.956°
Index ranges	-10 ≤ h ≤ 10, -12 ≤ k ≤ 12, -22 ≤ l ≤ 22
Reflections collected	34619
Independent reflections	3093[R(int) = 0.0167]
Data/restraints/parameters	3093/0/172
Goodness-of-fit on F ²	1.072
Final R indexes [l>=2σ (l)]	R ₁ = 0.0197, wR ₂ = 0.0539
Final R indexes [all data]	R ₁ = 0.0204, wR ₂ = 0.0546
Largest diff. peak/hole	0.21/-0.15 eÅ ⁻³
Flack parameter	0.019(7)

Table 2 . Refined Positional Parameters for Compound 1436

Atom	x	y	z	U(eq)
Cl1	0.09107(5)	0.70615(4)	0.33214(2)	0.02712(10)
Cl2	1.09986(5)	0.20840(5)	0.40390(2)	0.03140(11)
N1	0.47760(16)	0.52924(13)	0.41620(7)	0.0174(3)
N2	0.27362(18)	0.66304(14)	0.46030(8)	0.0228(3)
C1	0.4113(2)	0.59712(16)	0.47801(9)	0.0211(3)
C2	0.37380(18)	0.55263(15)	0.35335(8)	0.0169(3)
C3	0.25187(19)	0.63474(16)	0.38344(9)	0.0196(3)
C4	0.62683(19)	0.44939(15)	0.41620(8)	0.0170(3)
C5	0.7695(2)	0.50647(16)	0.44722(9)	0.0192(3)
C6	0.9153(2)	0.43018(16)	0.44545(9)	0.0213(3)
C7	0.9144(2)	0.29927(16)	0.41118(9)	0.0216(3)
C8	0.7721(2)	0.24107(17)	0.38158(10)	0.0241(3)
C9	0.6256(2)	0.31601(16)	0.38482(9)	0.0214(3)
C10	0.40238(19)	0.49792(14)	0.27482(8)	0.0159(3)
C11	0.55152(18)	0.52238(16)	0.23666(9)	0.0183(3)
C12	0.57762(19)	0.46838(15)	0.16287(8)	0.0196(3)
C13	0.4549(2)	0.39032(16)	0.12695(9)	0.0197(3)
C14	0.30663(19)	0.36612(15)	0.16454(9)	0.0196(3)
C15	0.27985(19)	0.41918(15)	0.23853(9)	0.0182(3)

Table 3 . Positional Parameters for Hydrogens in Compound 1436

Atom	x	y	z	U(eq)
H1	0.458	0.597	0.5272	0.028
H5	0.7677	0.5949	0.469	0.026
H6	1.0118	0.4661	0.4668	0.028
H8	0.7741	0.1527	0.3597	0.032
H9	0.5279	0.2776	0.3663	0.028
H11	0.6335	0.5748	0.2606	0.024
H12	0.6772	0.4845	0.1375	0.026
H13	0.4725	0.3543	0.0776	0.026
H14	0.2246	0.3142	0.1403	0.026
H15	0.1804	0.4022	0.2638	0.024

Table 4 . Refined Thermal Parameters (U's) for Compound 1436

Atom	U ₁₁	U ₂₂	U ₃₃	U ₂₃	U ₁₃	U ₁₂
Cl1	0.01982(17)	0.03064(19)	0.0309(2)	0.00261(16)	0.00326(15)	0.00733(17)
Cl2	0.0306(2)	0.0347(2)	0.0289(2)	0.00907(17)	0.00530(17)	0.0145(2)
N1	0.0210(6)	0.0155(6)	0.0157(6)	-0.0012(5)	0.0007(5)	-0.0001(5)
N2	0.0259(7)	0.0211(6)	0.0213(6)	-0.0012(5)	0.0069(5)	-0.0008(5)
C1	0.0276(8)	0.0197(7)	0.0161(6)	-0.0024(5)	0.0045(6)	-0.0015(7)
C2	0.0174(7)	0.0160(6)	0.0174(6)	0.0012(5)	0.0012(5)	-0.0012(5)
C3	0.0182(7)	0.0190(7)	0.0215(7)	0.0005(6)	0.0039(6)	0.0006(6)
C4	0.0218(7)	0.0155(6)	0.0137(6)	0.0014(5)	0.0007(5)	0.0008(5)
C5	0.0252(7)	0.0163(7)	0.0161(7)	-0.0003(5)	0.0002(6)	-0.0027(6)
C6	0.0222(7)	0.0229(7)	0.0187(7)	0.0032(6)	-0.0010(6)	-0.0027(6)
C7	0.0249(7)	0.0220(7)	0.0180(6)	0.0049(6)	0.0022(6)	0.0069(7)
C8	0.0351(9)	0.0166(7)	0.0206(7)	-0.0021(6)	-0.0030(7)	0.0042(6)
C9	0.0270(8)	0.0168(7)	0.0204(7)	-0.0019(6)	-0.0048(6)	-0.0007(6)
C10	0.0174(6)	0.0145(6)	0.0159(6)	0.0007(5)	0.0004(6)	0.0017(5)
C11	0.0181(7)	0.0175(7)	0.0192(7)	-0.0010(6)	-0.0012(6)	-0.0017(5)
C12	0.0186(7)	0.0204(7)	0.0196(7)	0.0002(6)	0.0040(6)	0.0006(6)
C13	0.0257(8)	0.0168(7)	0.0165(7)	-0.0009(5)	-0.0004(6)	0.0025(6)
C14	0.0206(7)	0.0182(7)	0.0201(7)	0.0005(6)	-0.0058(6)	-0.0017(6)
C15	0.0172(6)	0.0186(7)	0.0189(7)	0.0029(6)	0.0005(6)	-0.0011(5)

Table 5 . Bond Distances in Compound 1436, Å

Cl1-C3	1.7178(16)	Cl2-C7	1.7419(16)	N1-C1	1.3608(19)
N1-C2	1.3906(19)	N1-C4	1.4318(19)	N2-C1	1.319(2)
N2-C3	1.366(2)	C2-C3	1.367(2)	C2-C10	1.4721(19)
C4-C5	1.387(2)	C4-C9	1.392(2)	C5-C6	1.390(2)
C6-C7	1.391(2)	C7-C8	1.380(2)	C8-C9	1.389(2)
C10-C11	1.396(2)	C10-C15	1.396(2)	C11-C12	1.392(2)
C12-C13	1.391(2)	C13-C14	1.385(2)	C14-C15	1.392(2)

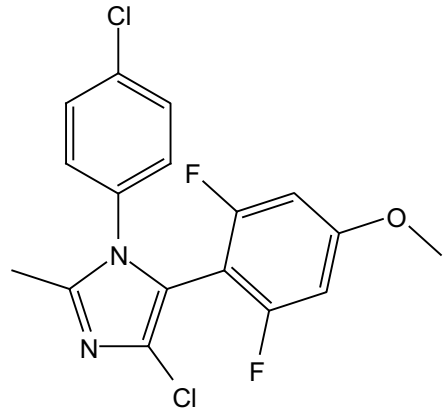
Table 6 . Bond Angles in Compound 1436, °

C1-N1-C2	107.19(13)	C1-N1-C4	126.15(13)	C2-N1-C4	126.66(12)
C1-N2-C3	103.80(13)	N2-C1-N1	112.48(14)	N1-C2-C10	124.42(13)
C3-C2-N1	103.52(13)	C3-C2-C10	132.05(14)	N2-C3-Cl1	121.25(12)
N2-C3-C2	113.01(14)	C2-C3-Cl1	125.64(12)	C5-C4-N1	119.43(13)
C5-C4-C9	121.38(14)	C9-C4-N1	119.19(14)	C4-C5-C6	119.38(14)
C5-C6-C7	118.83(15)	C6-C7-Cl2	118.69(13)	C8-C7-Cl2	119.37(12)
C8-C7-C6	121.93(15)	C7-C8-C9	119.24(14)	C8-C9-C4	119.16(15)
C11-C10-C2	120.68(13)	C11-C10-C15	119.65(13)	C15-C10-C2	119.66(14)
C12-C11-C10	120.03(13)	C13-C12-C11	120.04(14)	C14-C13-C12	120.09(14)
C13-C14-C15	120.23(14)	C14-C15-C10	119.96(14)		

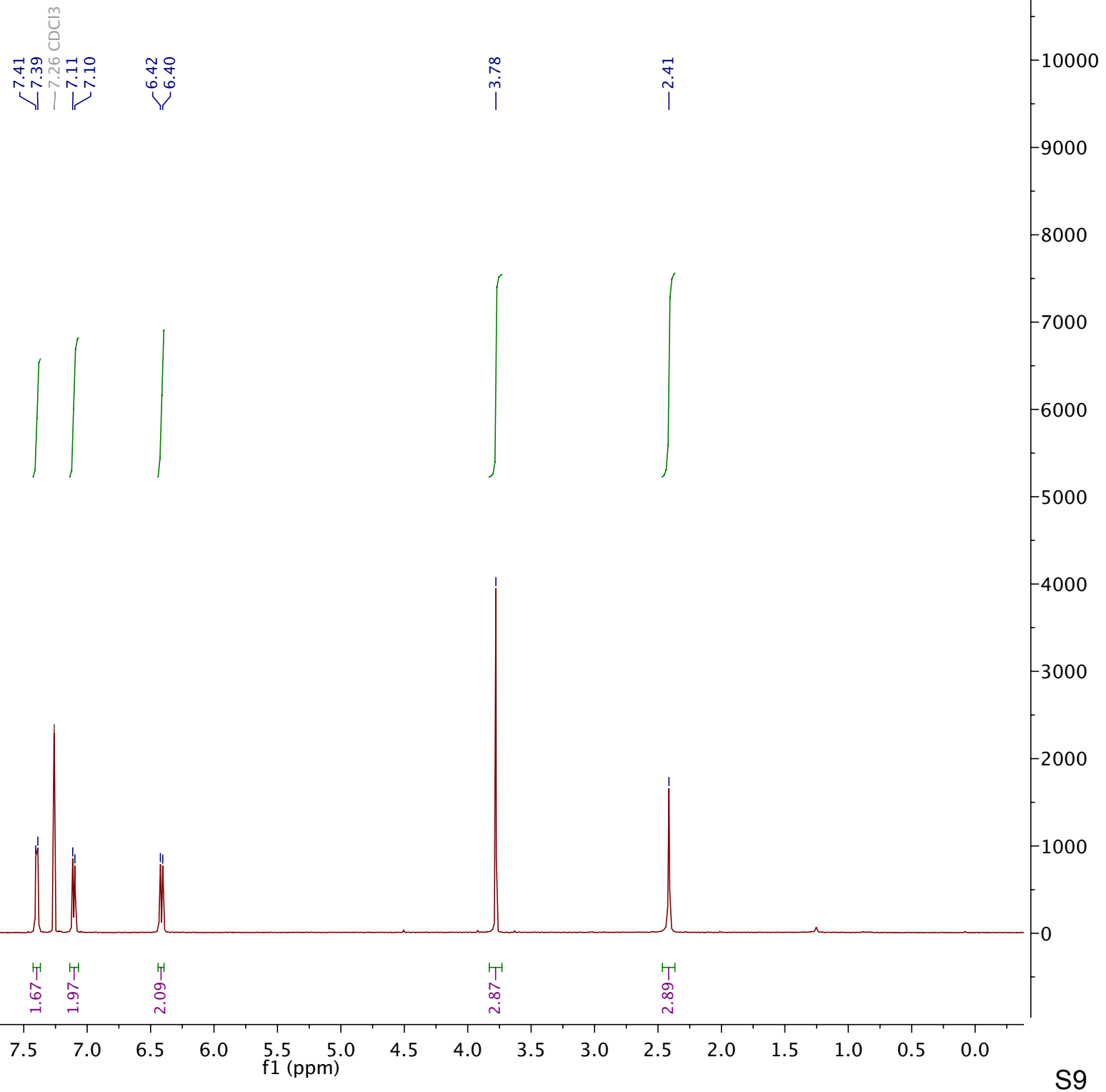
This report has been created with Olex2 [6], compiled on 2016.02.19 svn.r3266 for OlexSys.

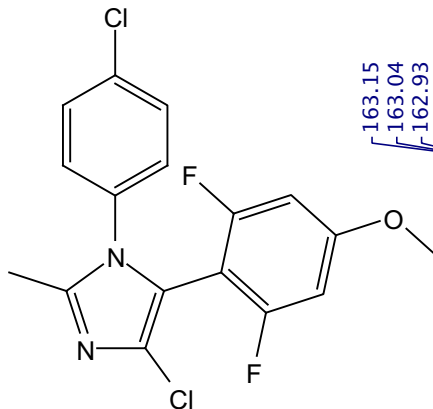
Reference

- [1] APEX2 2014.11-0
- [2] SAINT v8.34A
- [3] SADABS v2014/5
- [4] SHELXS-97
- [5] SHELXL-2014/7
- [6] Olex2 (Dolomanov et al., 2009)

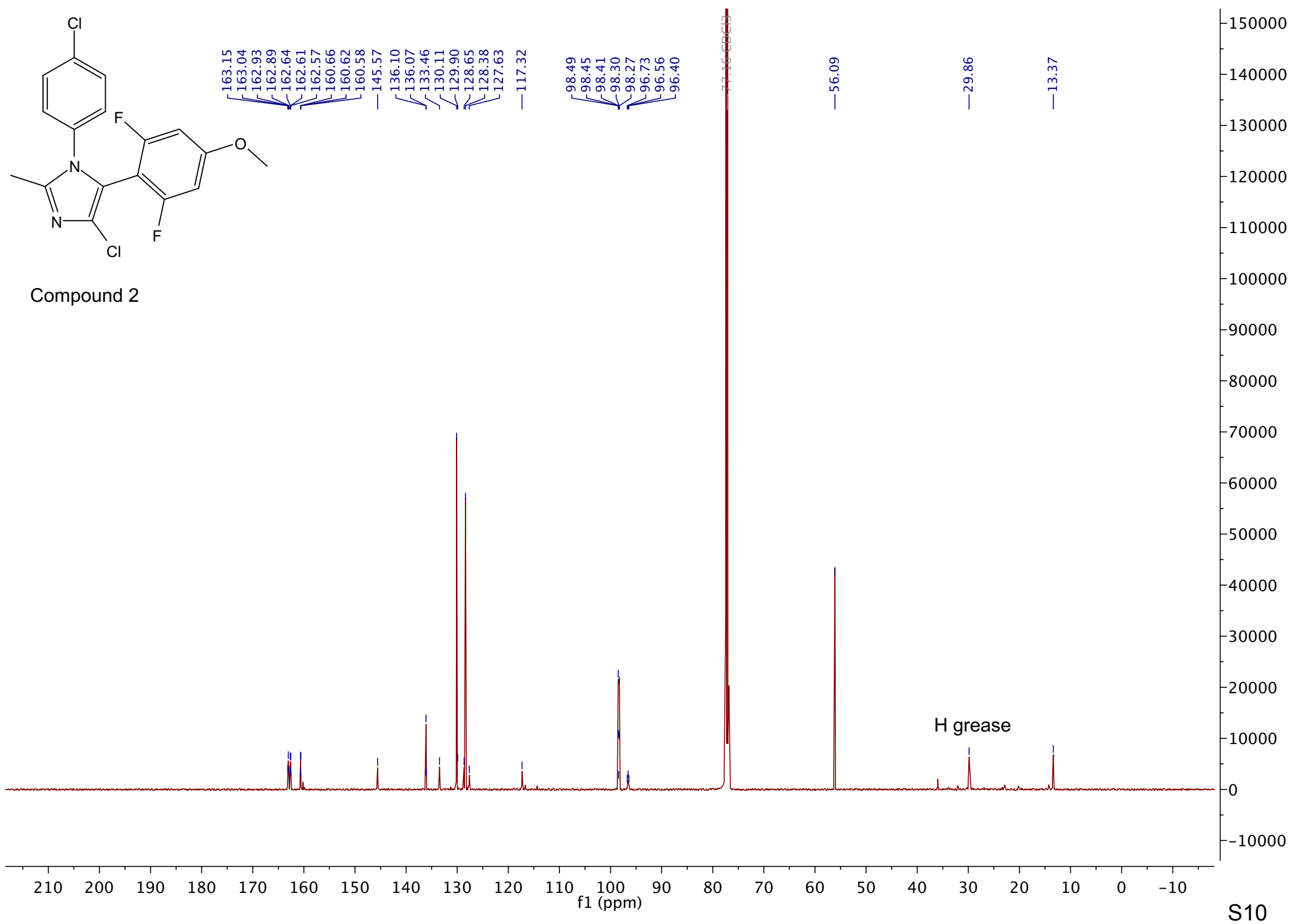


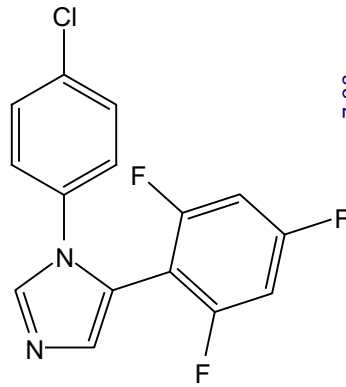
Compound 2



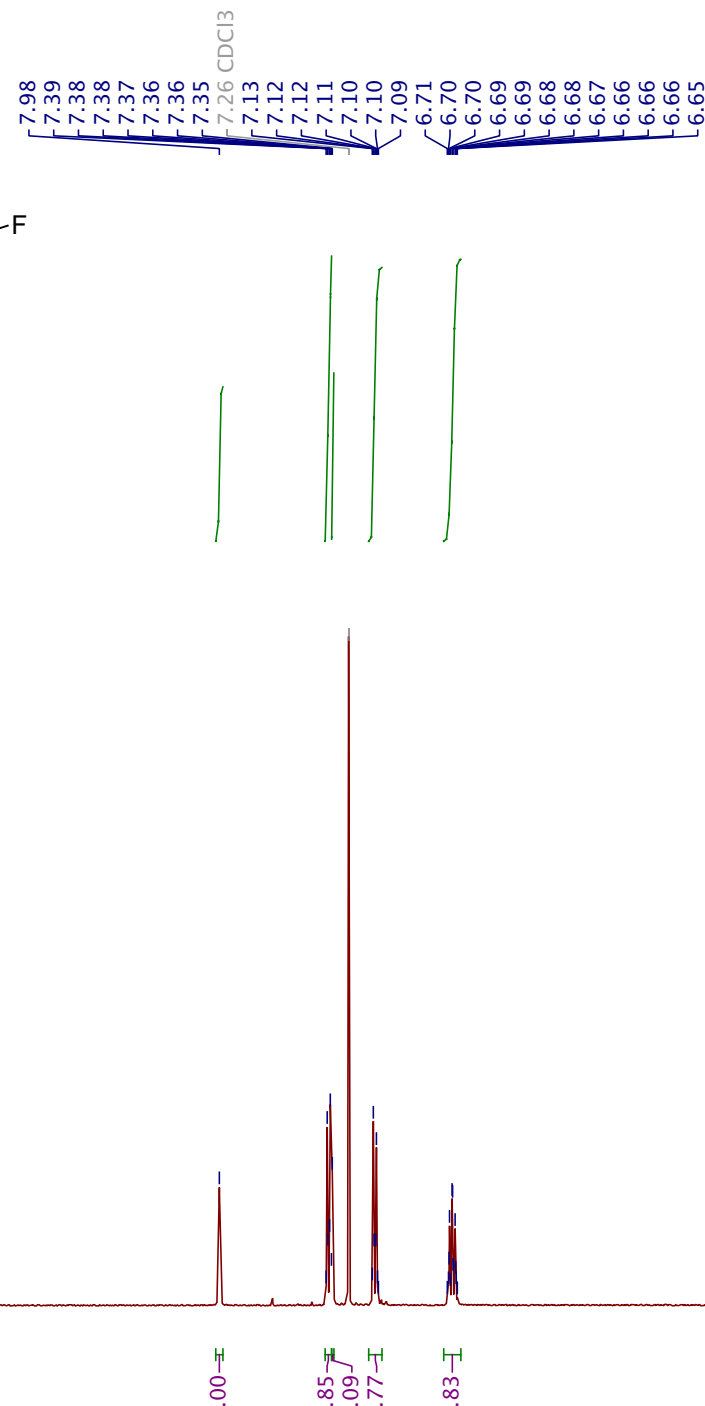


Compound 2

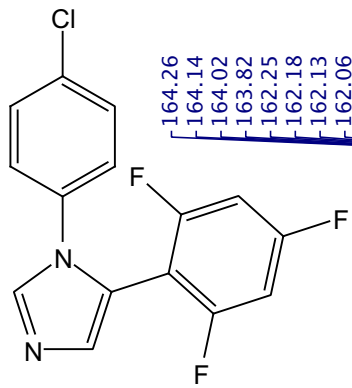




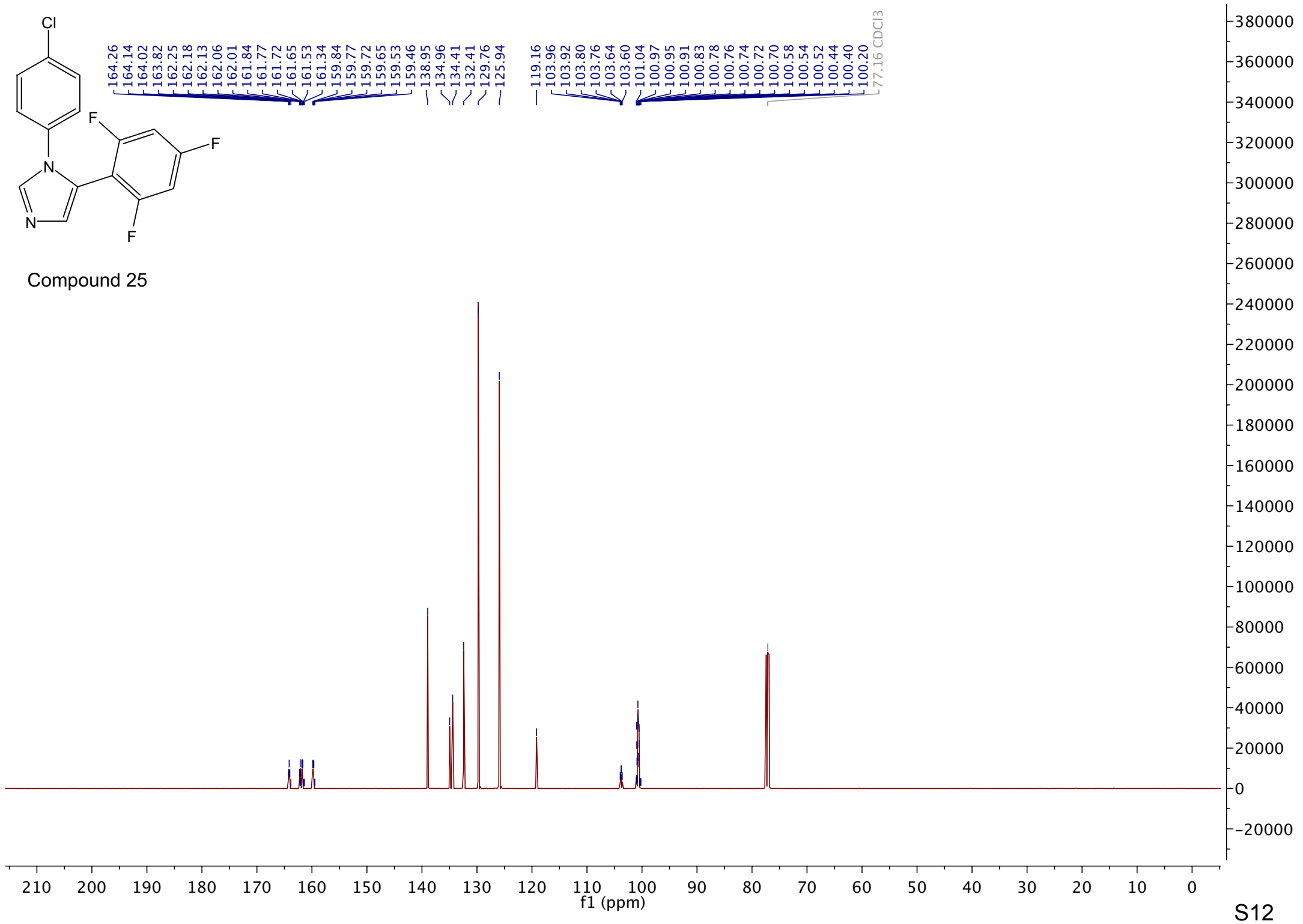
Compound 25



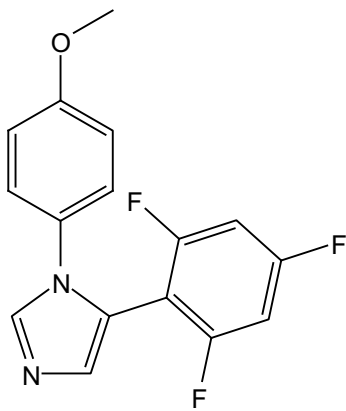
S11



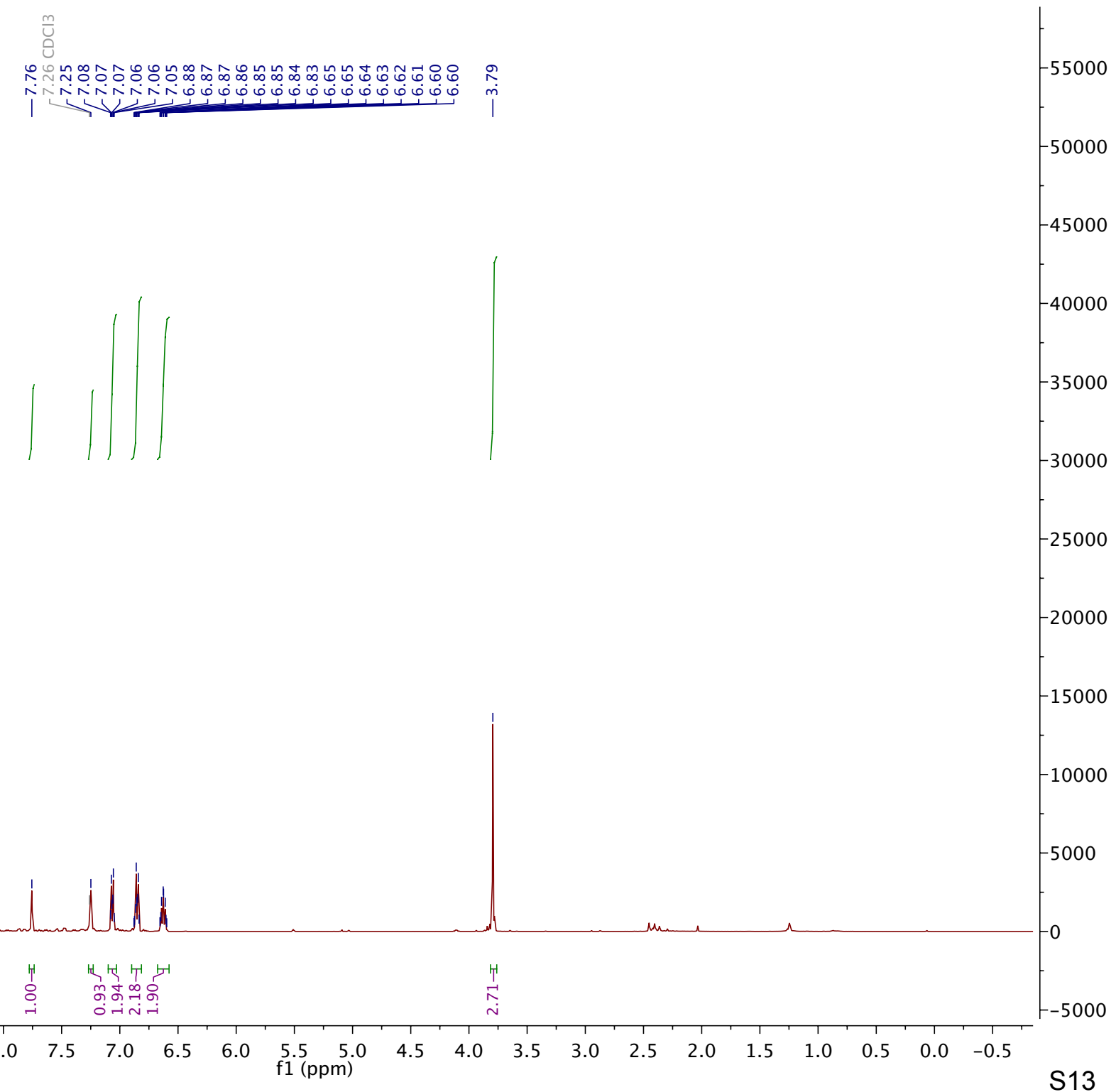
Compound 25

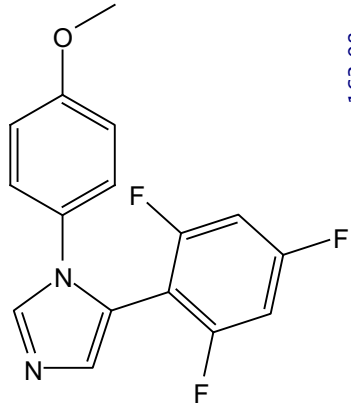


S12

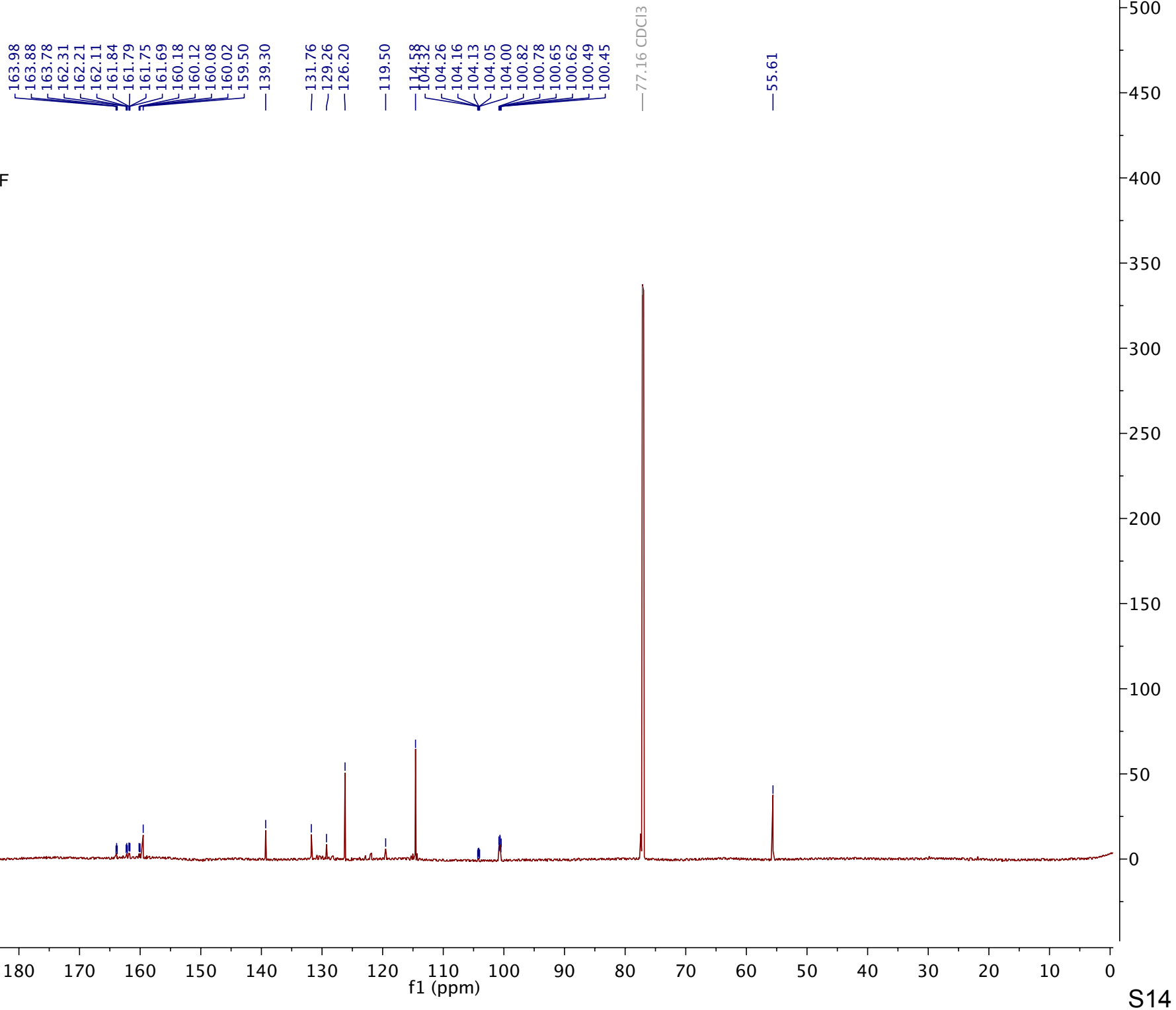


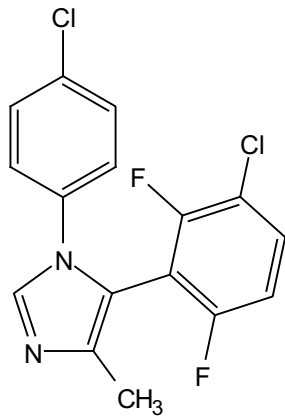
Compound 26



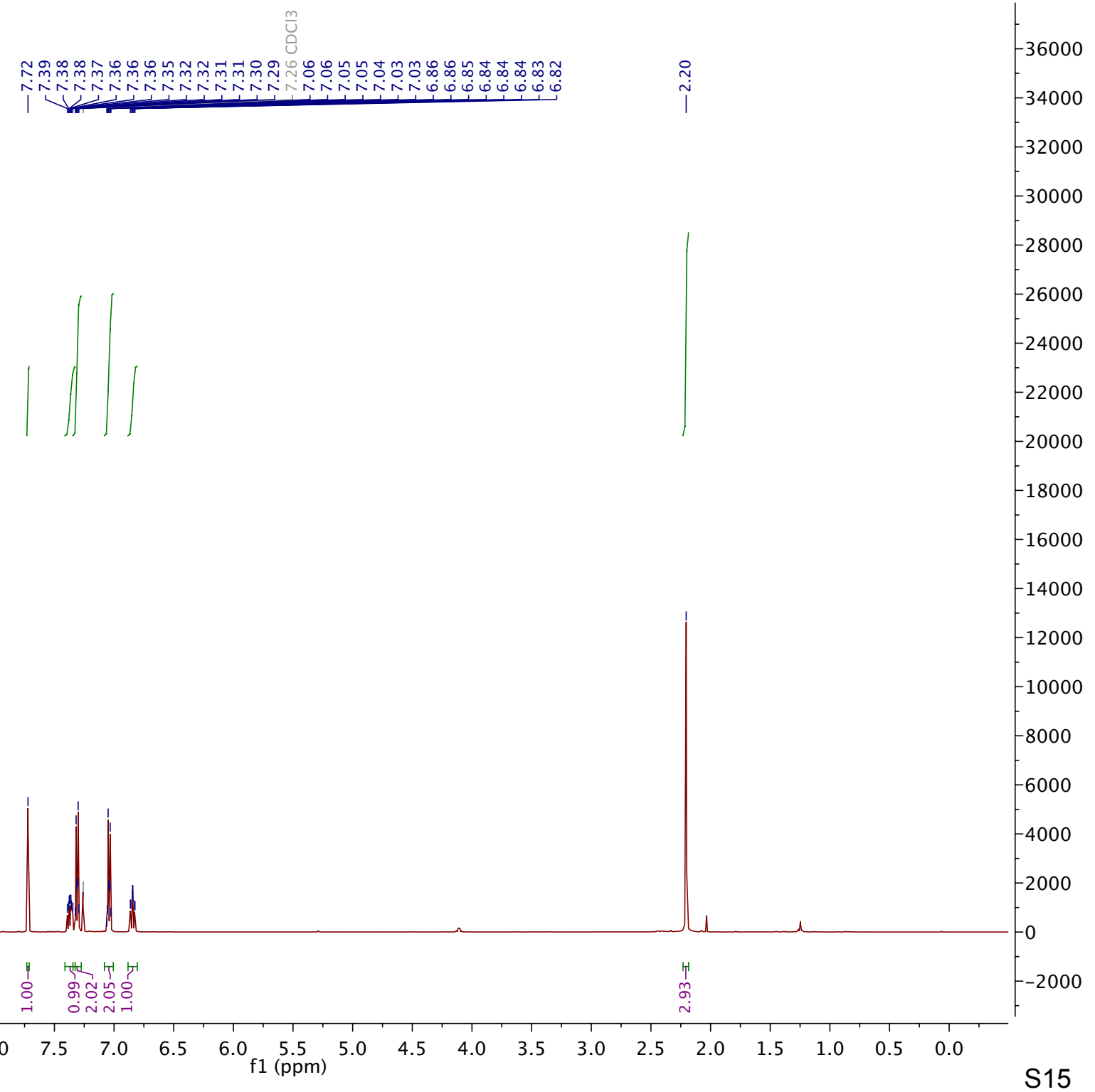


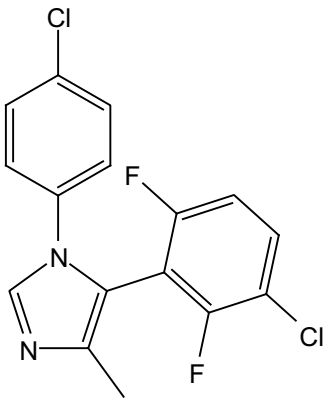
Compound 26



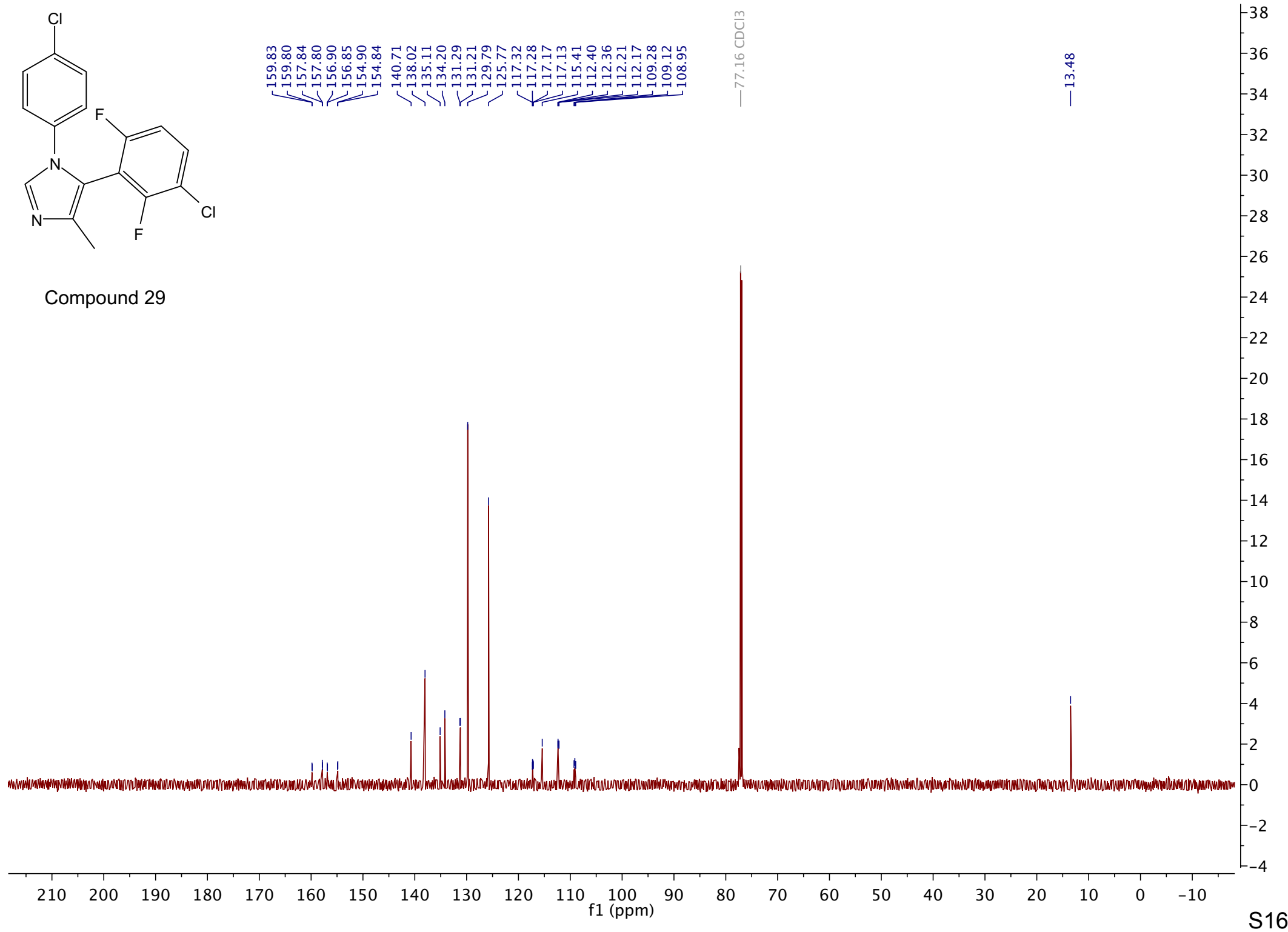


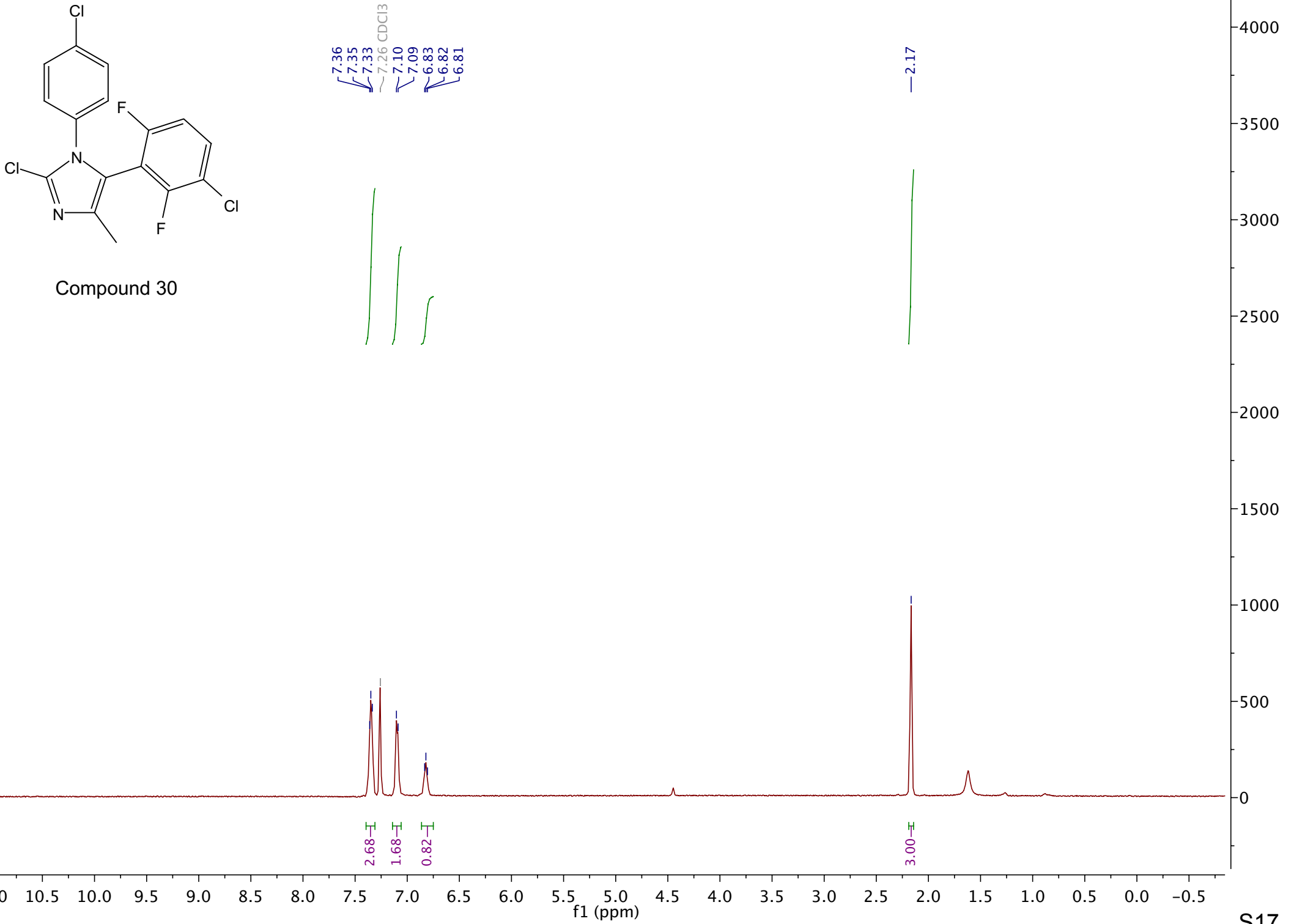
Compound 29

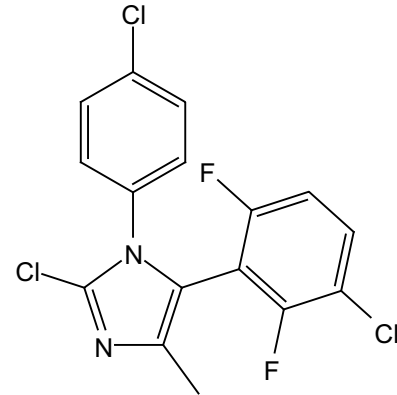




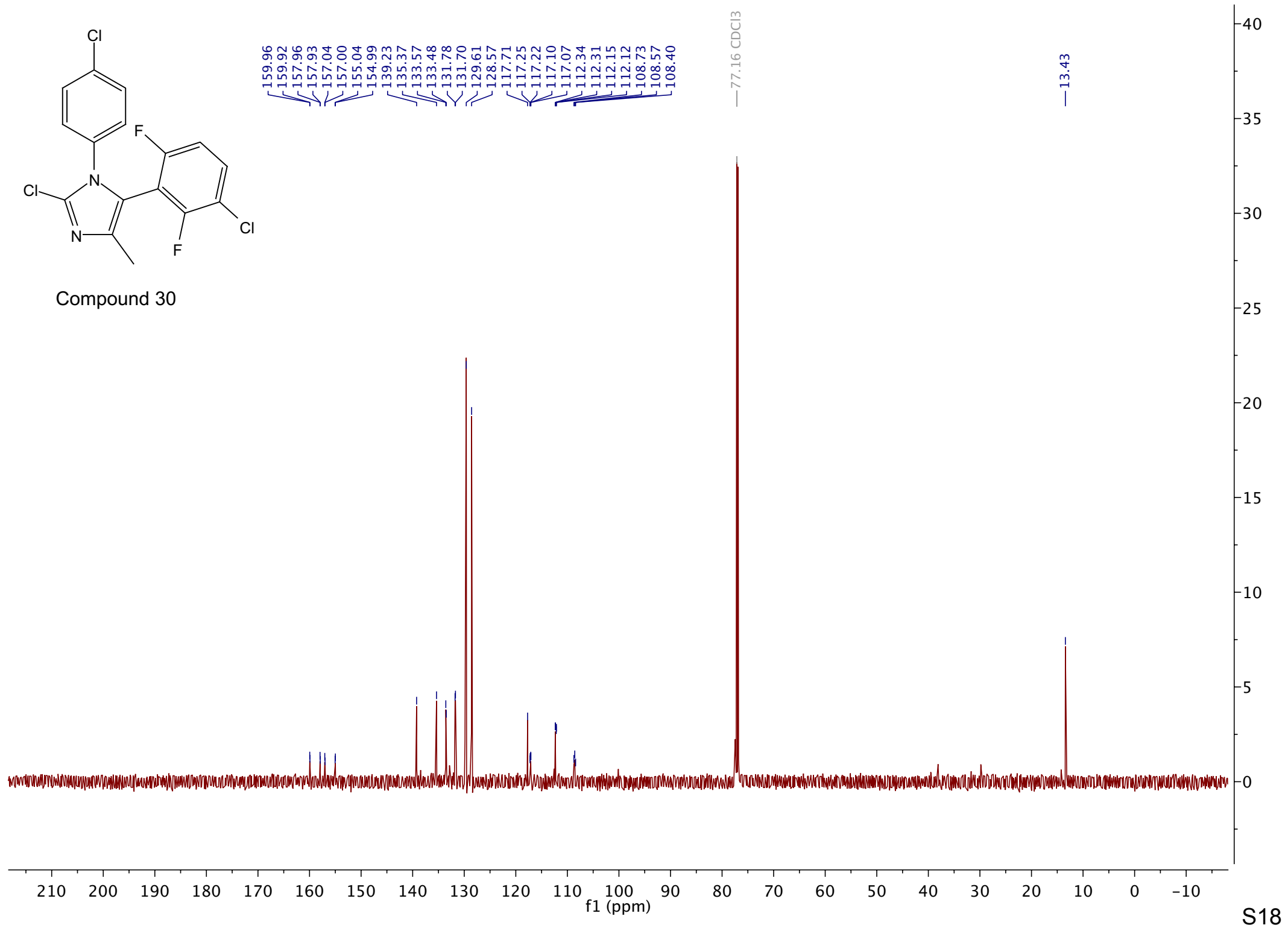
Compound 29

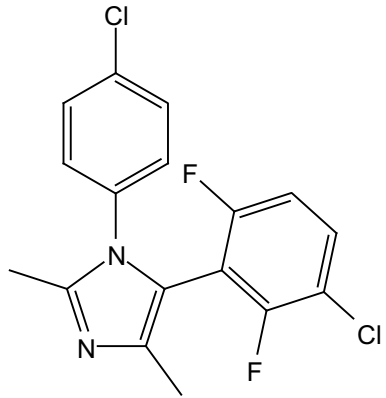




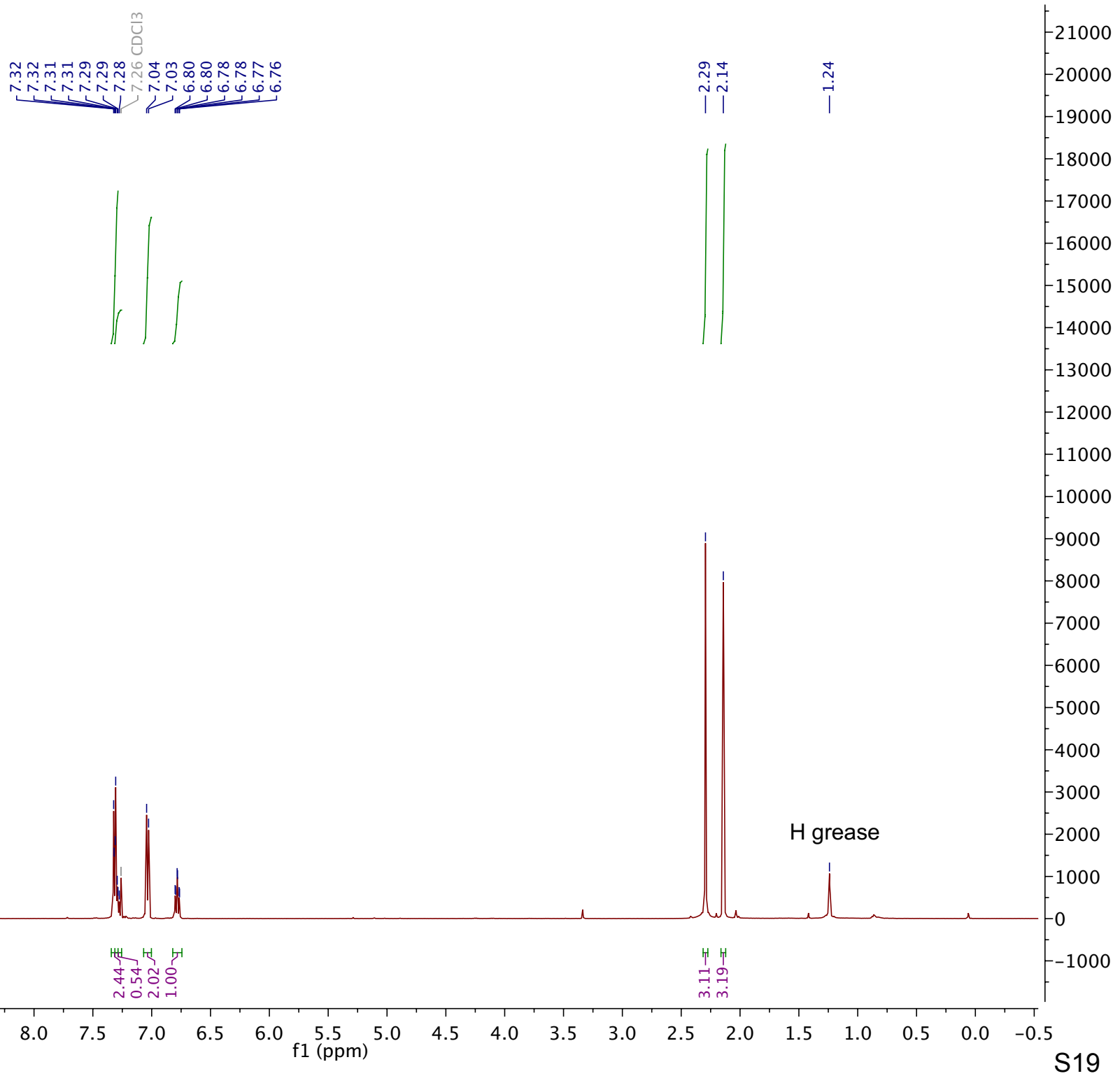


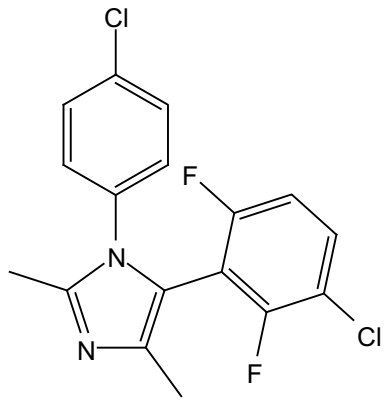
Compound 30



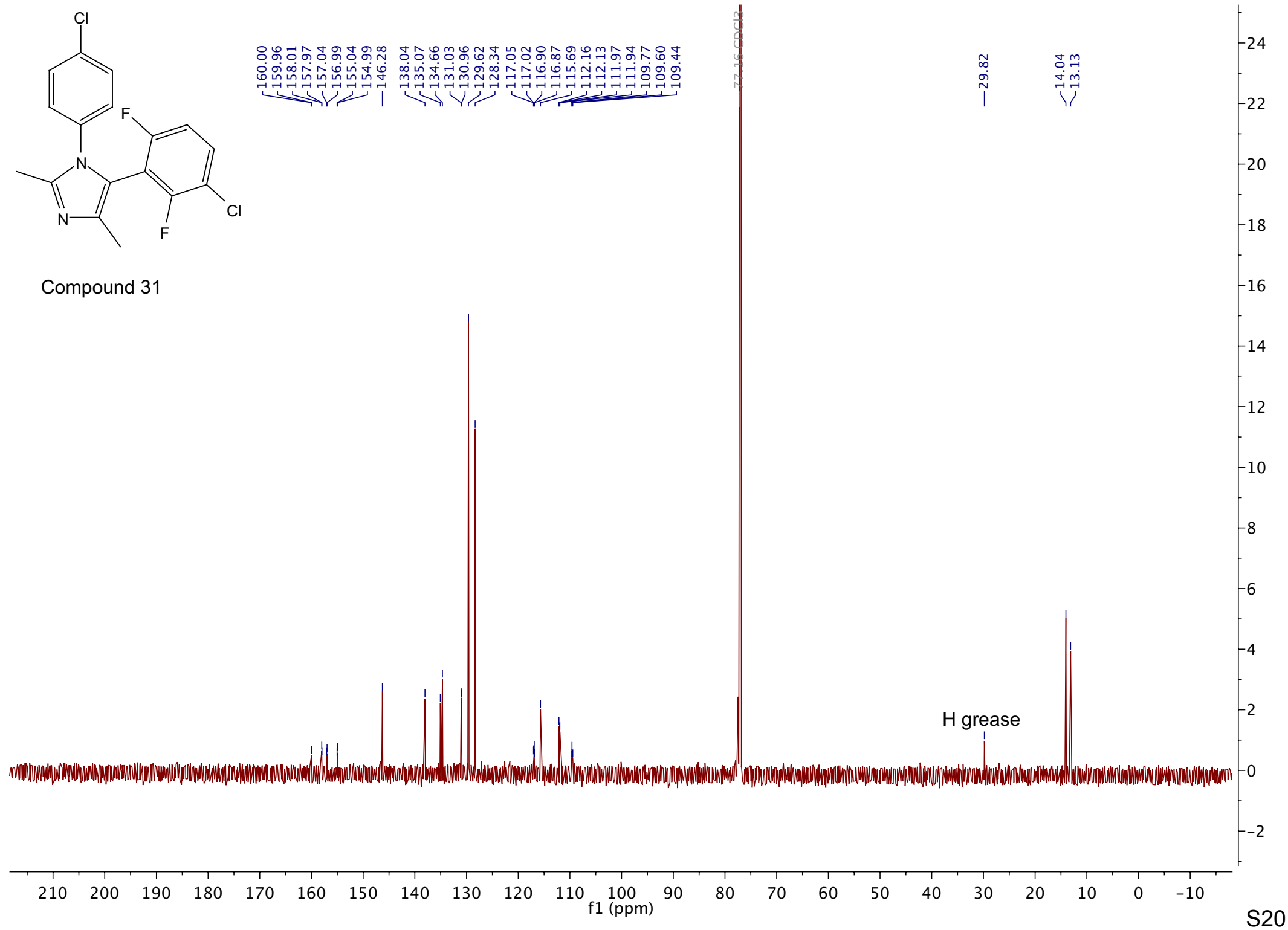


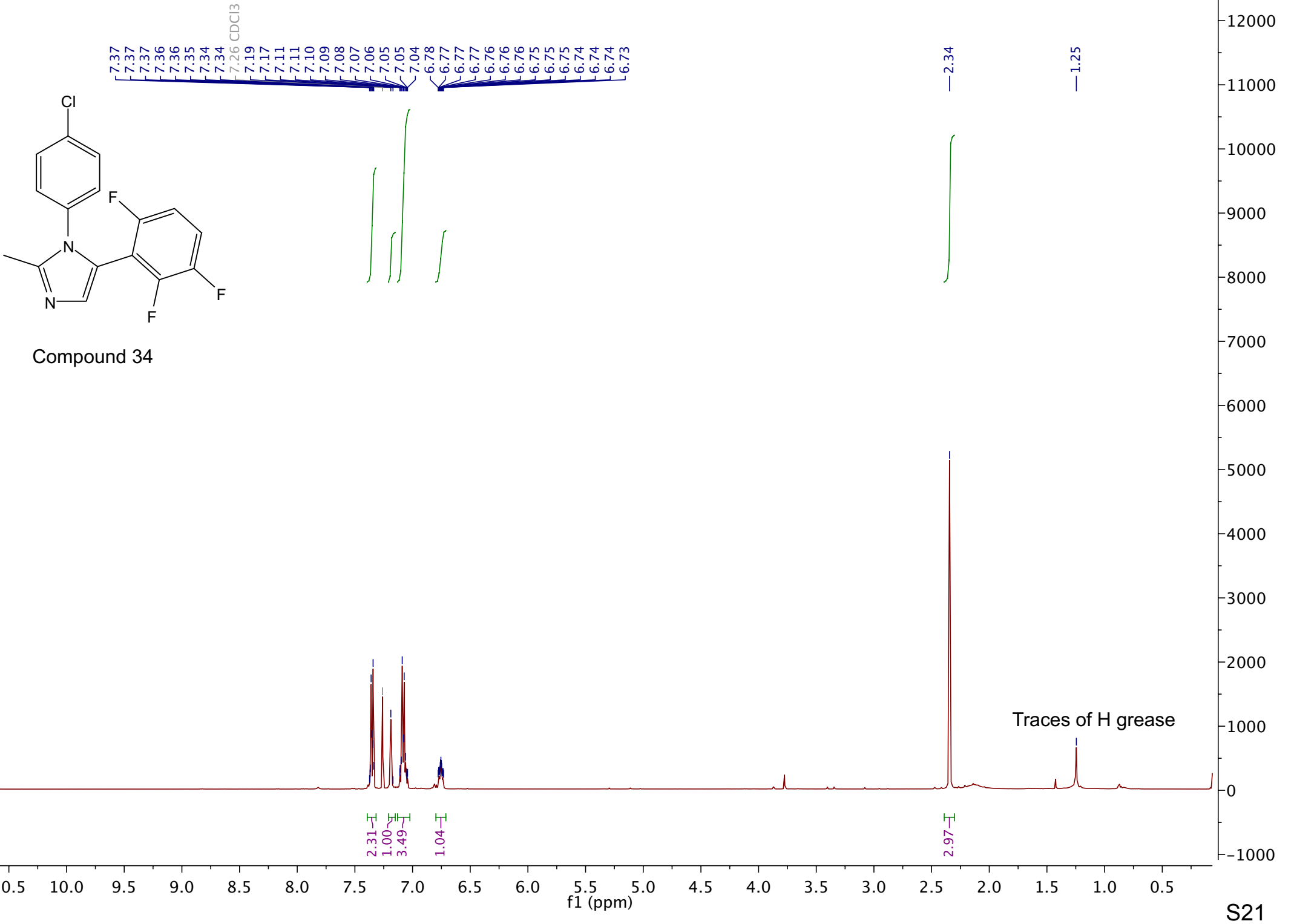
Compound 31

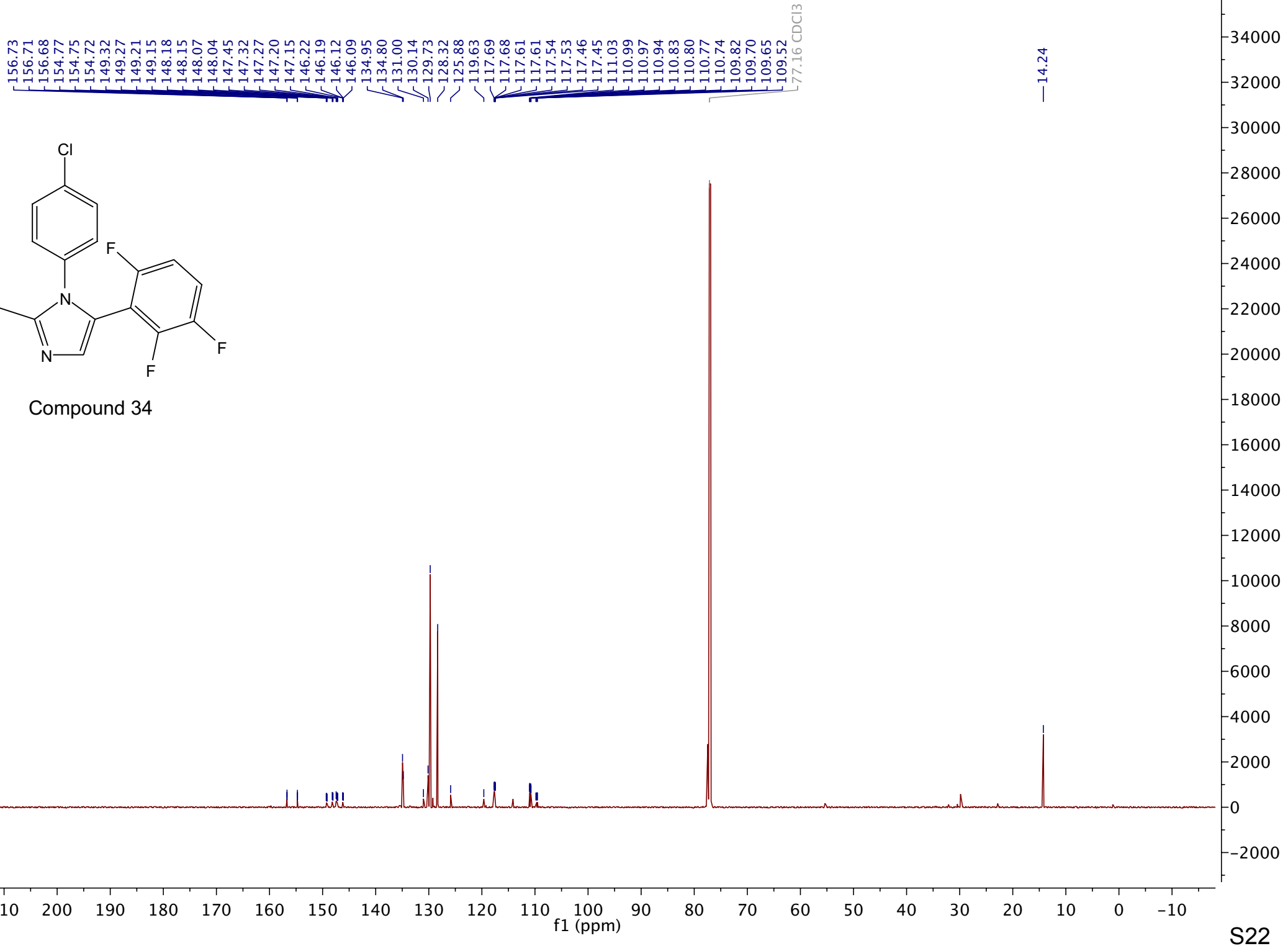




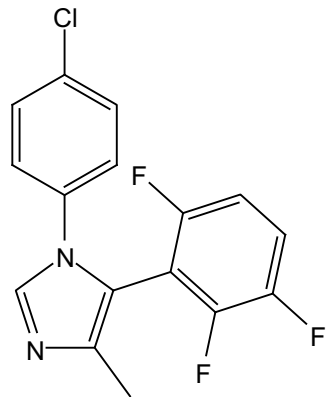
Compound 31



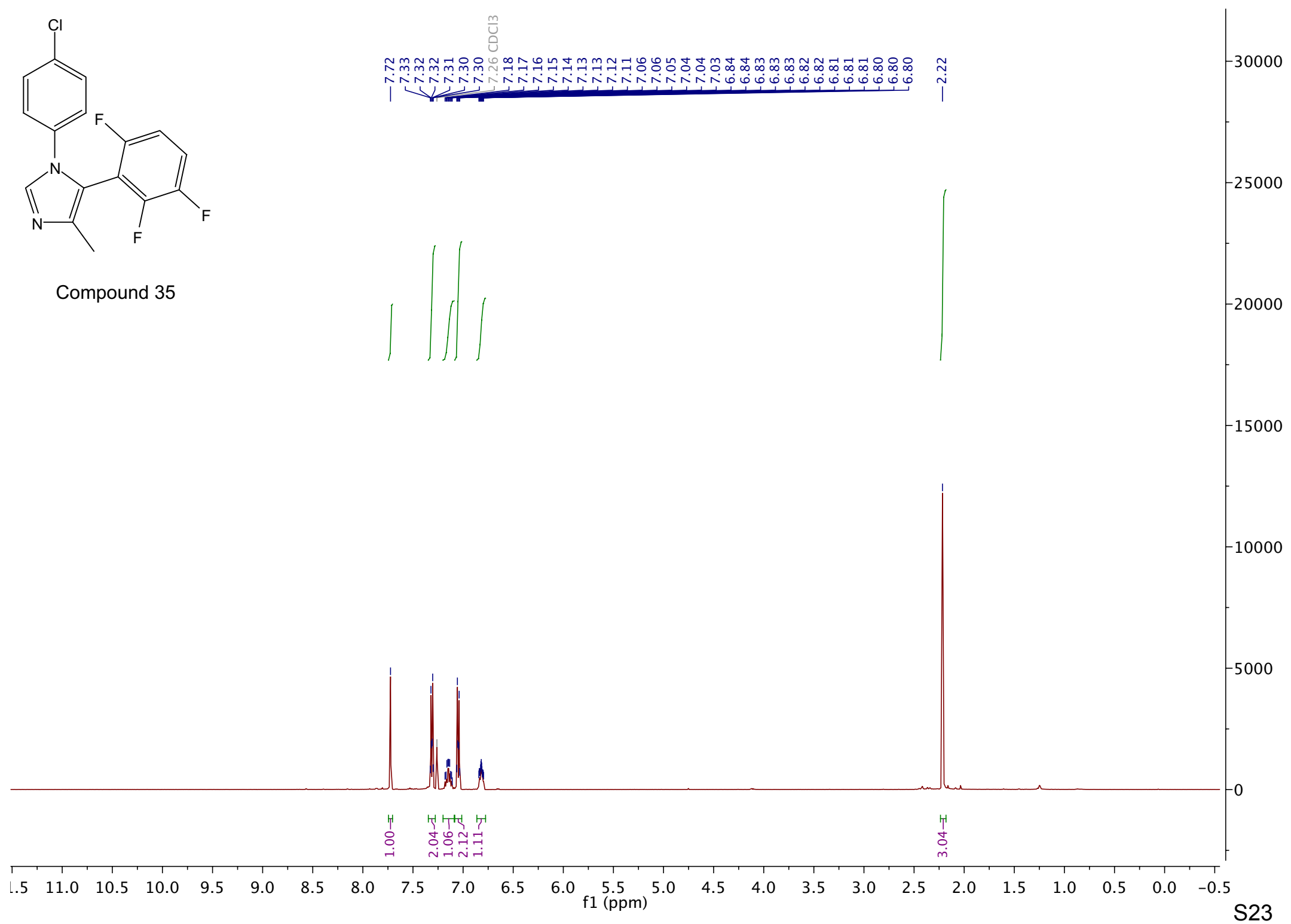


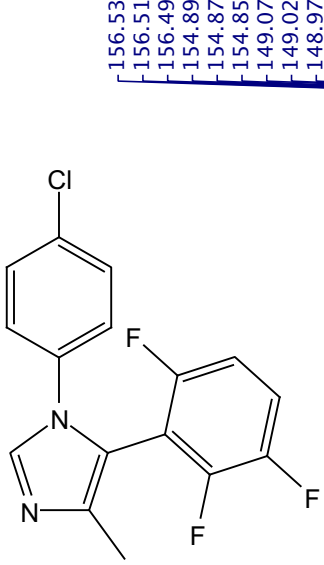


Compound 34

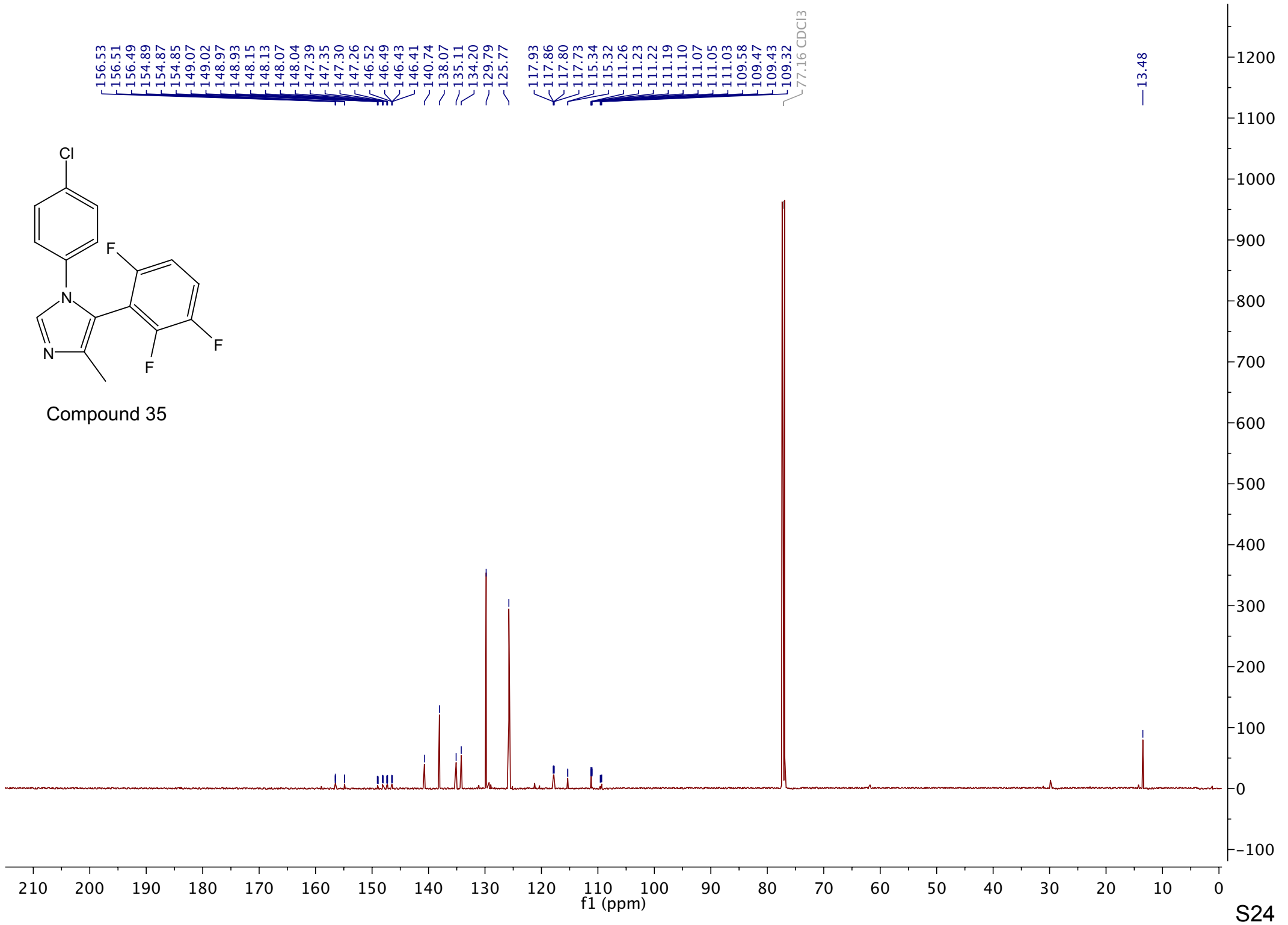


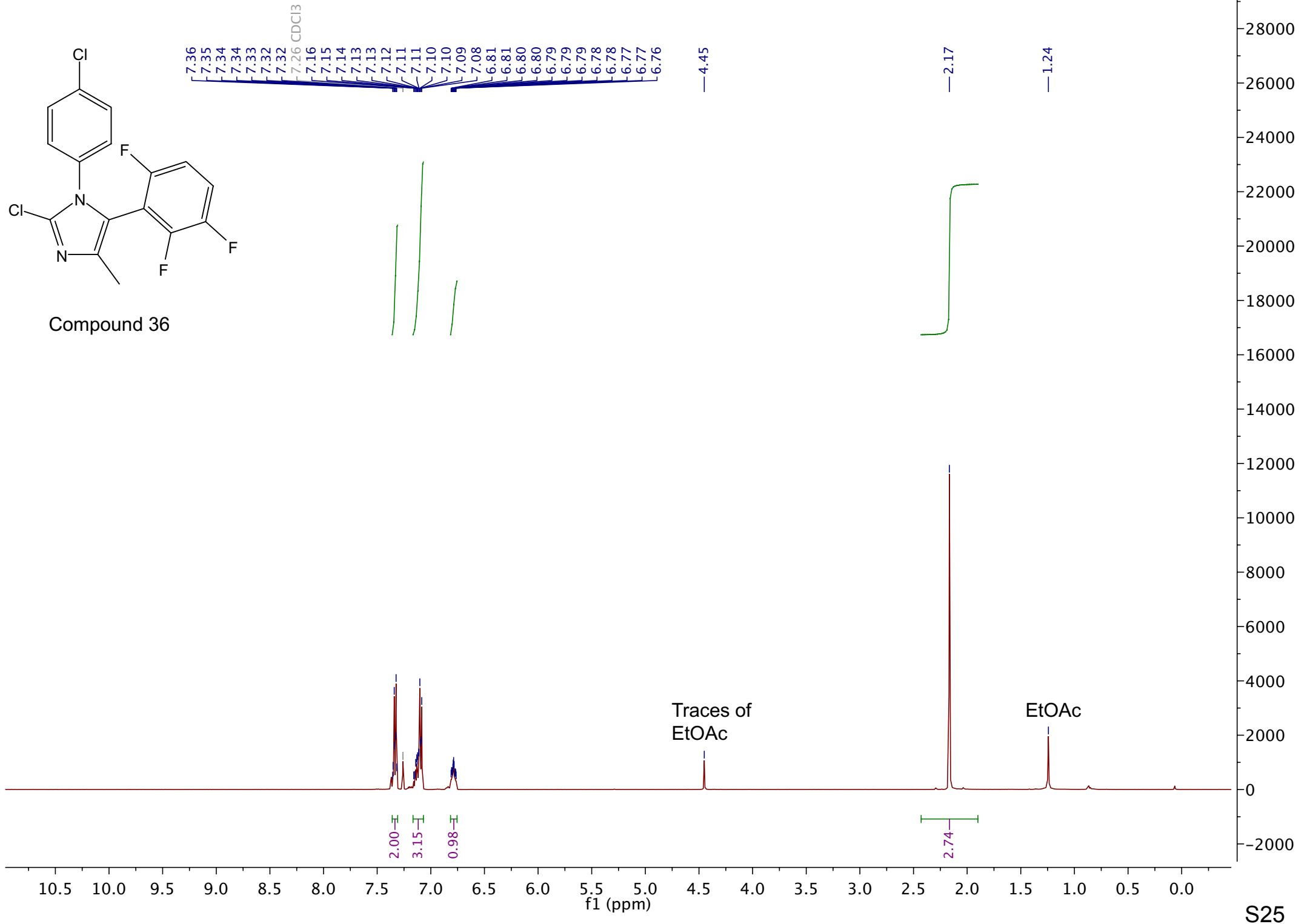
Compound 35

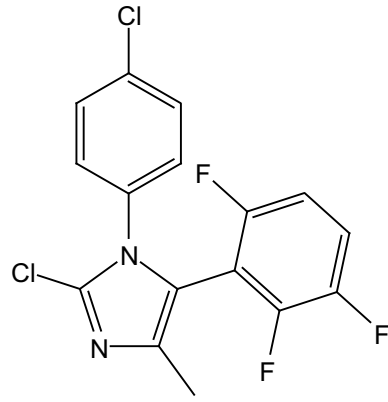




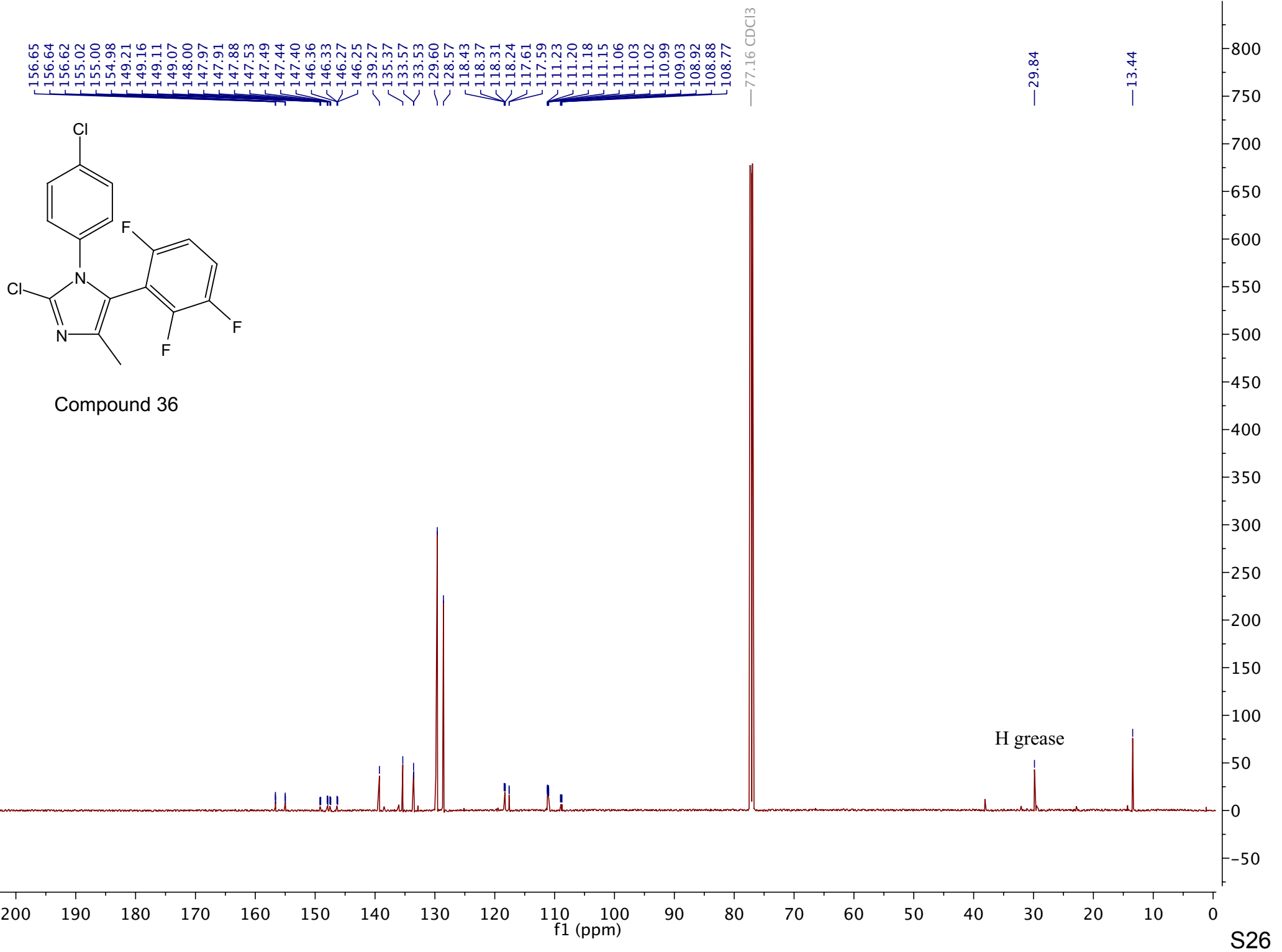
Compound 35

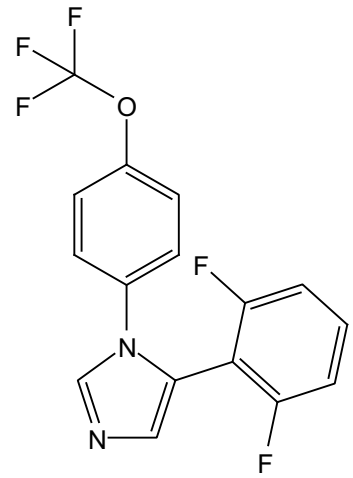




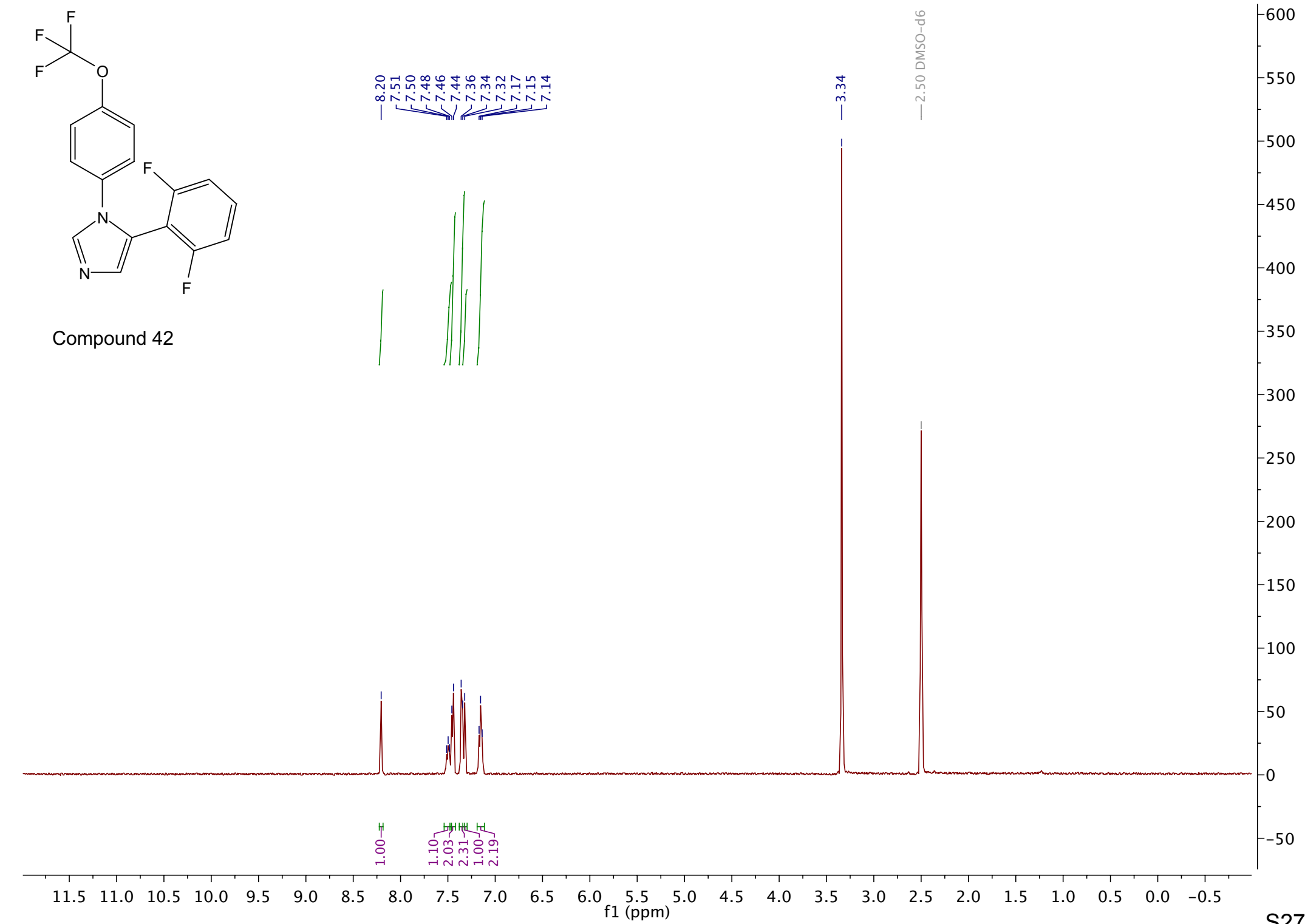


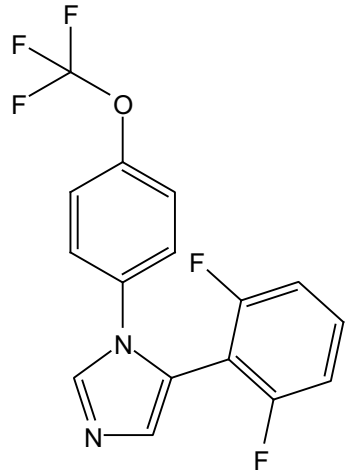
Compound 36



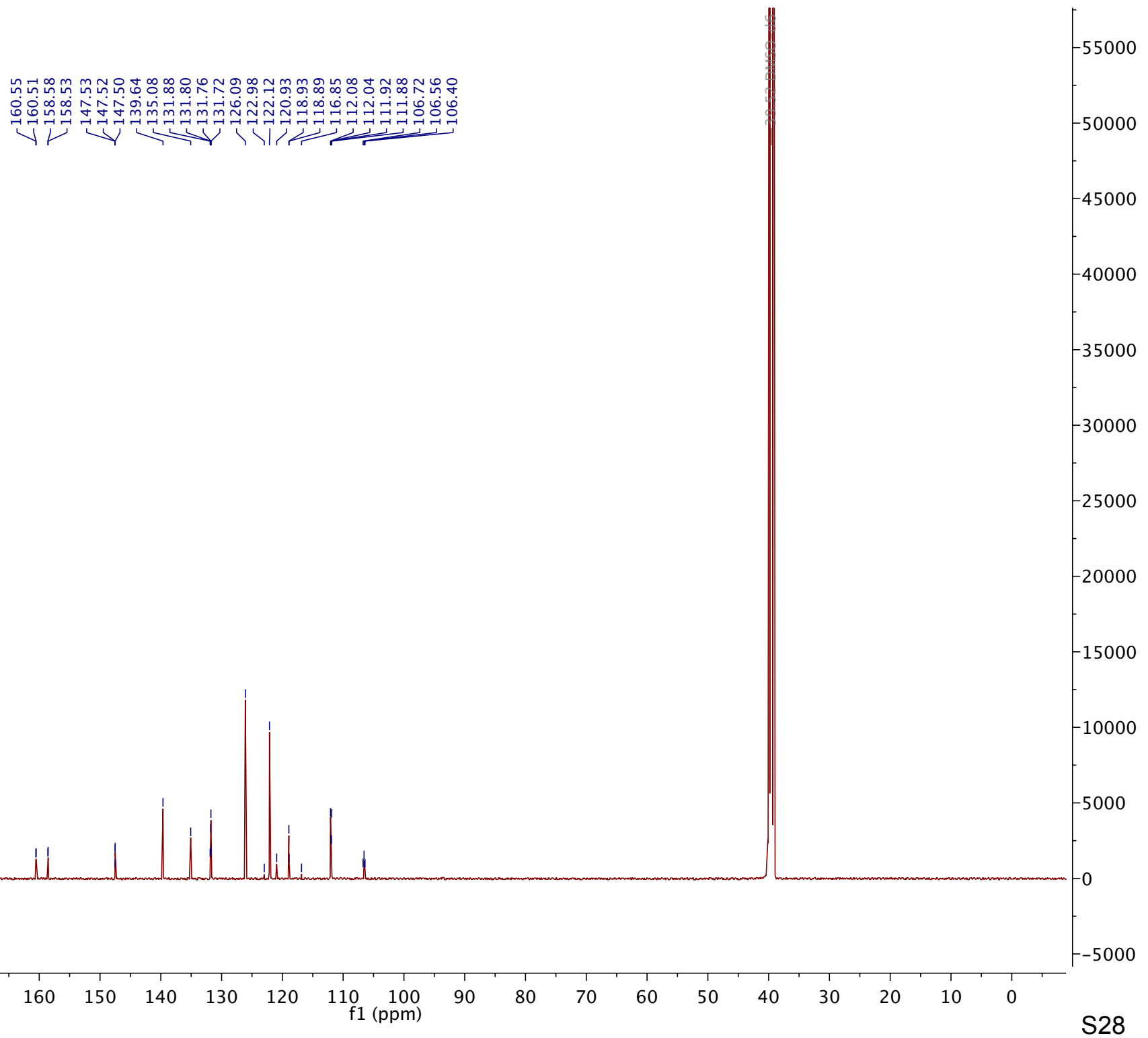


Compound 42

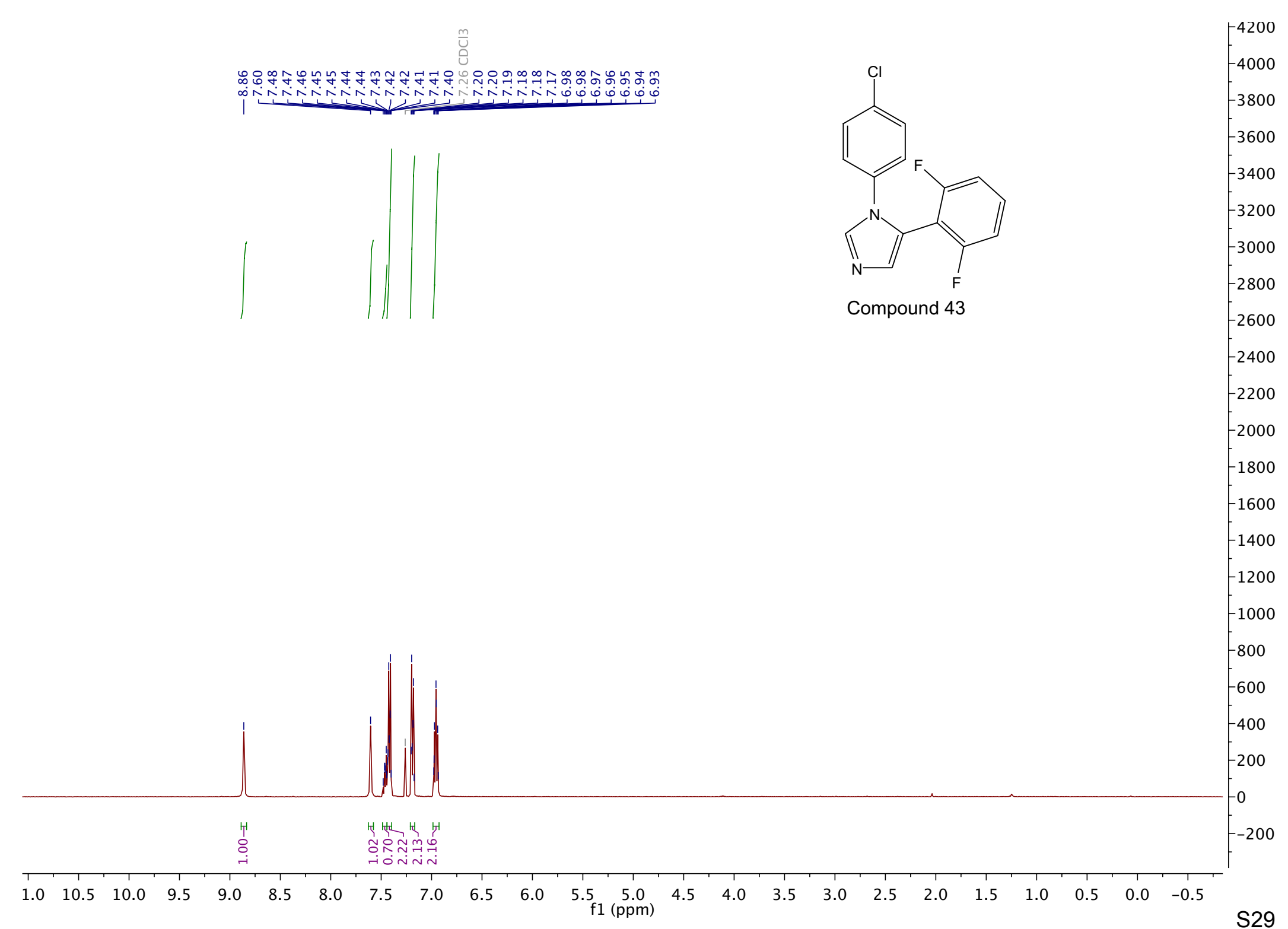


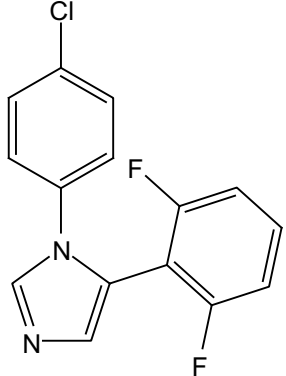


Compound 42

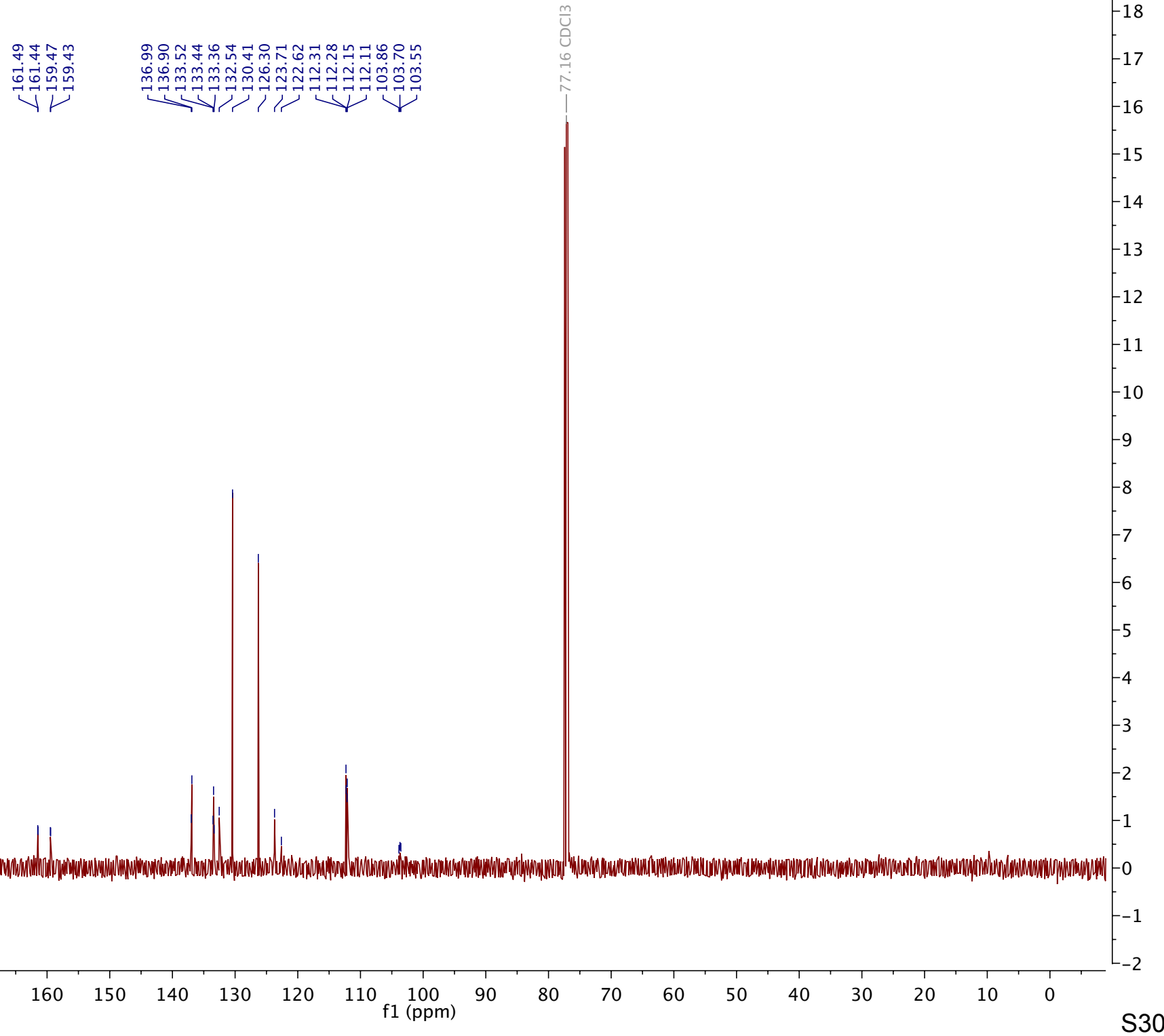


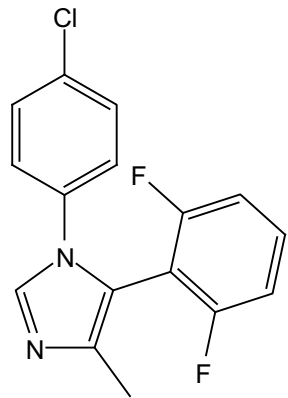
S28



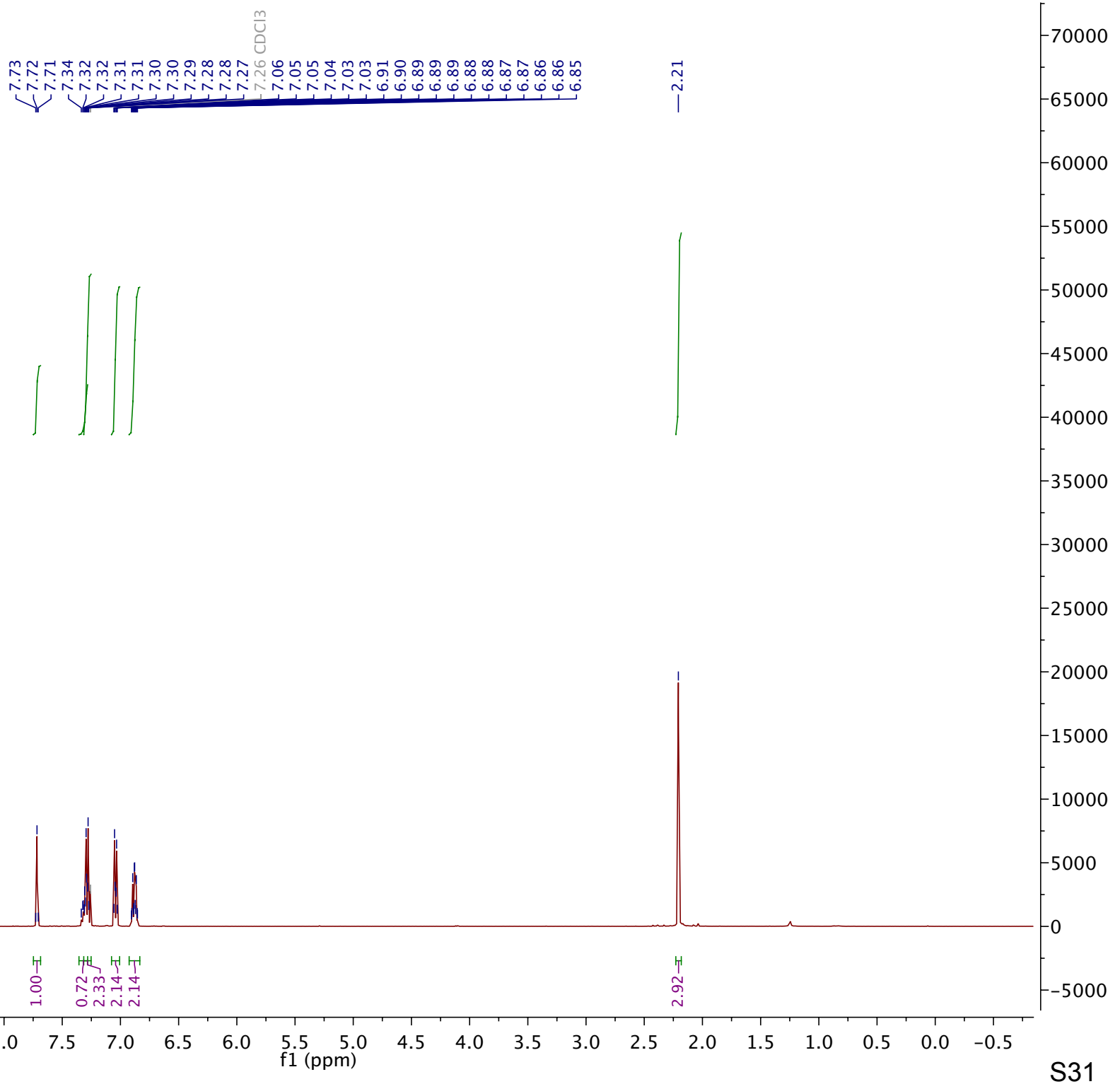


Compound 43

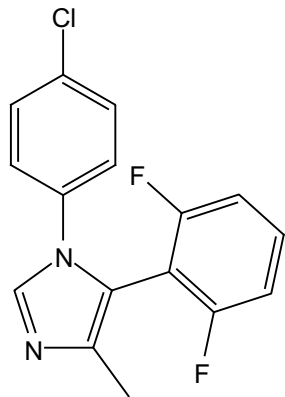




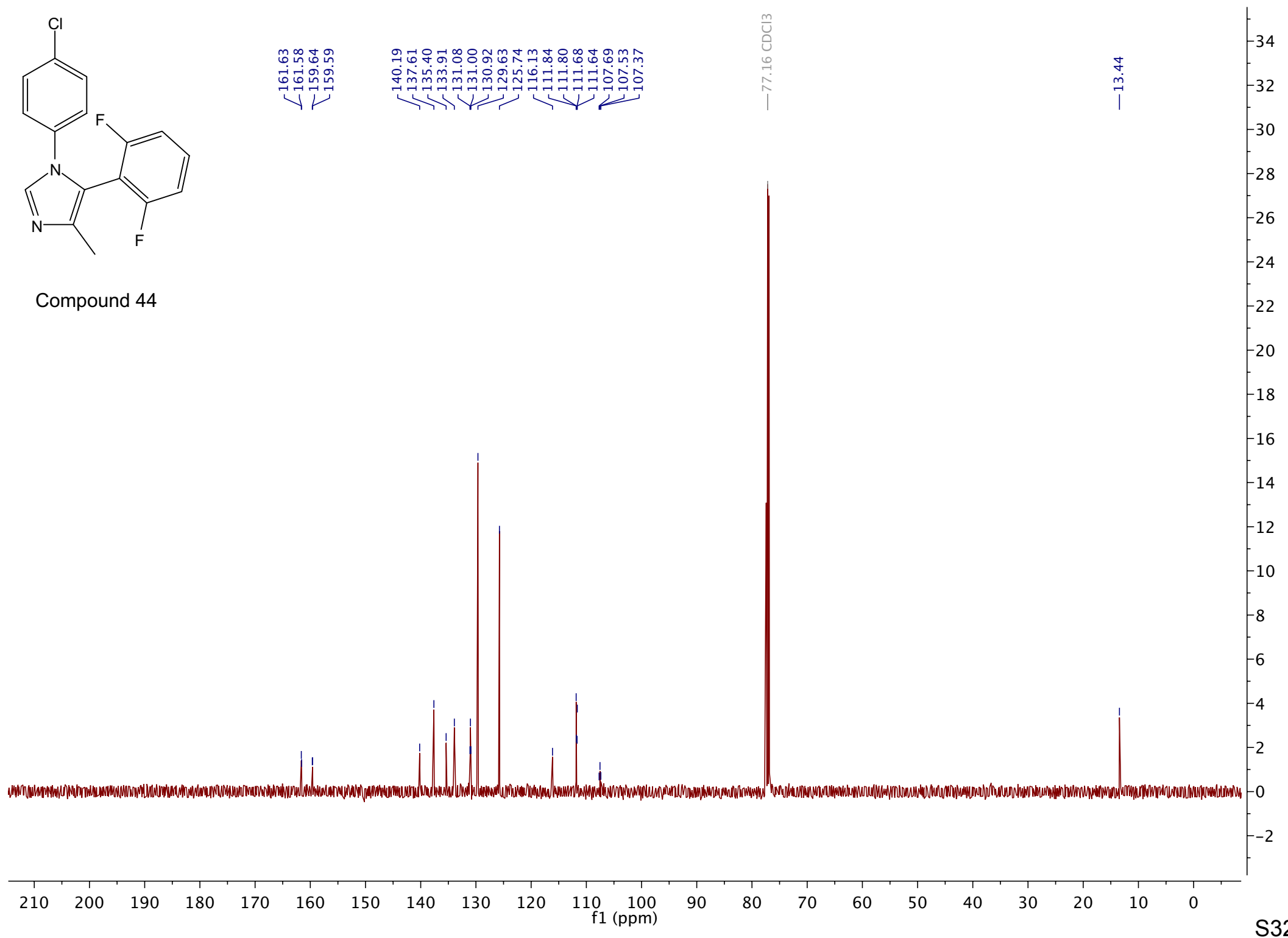
Compound 44

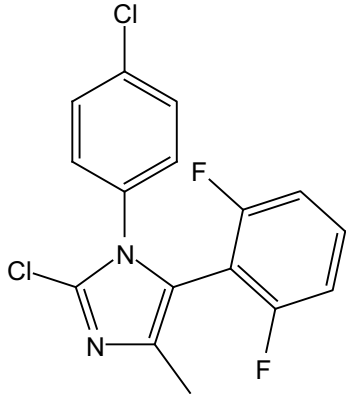


S31

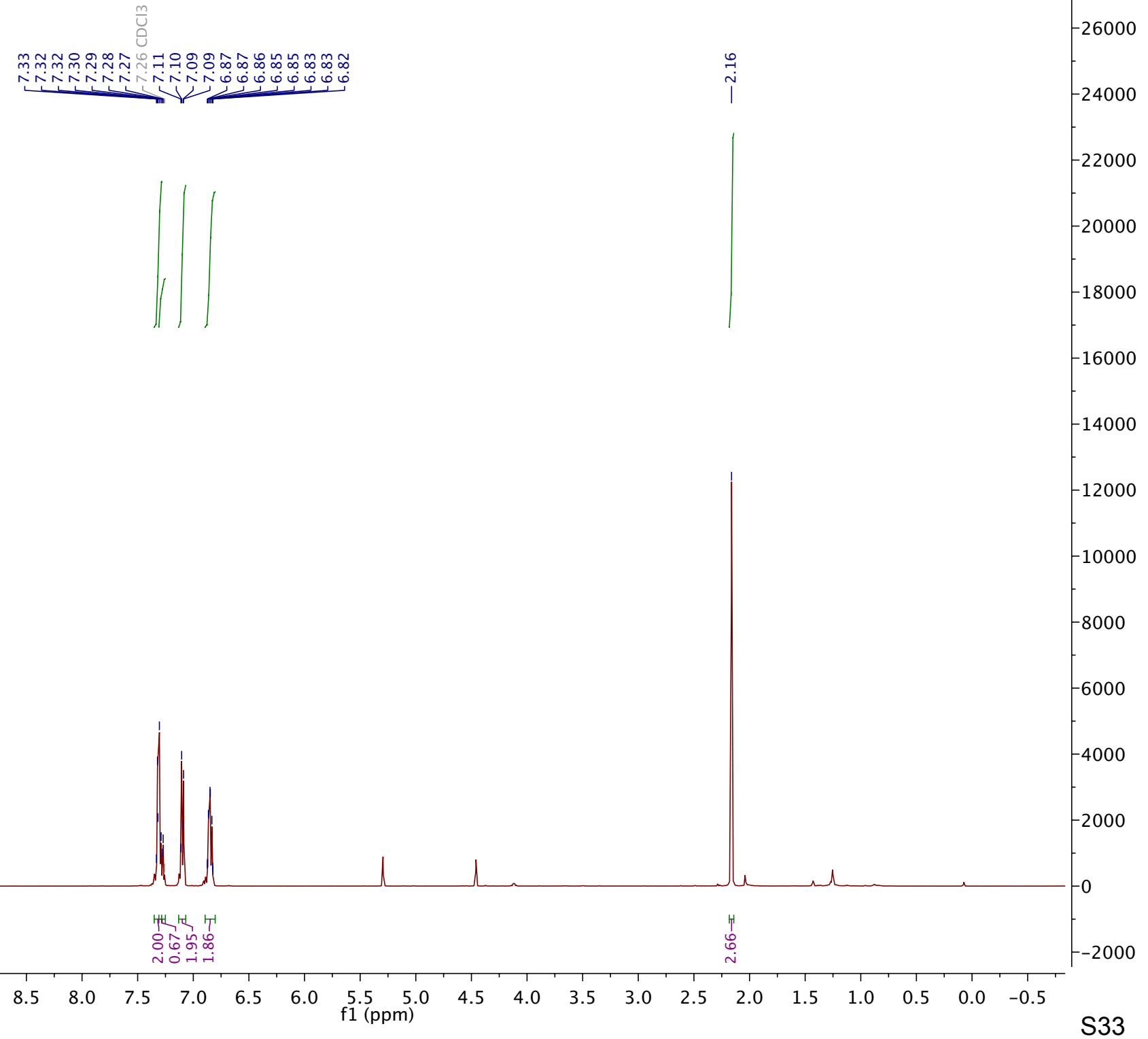


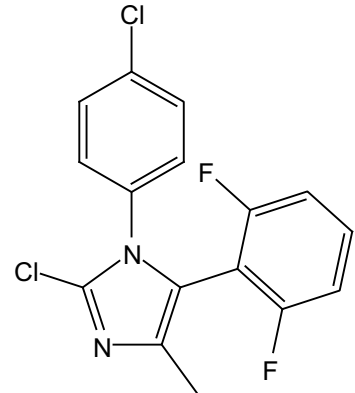
Compound 44



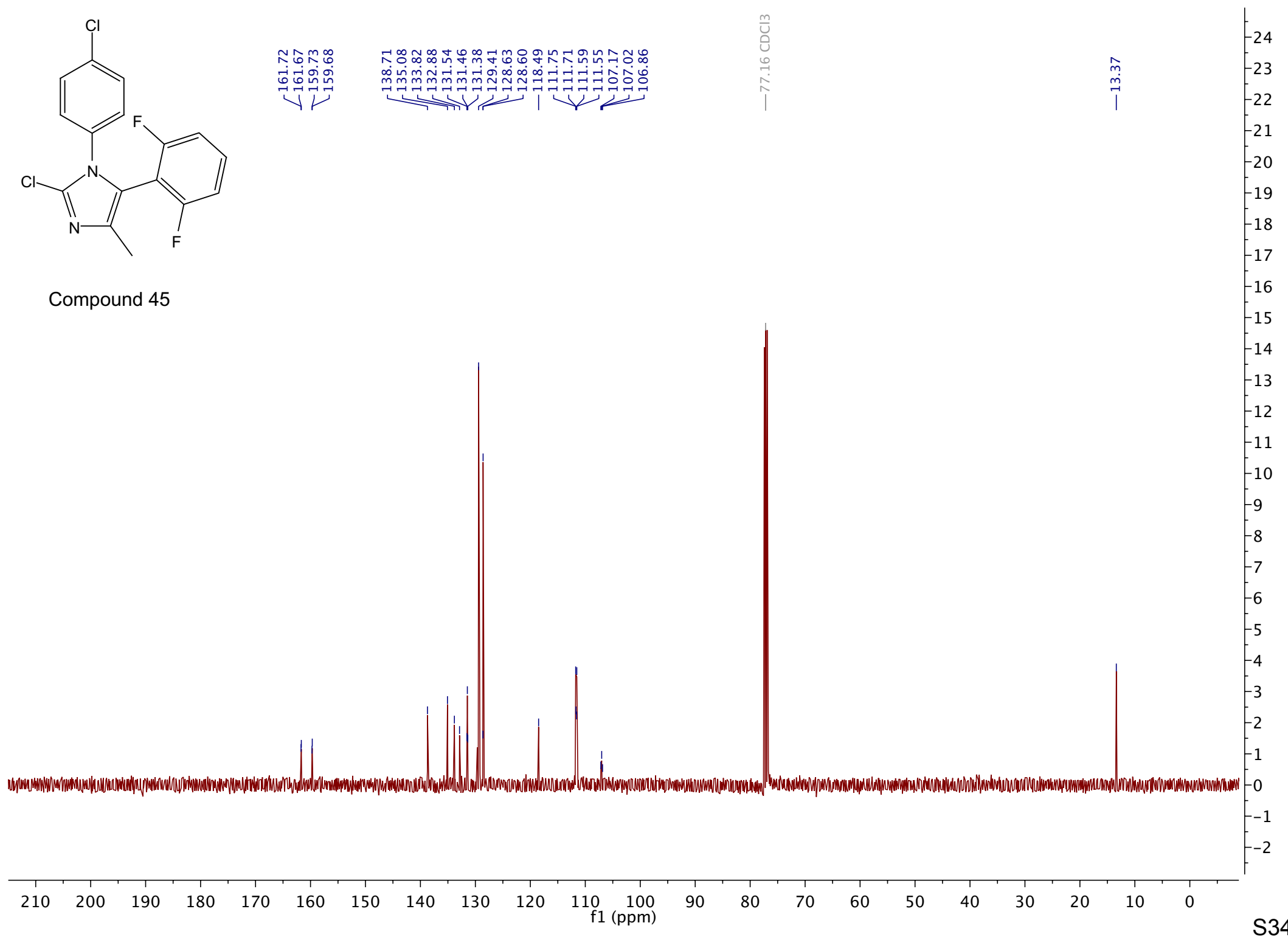


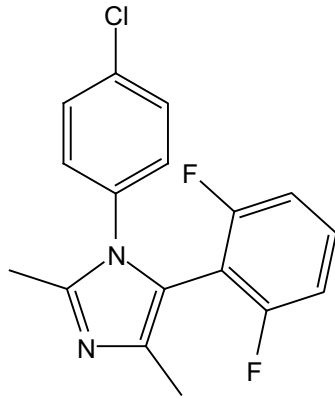
Compound 45



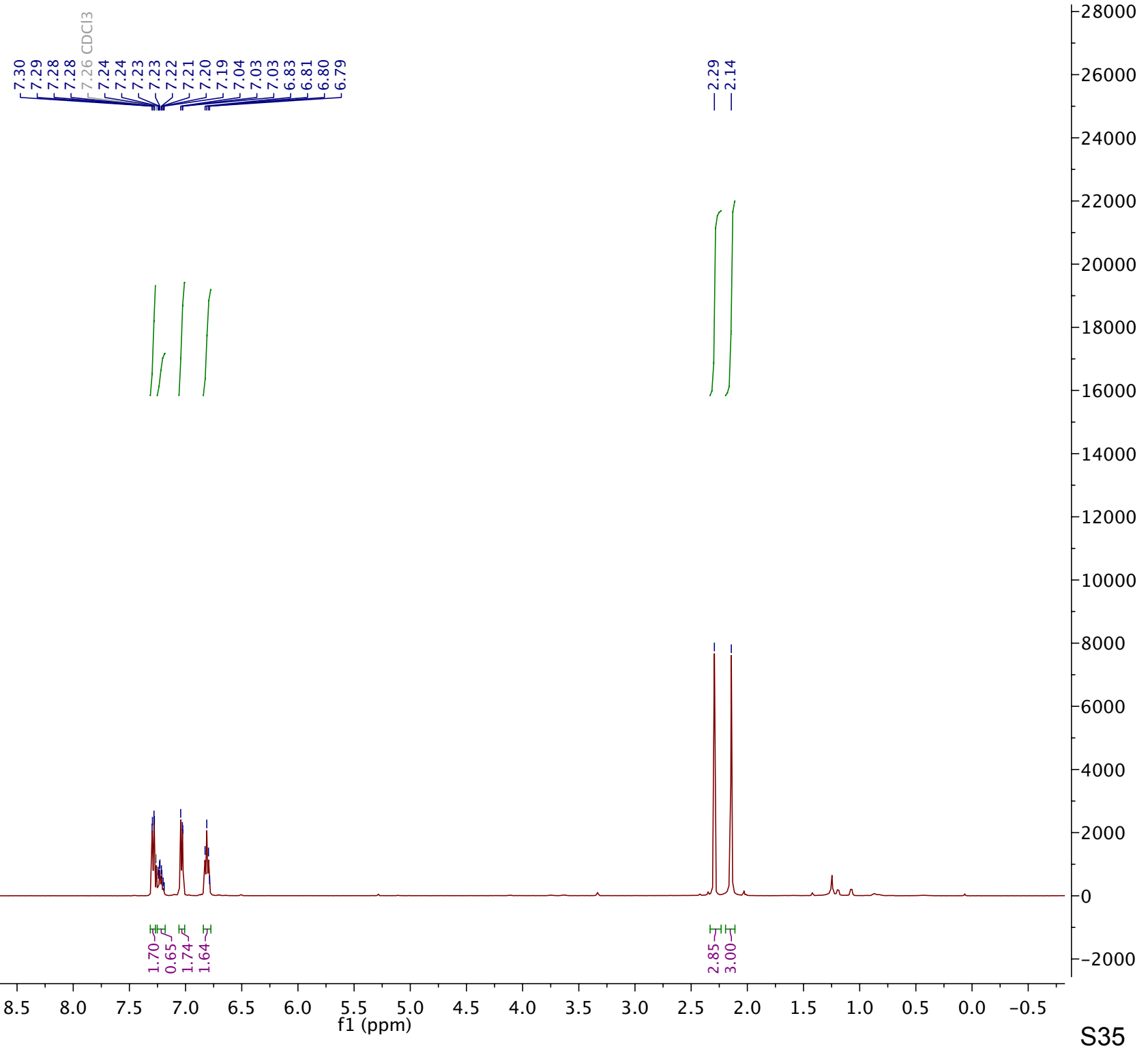


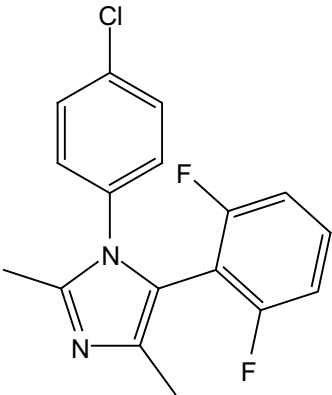
Compound 45



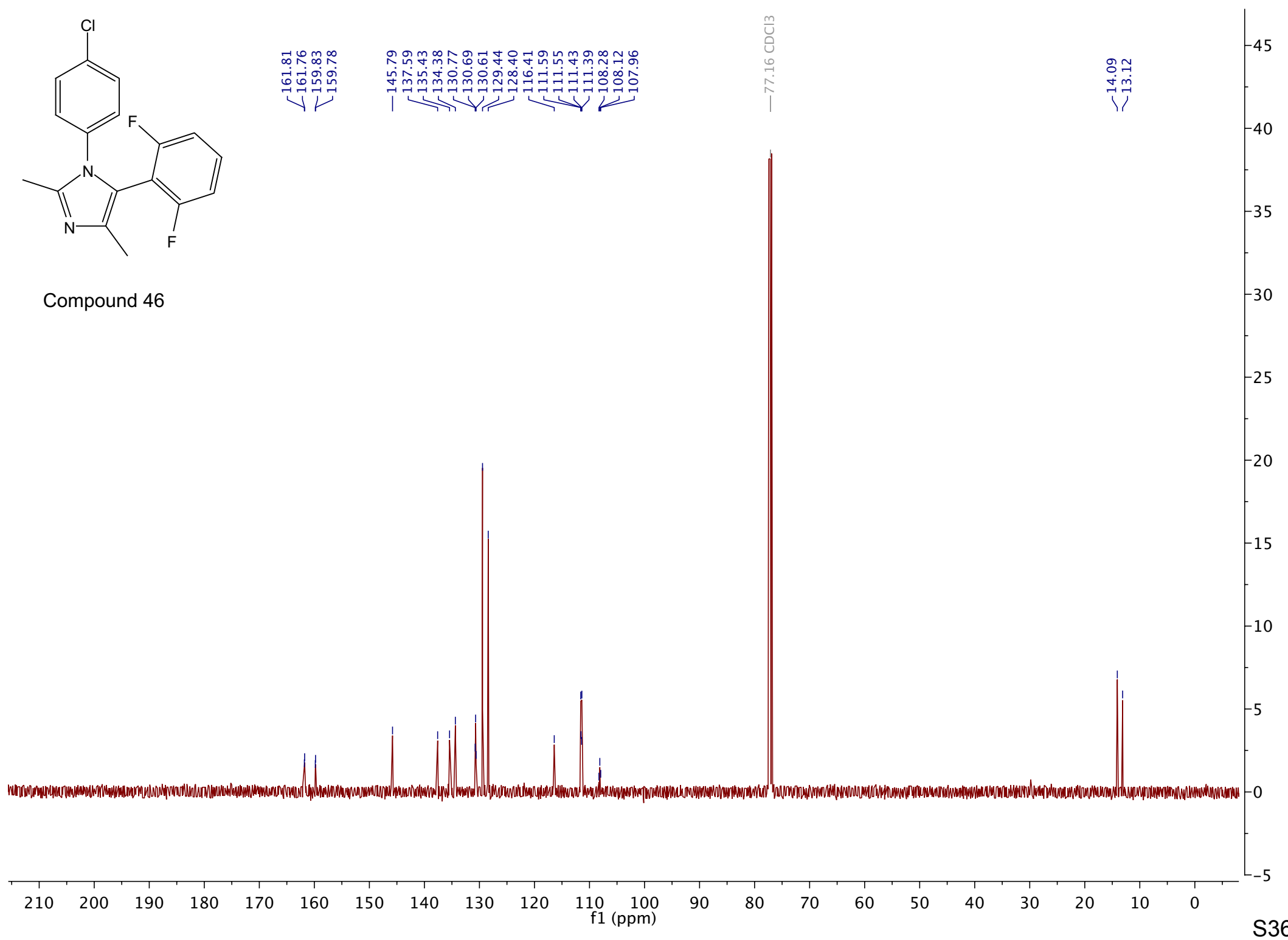


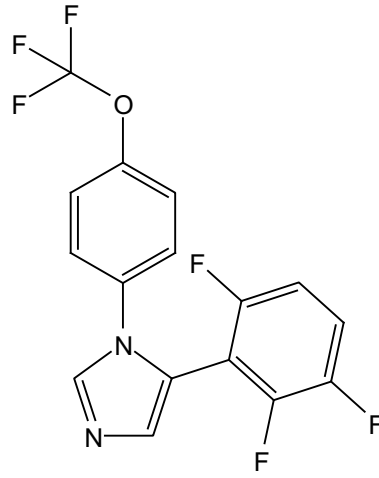
Compound 46



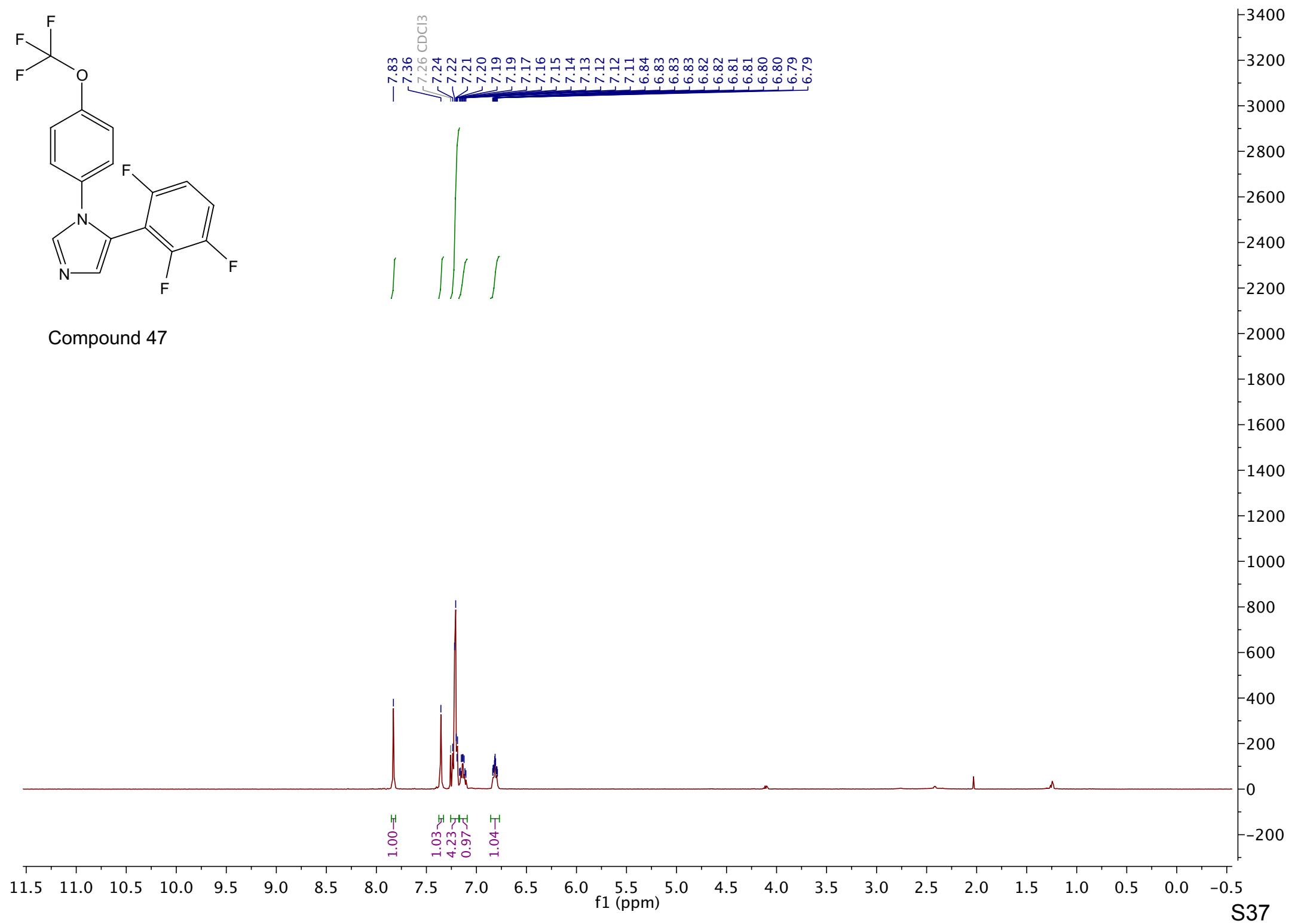


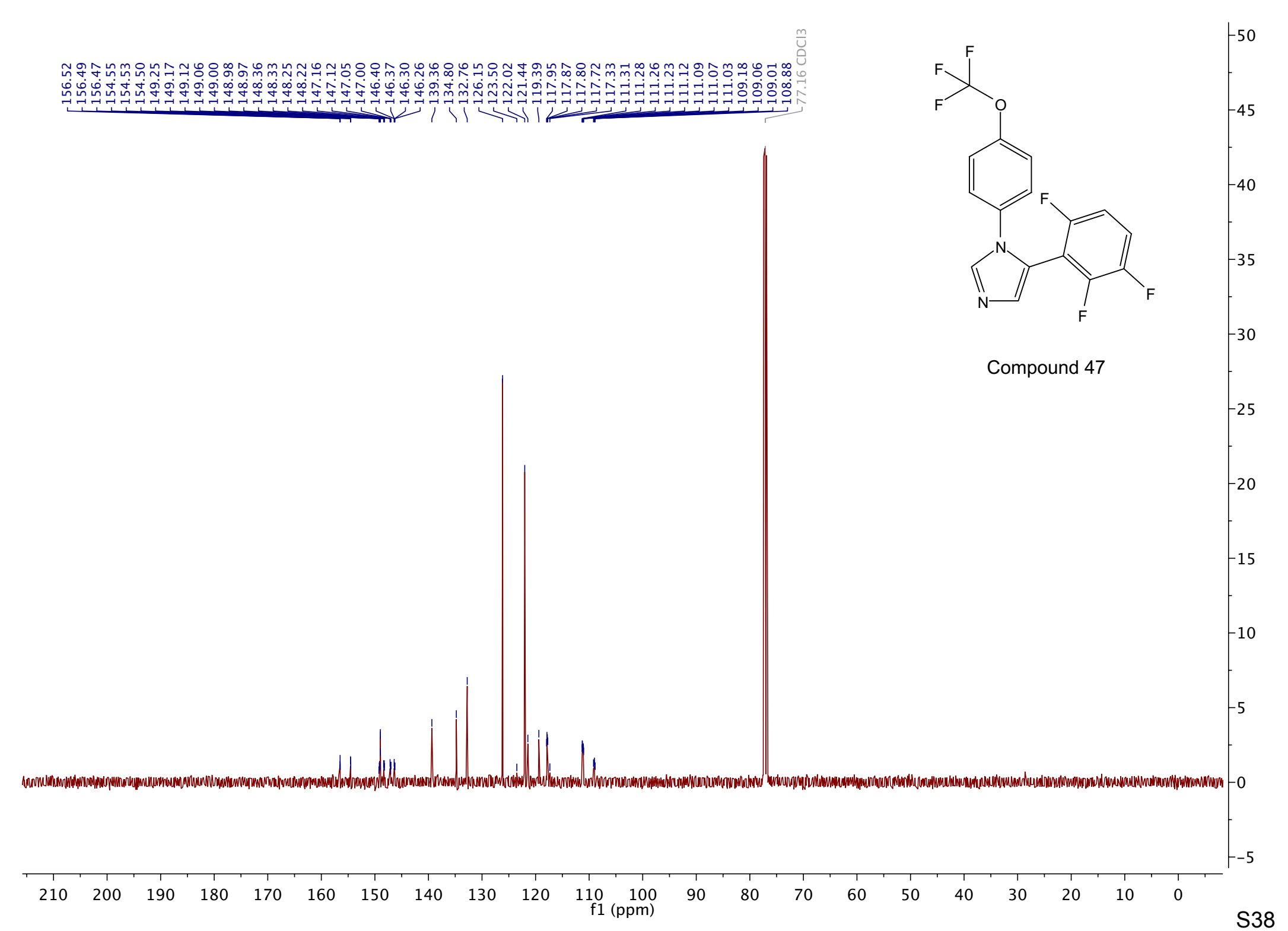
Compound 46

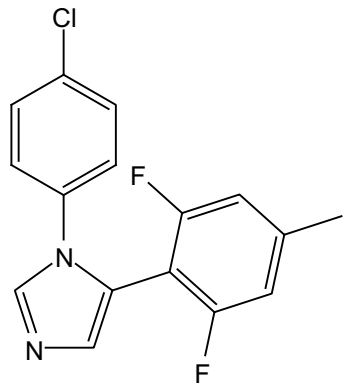




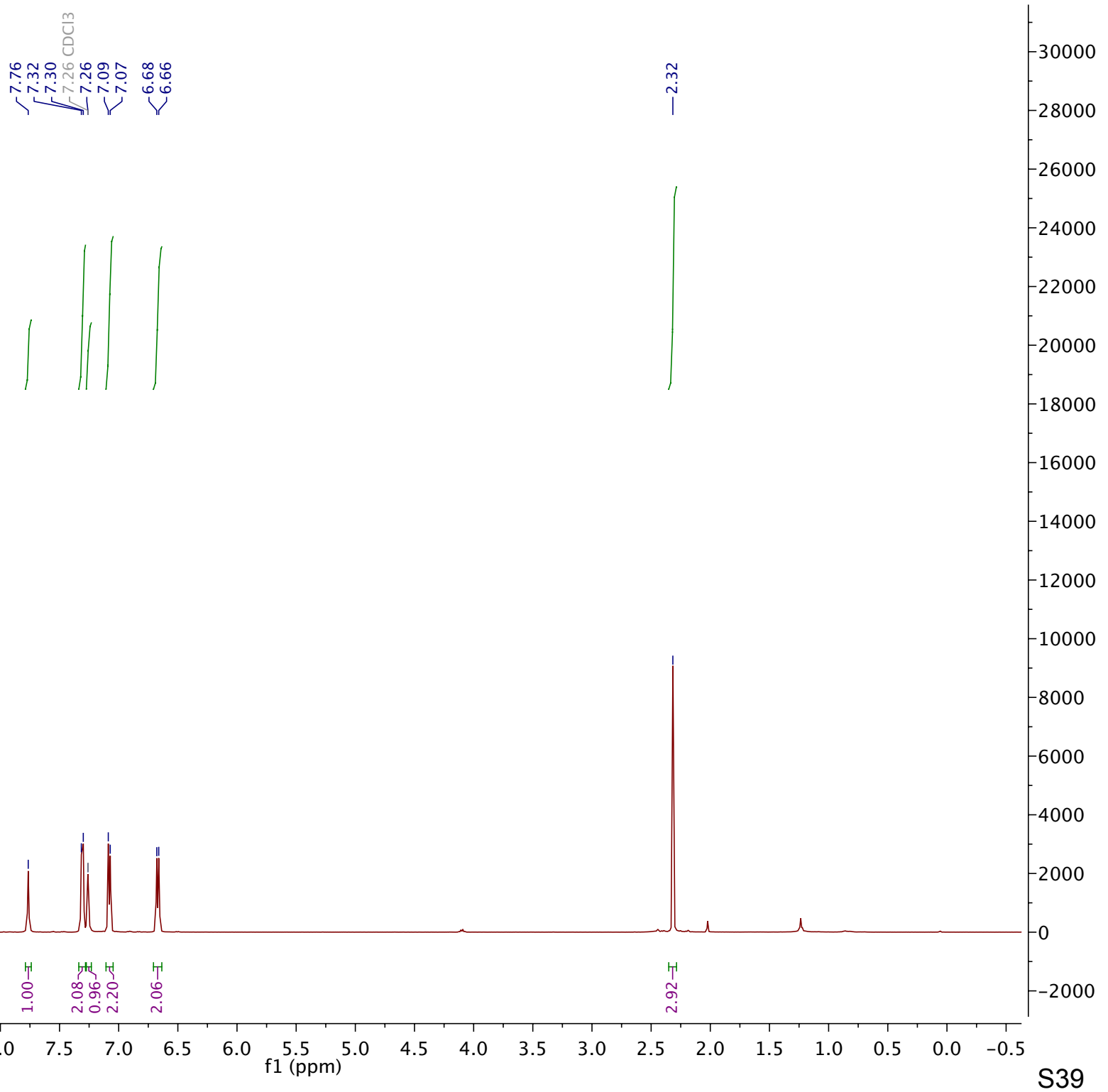
Compound 47

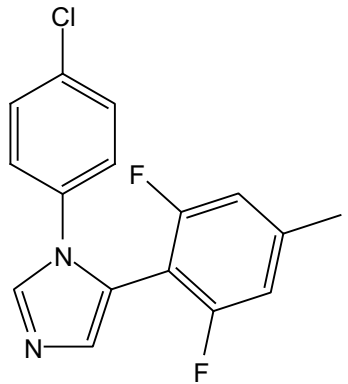




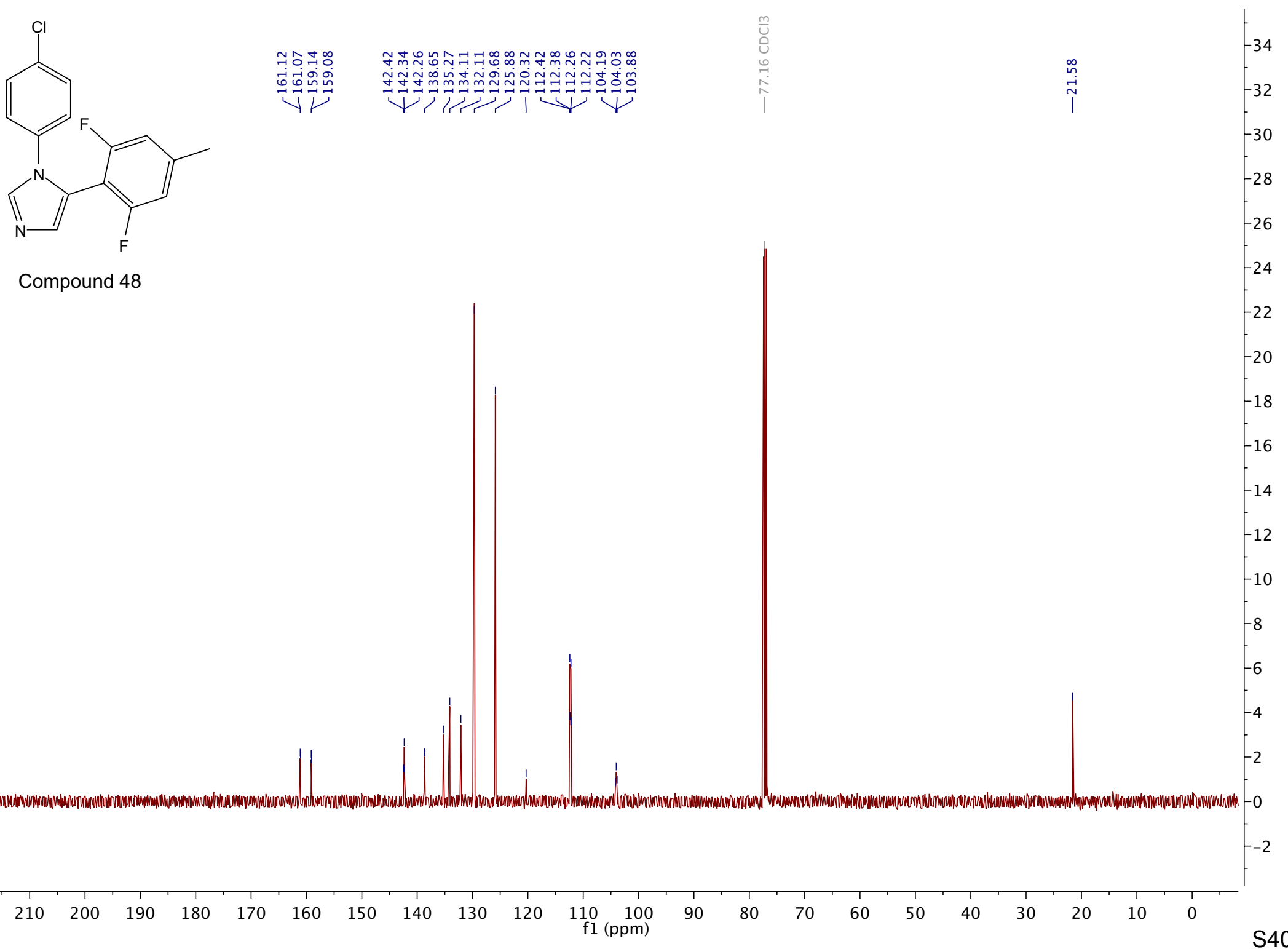


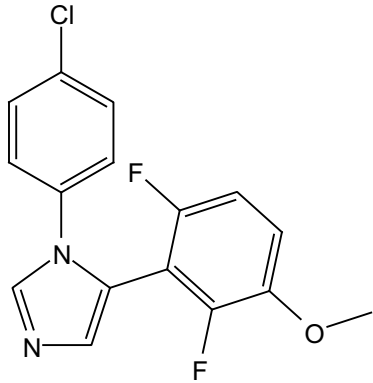
Compound 48



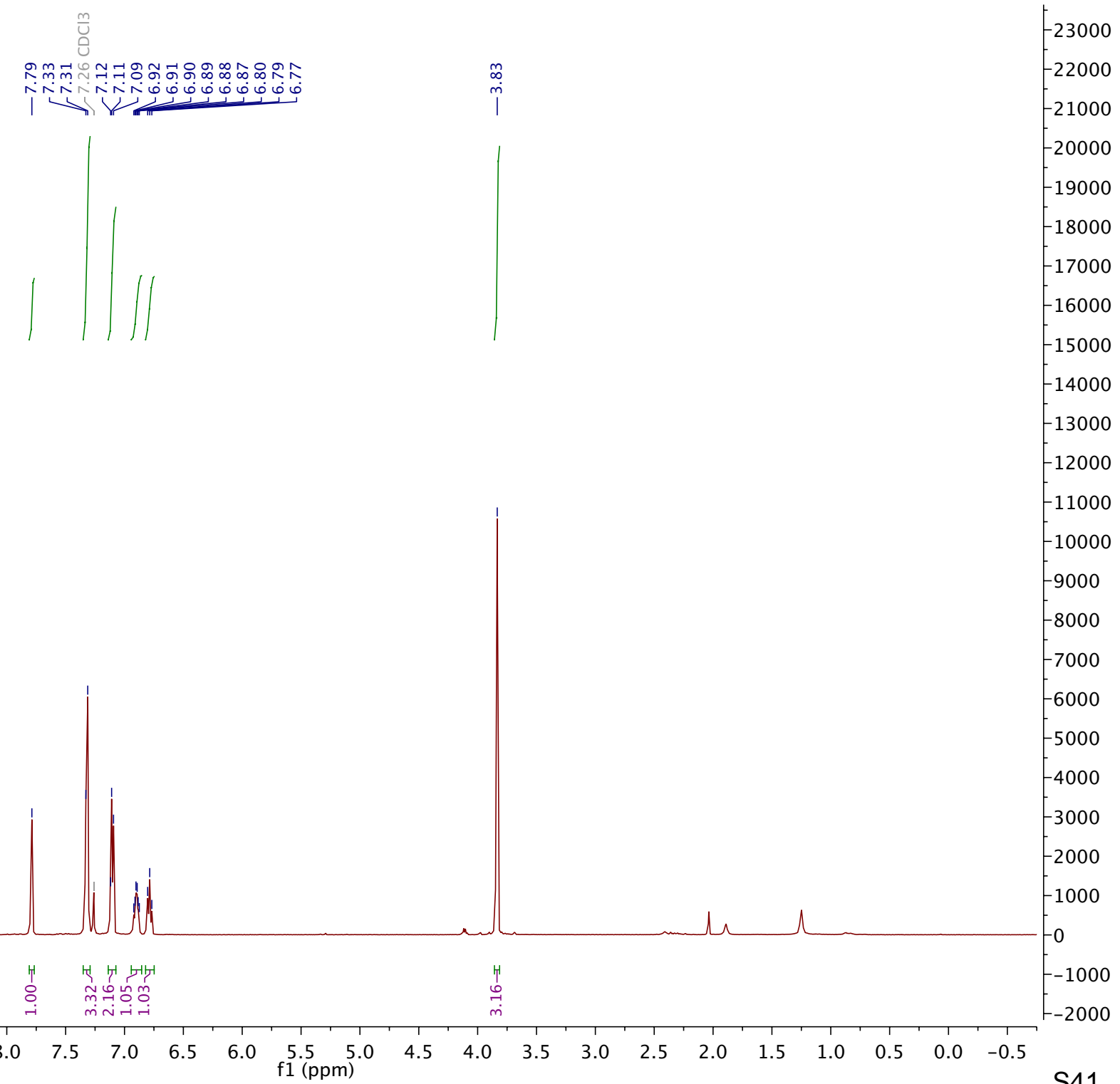


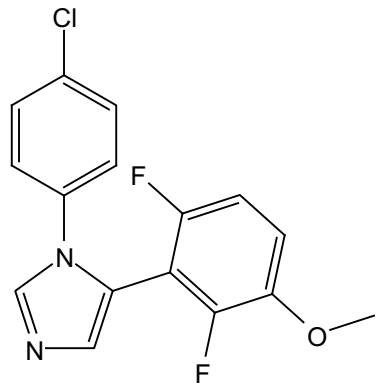
Compound 48



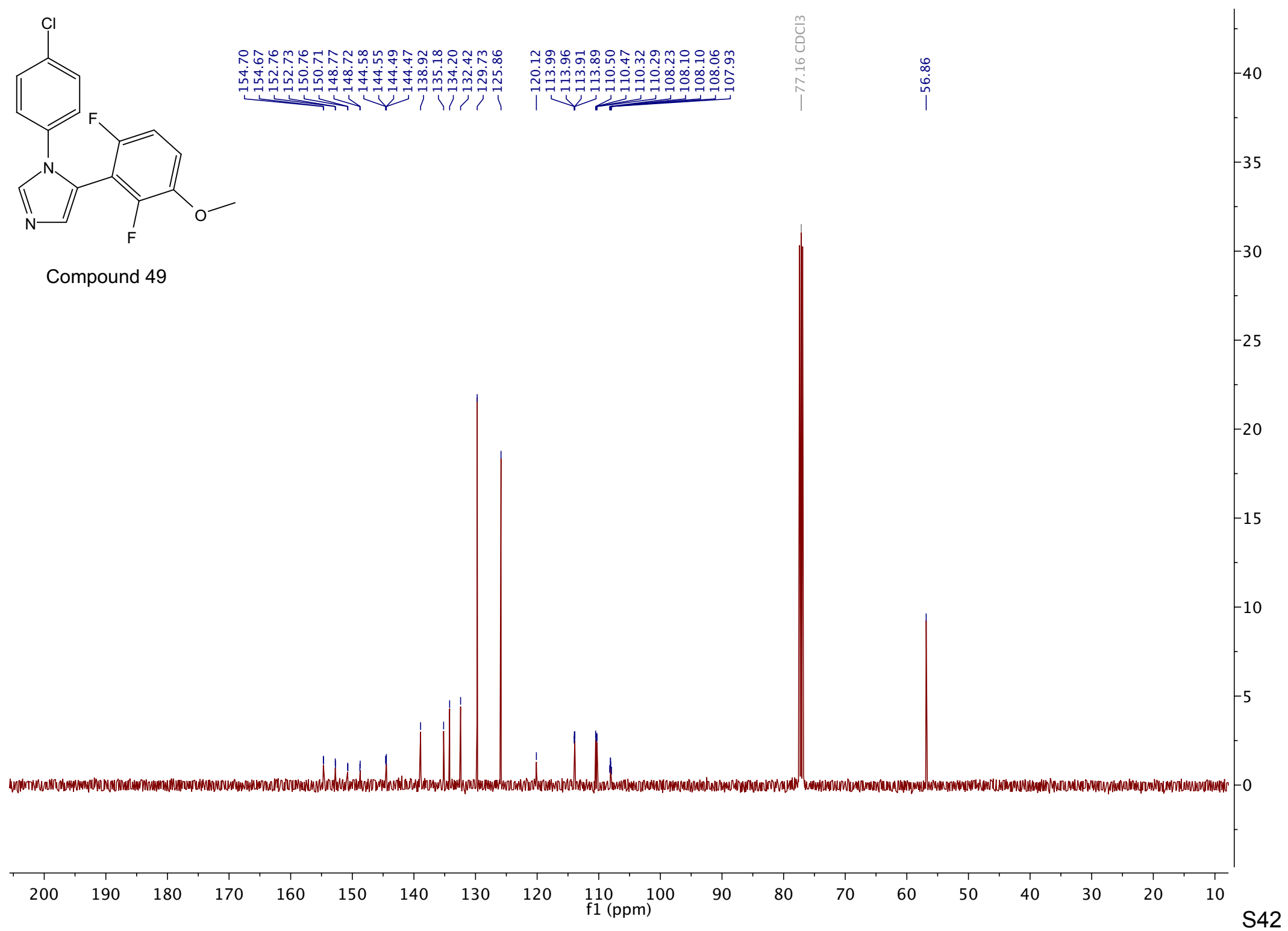


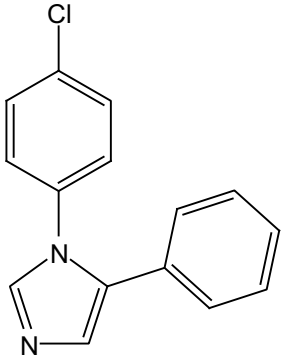
Compound 49



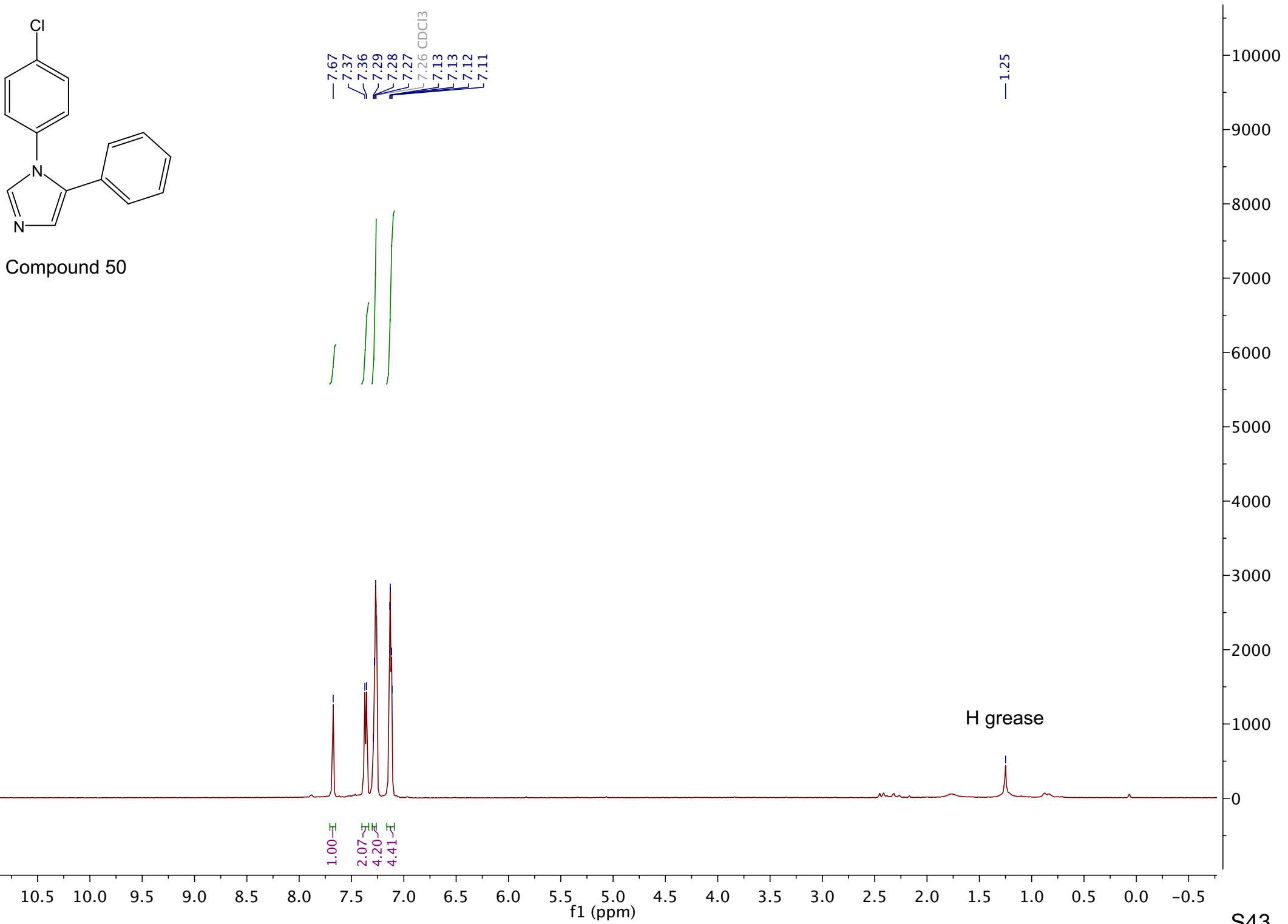


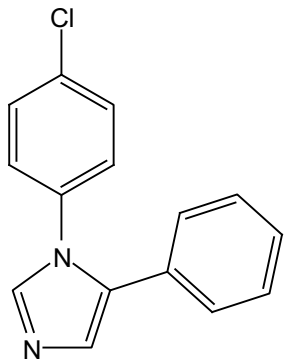
Compound 49



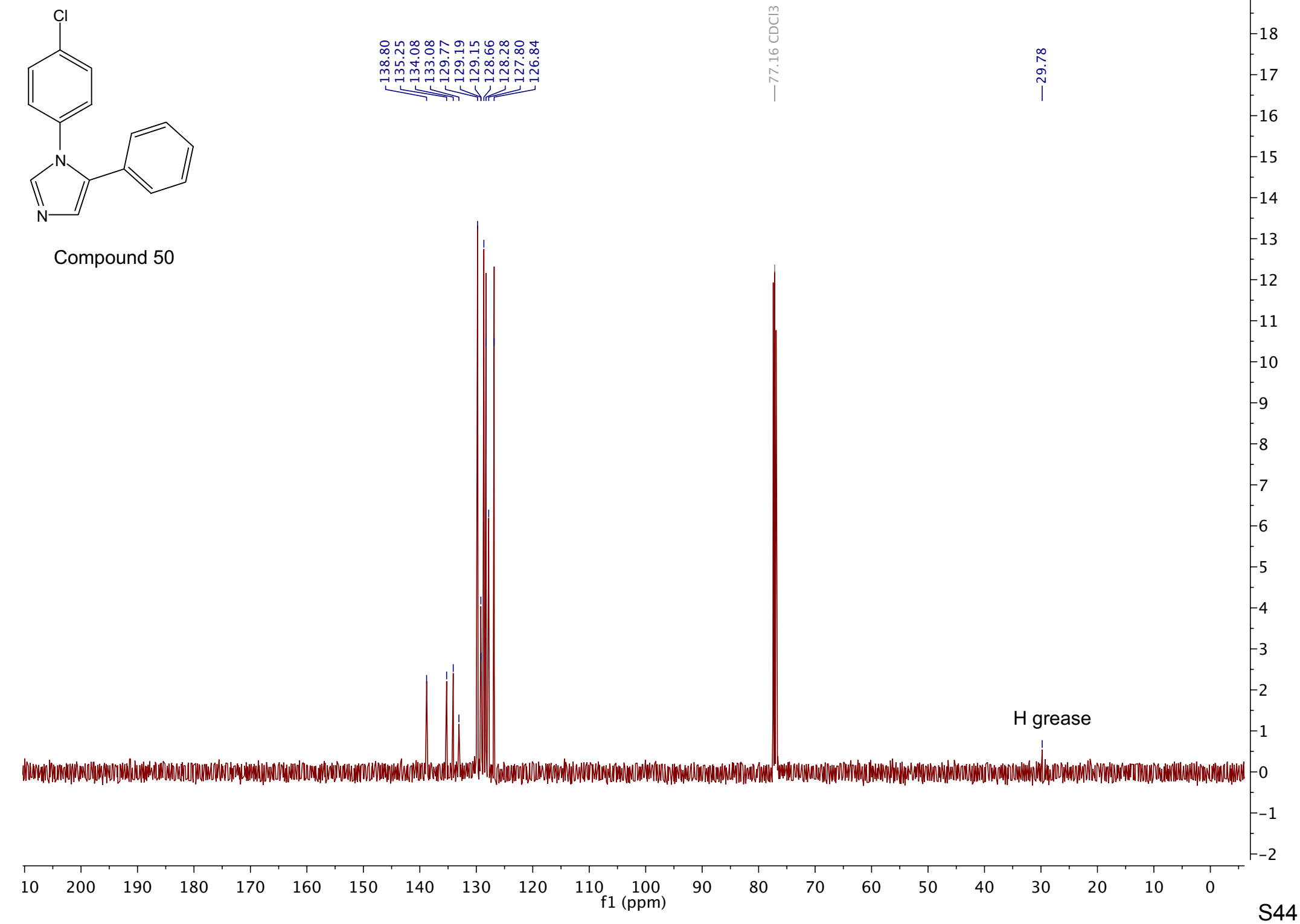


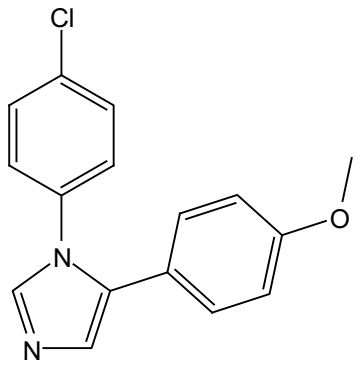
Compound 50



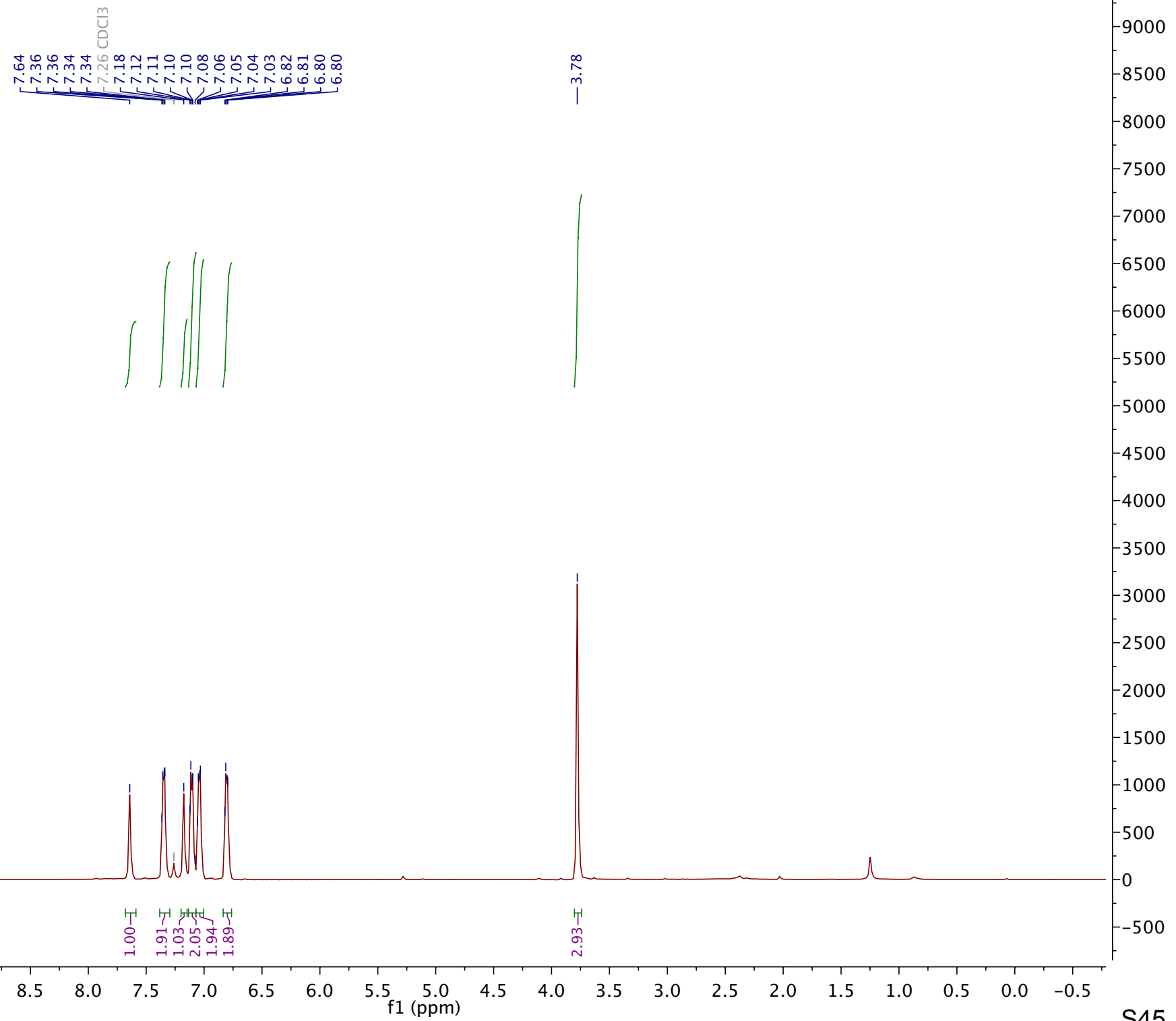


Compound 50





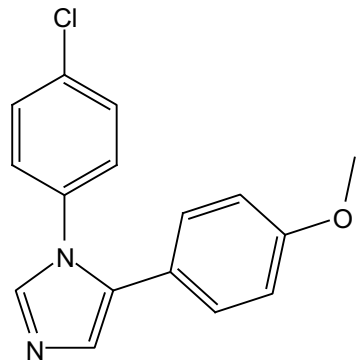
Compound 51



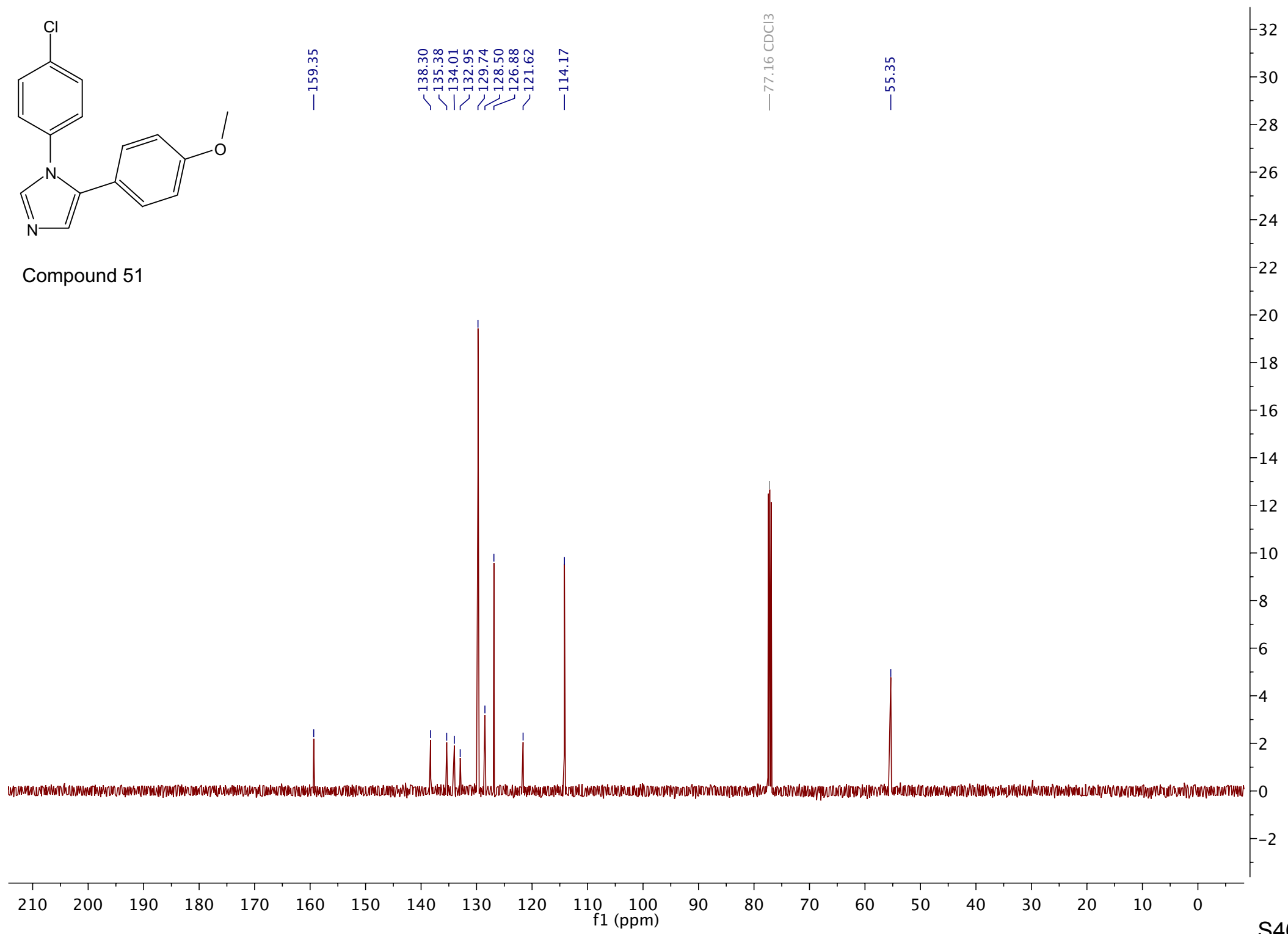
10.5 10.0 9.5 9.0 8.5 8.0 7.5 7.0 6.5 6.0 5.5 5.0 4.5 4.0 3.5 3.0 2.5 2.0 1.5 1.0 0.5 0.0 -0.5

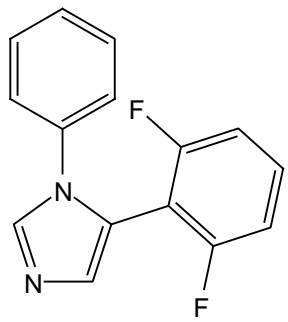
f1 (ppm)

S45

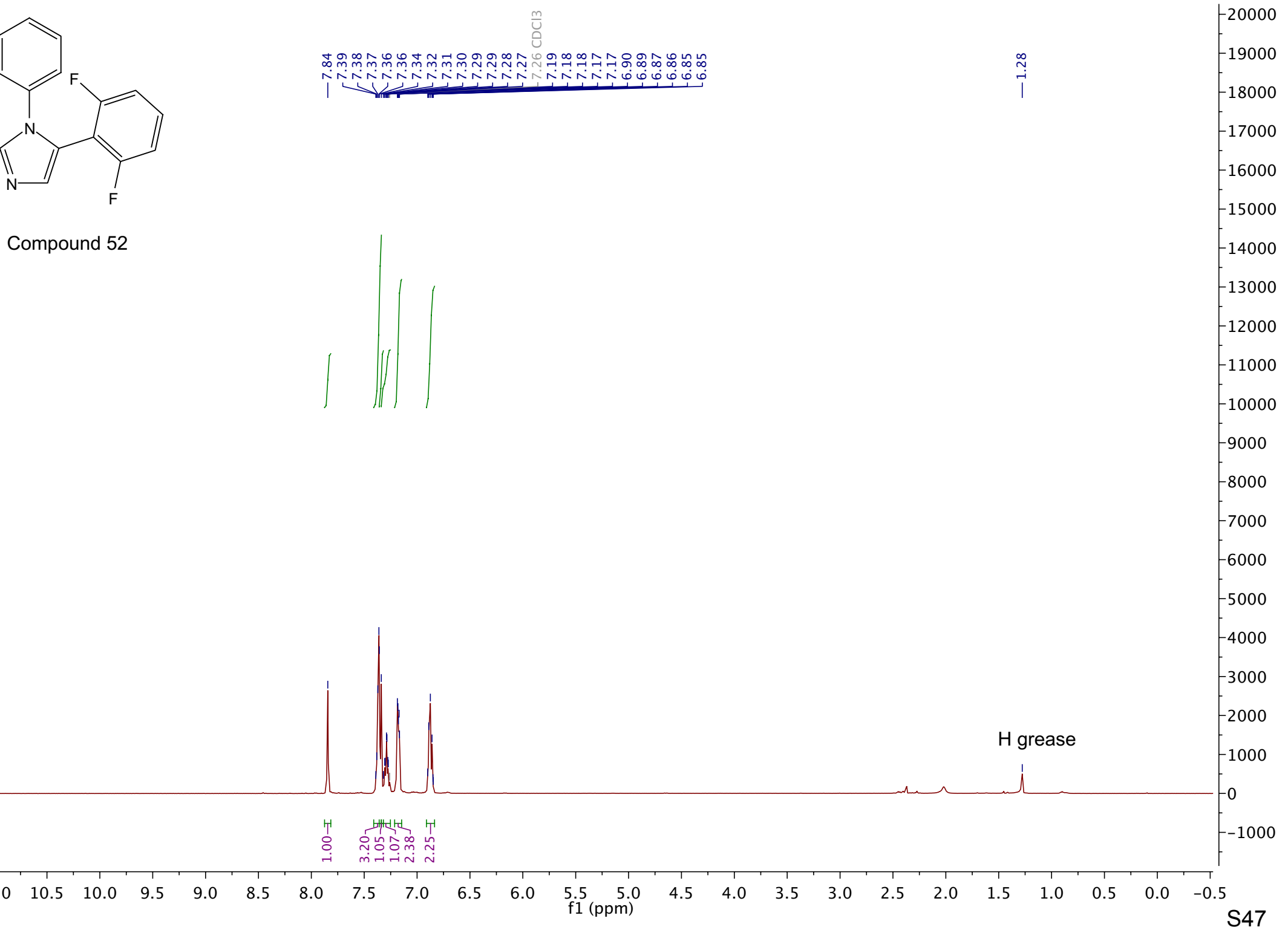


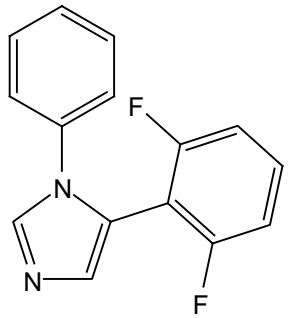
Compound 51



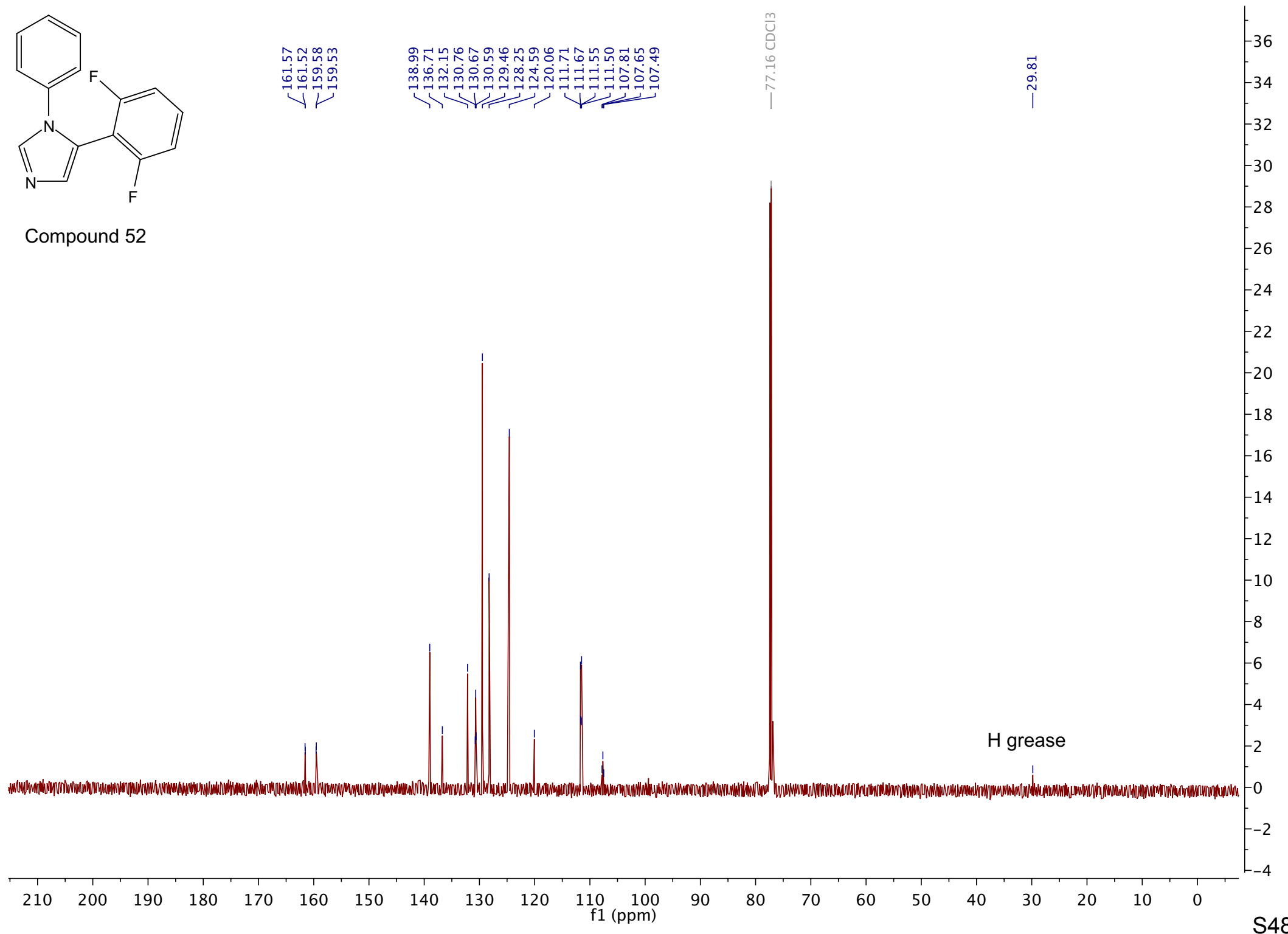


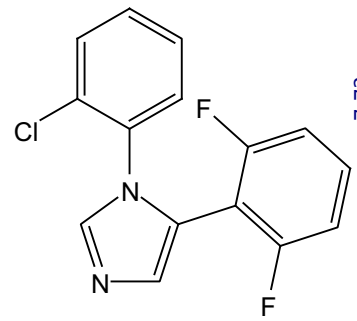
Compound 52



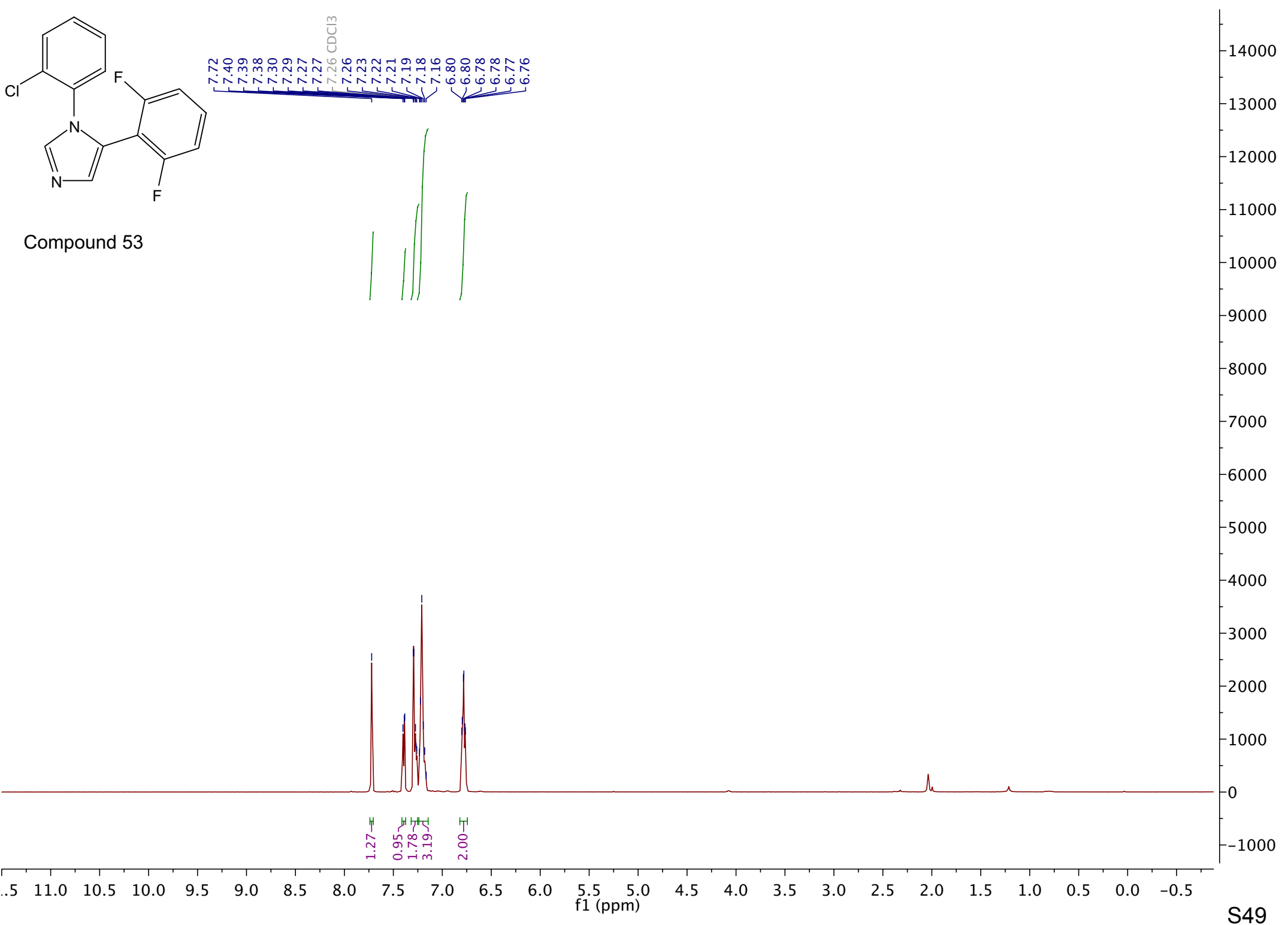


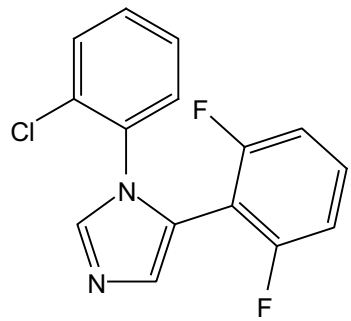
Compound 52



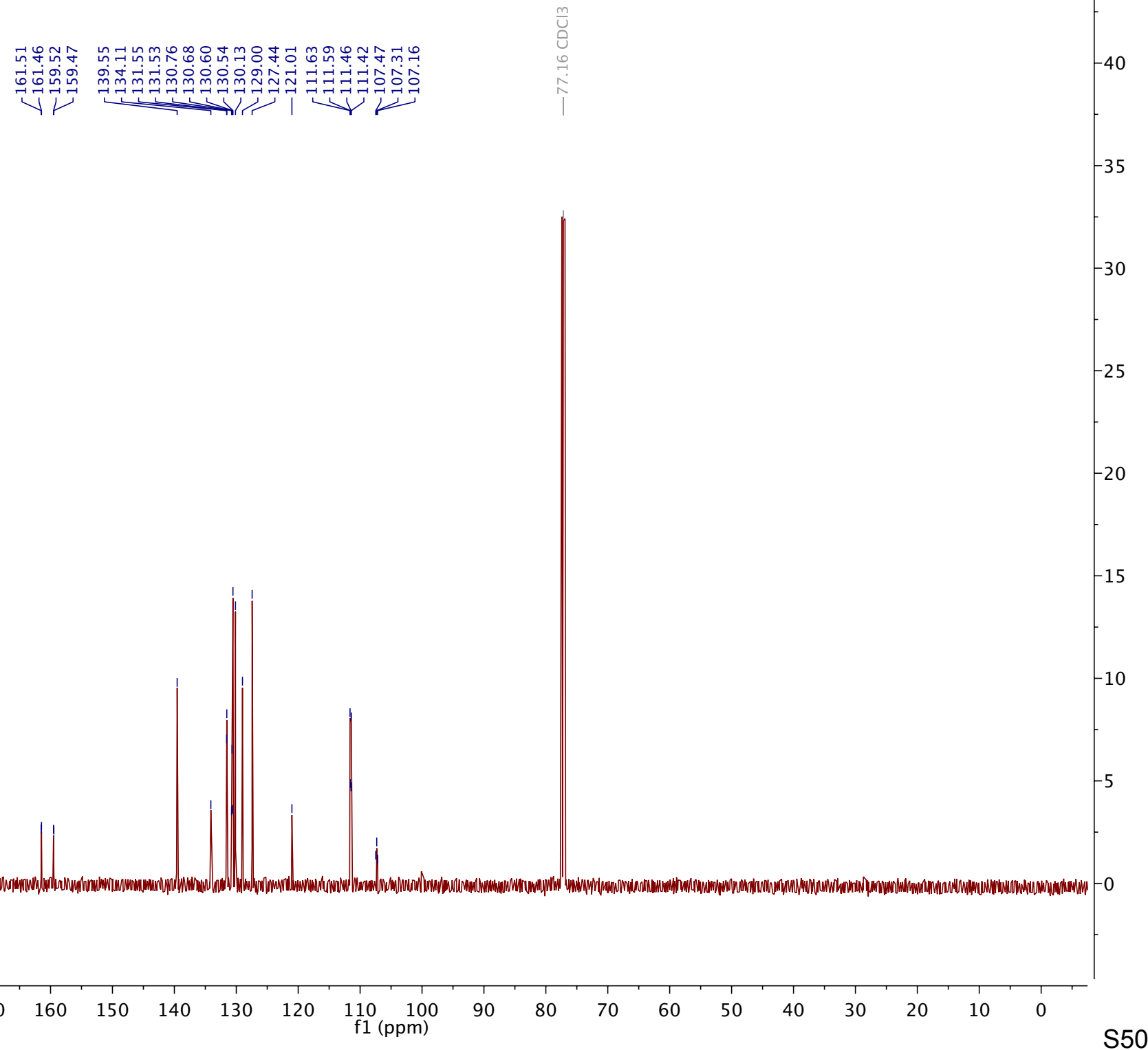


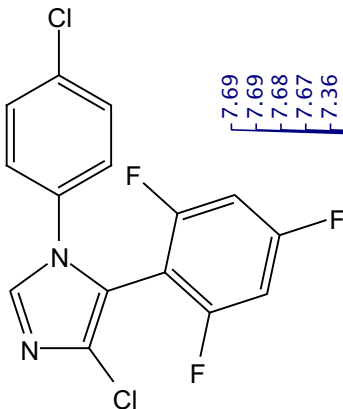
Compound 53



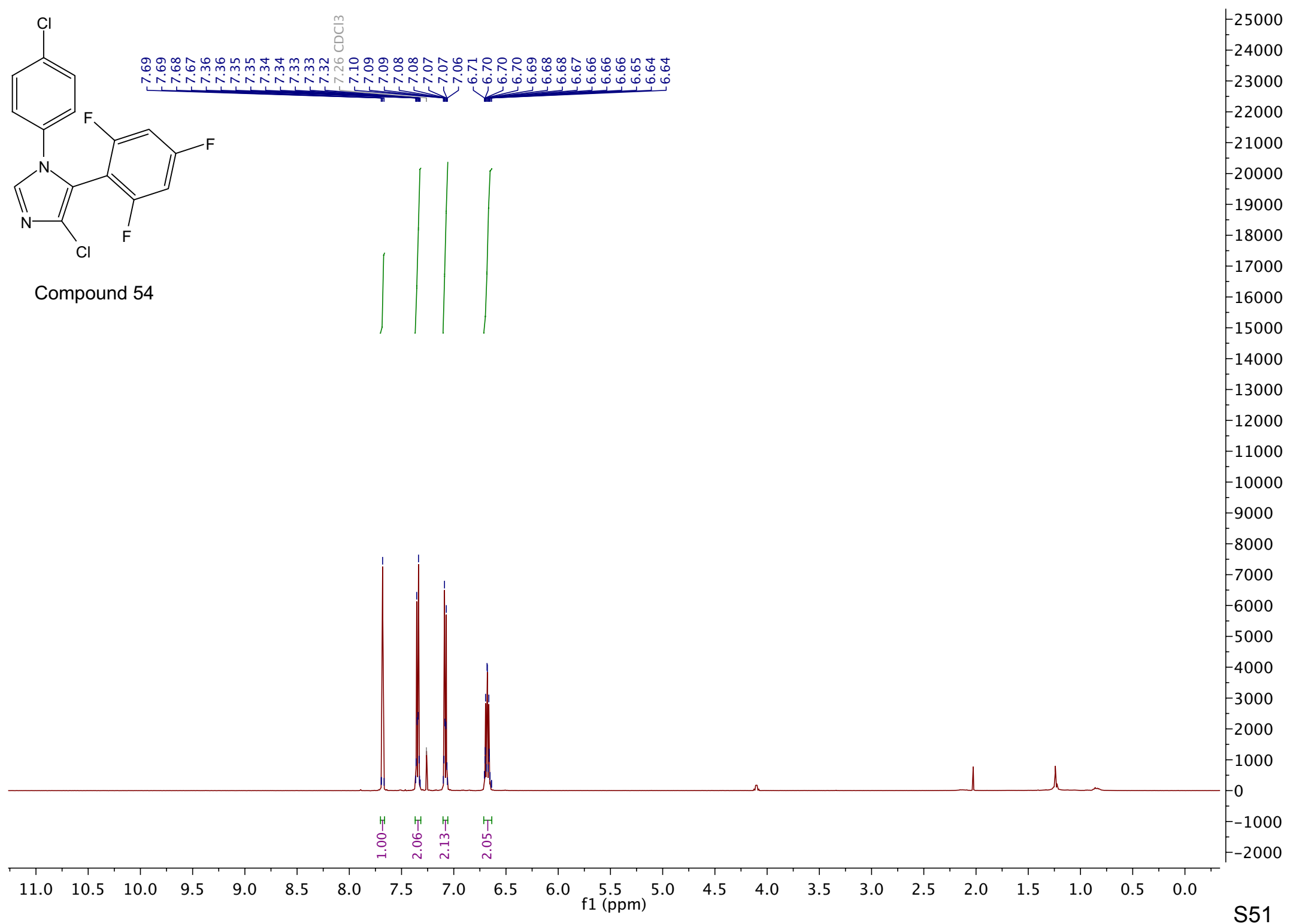


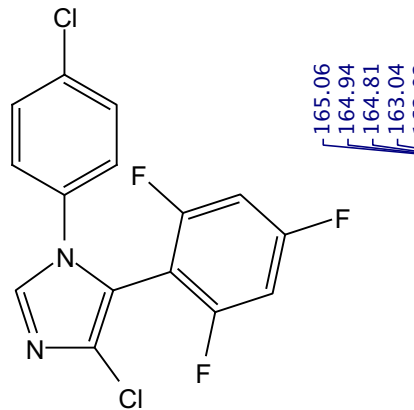
Compound 53



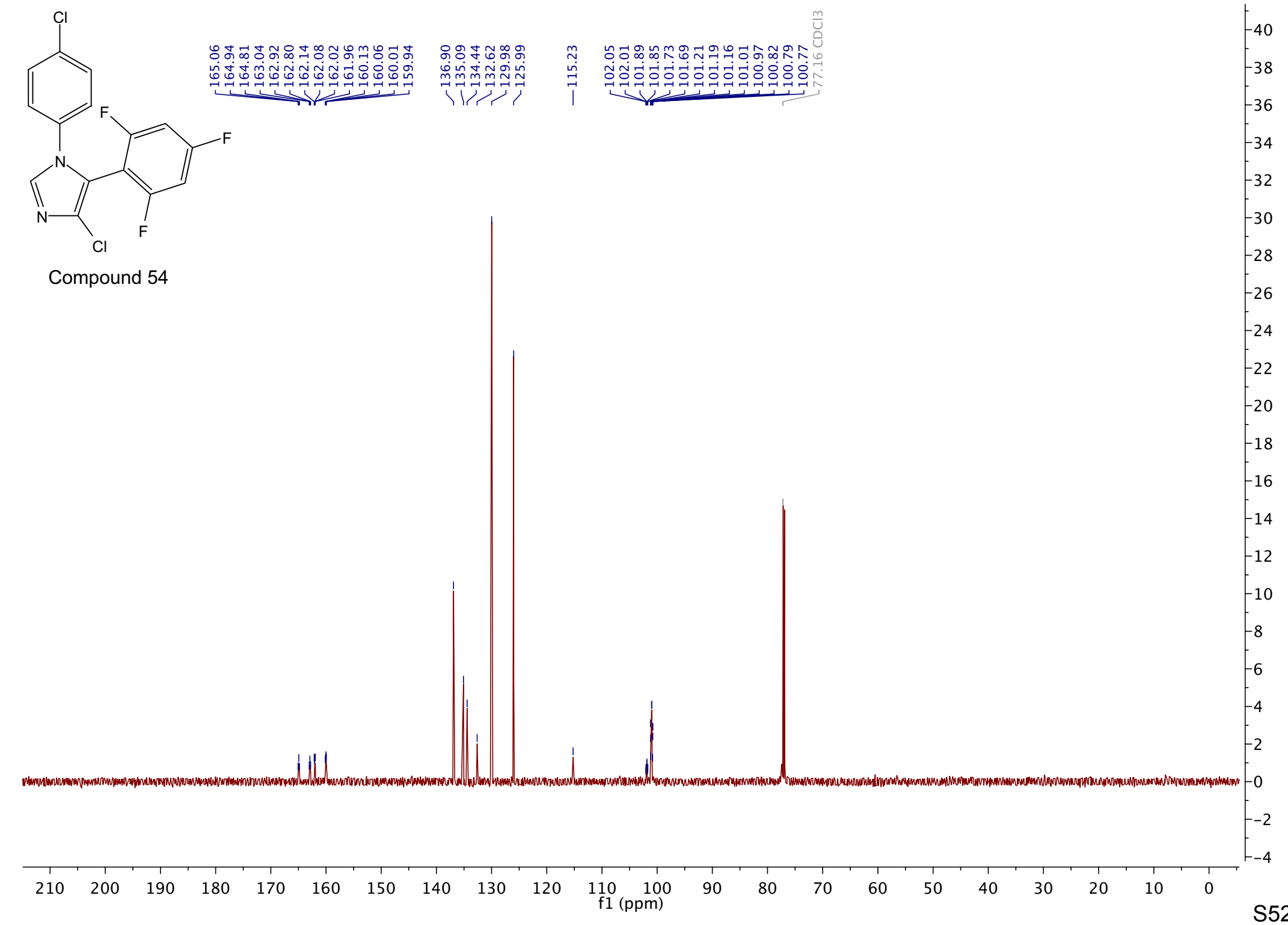


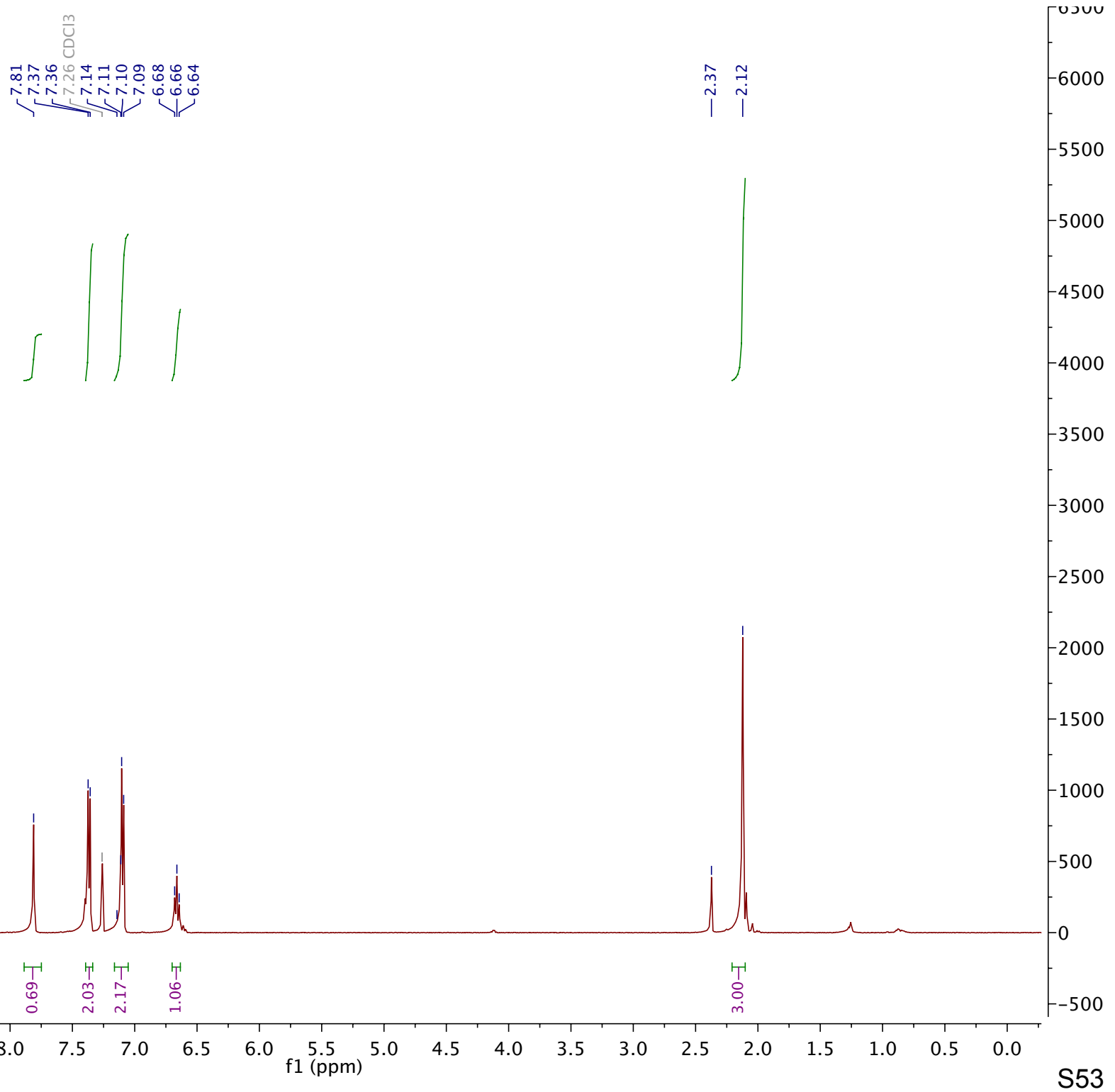
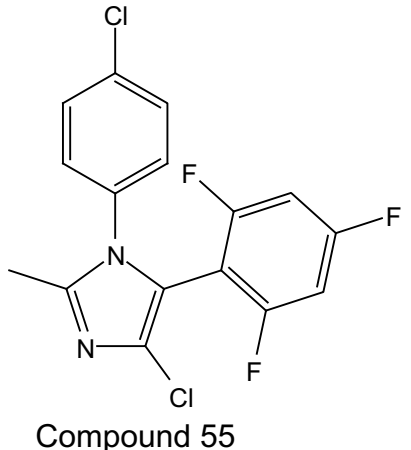
Compound 54

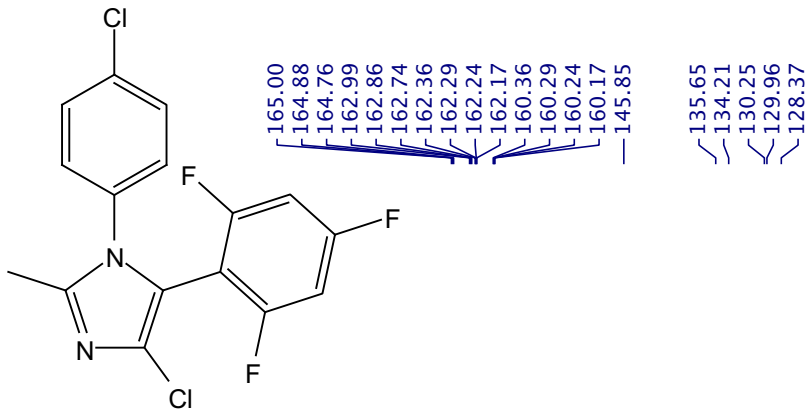




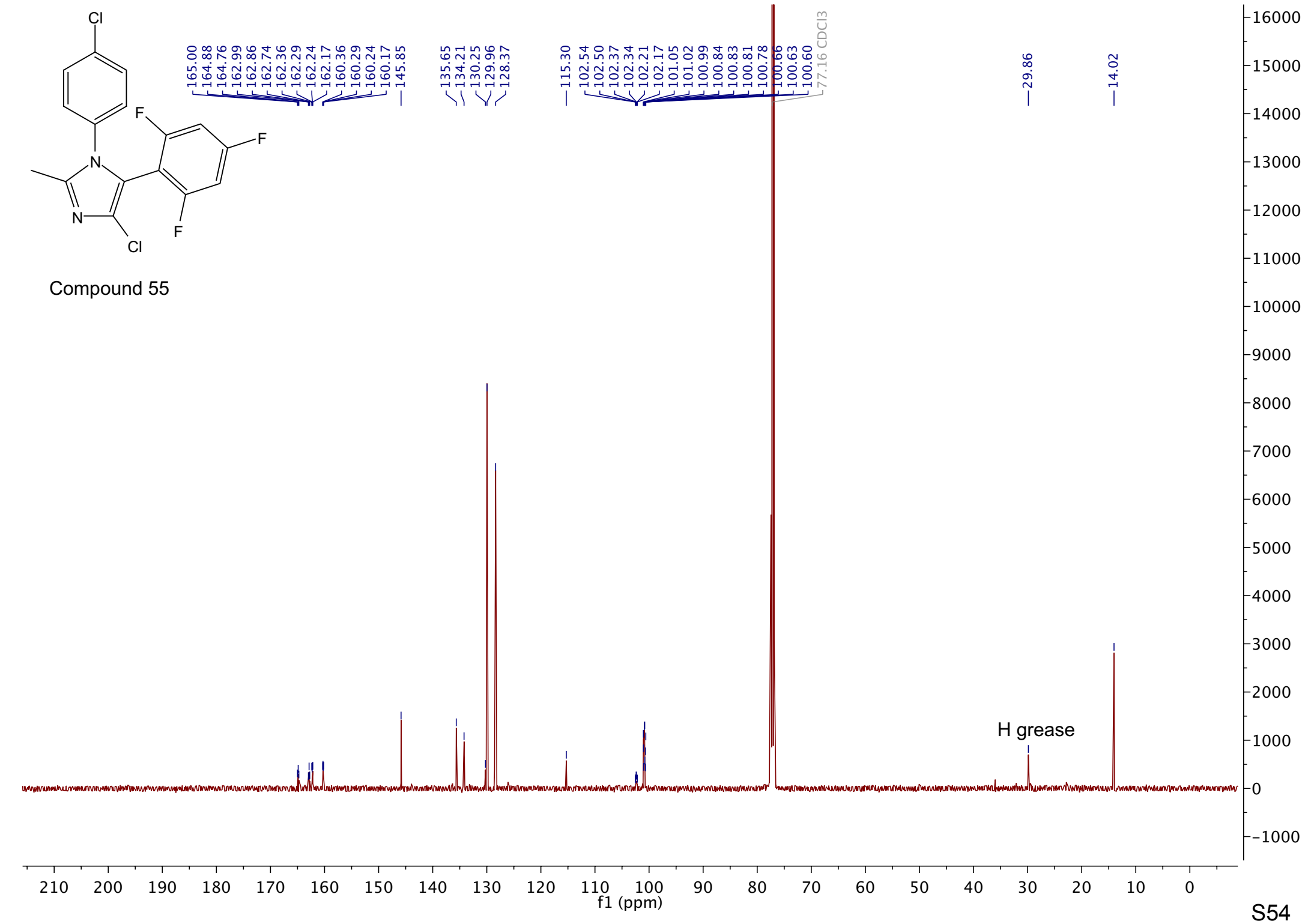
Compound 54

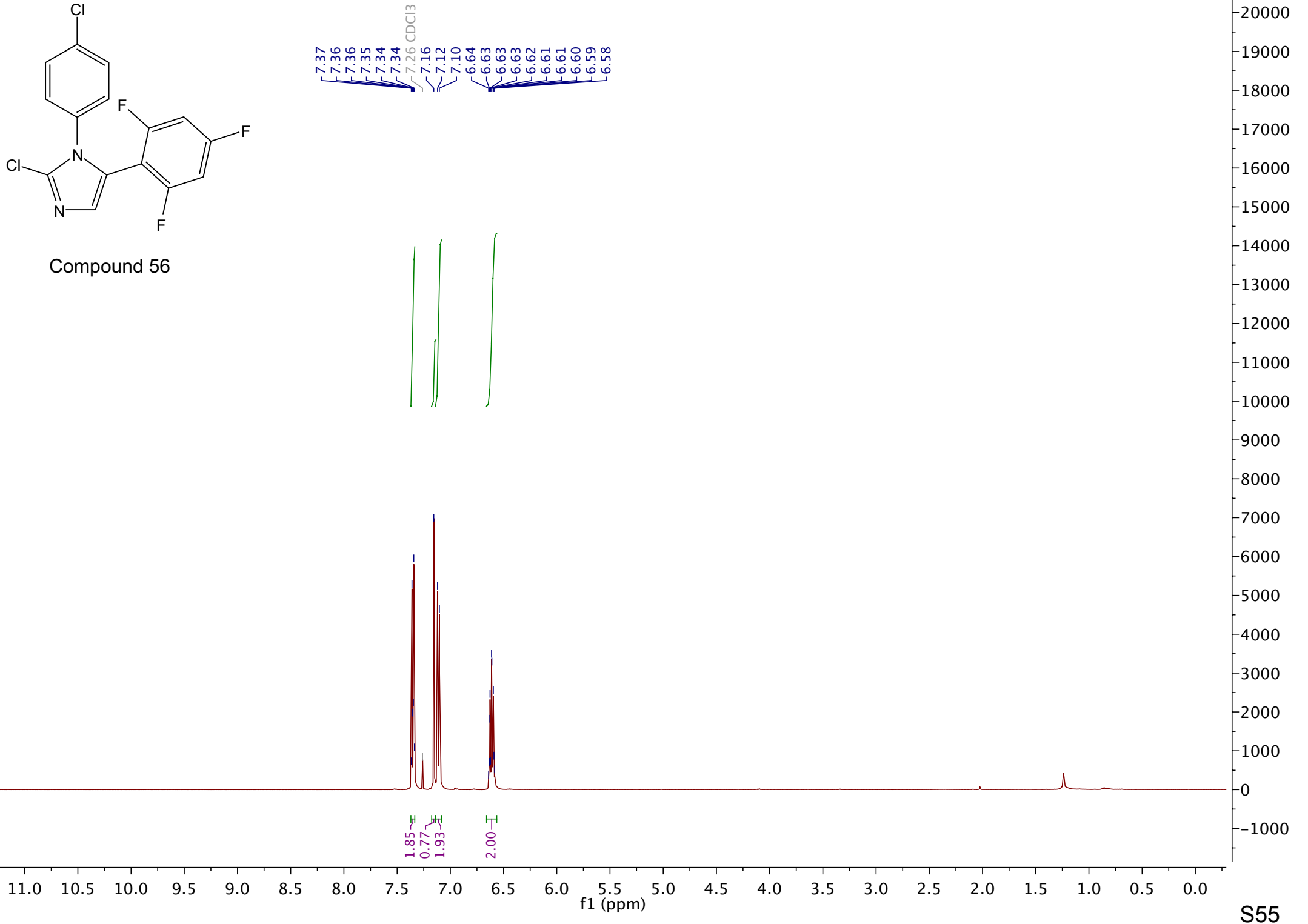


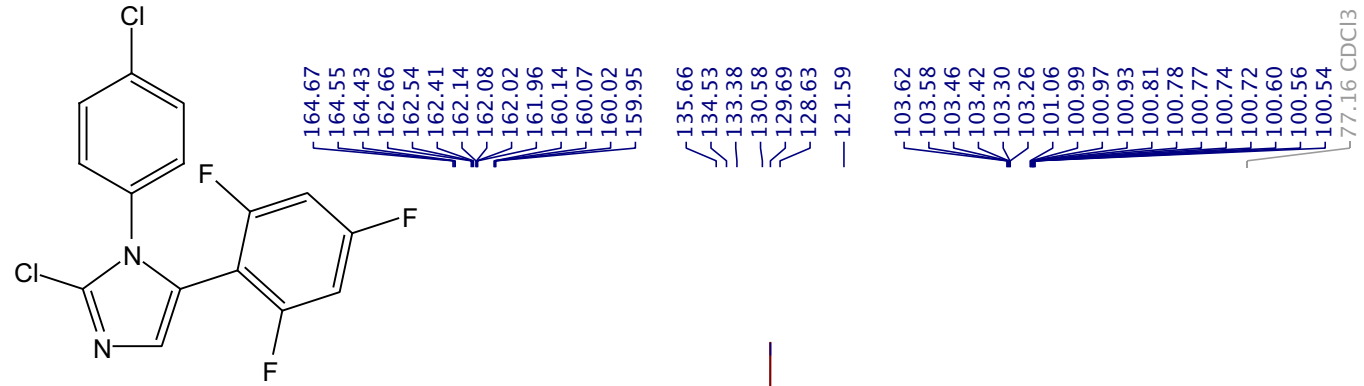




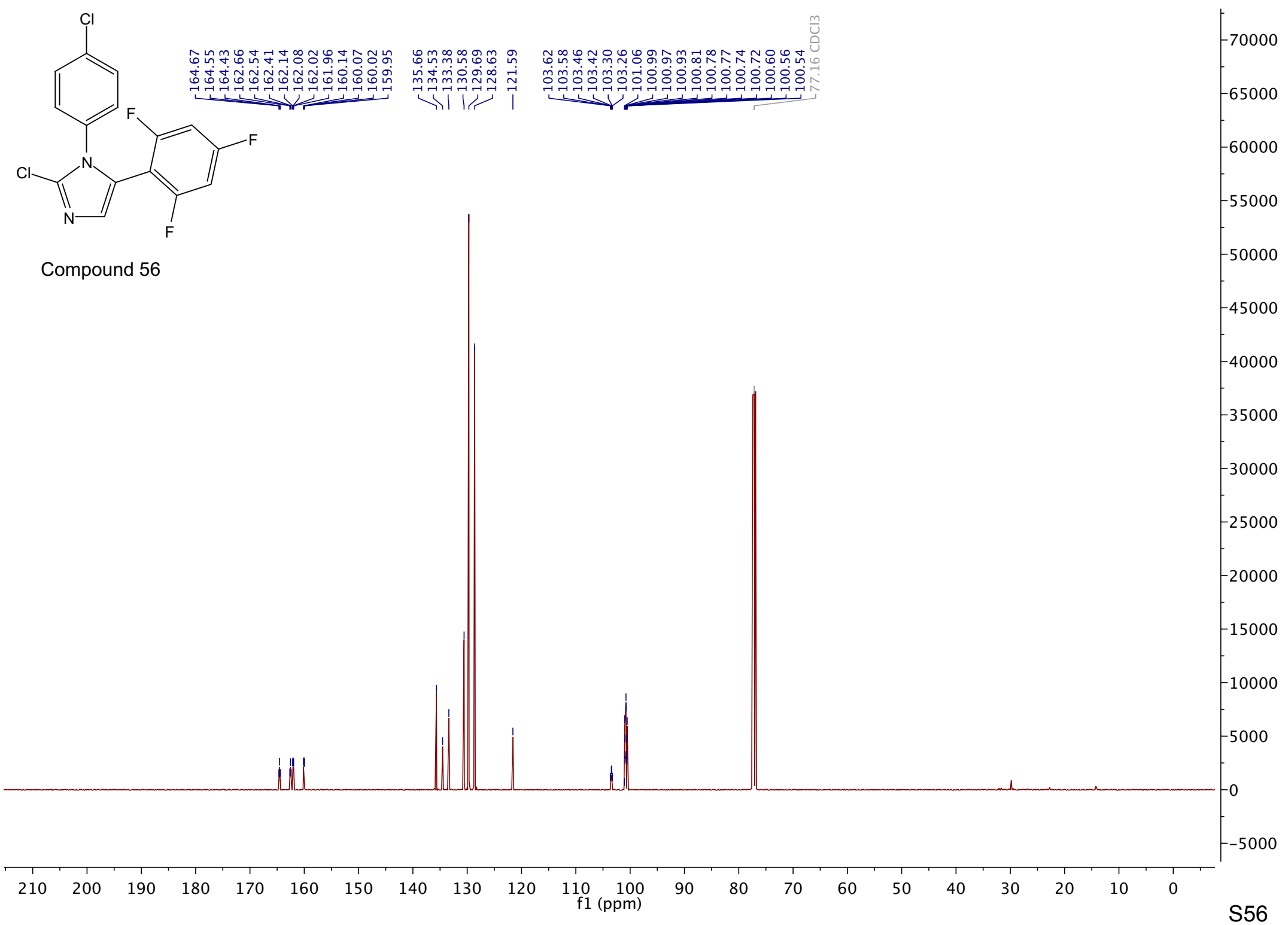
Compound 55

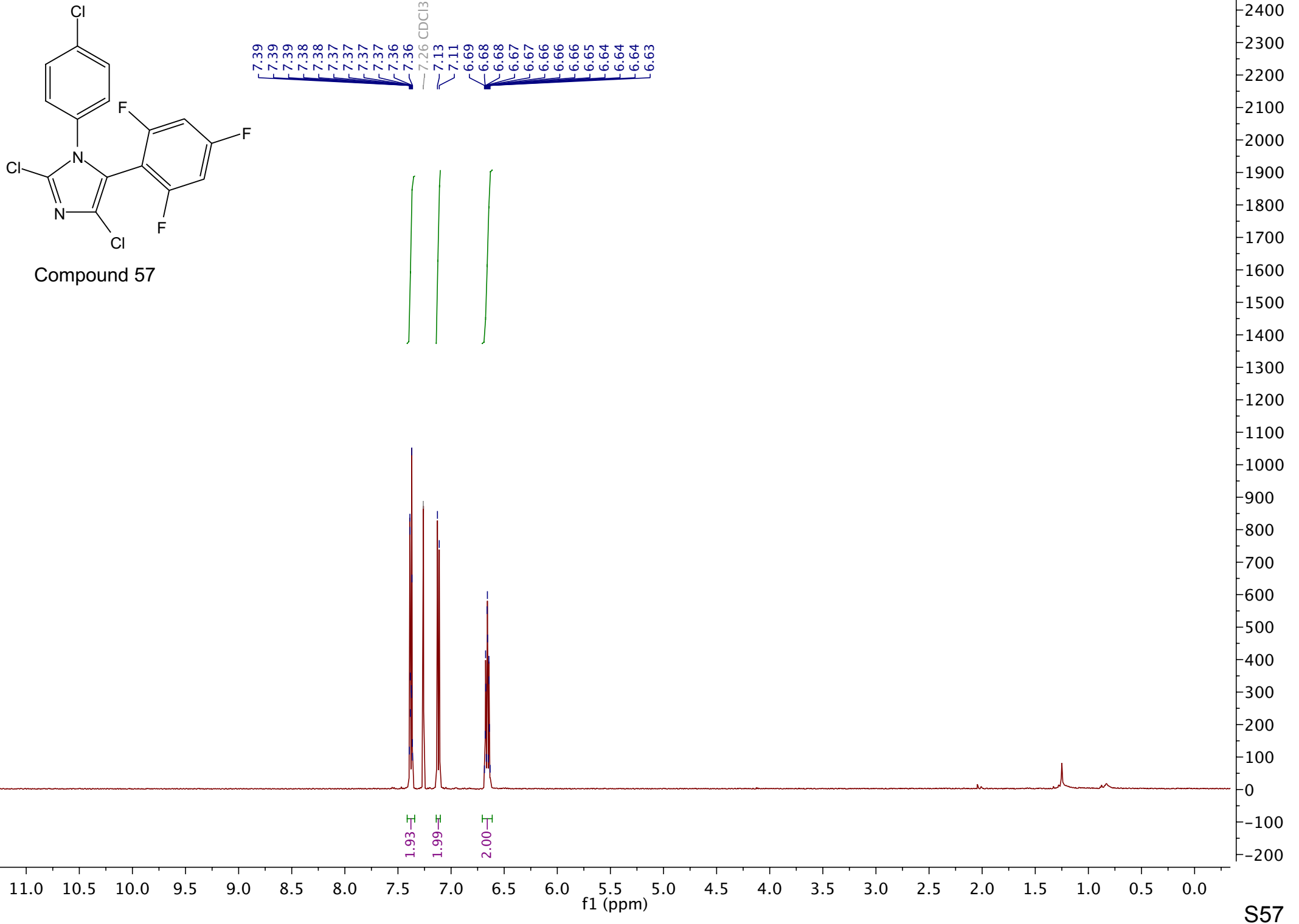


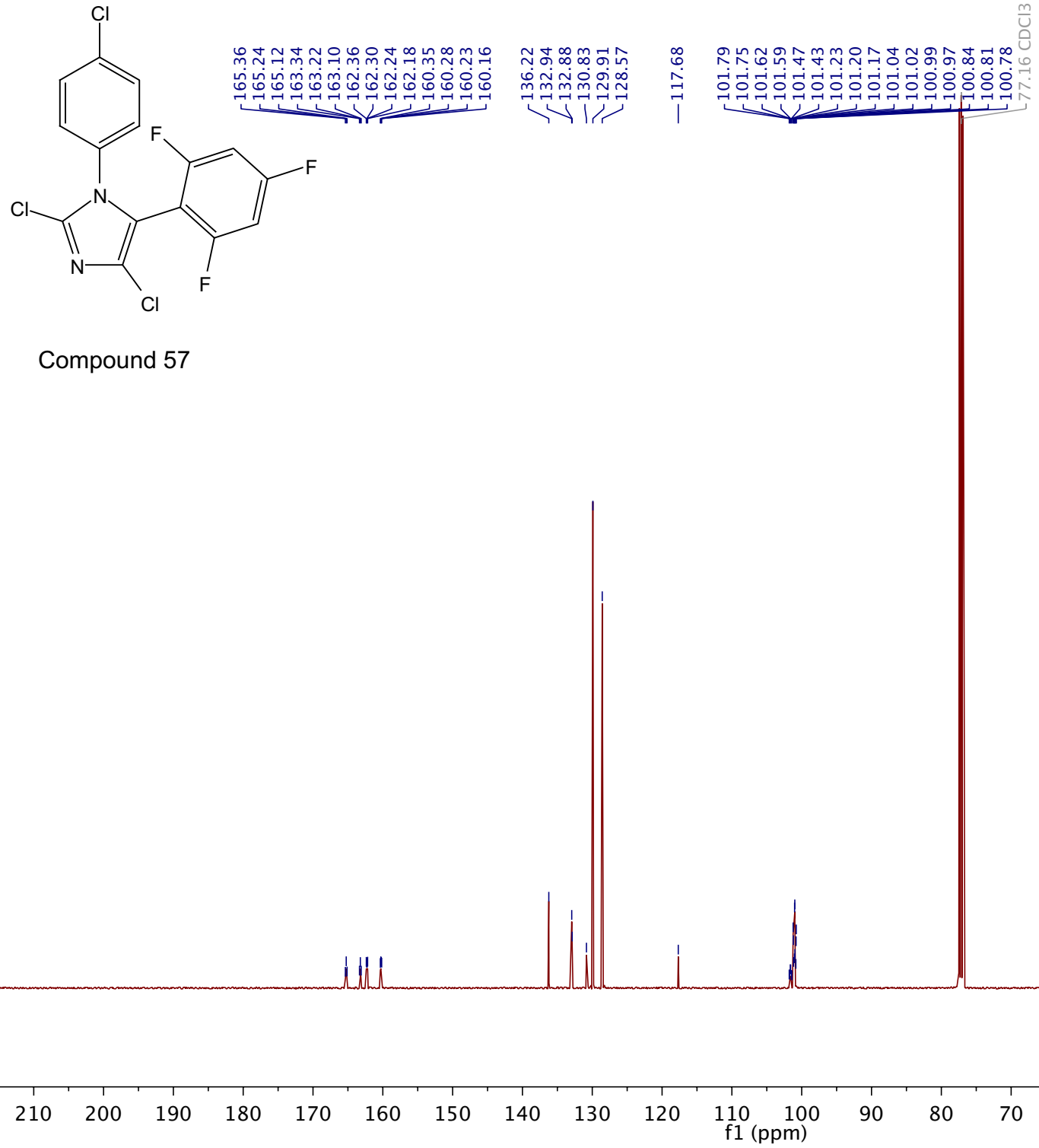


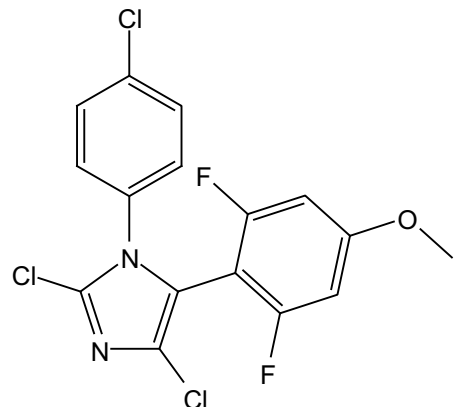


Compound 56

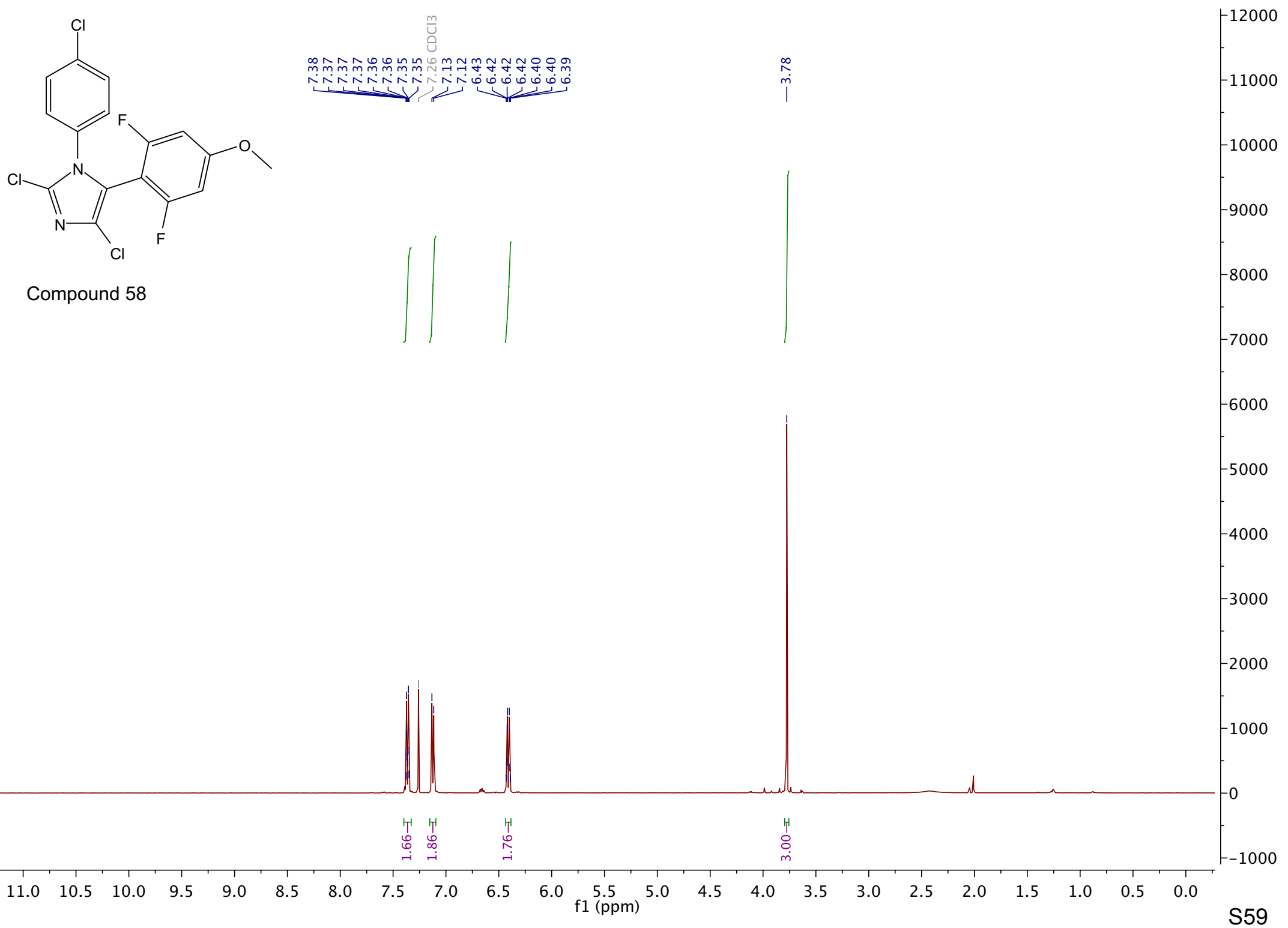




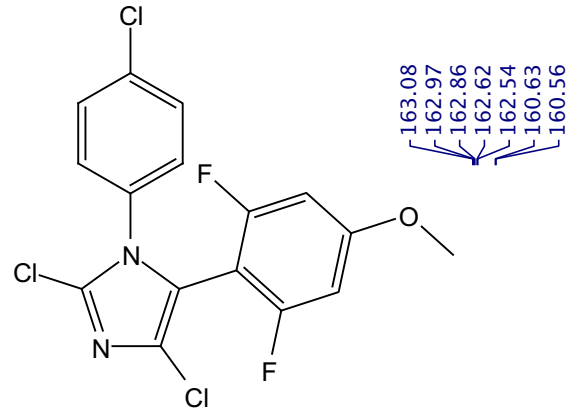




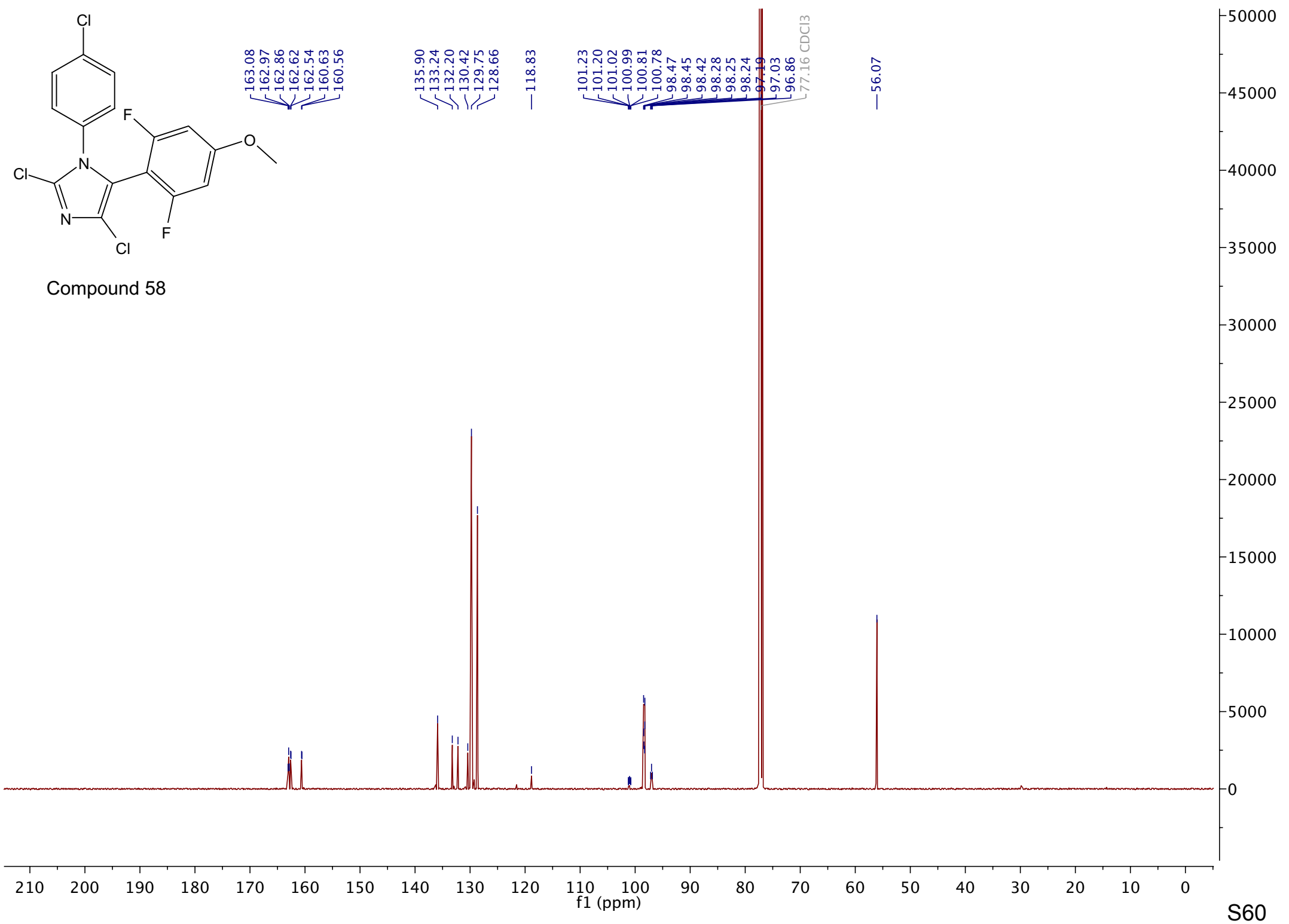
Compound 58

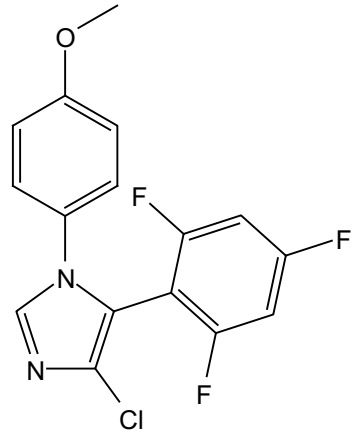


S59

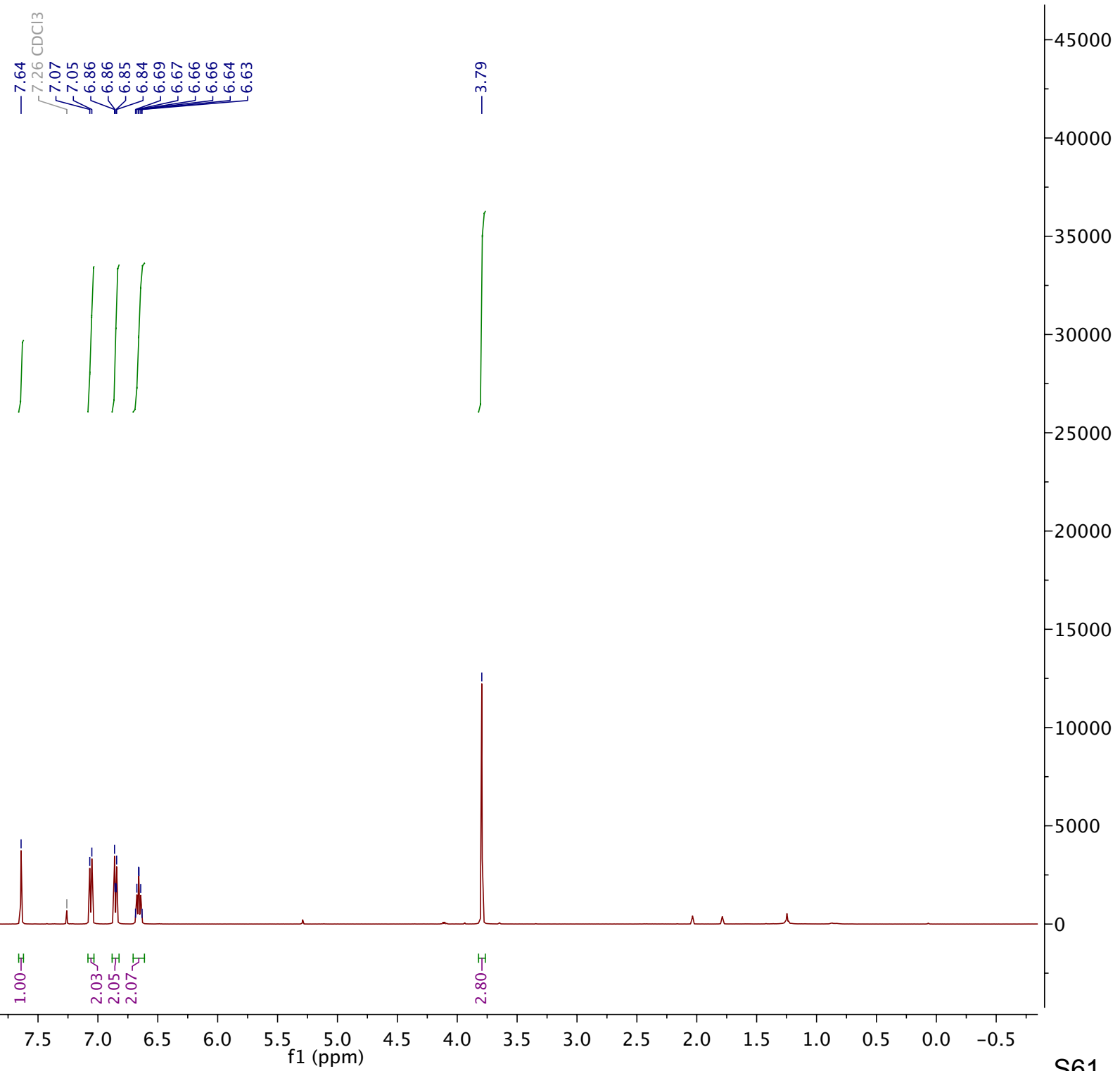


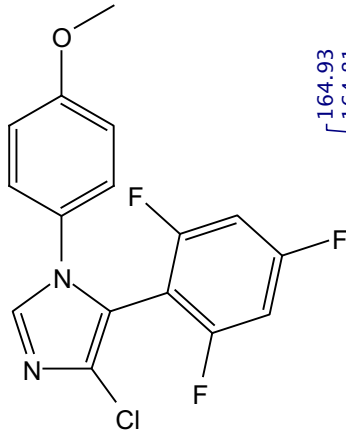
Compound 58



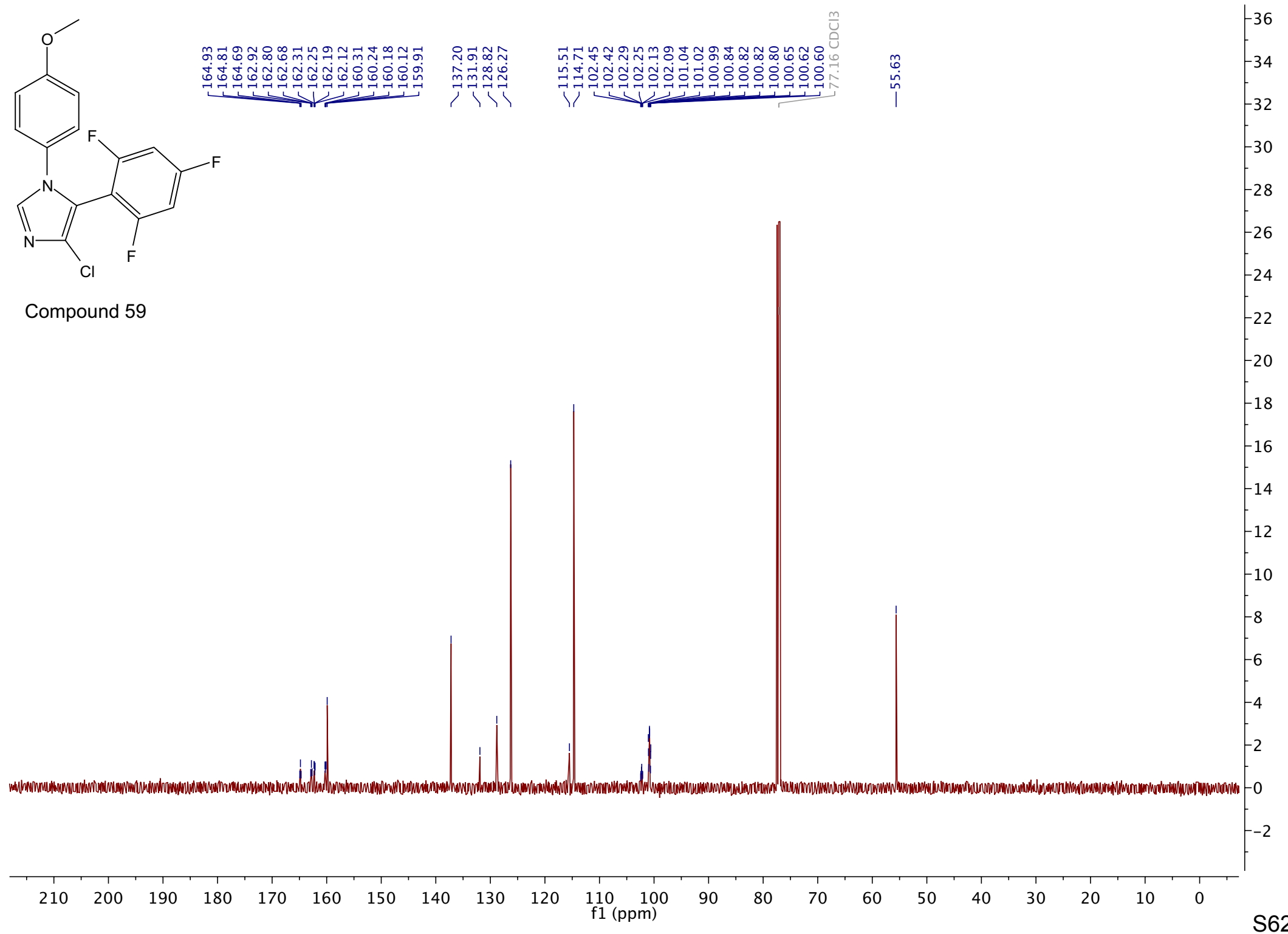


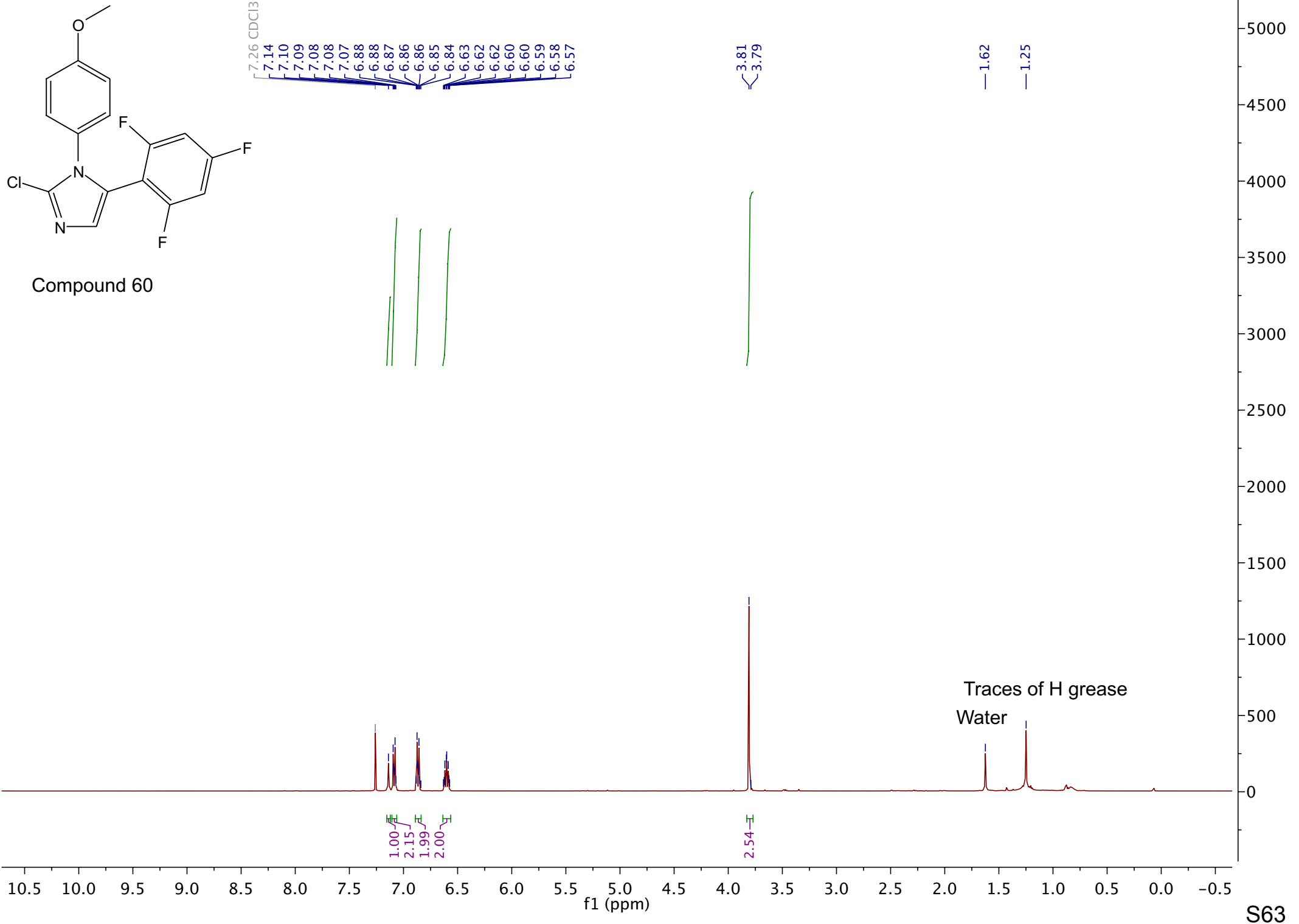
Compound 59

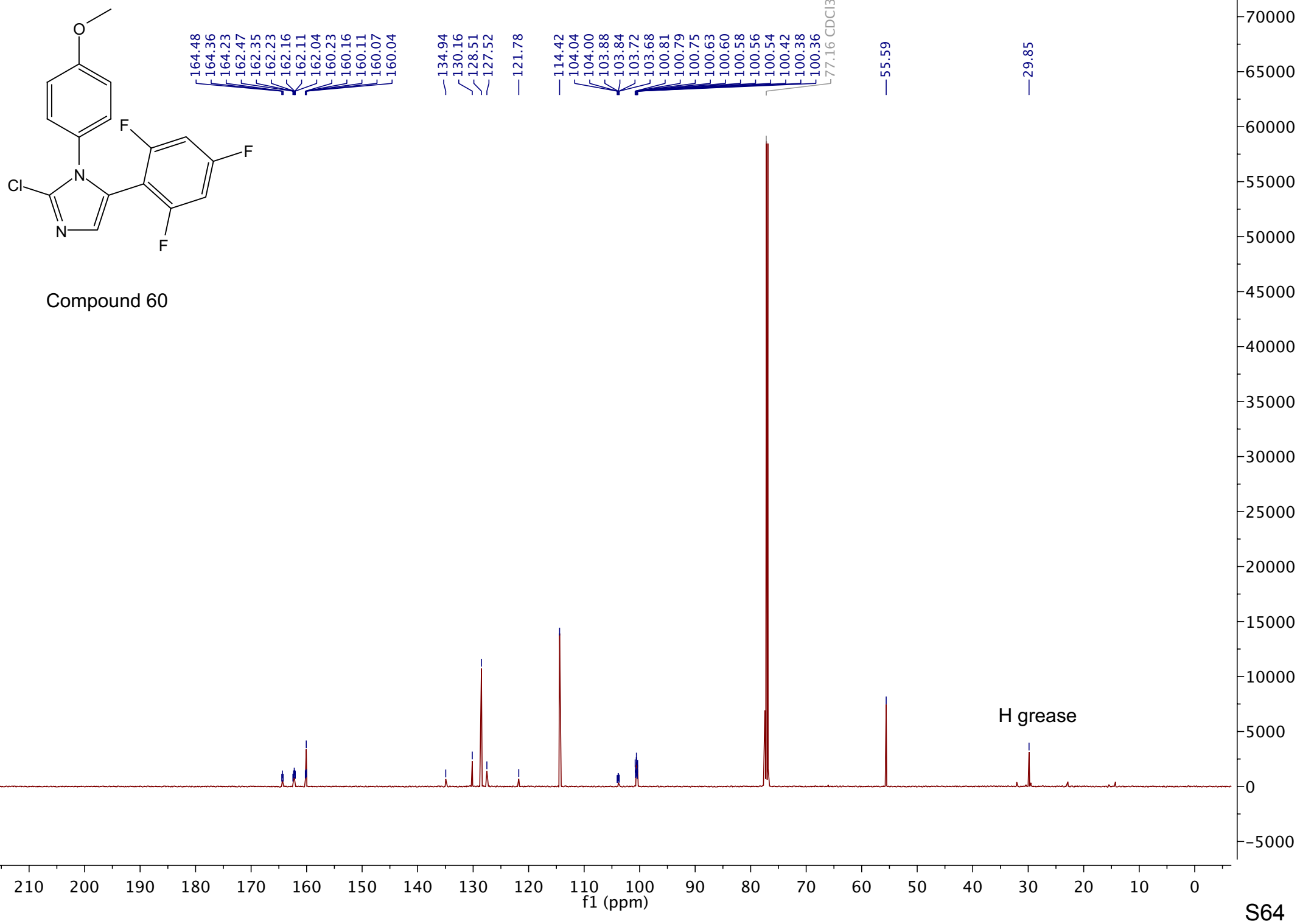


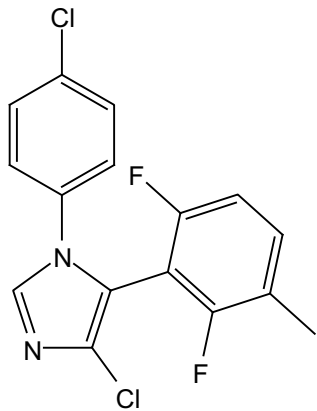


Compound 59

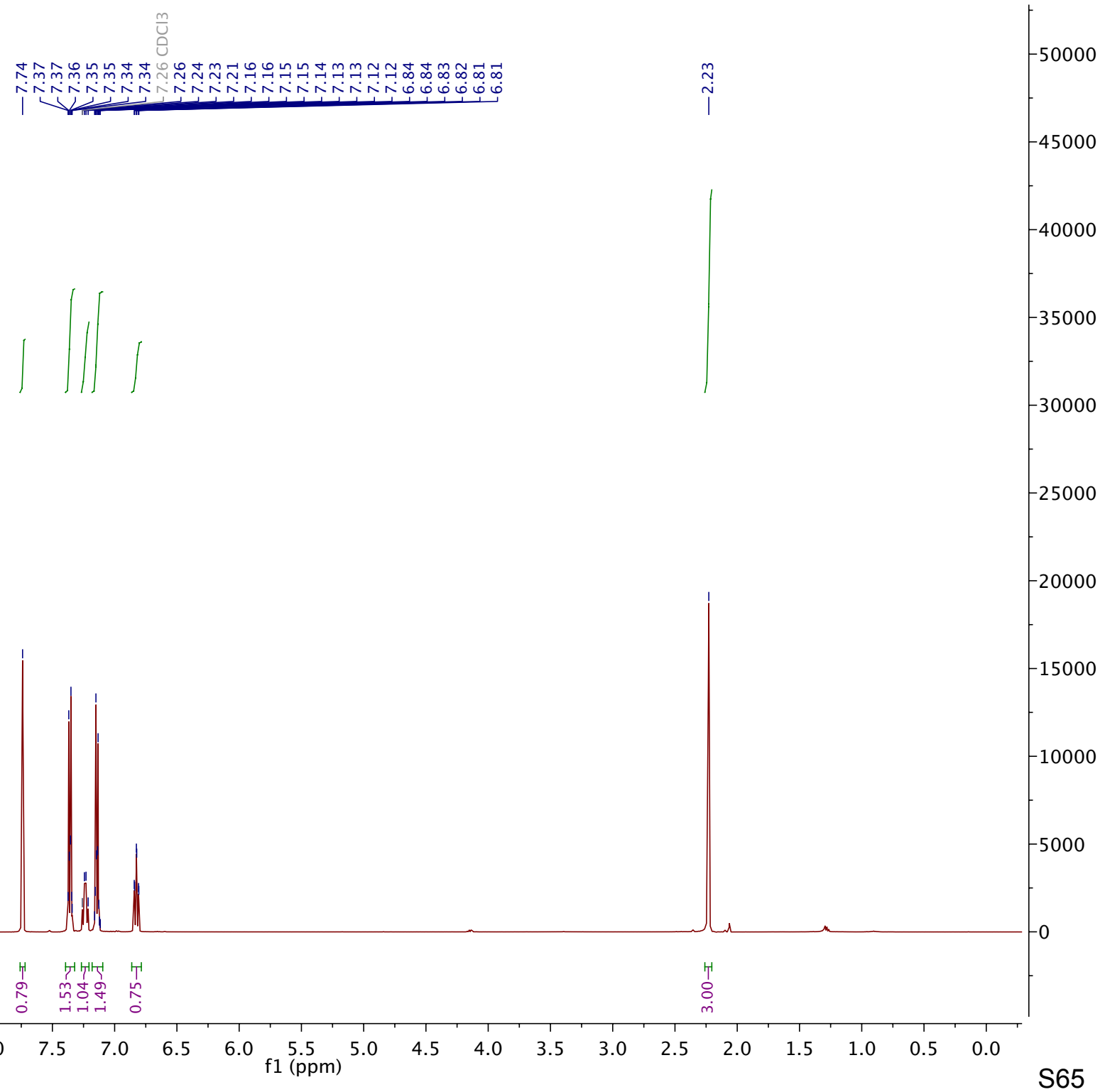


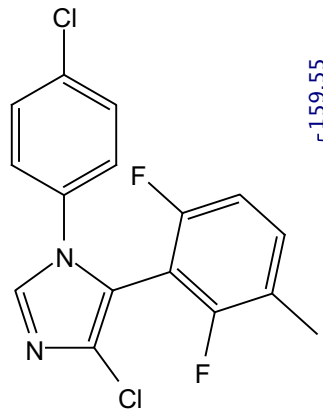




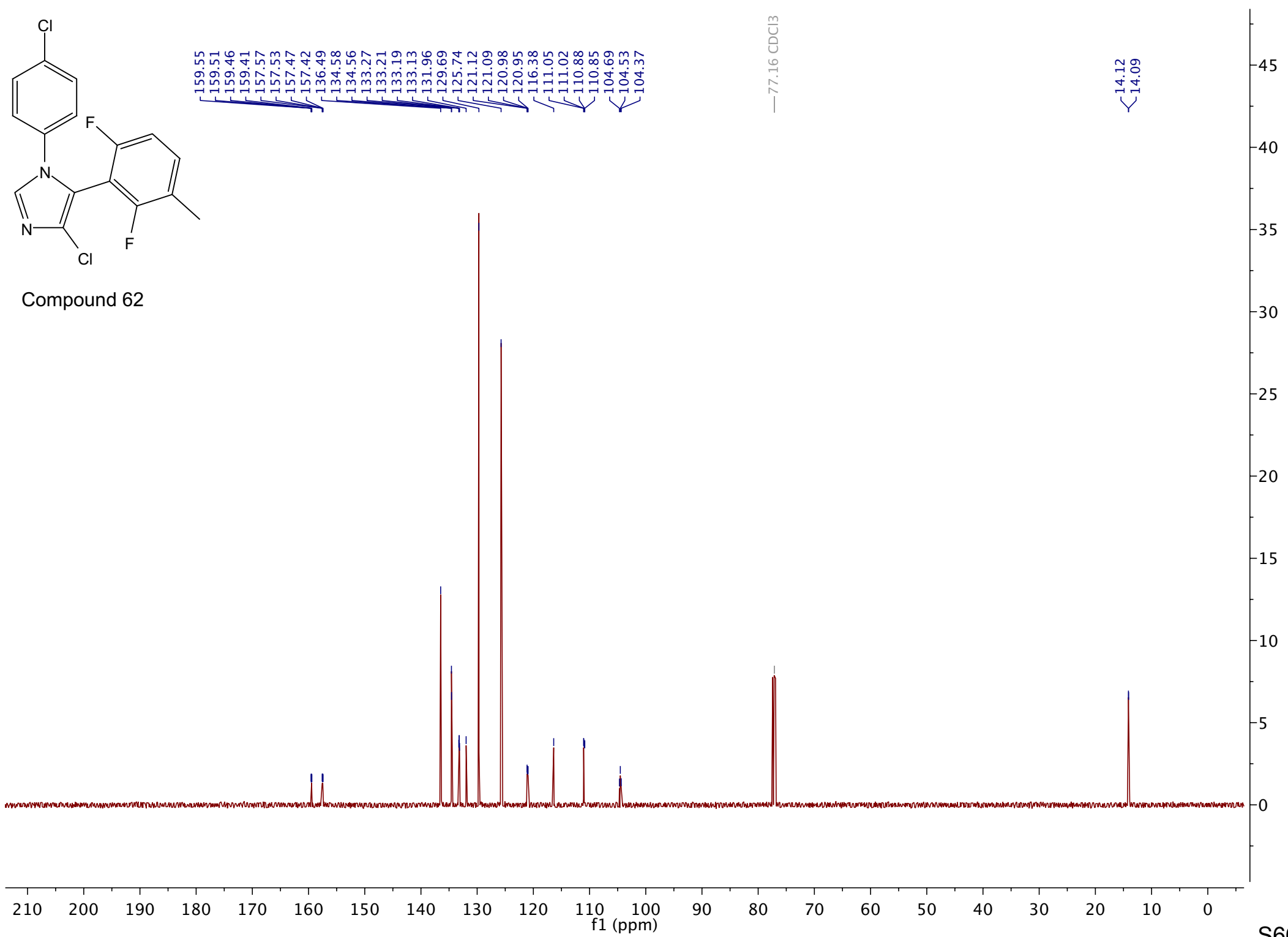


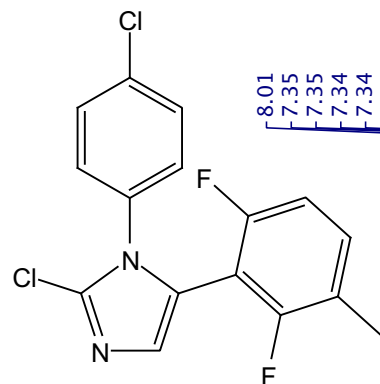
Compound 62



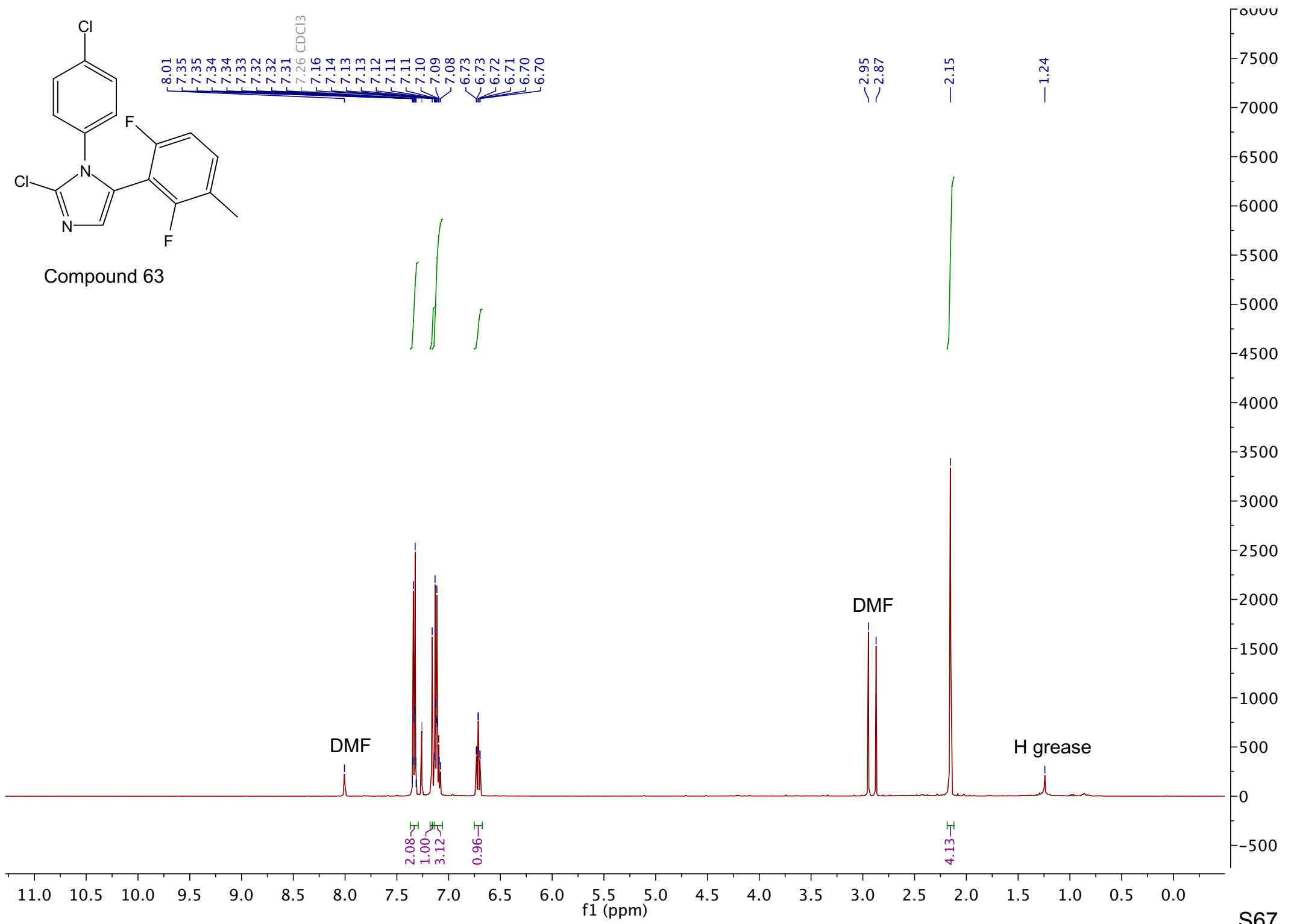


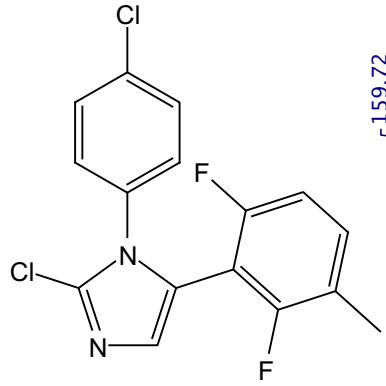
Compound 62



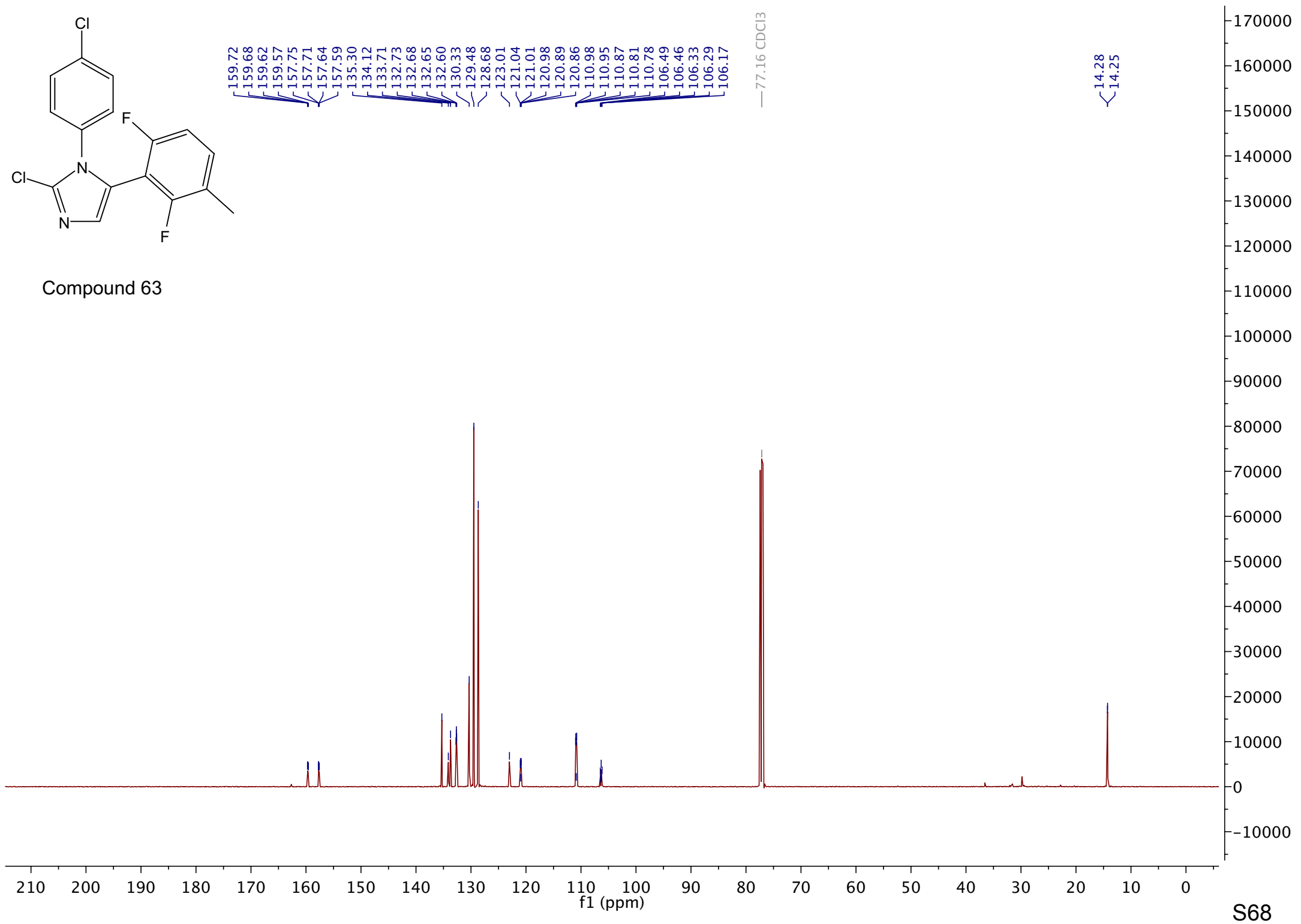


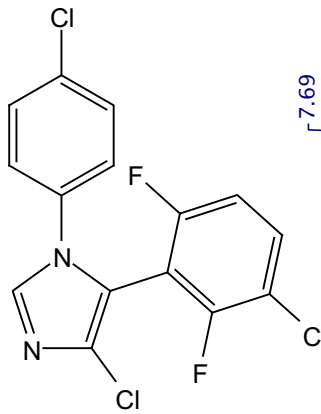
Compound 63



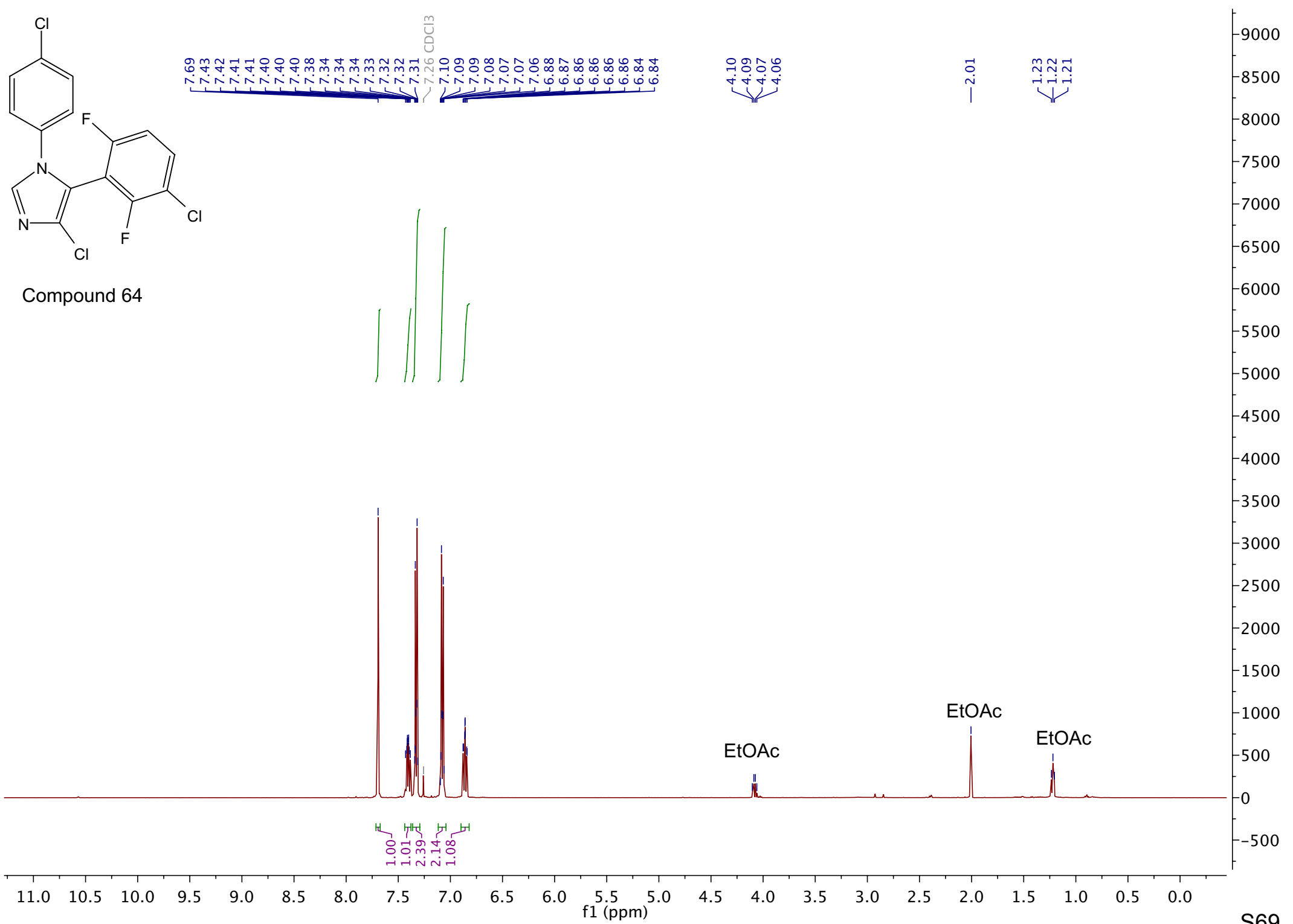


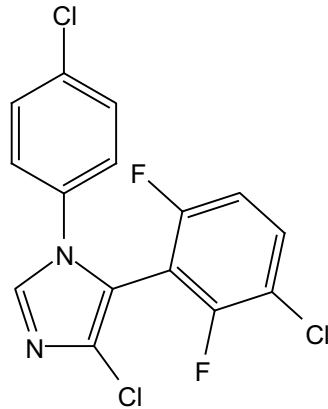
Compound 63



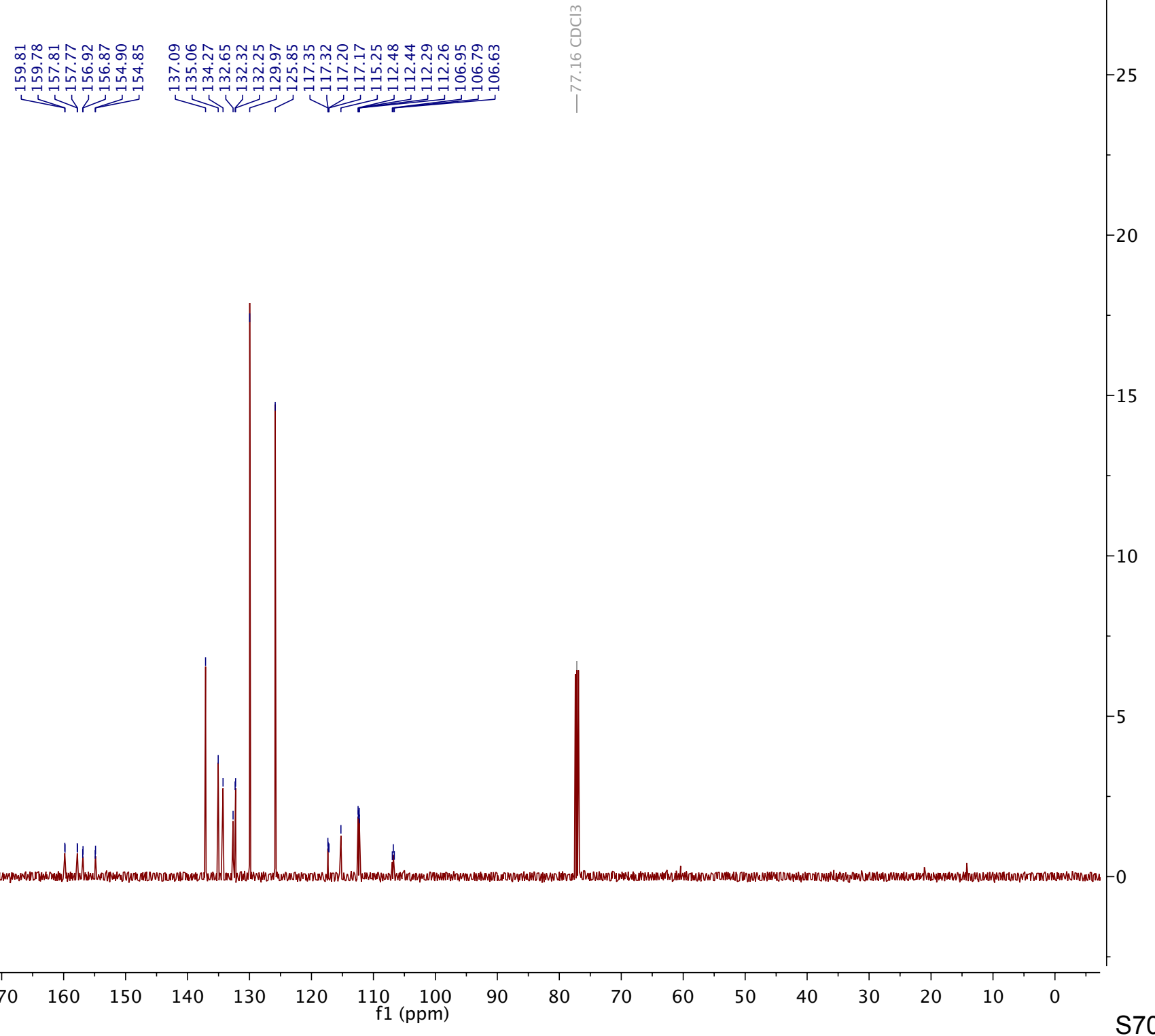


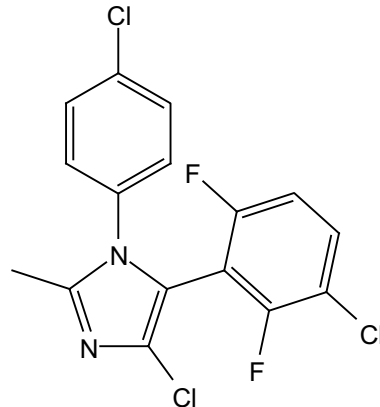
Compound 64



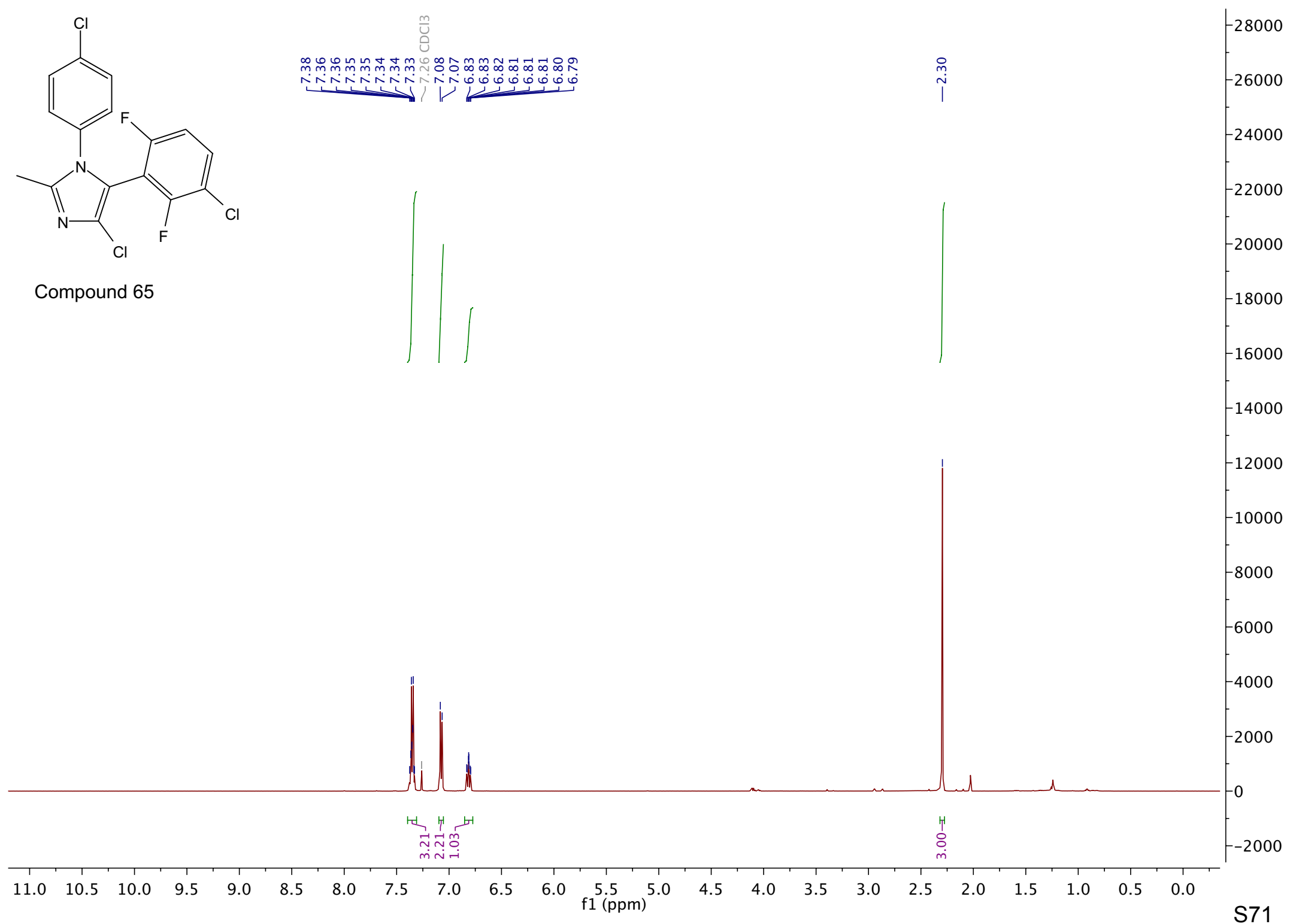


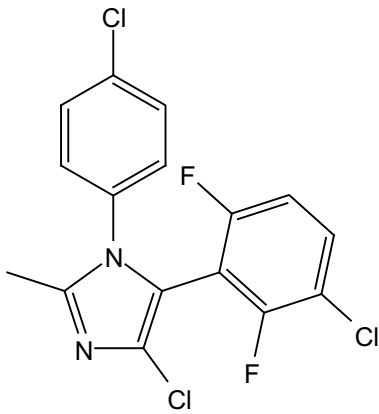
Compound 64



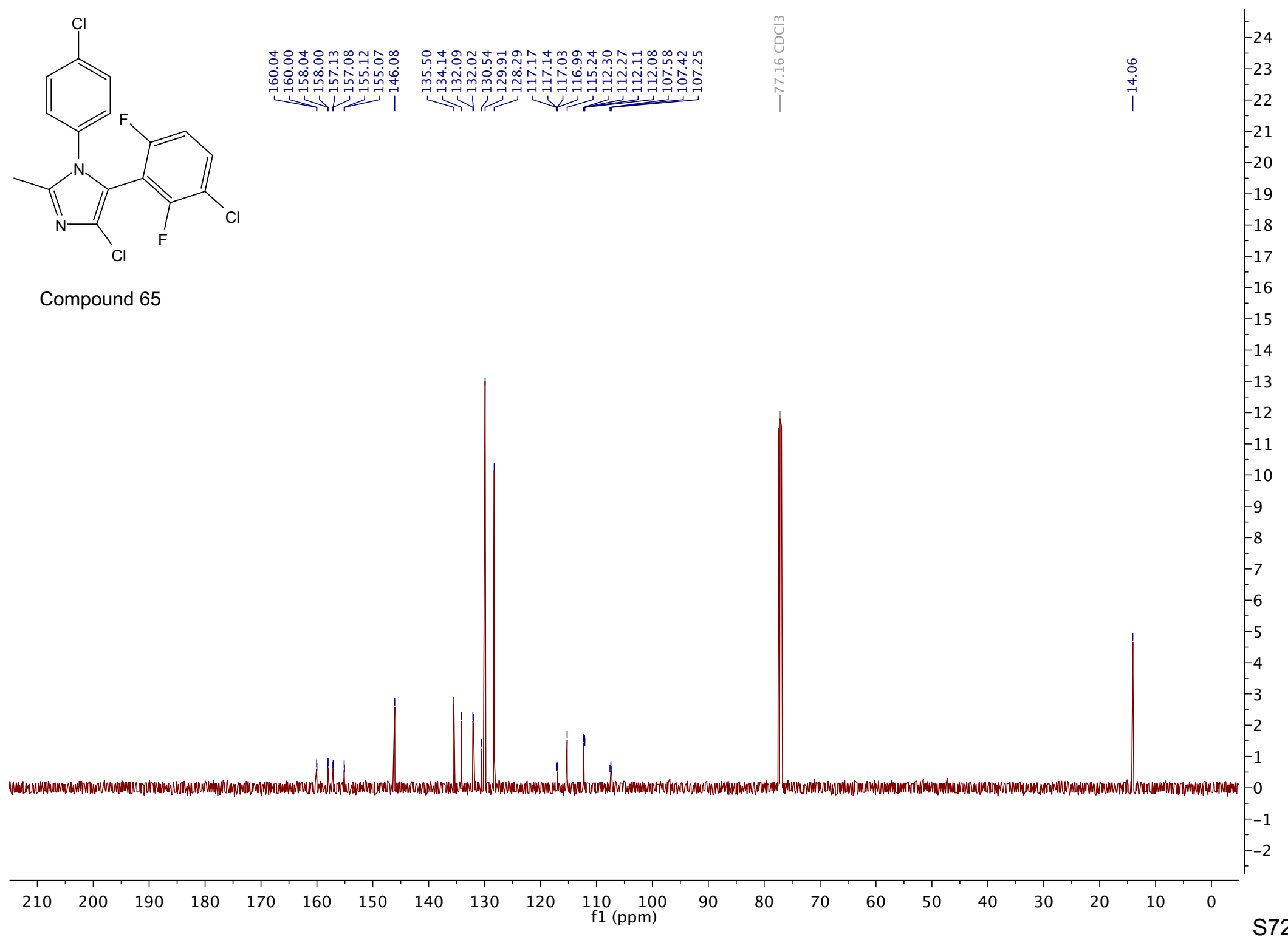


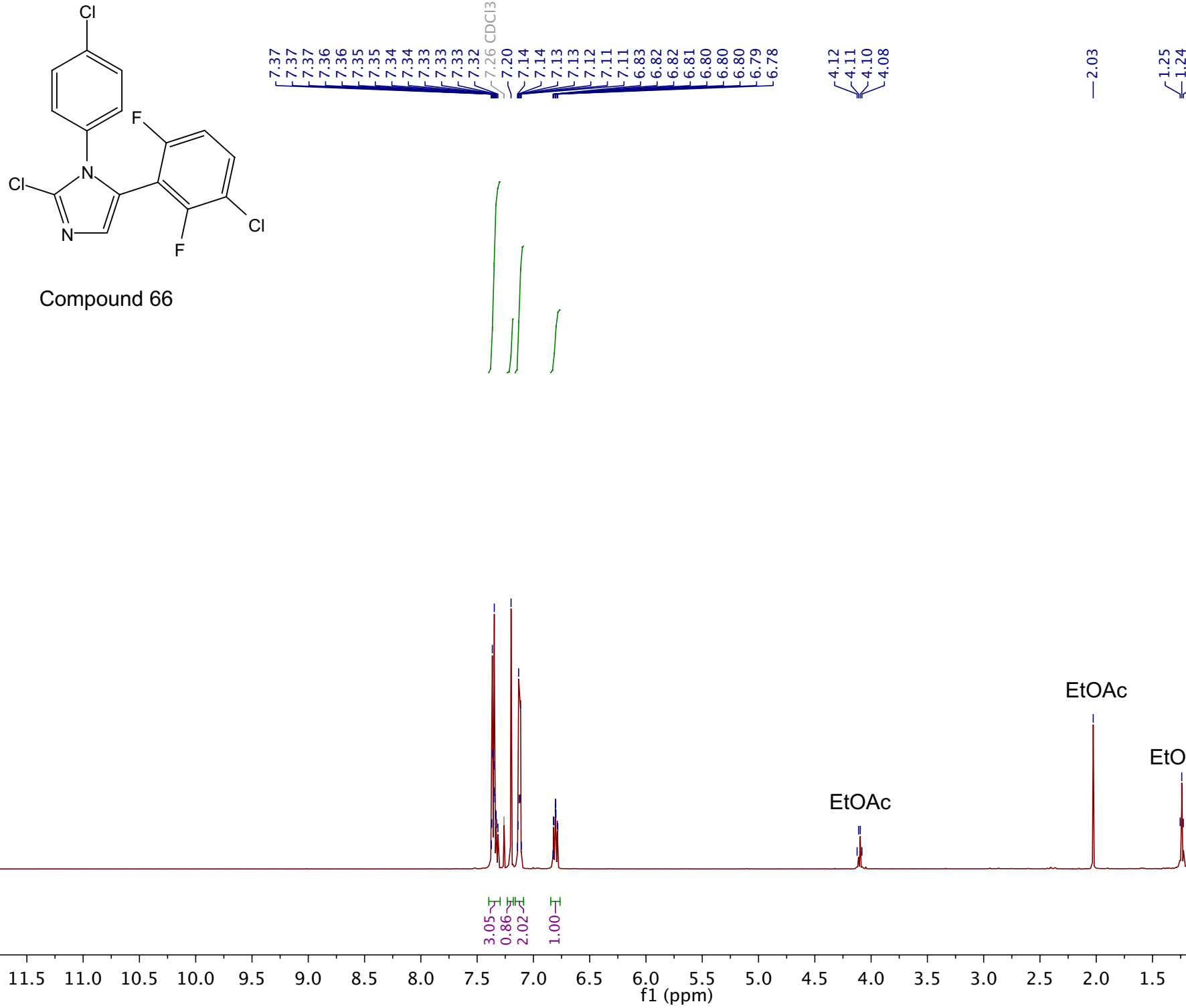
Compound 65

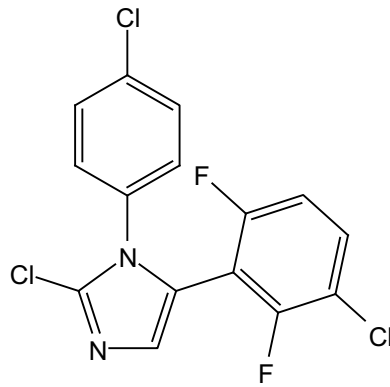




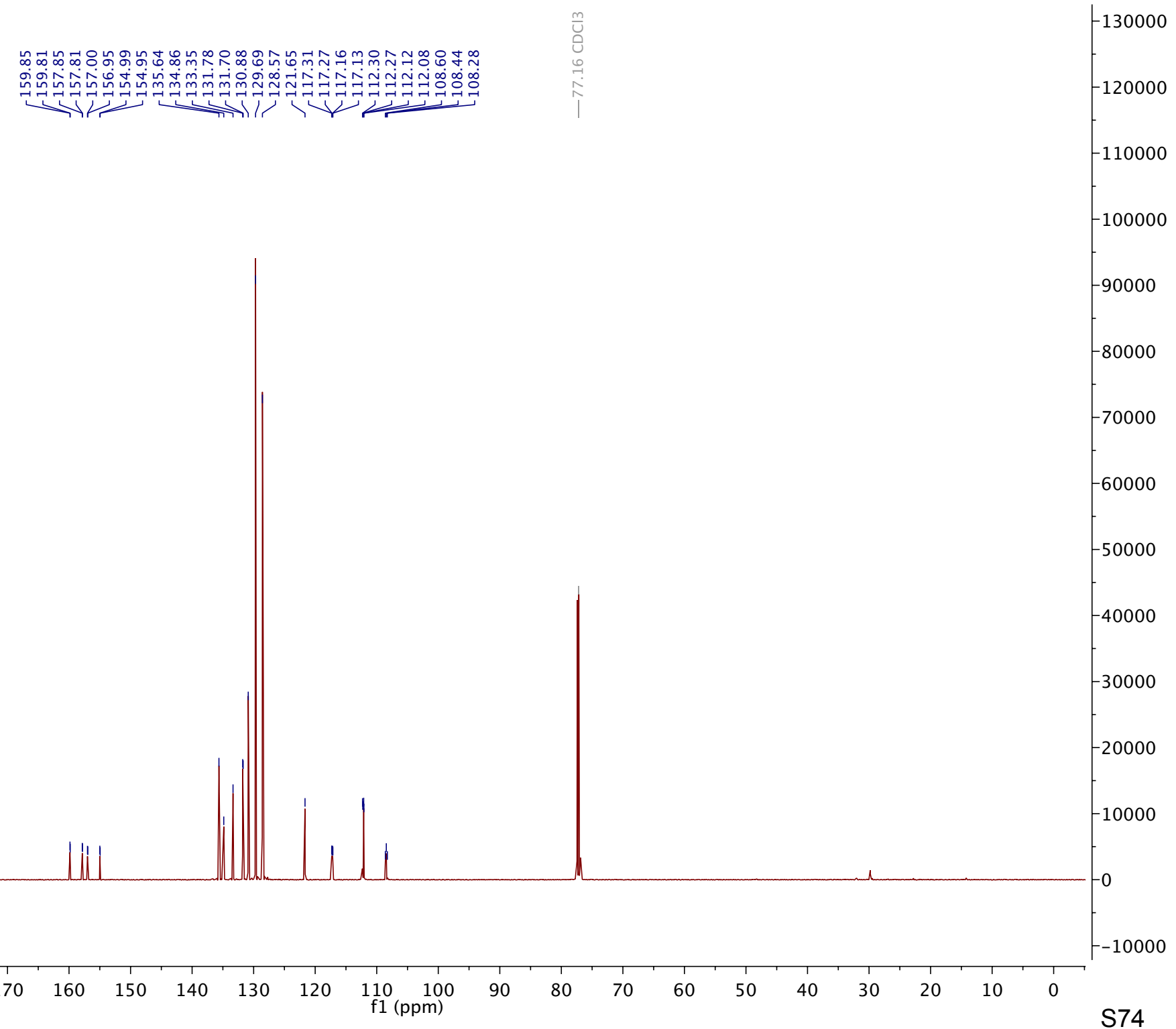
Compound 65

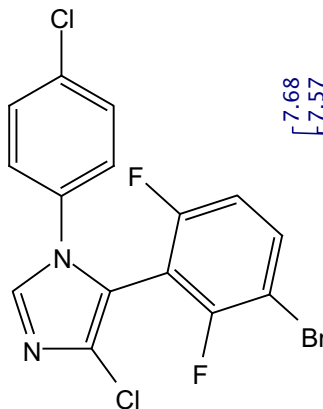




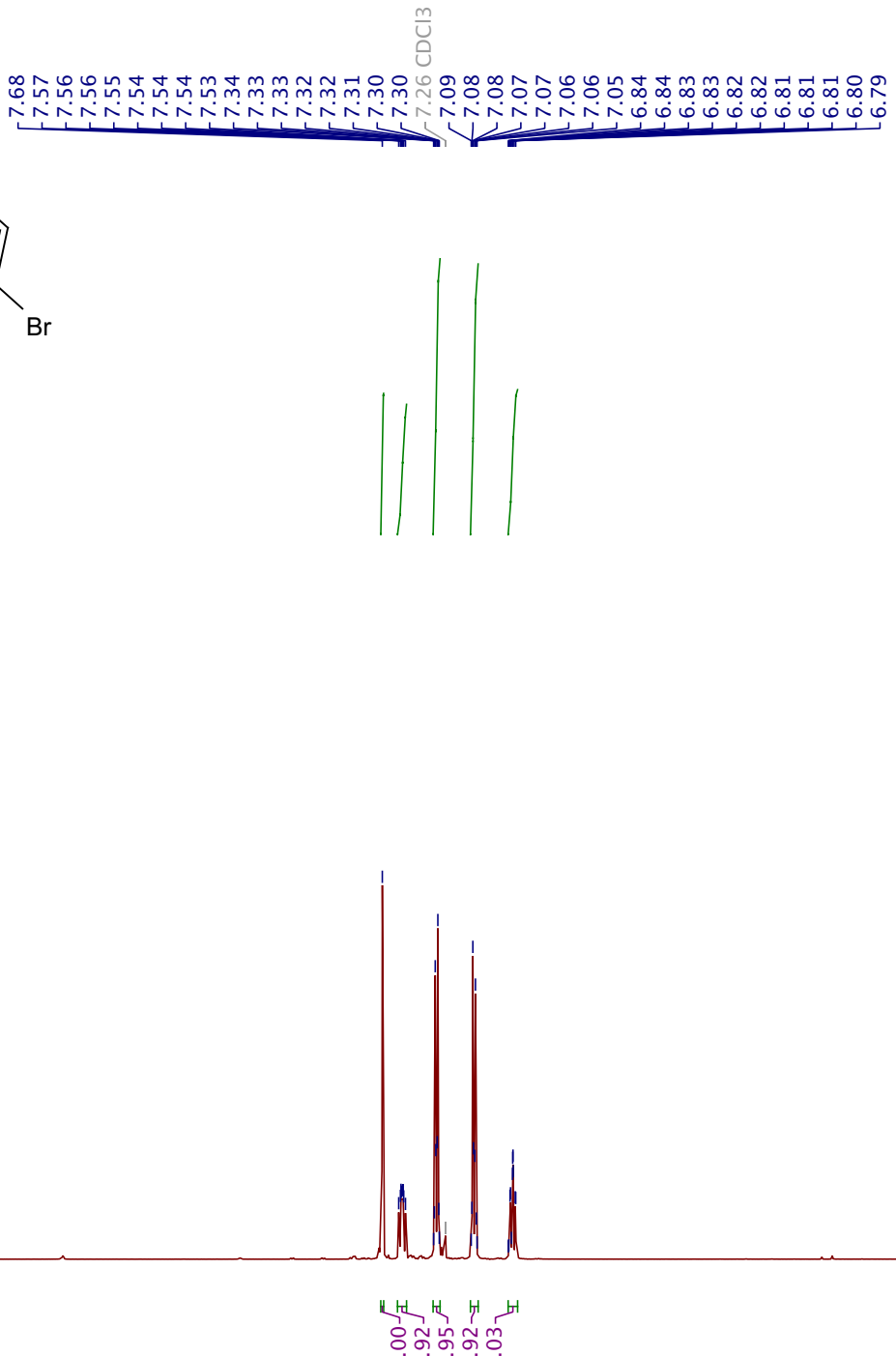


Compound 66





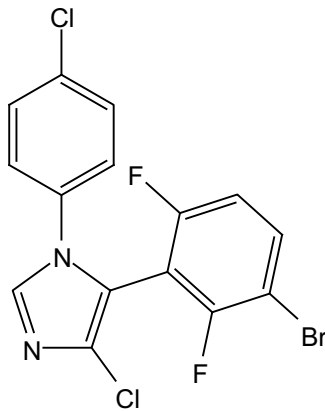
Compound 67



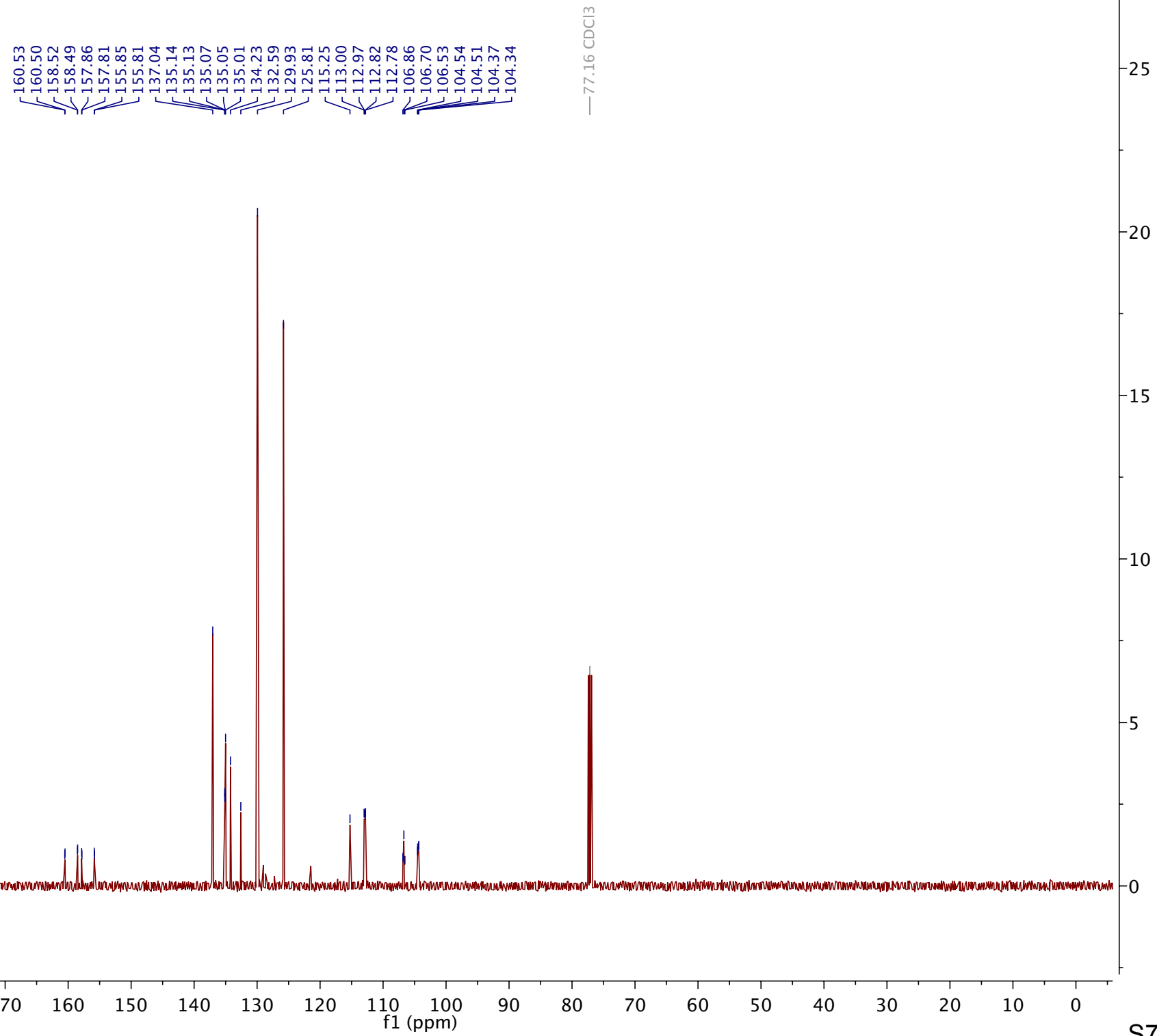
11.5 11.0 10.5 10.0 9.5 9.0 8.5 8.0 7.5 7.0 6.5 6.0 5.5 5.0 4.5 4.0 3.5 3.0 2.5 2.0 1.5 1.0 0.5 0.0 -0.5 -1.0

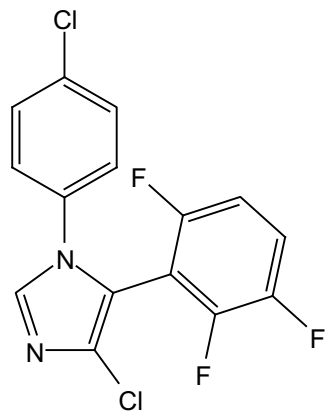
f1 (ppm)

S75

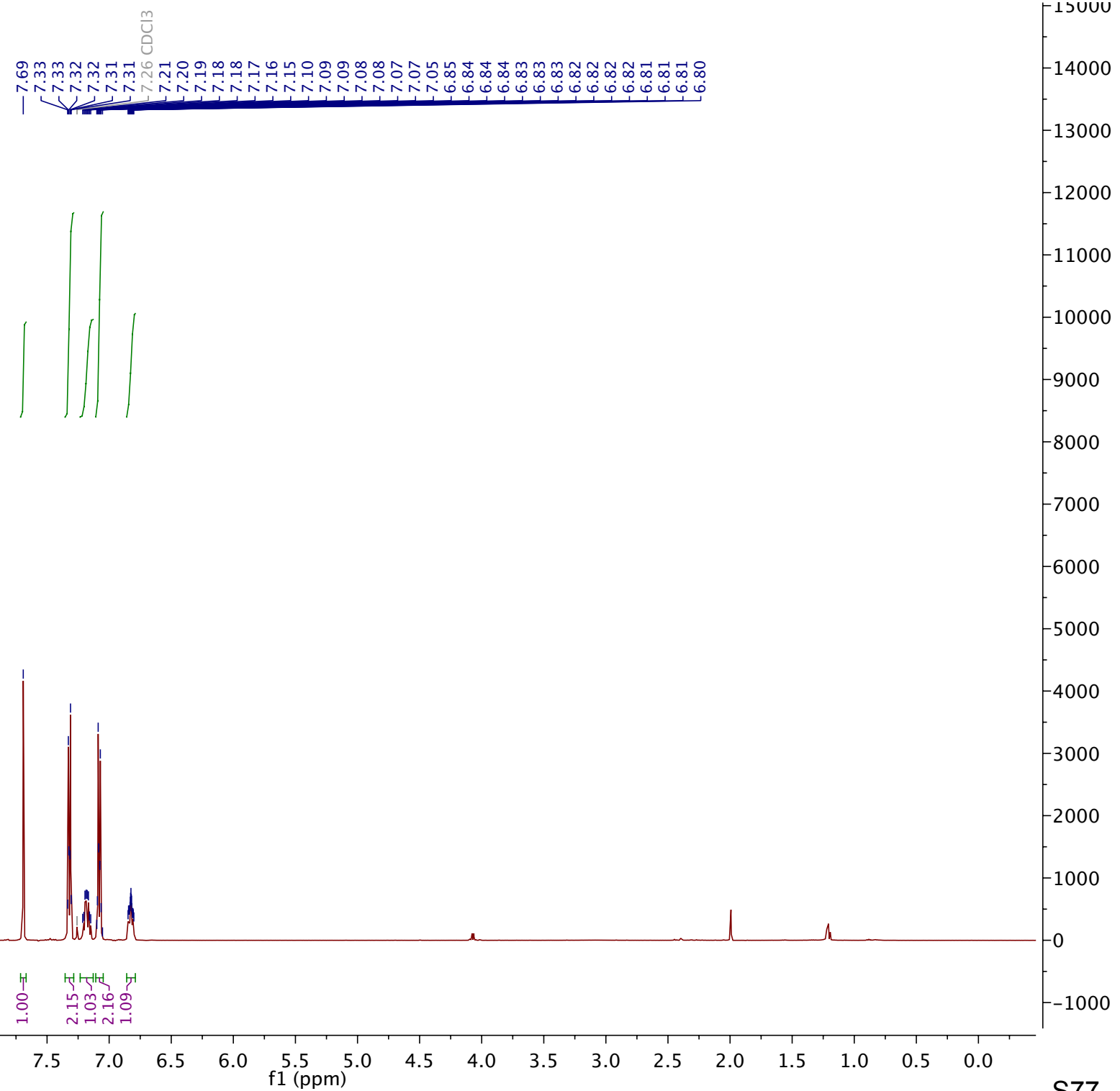


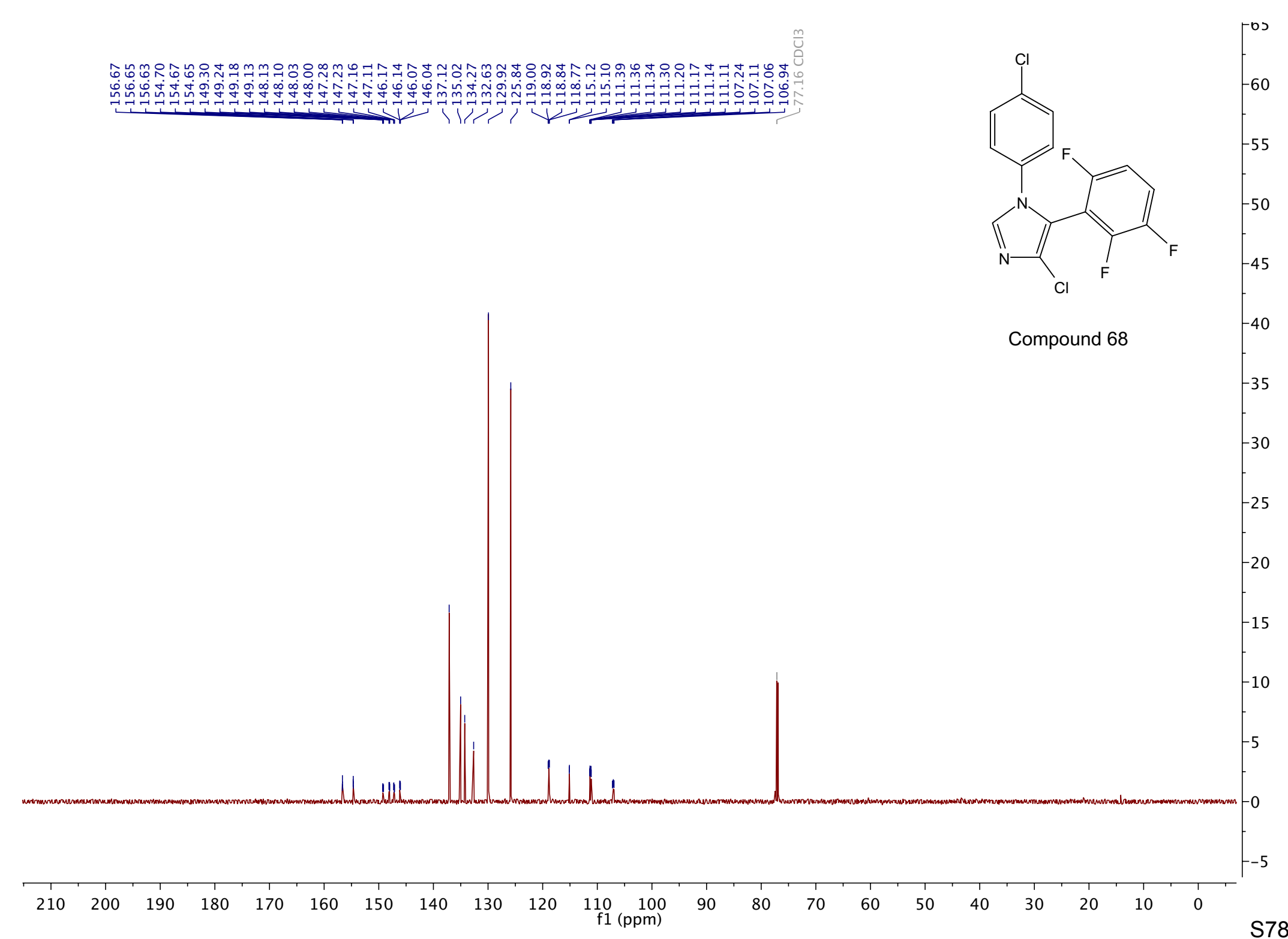
Compound 67

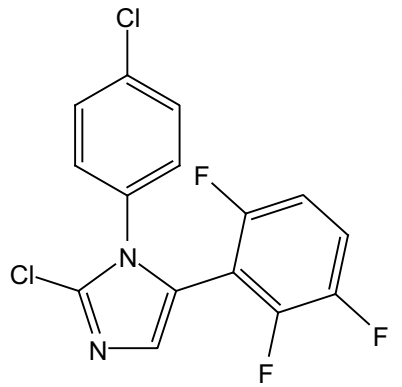




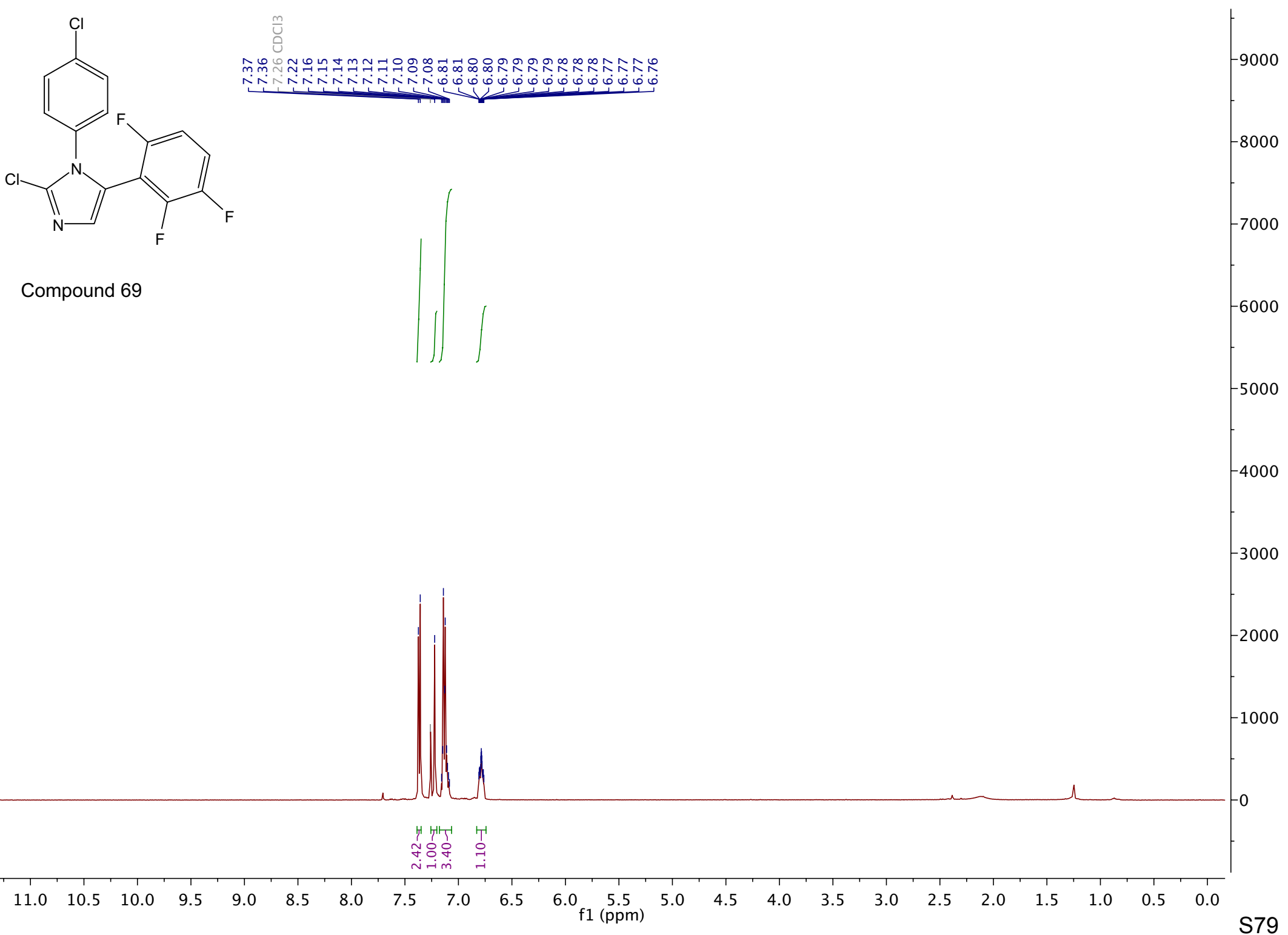
Compound 68

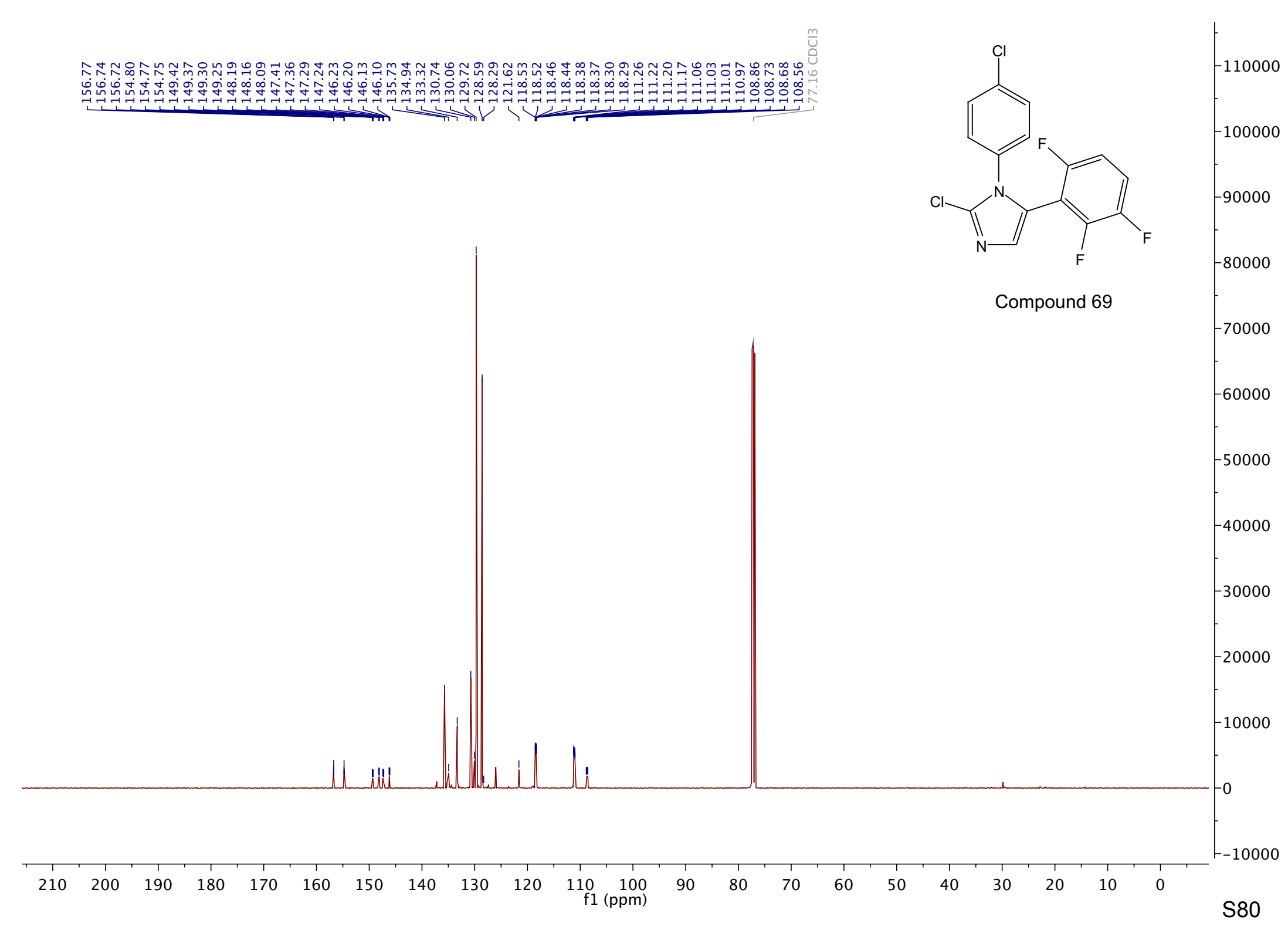


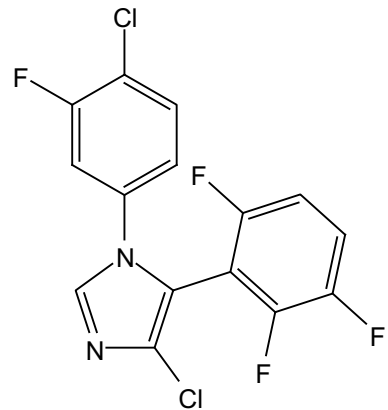




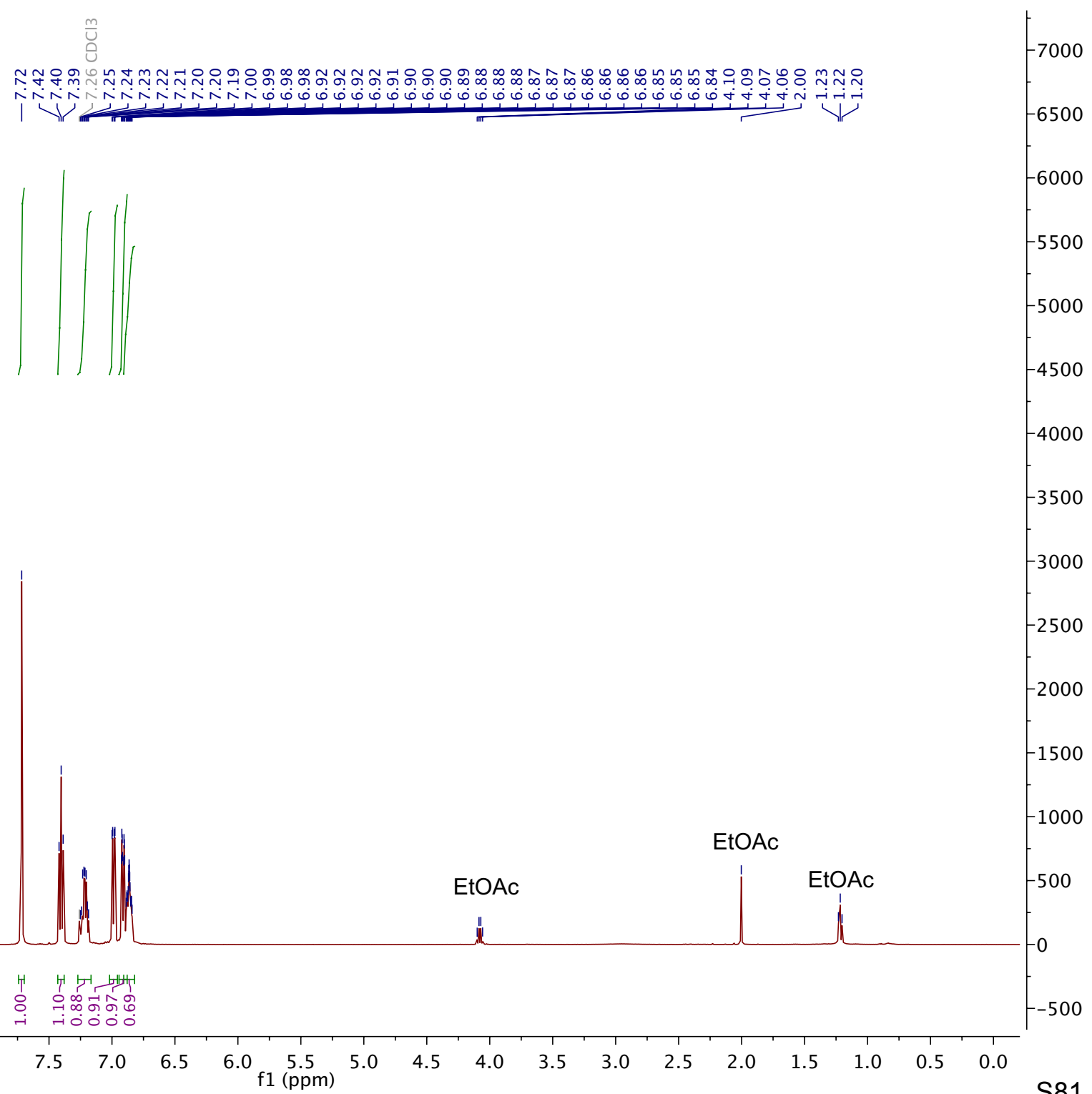
Compound 69



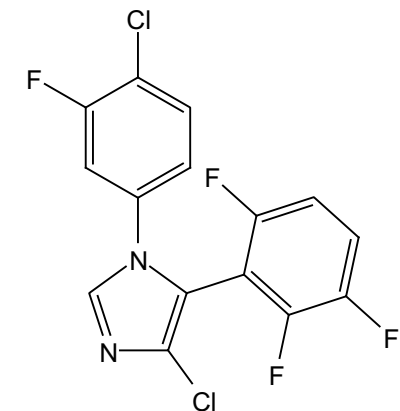




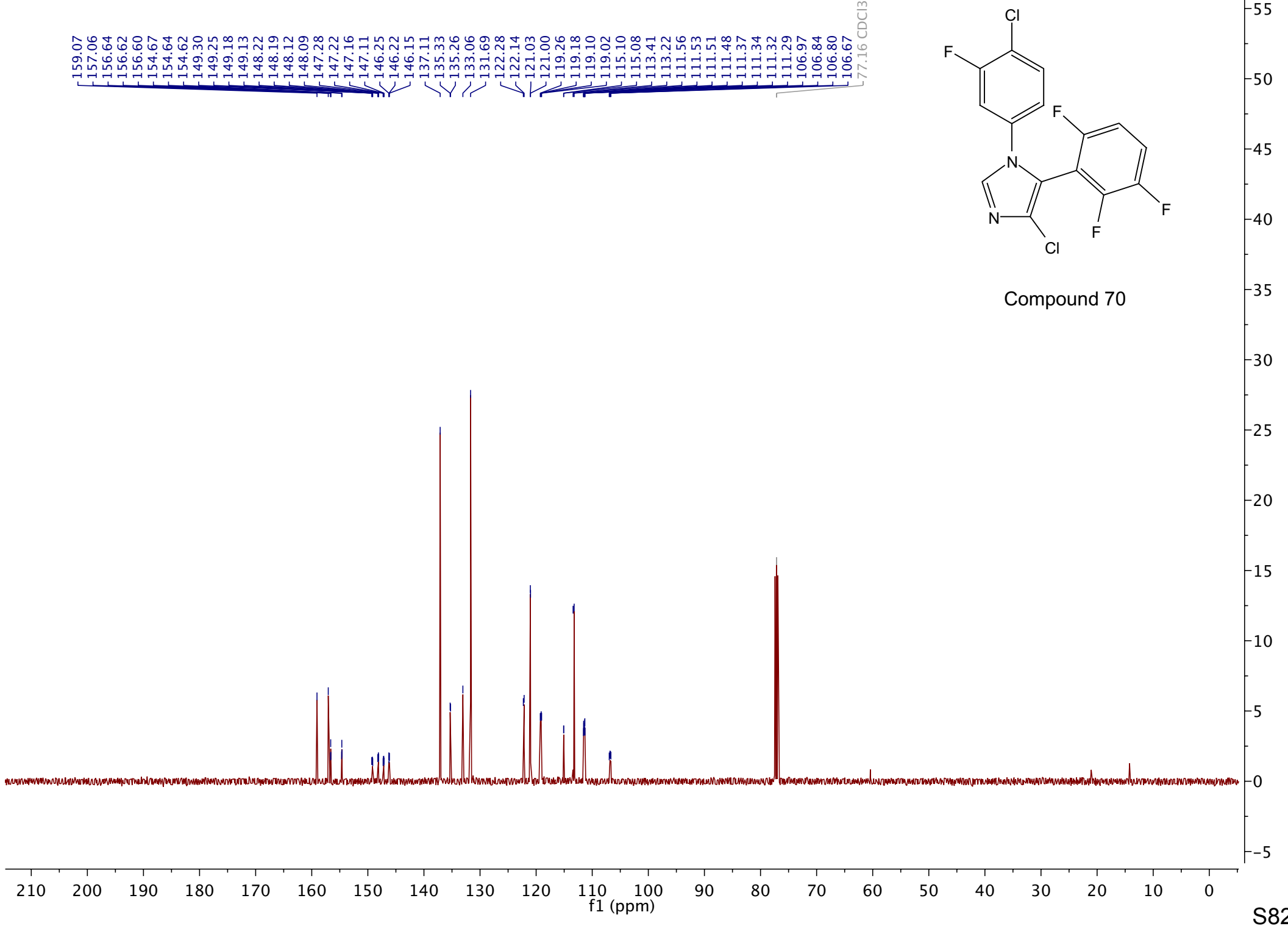
Compound 70

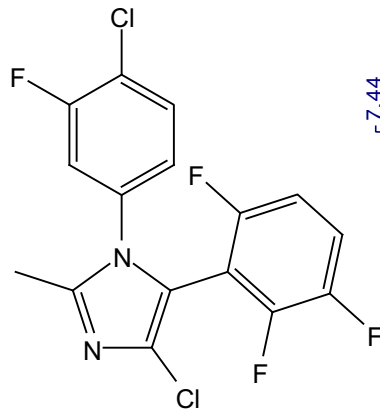


159.07
 157.06
 156.64
 156.62
 156.60
 154.67
 154.64
 154.62
 149.30
 149.25
 149.18
 149.13
 148.22
 148.19
 148.12
 148.09
 147.28
 147.22
 147.16
 147.11
 146.25
 146.22
 146.15
 137.11
 135.33
 135.26
 133.06
 131.69
 122.28
 122.14
 121.03
 121.00
 119.26
 119.18
 119.10
 119.02
 115.10
 115.08
 113.41
 113.22
 111.56
 111.53
 111.51
 111.48
 111.37
 111.34
 111.32
 111.29
 106.97
 106.84
 106.80
 106.67
 77.16 CDCl₃

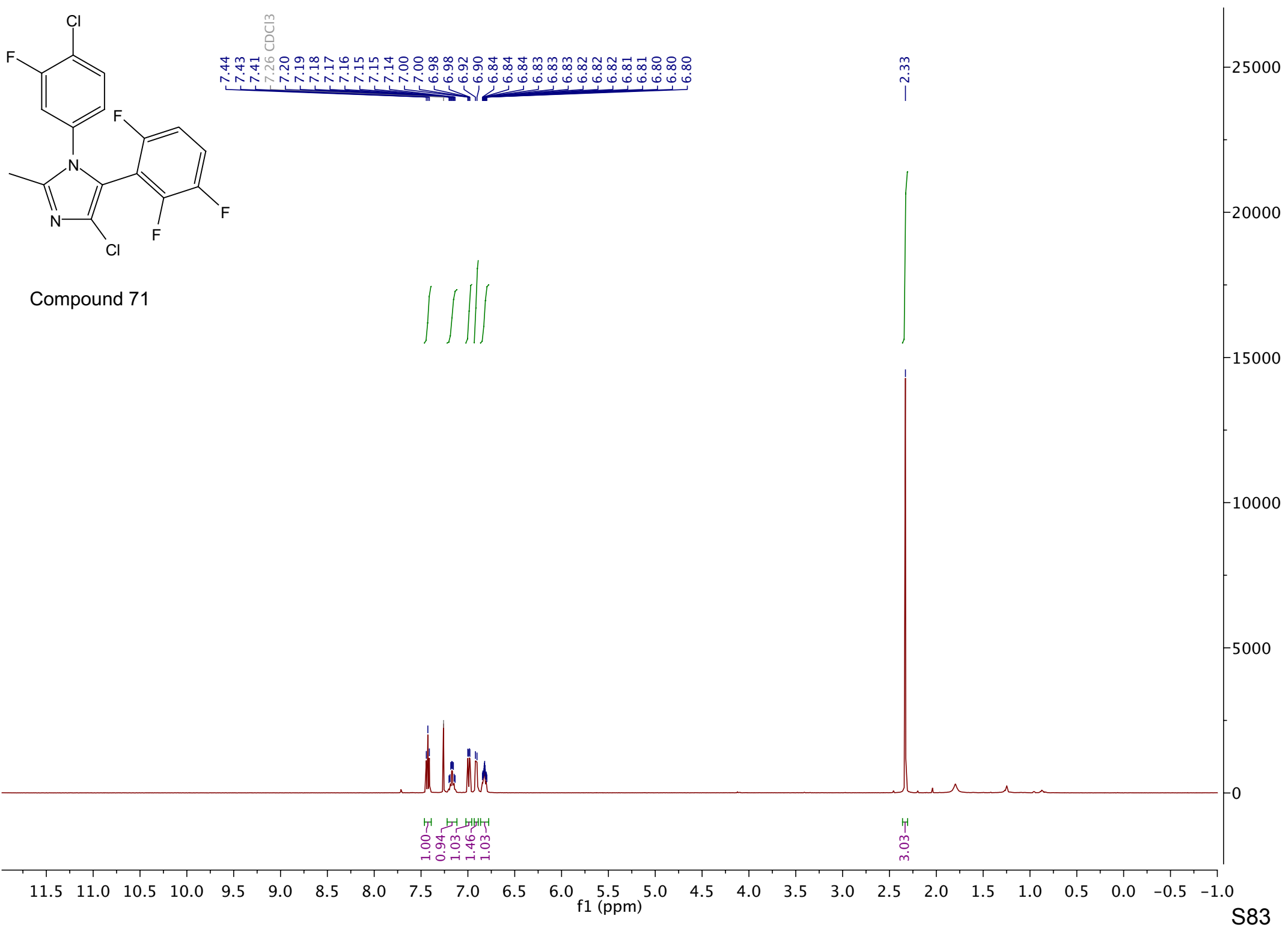


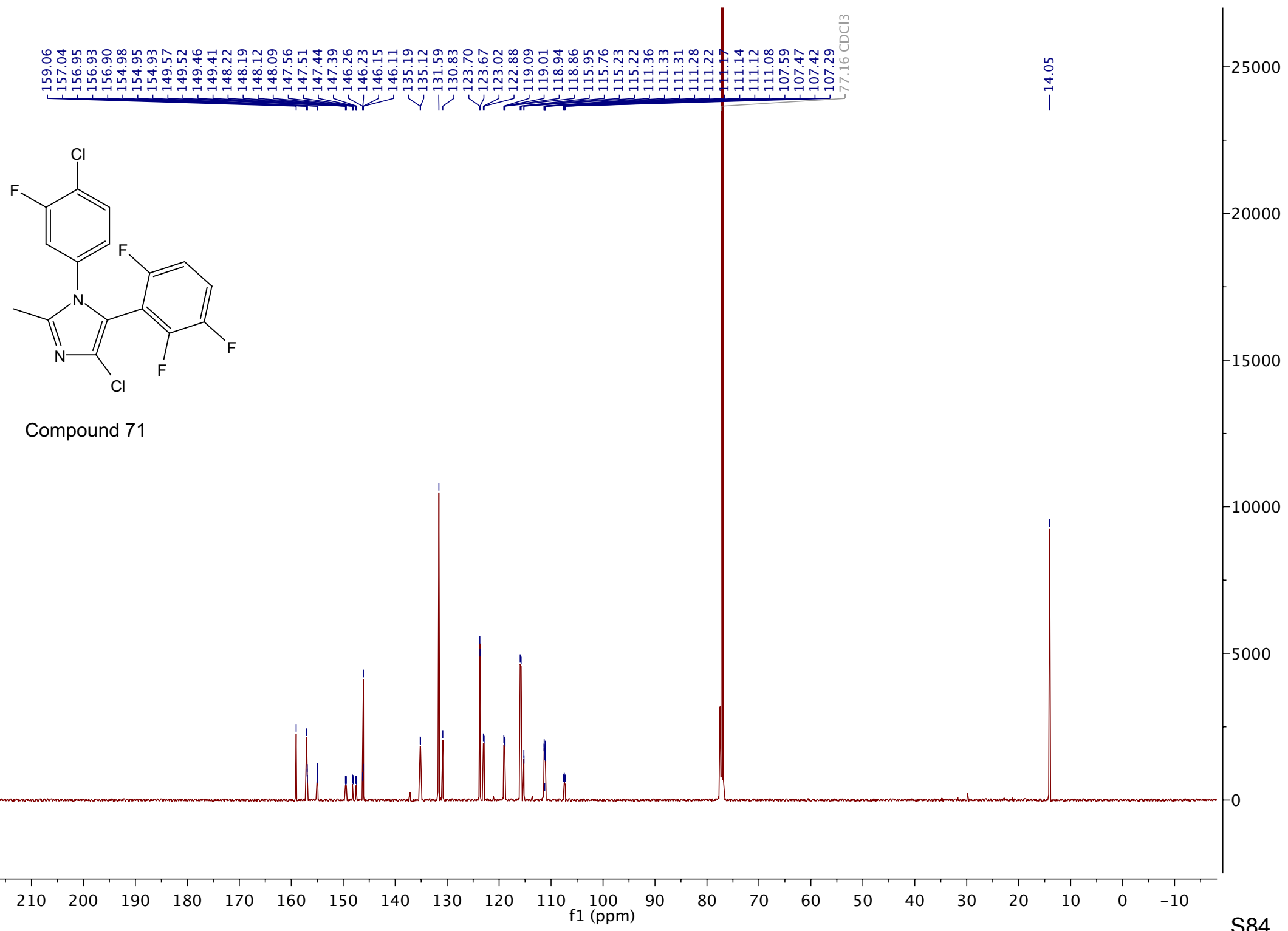
Compound 70

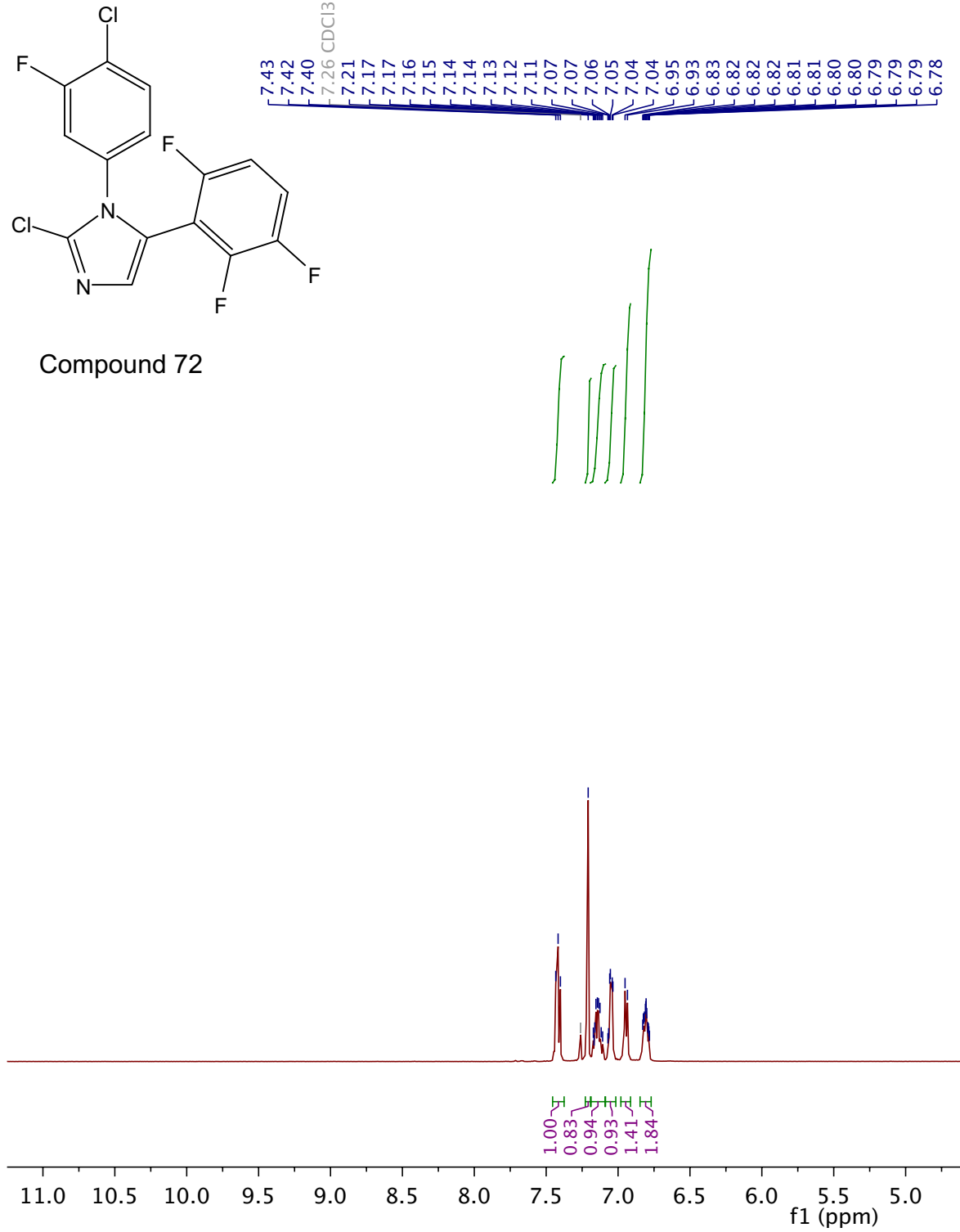


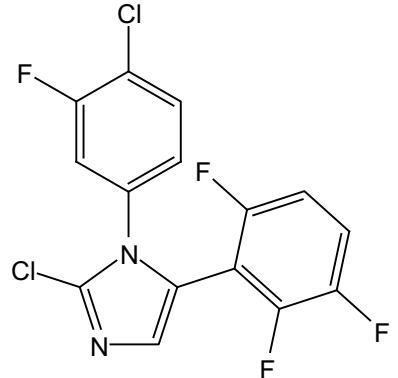
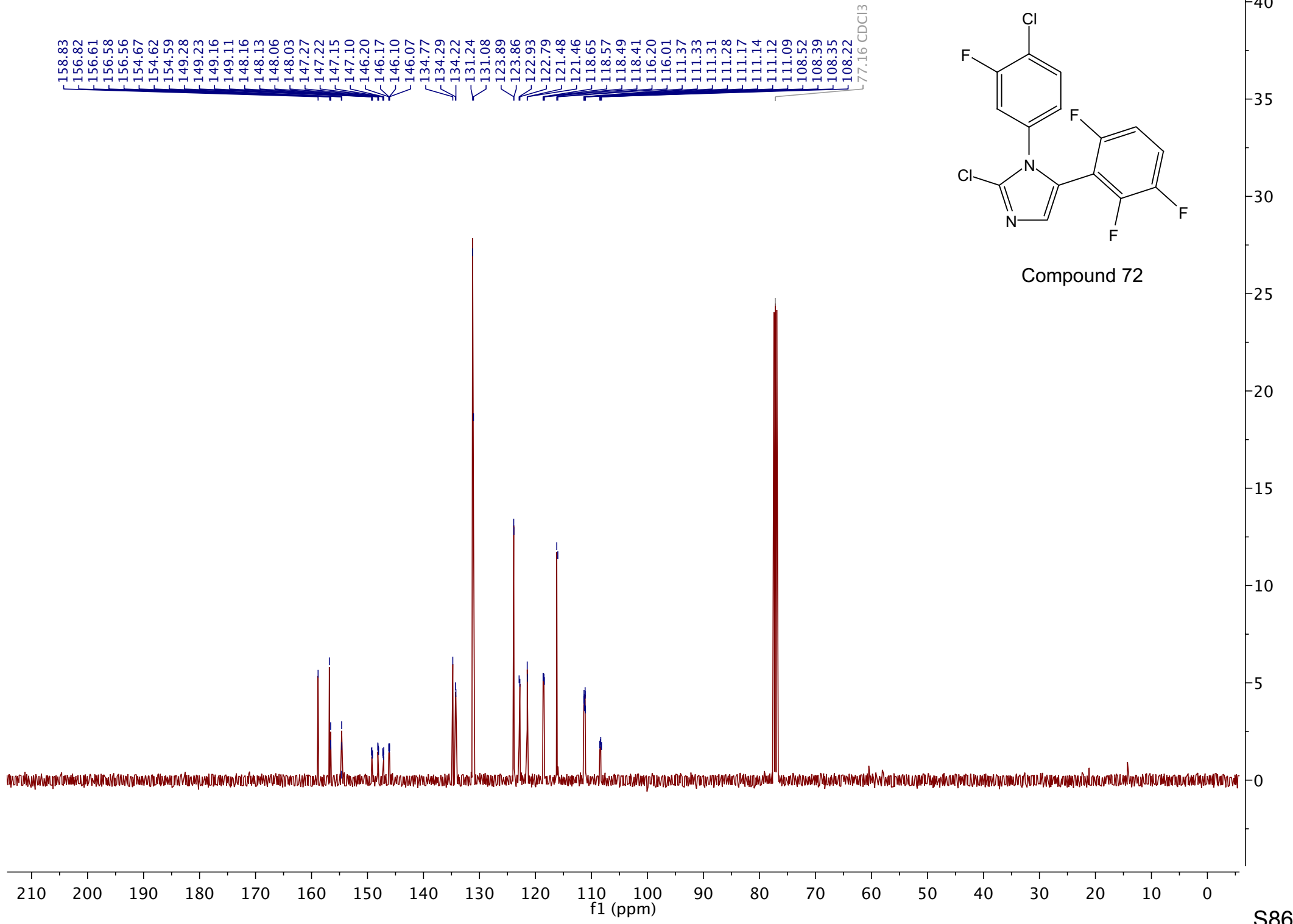


Compound 71

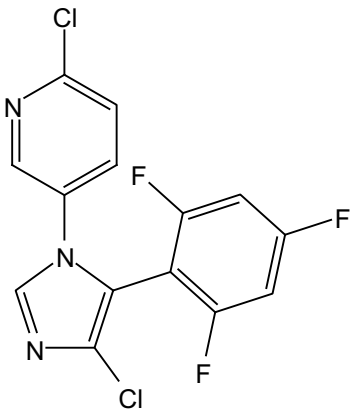




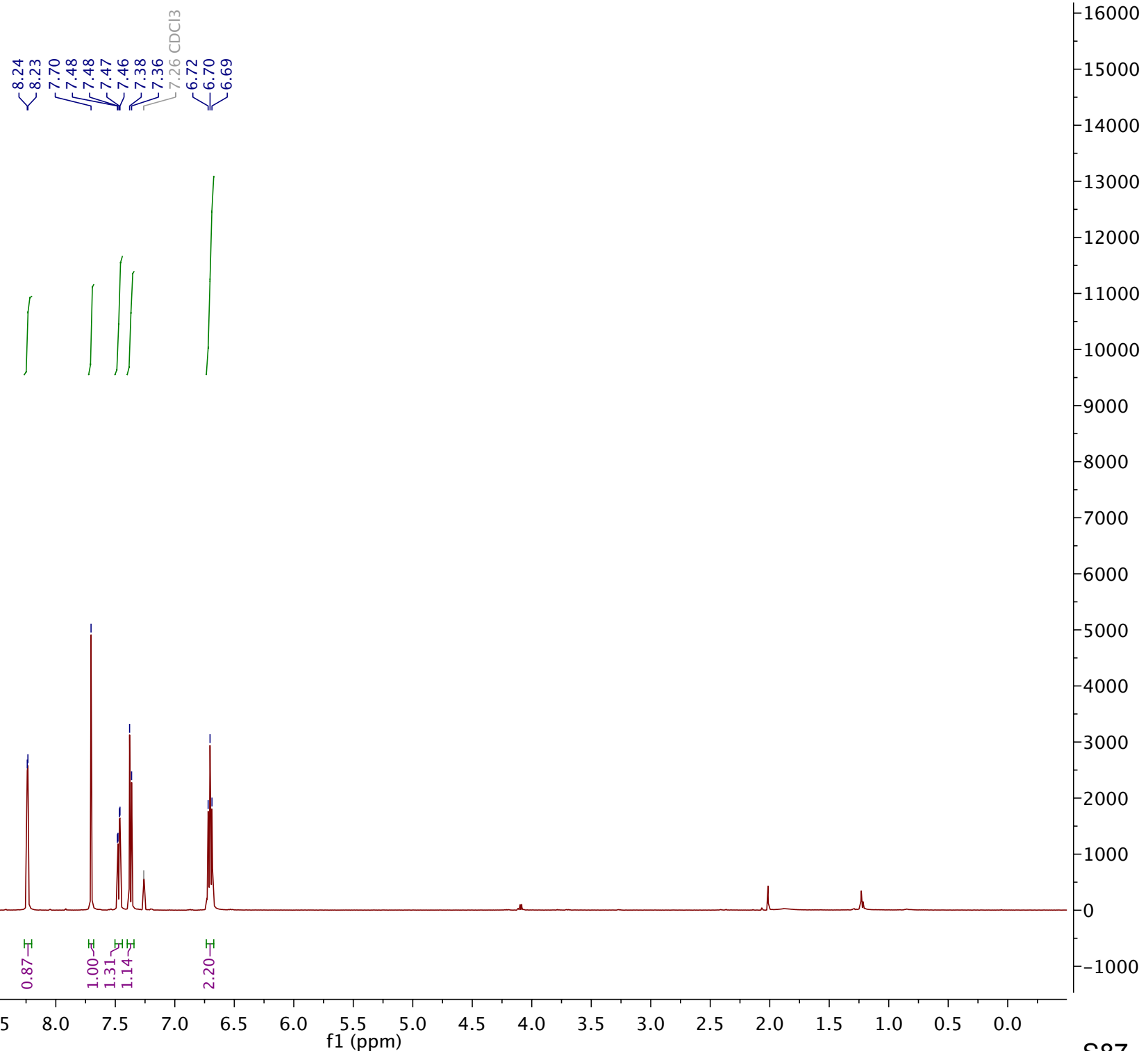


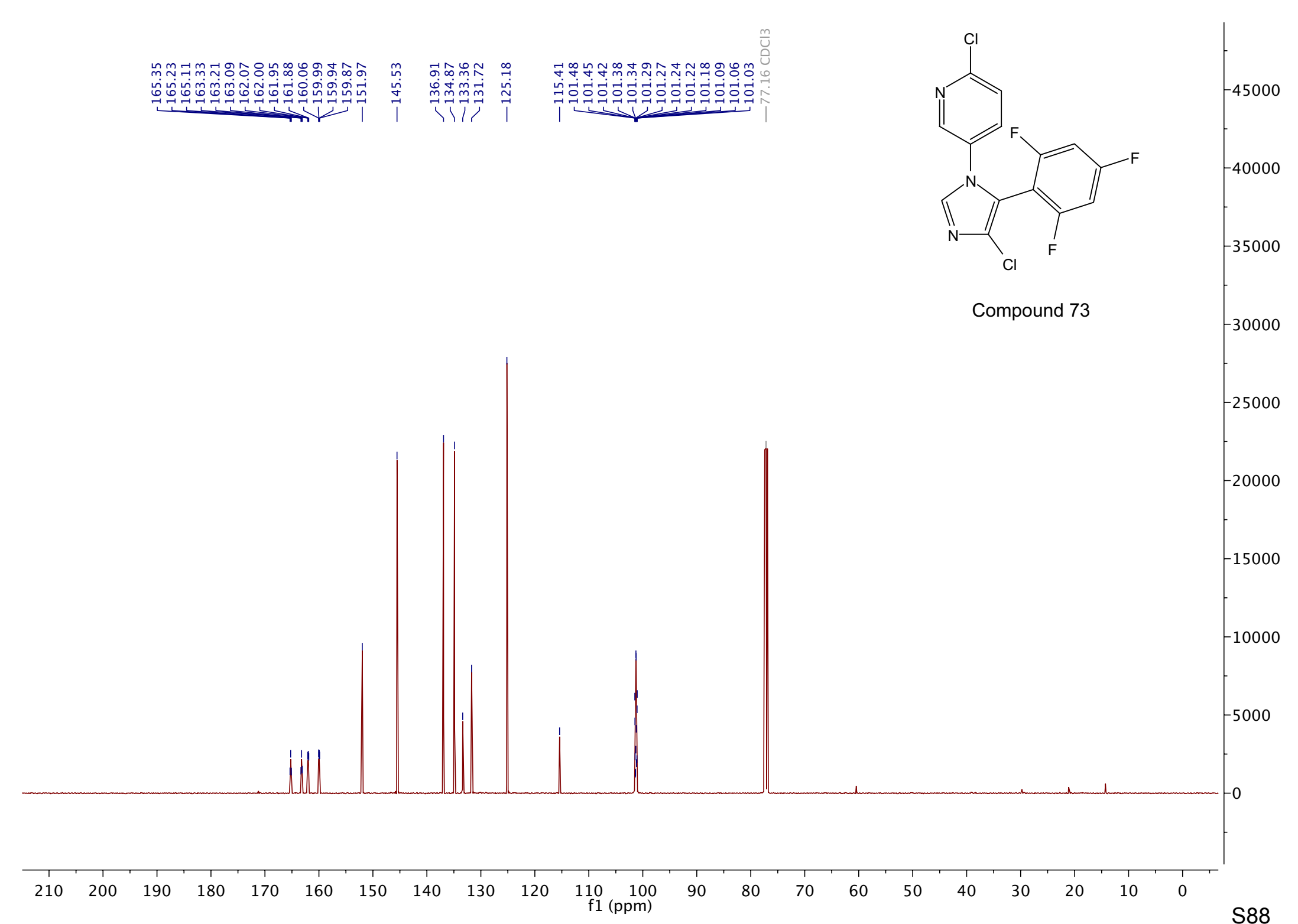


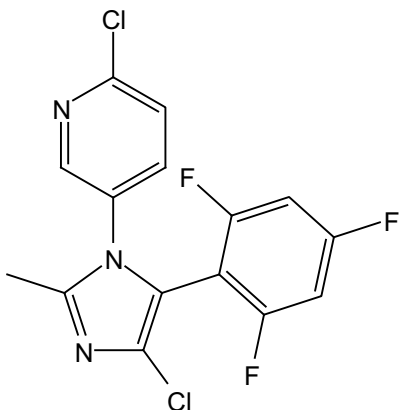
Compound 72



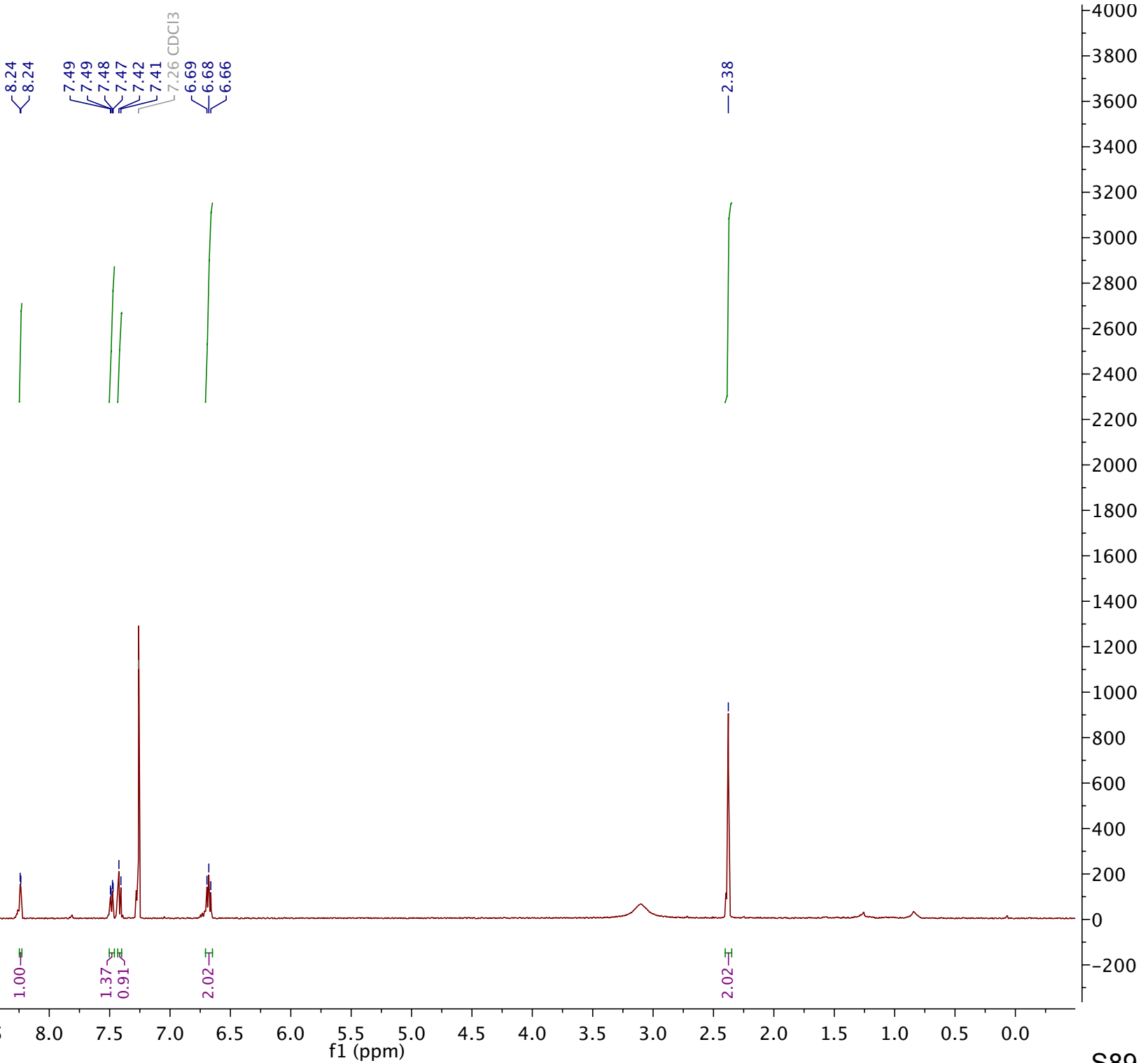
Compound 73

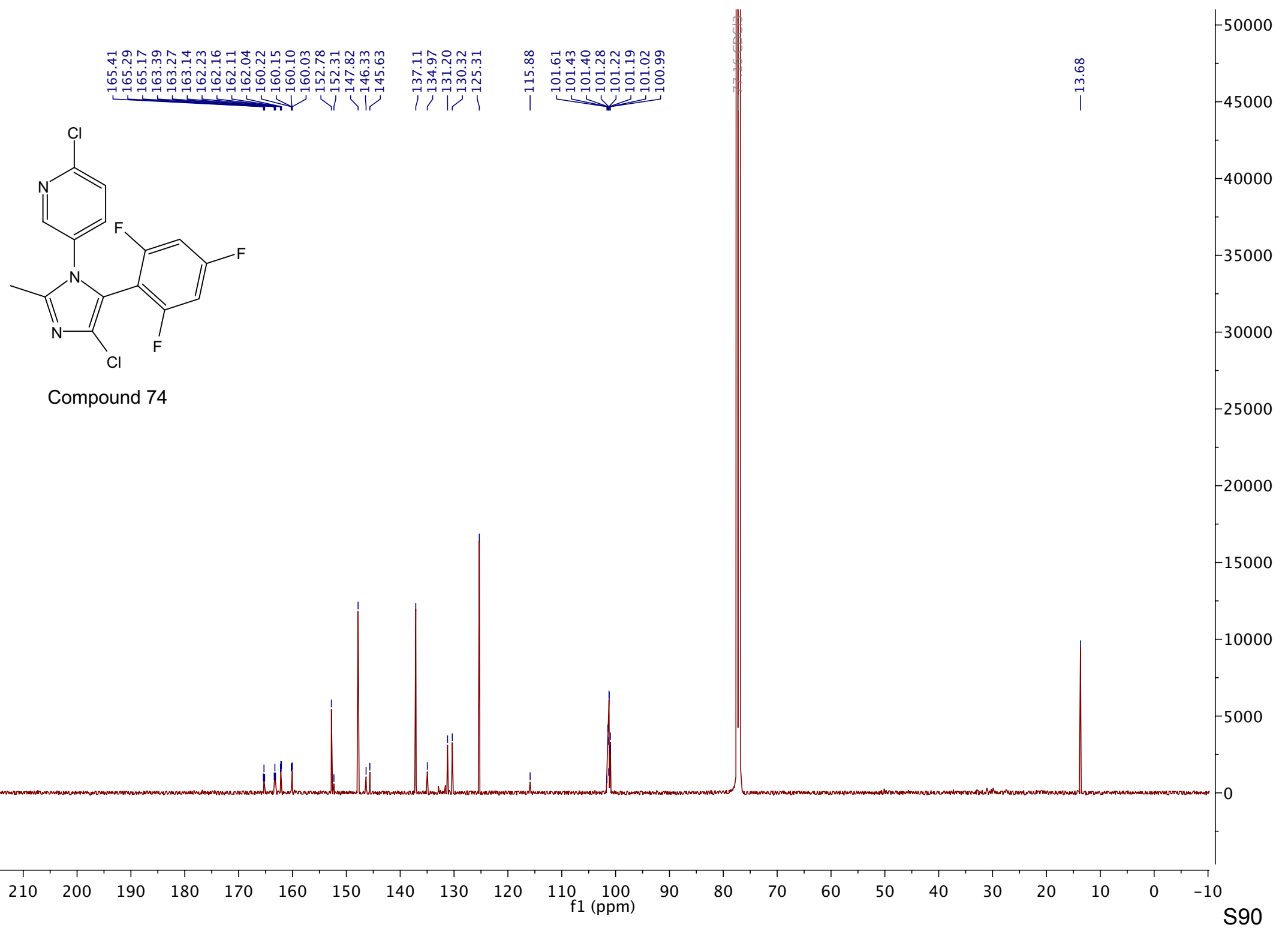


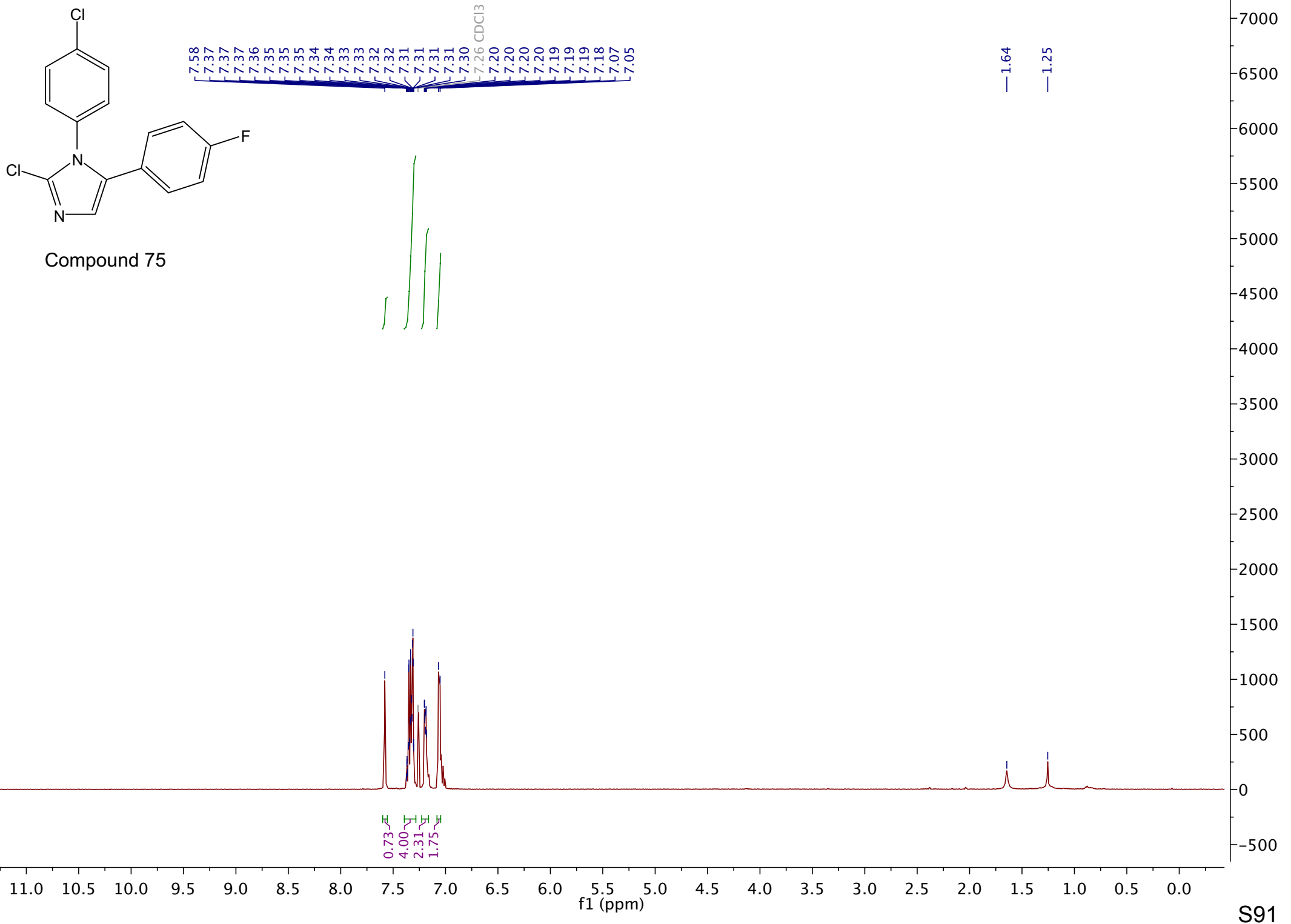


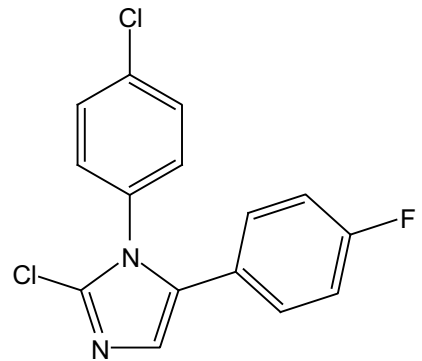


Compound 74

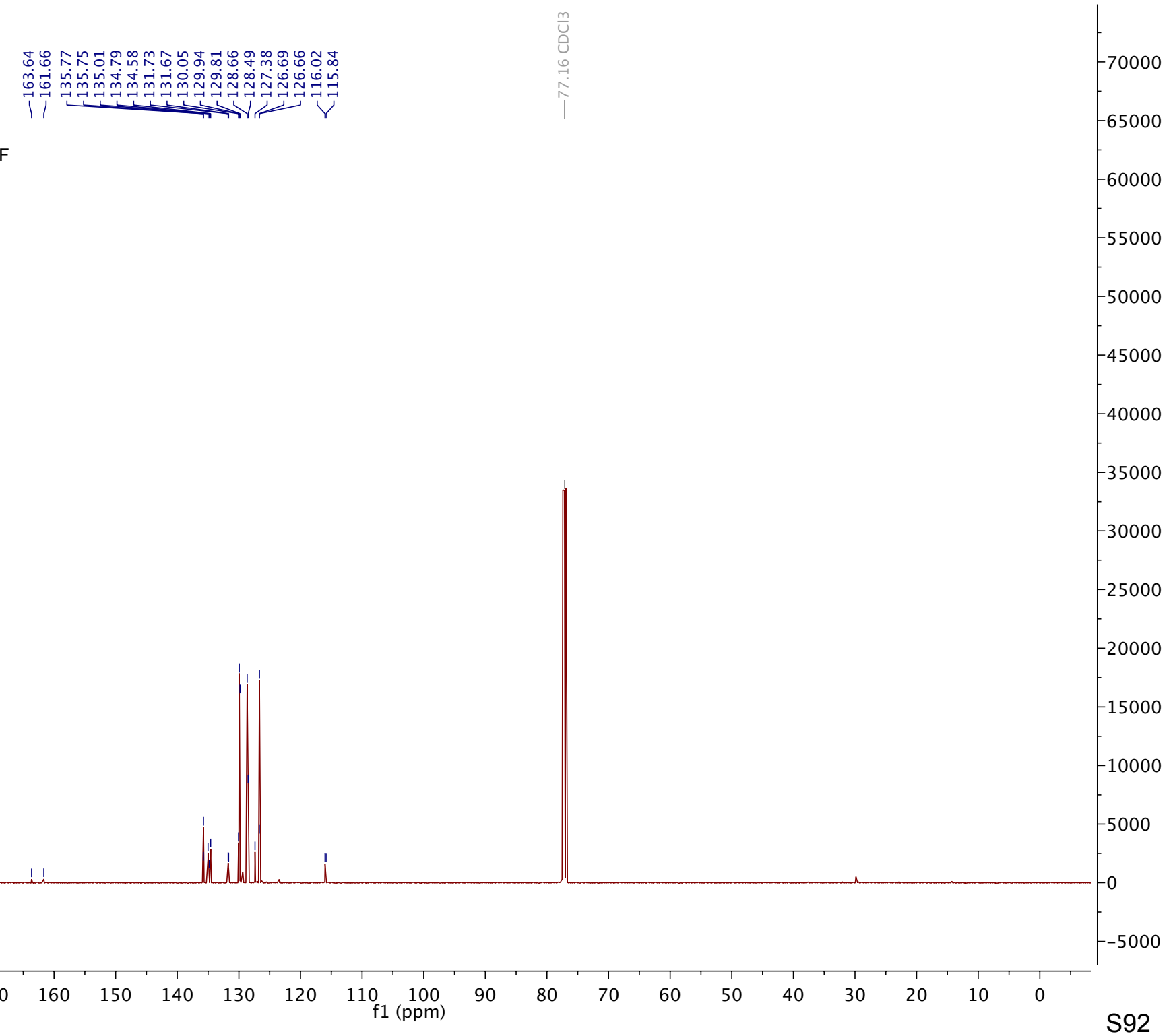


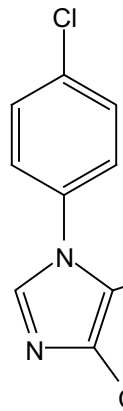




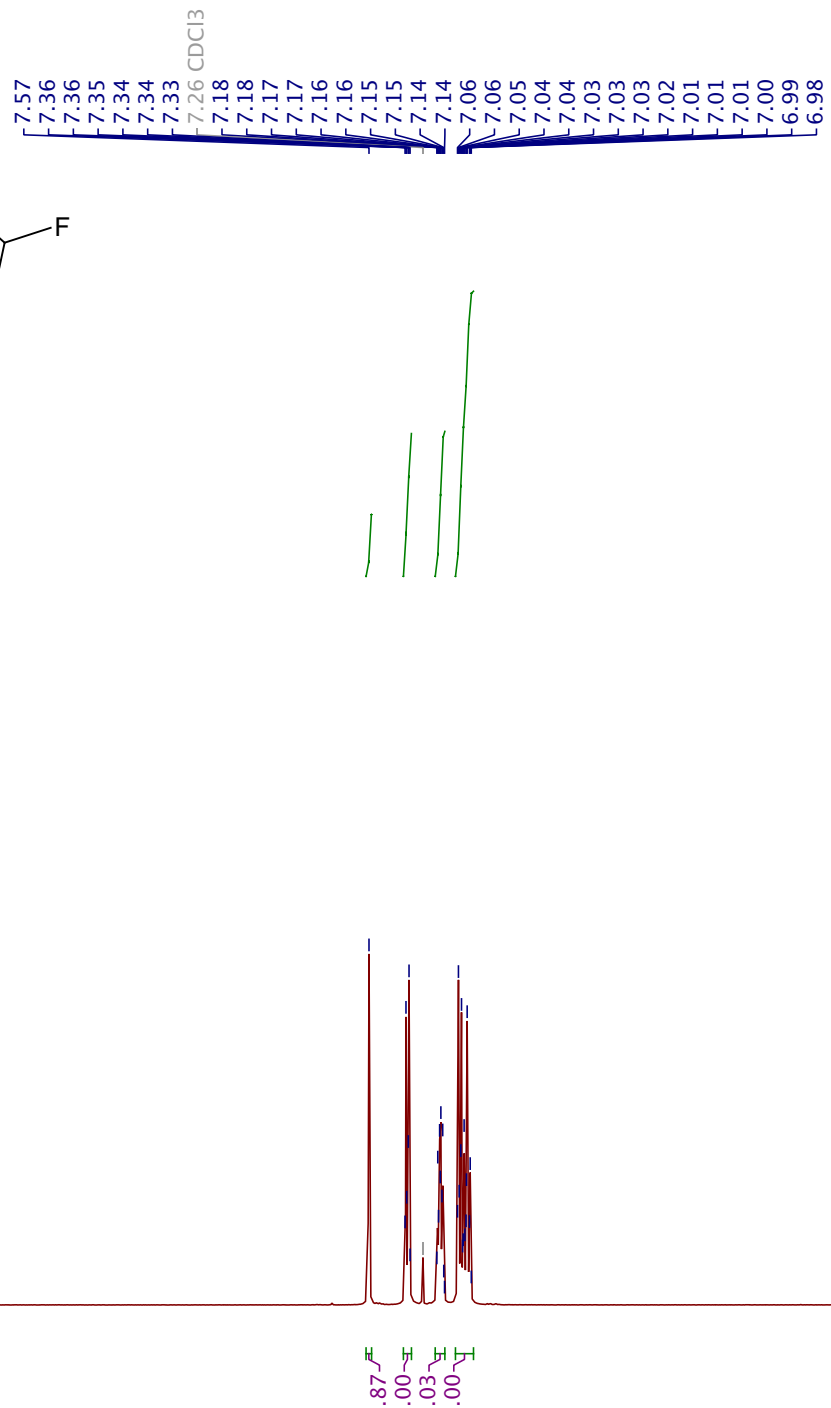


Compound 75





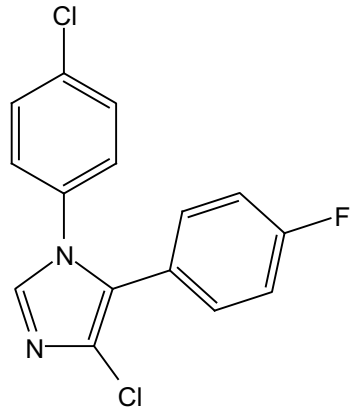
Compound 76



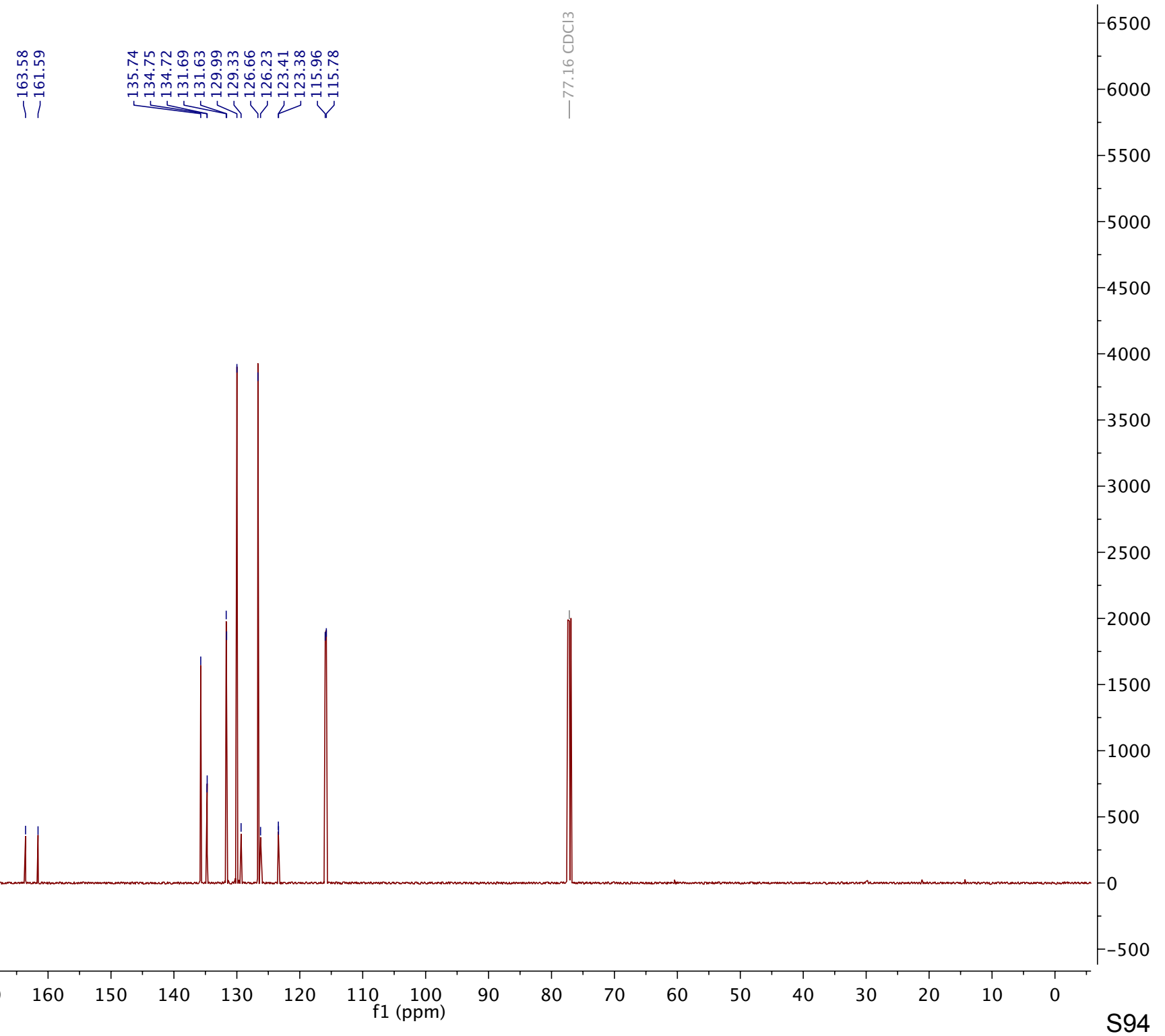
11.0 10.5 10.0 9.5 9.0 8.5 8.0 7.5 7.0 6.5 6.0 5.5 5.0 4.5 4.0 3.5 3.0 2.5 2.0 1.5 1.0 0.5 0.0

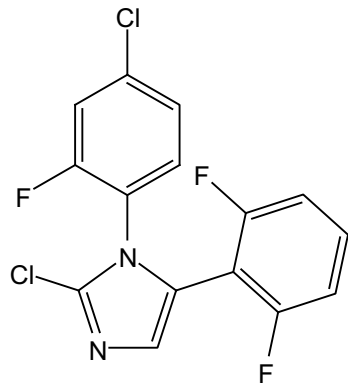
f1 (ppm)

S93

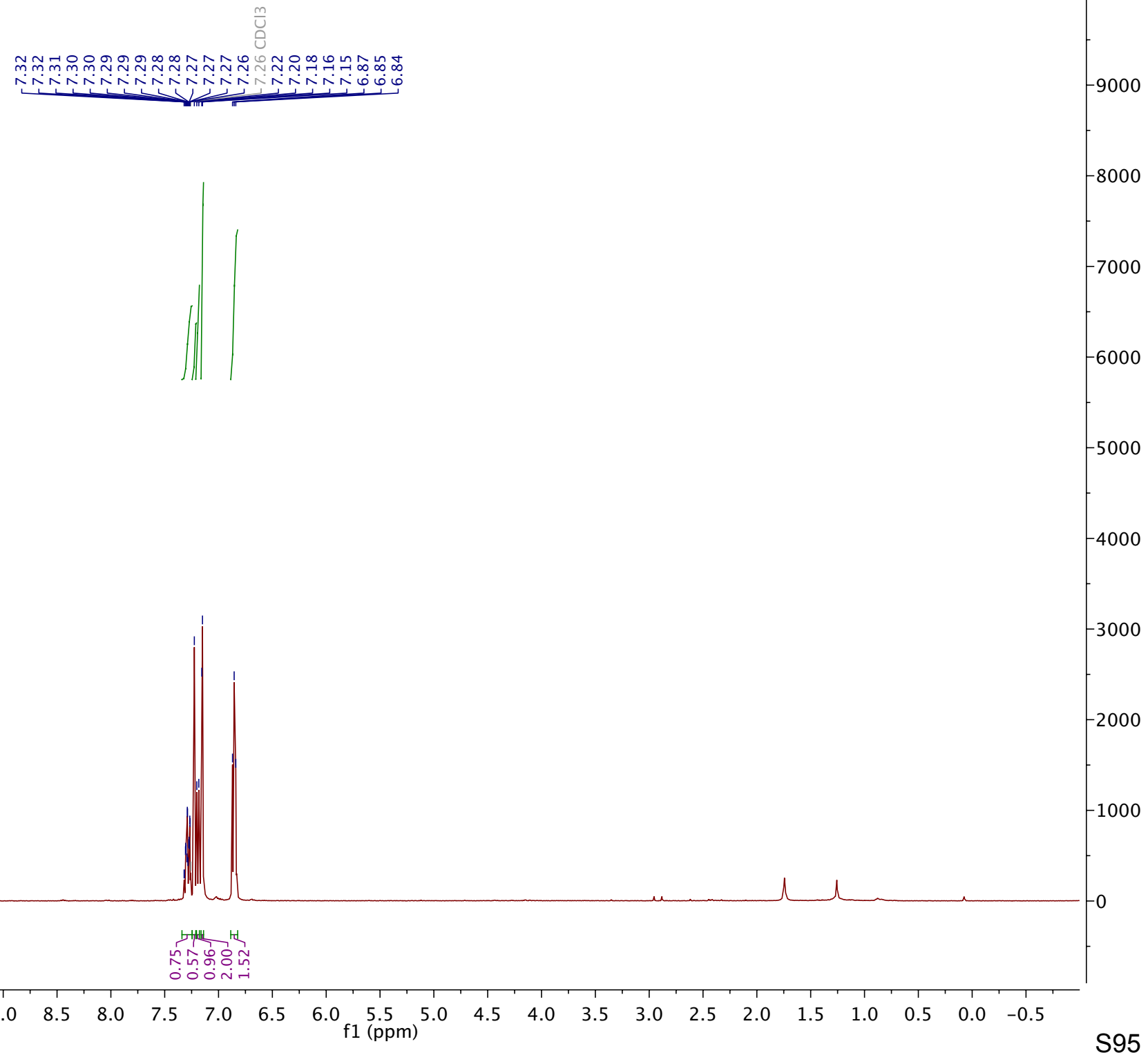


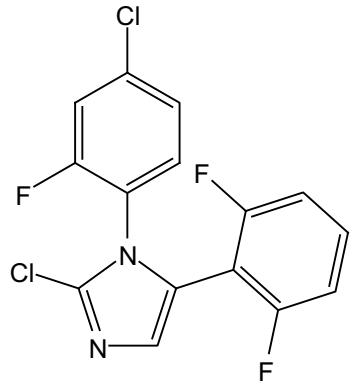
Compound 76



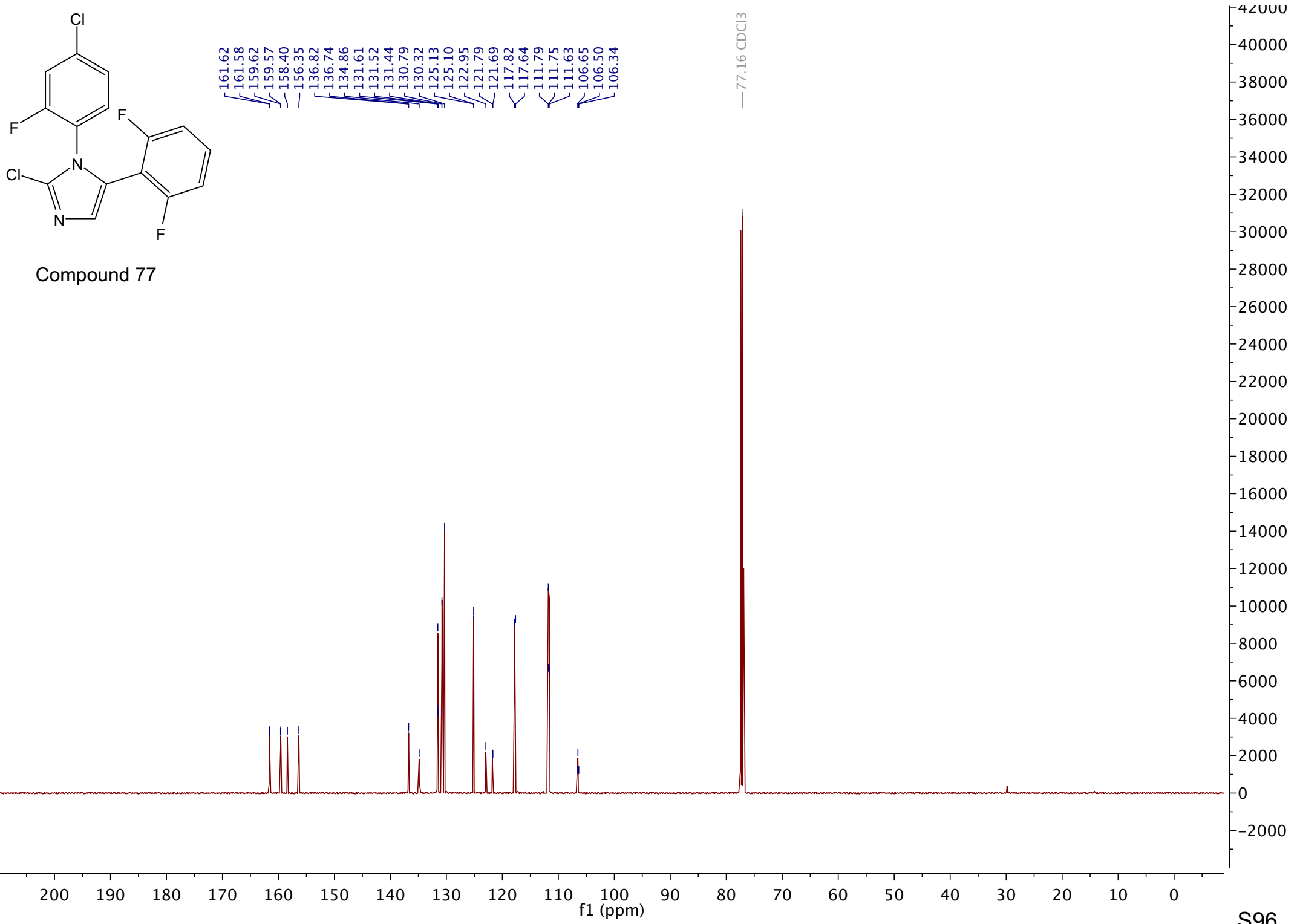


Compound 77





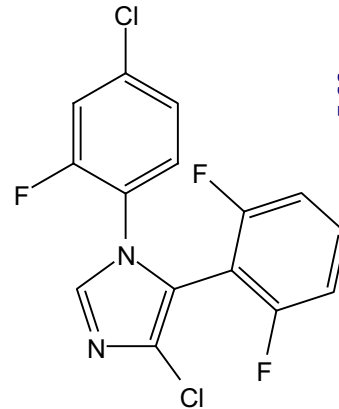
Compound 77



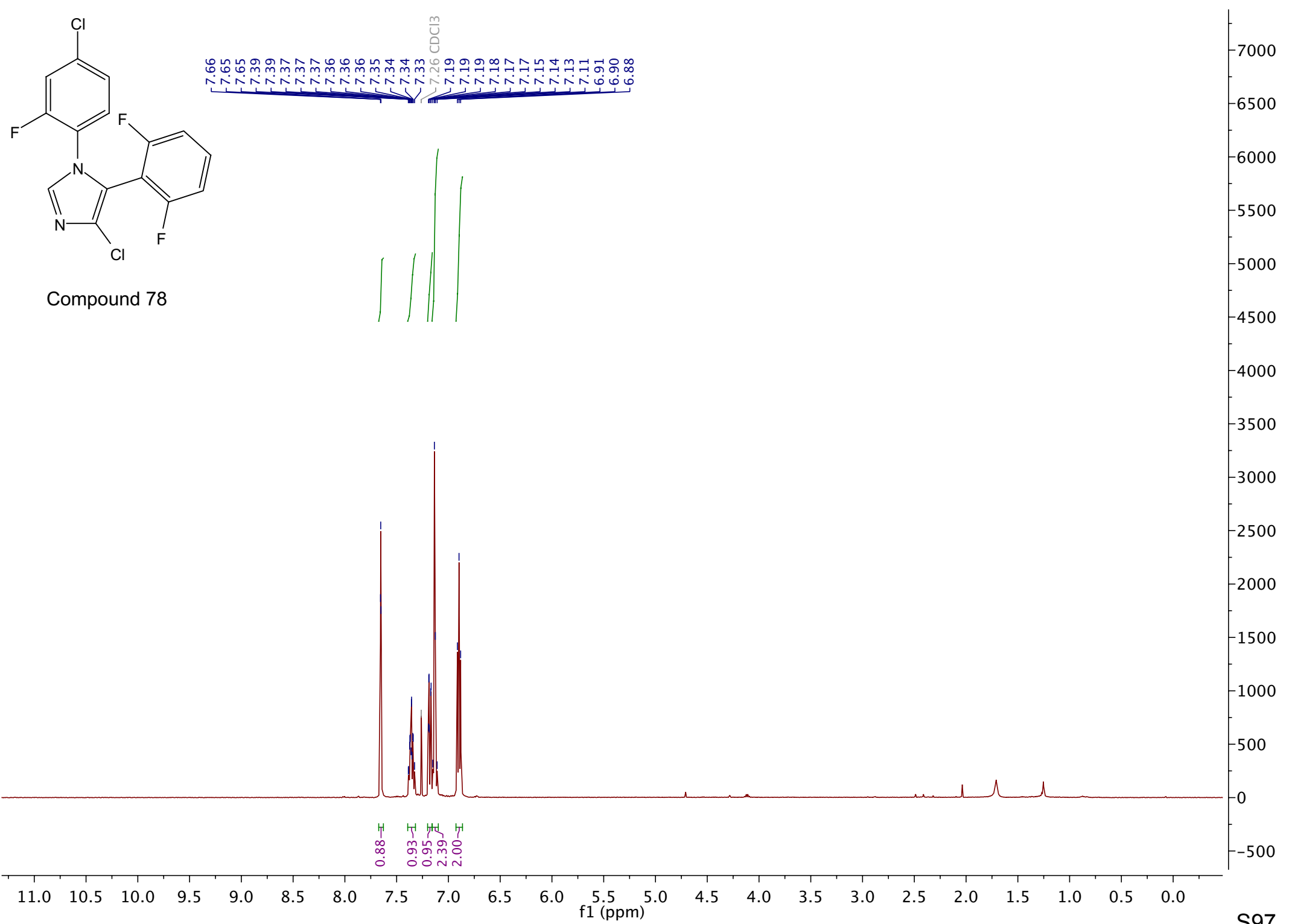
200 190 180 170 160 150 140 130 120 110 100 90 80 70 60 50 40 30 20 10 0

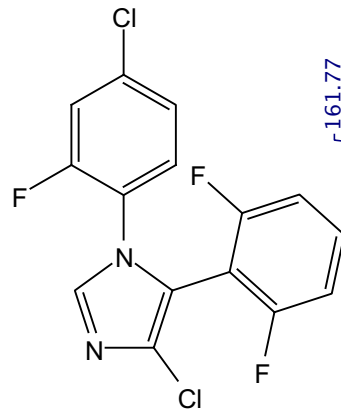
f1 (ppm)

S96

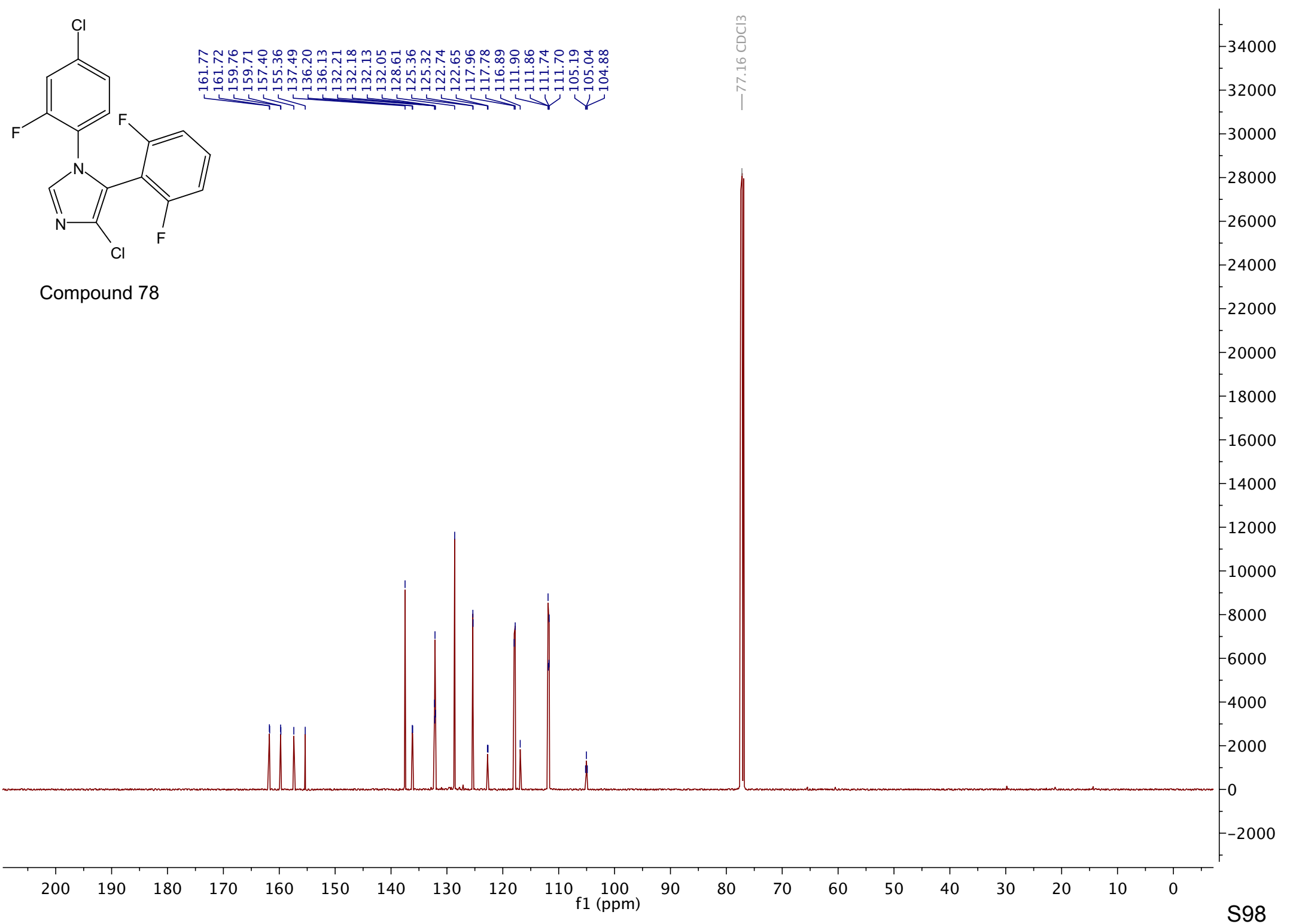


Compound 78





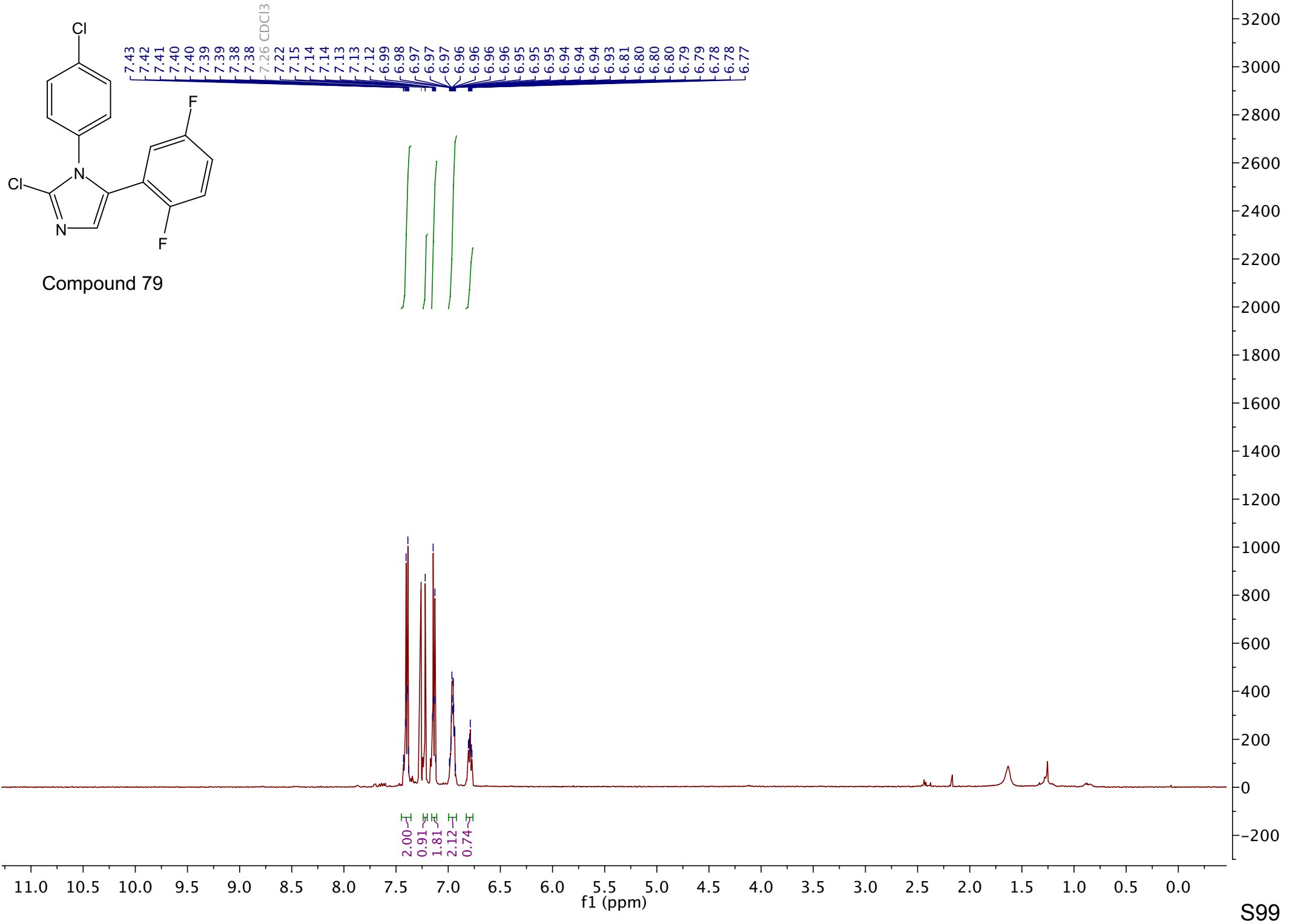
Compound 78

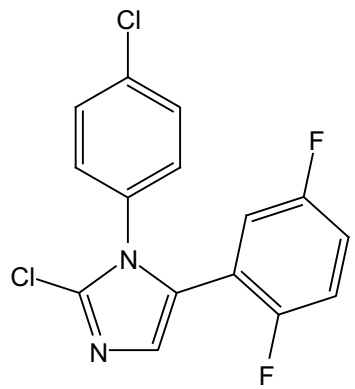


200 190 180 170 160 150 140 130 120 110 100 90 80 70 60 50 40 30 20 10 0

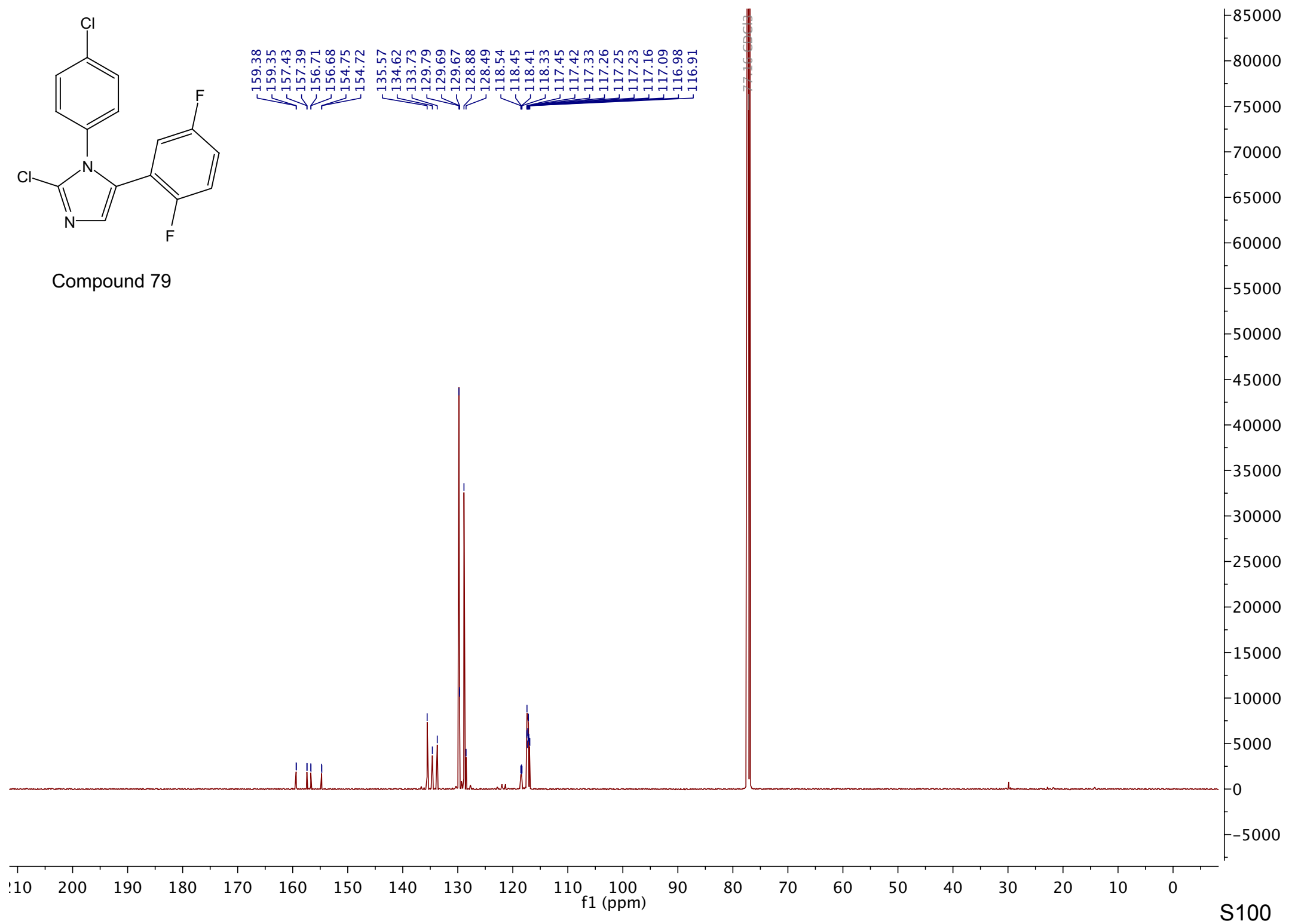
f1 (ppm)

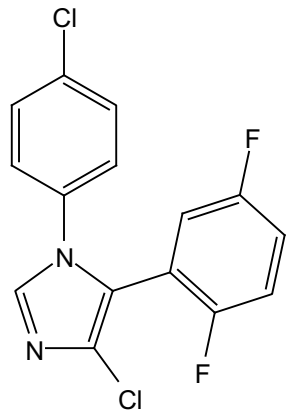
S98



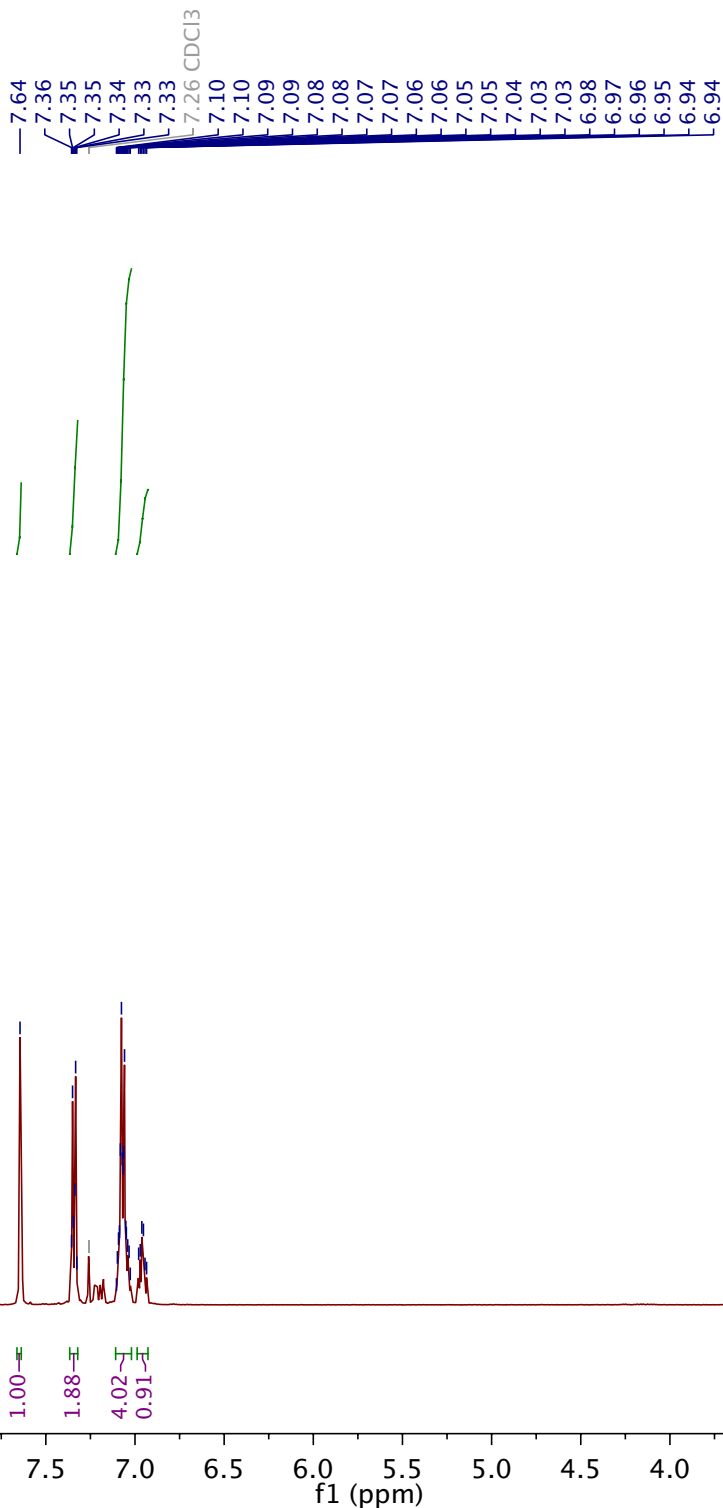


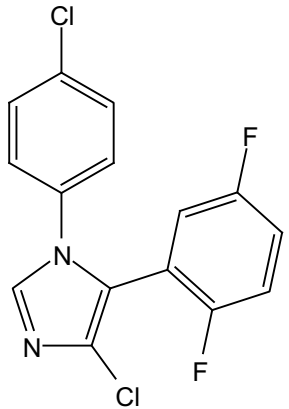
Compound 79



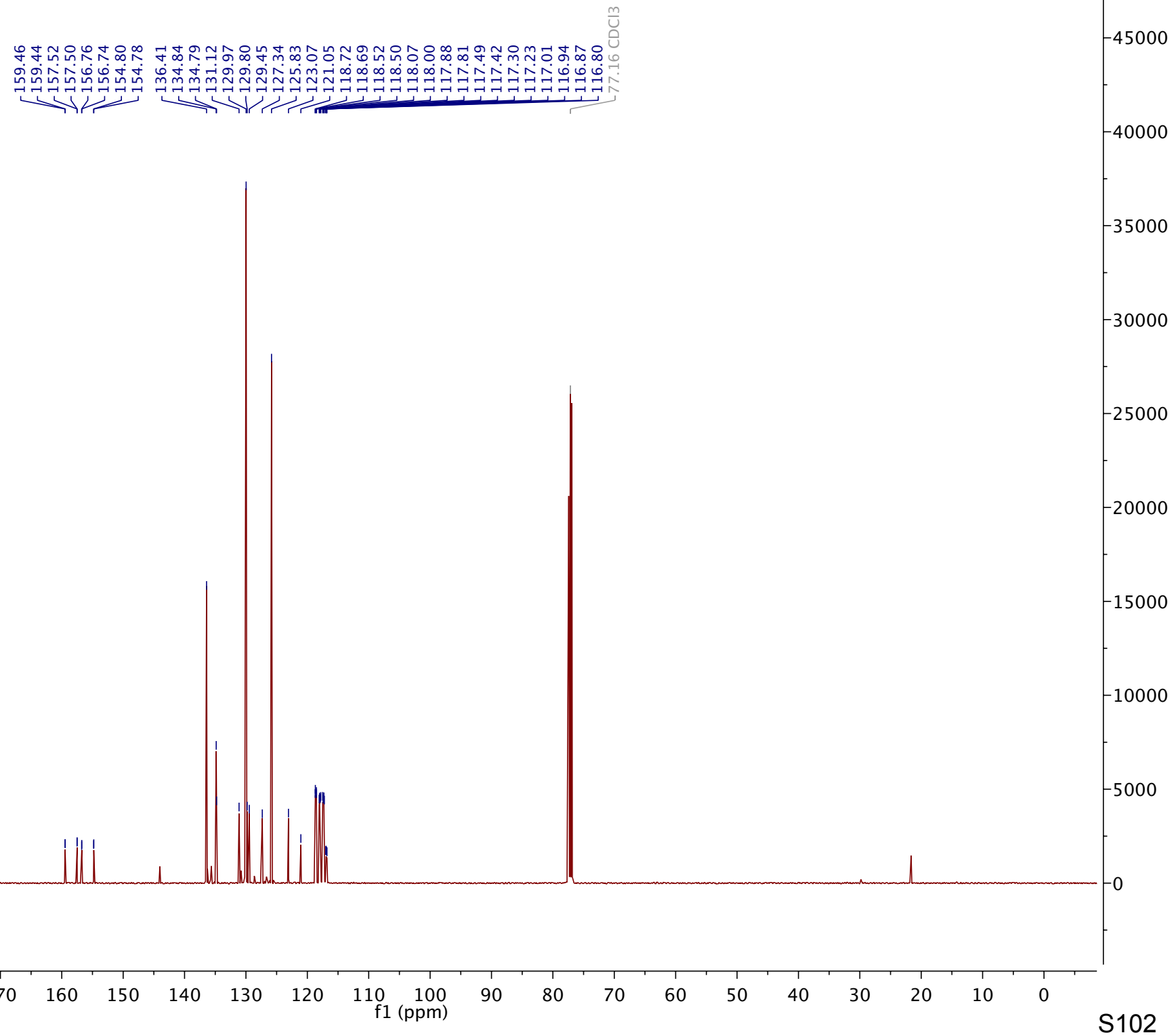


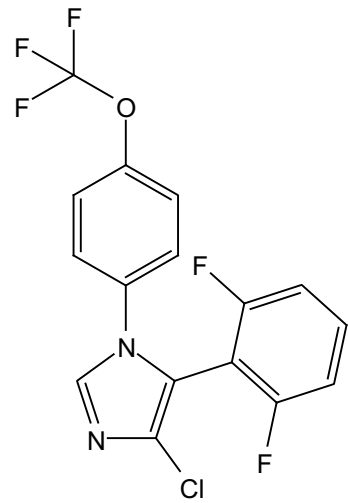
Compound 80



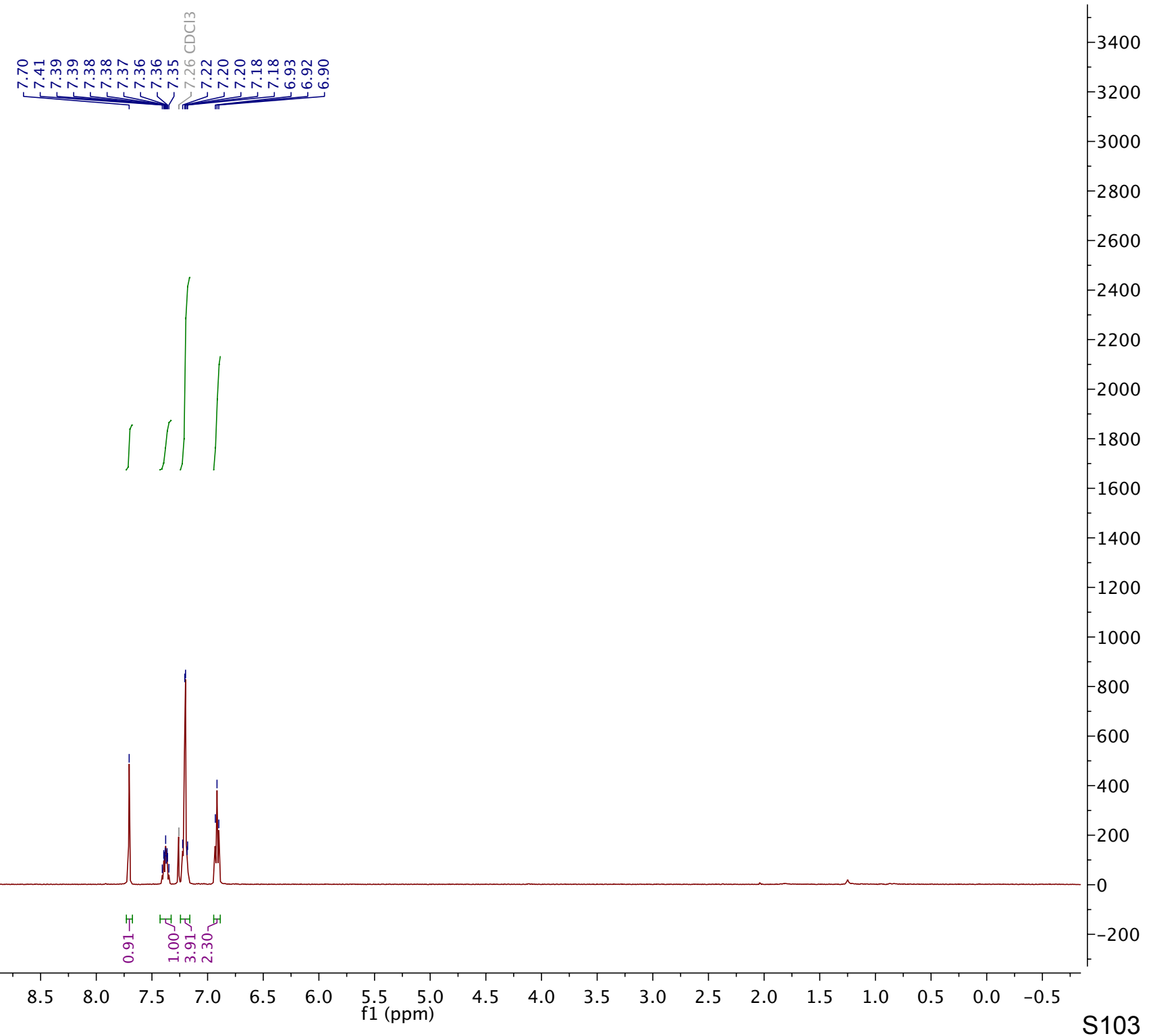


Compound 80

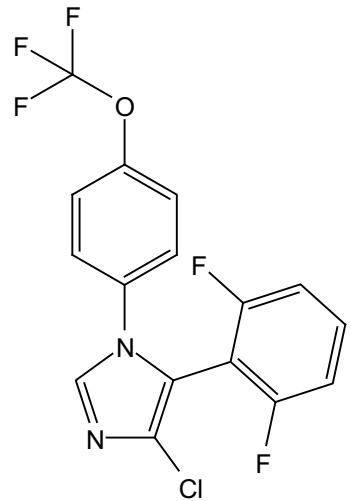




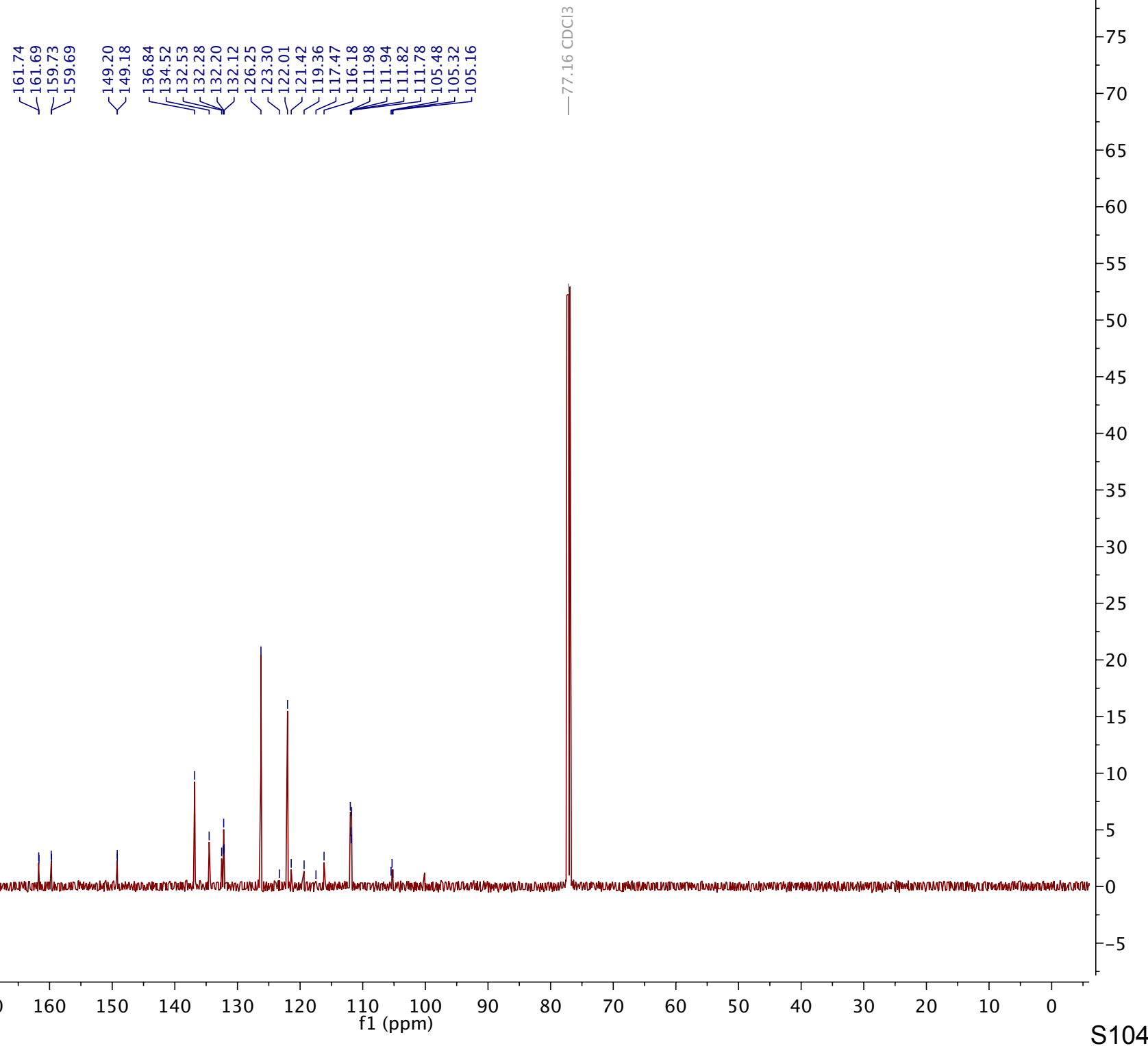
Compound 81

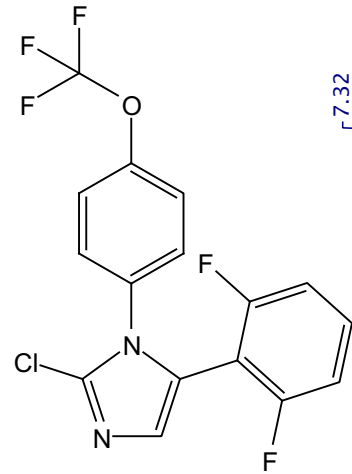


S103

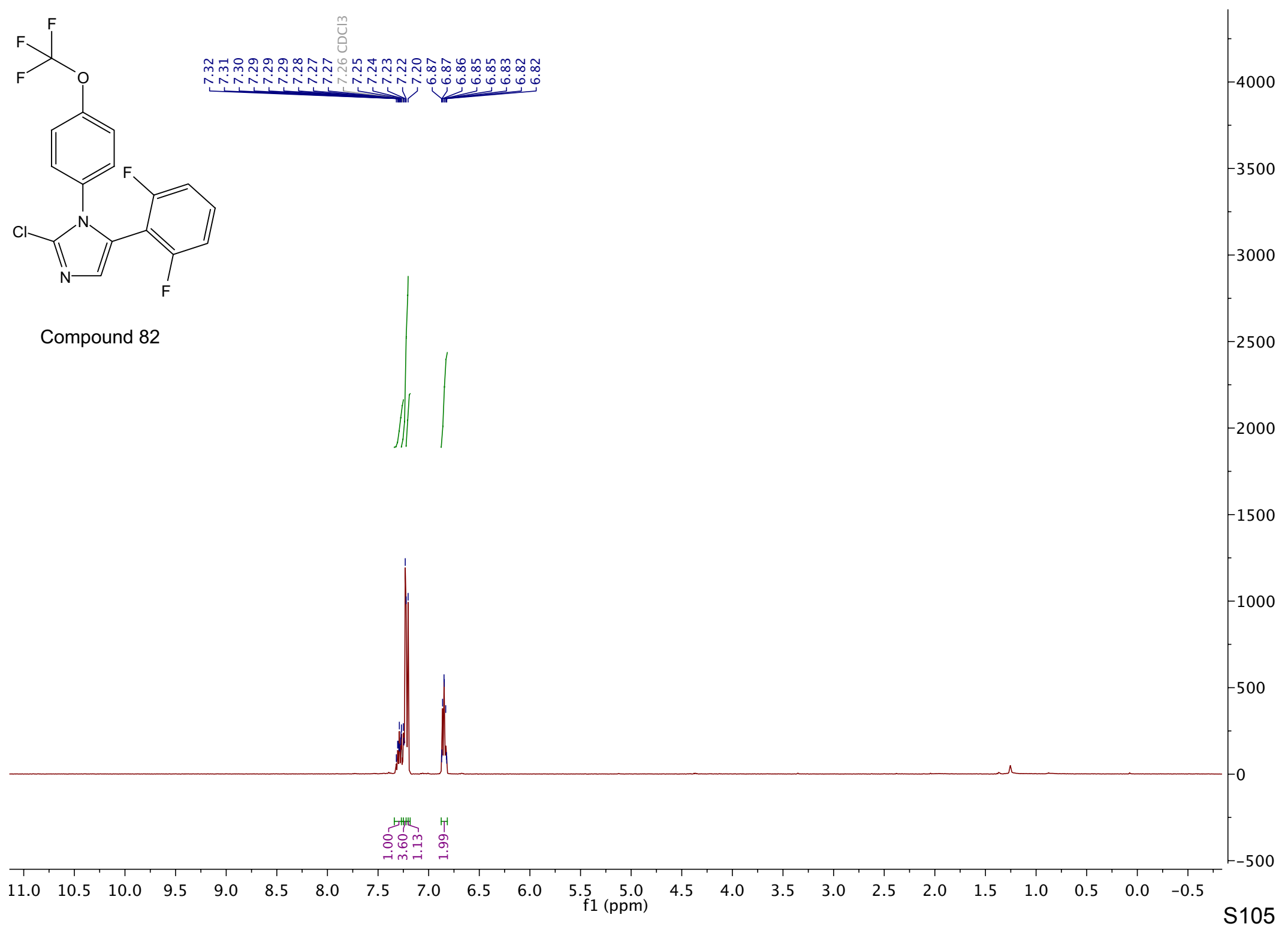


Compound 81

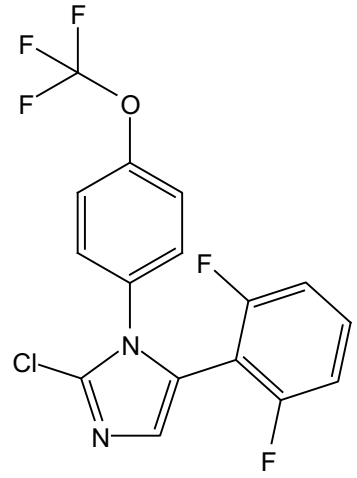




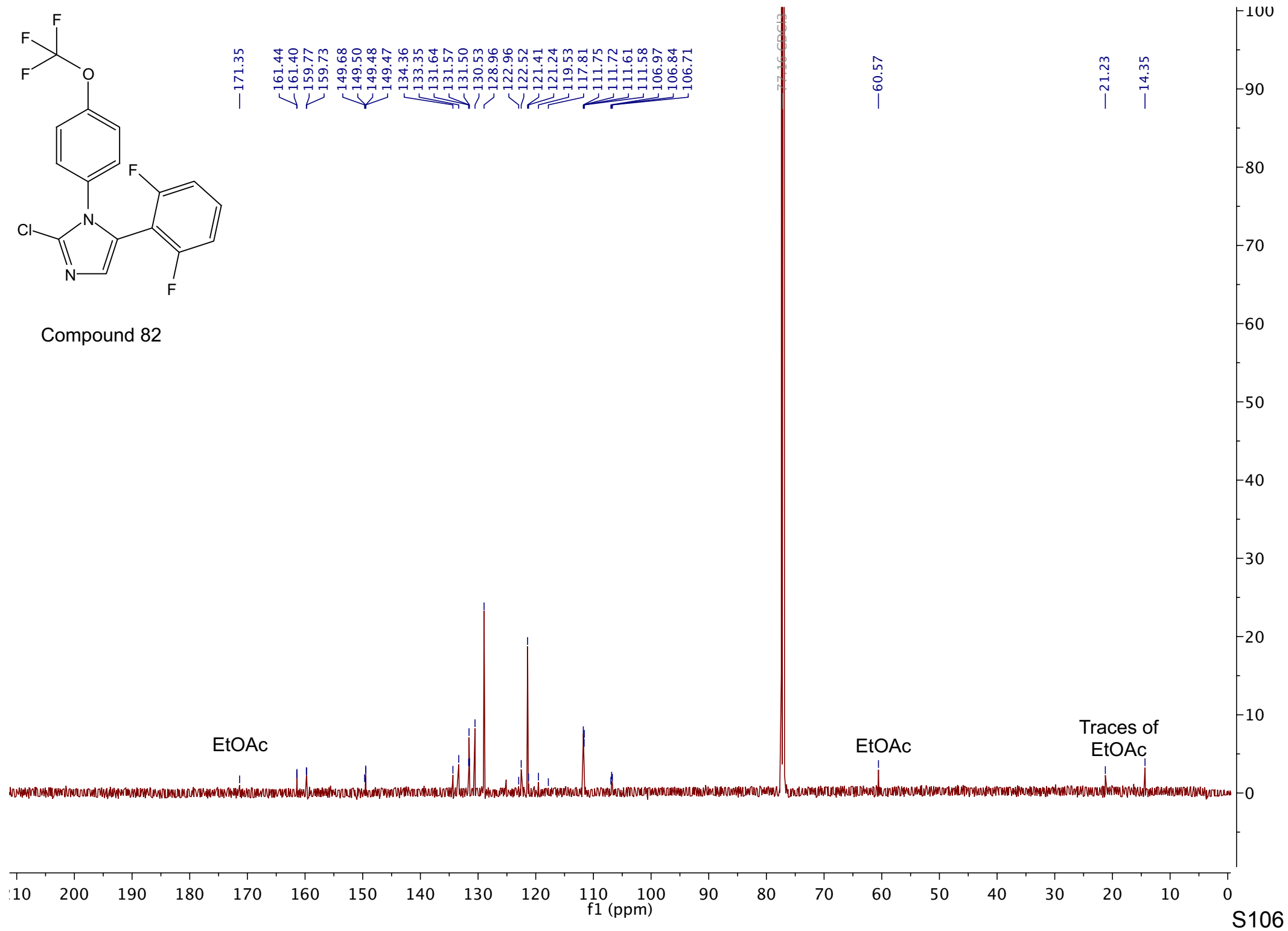
Compound 82

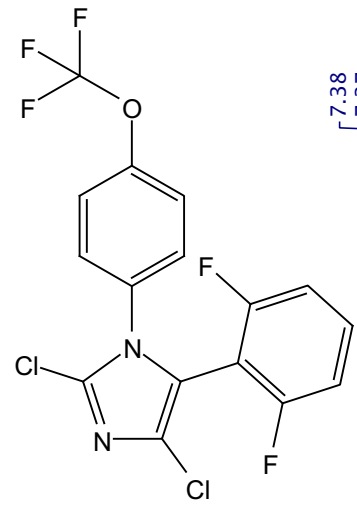


S105

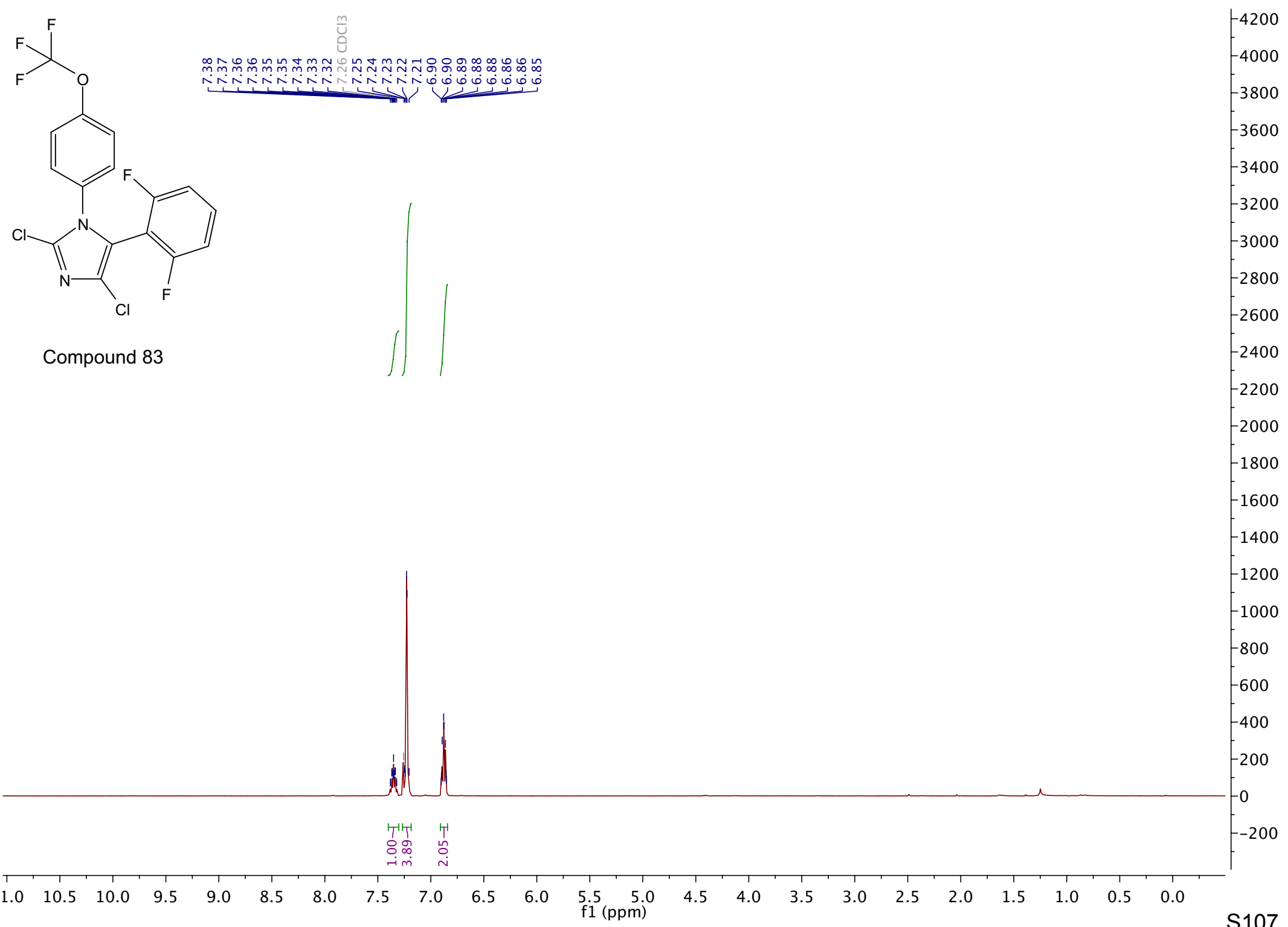


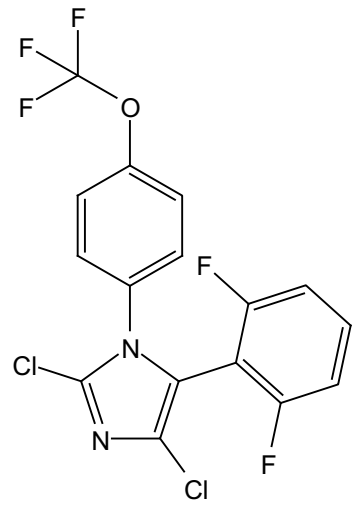
Compound 82



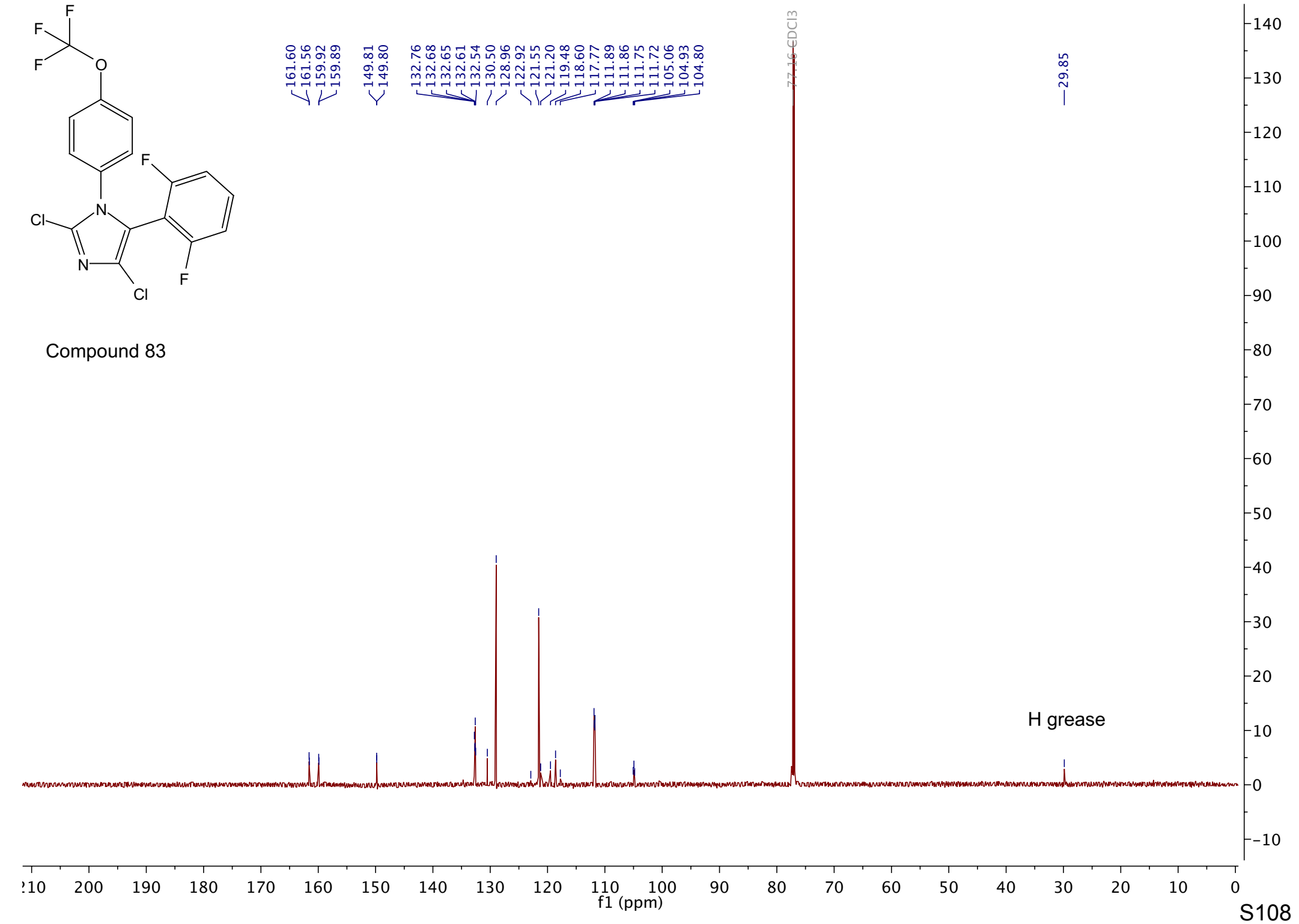


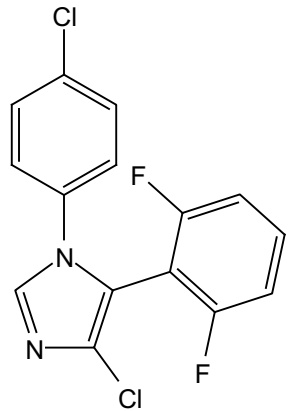
Compound 83



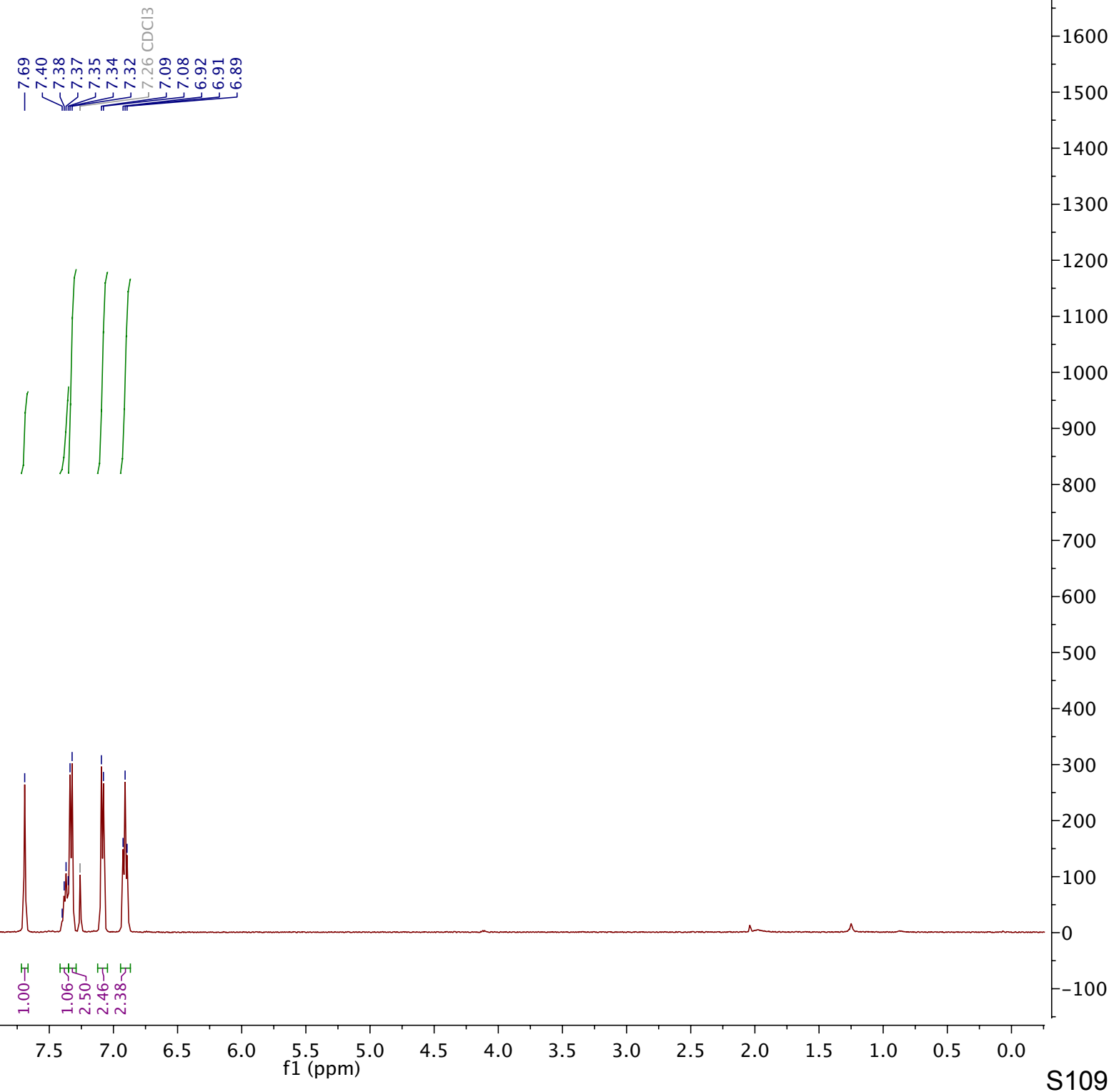


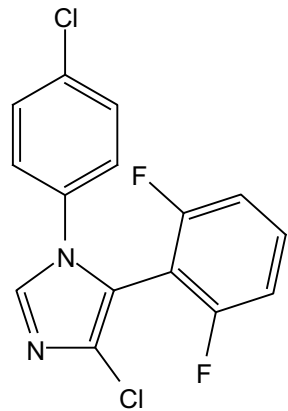
Compound 83



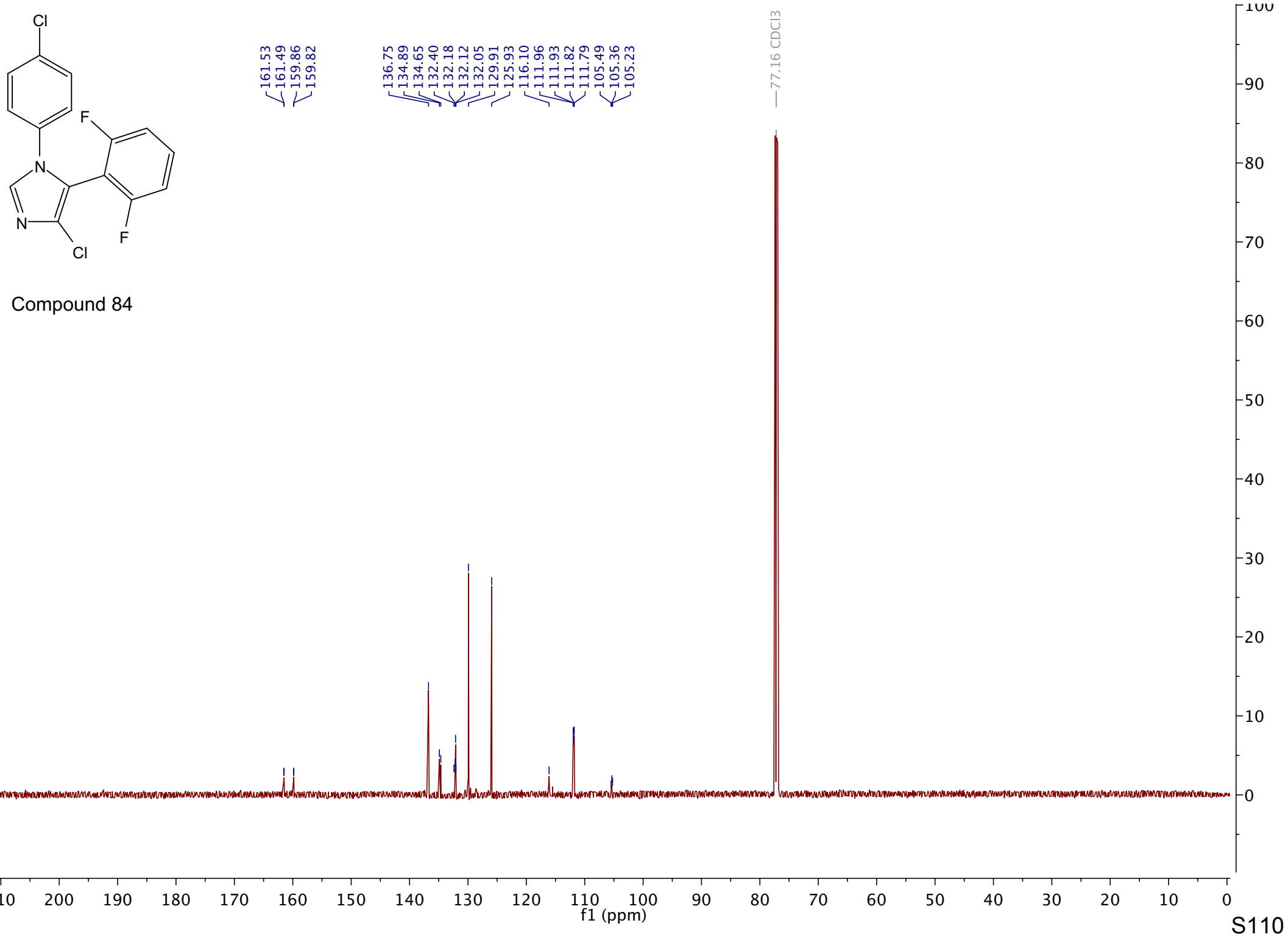


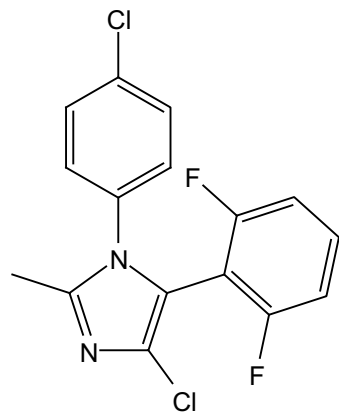
Compound 84



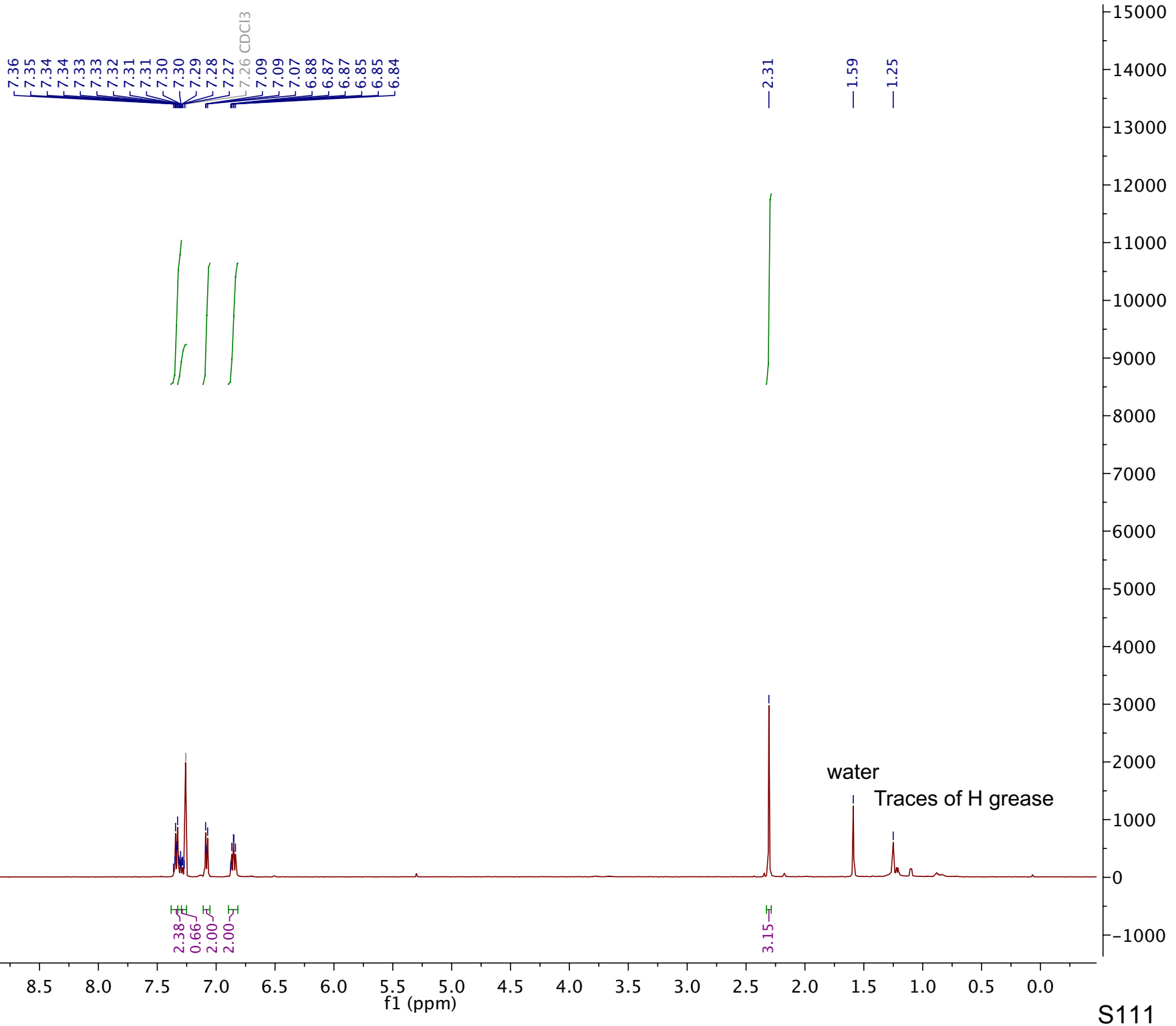


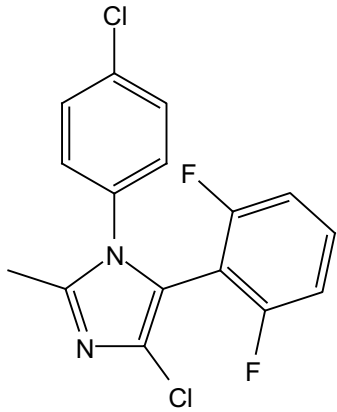
Compound 84



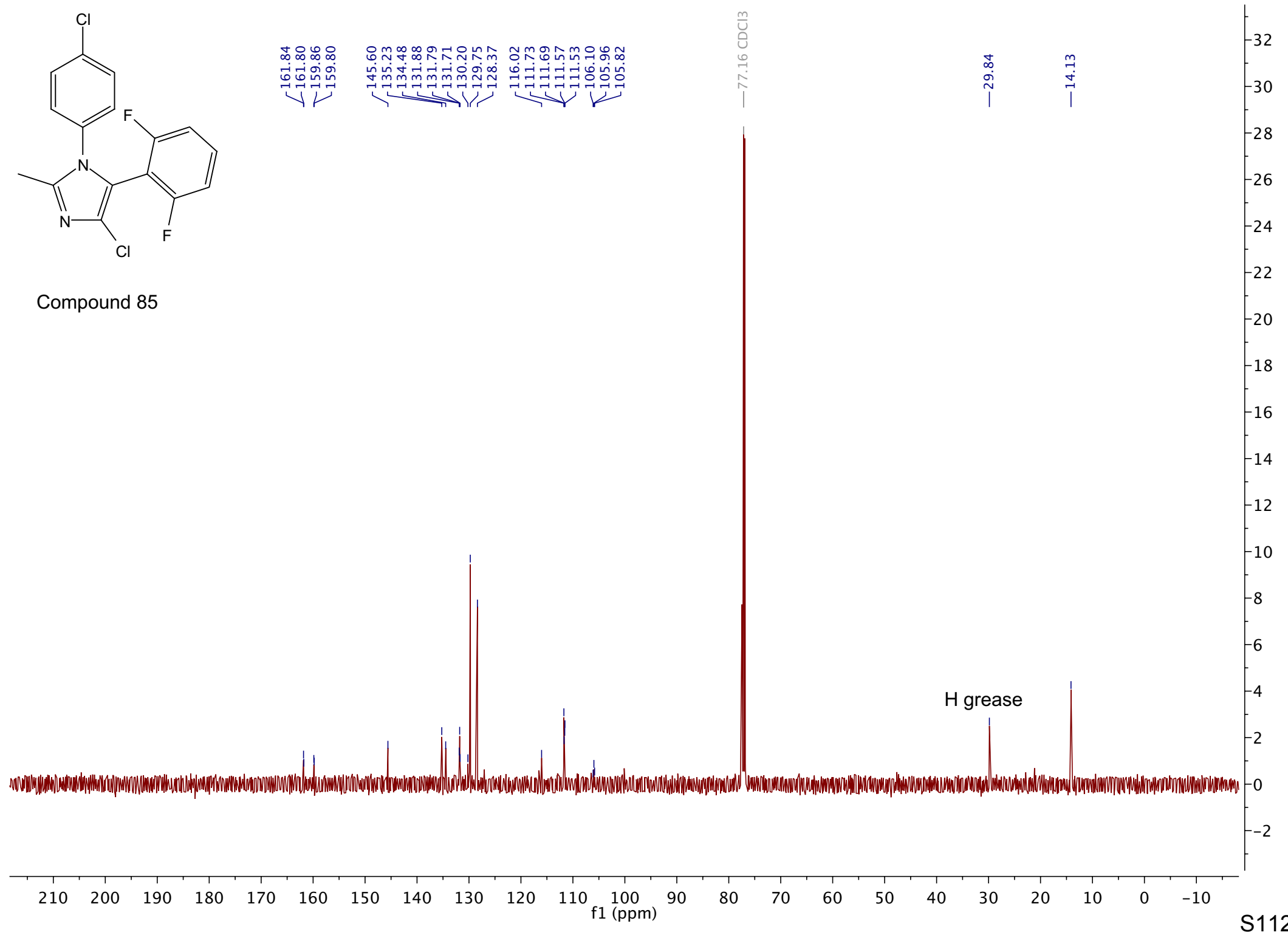


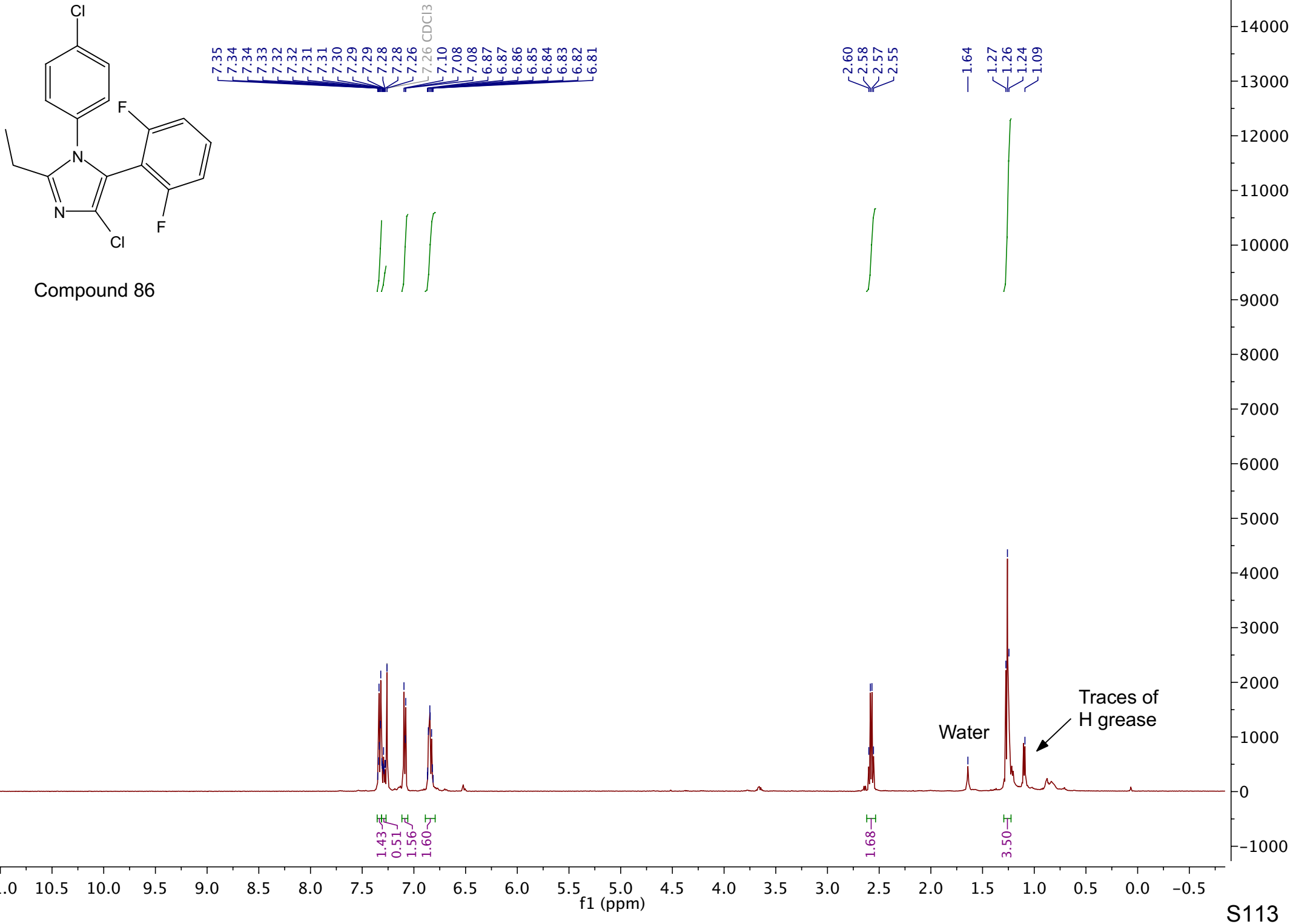
Compound 85

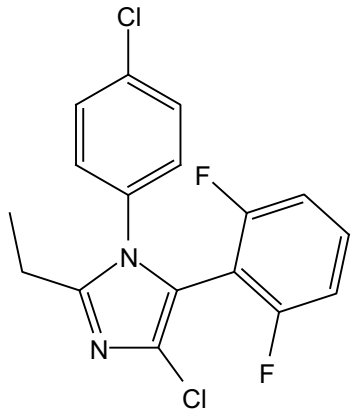




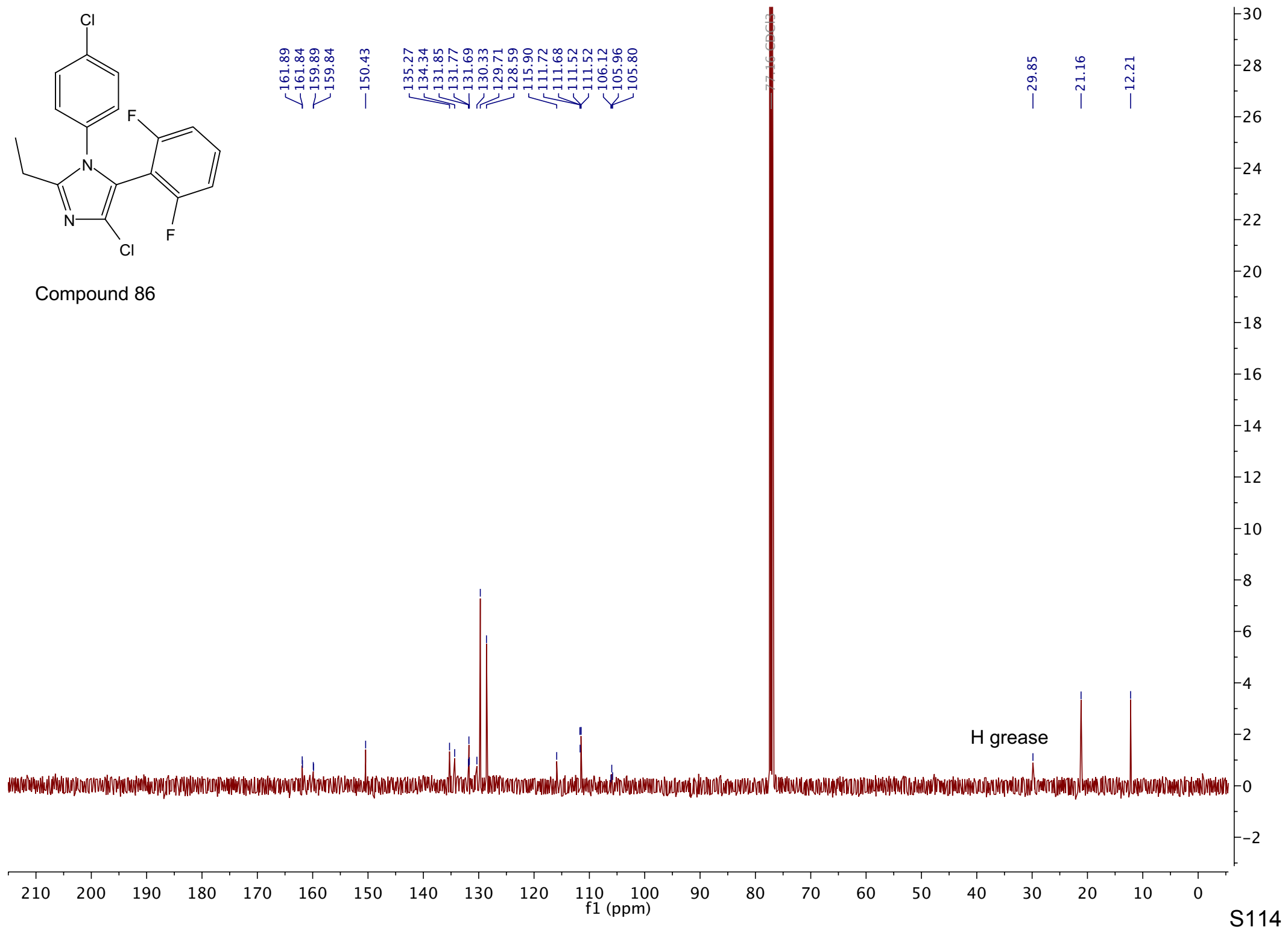
Compound 85

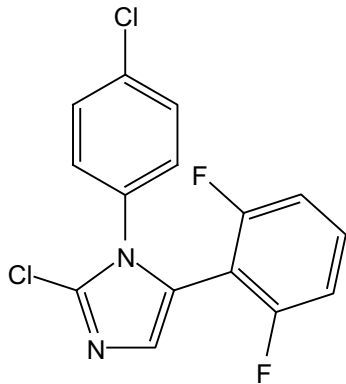




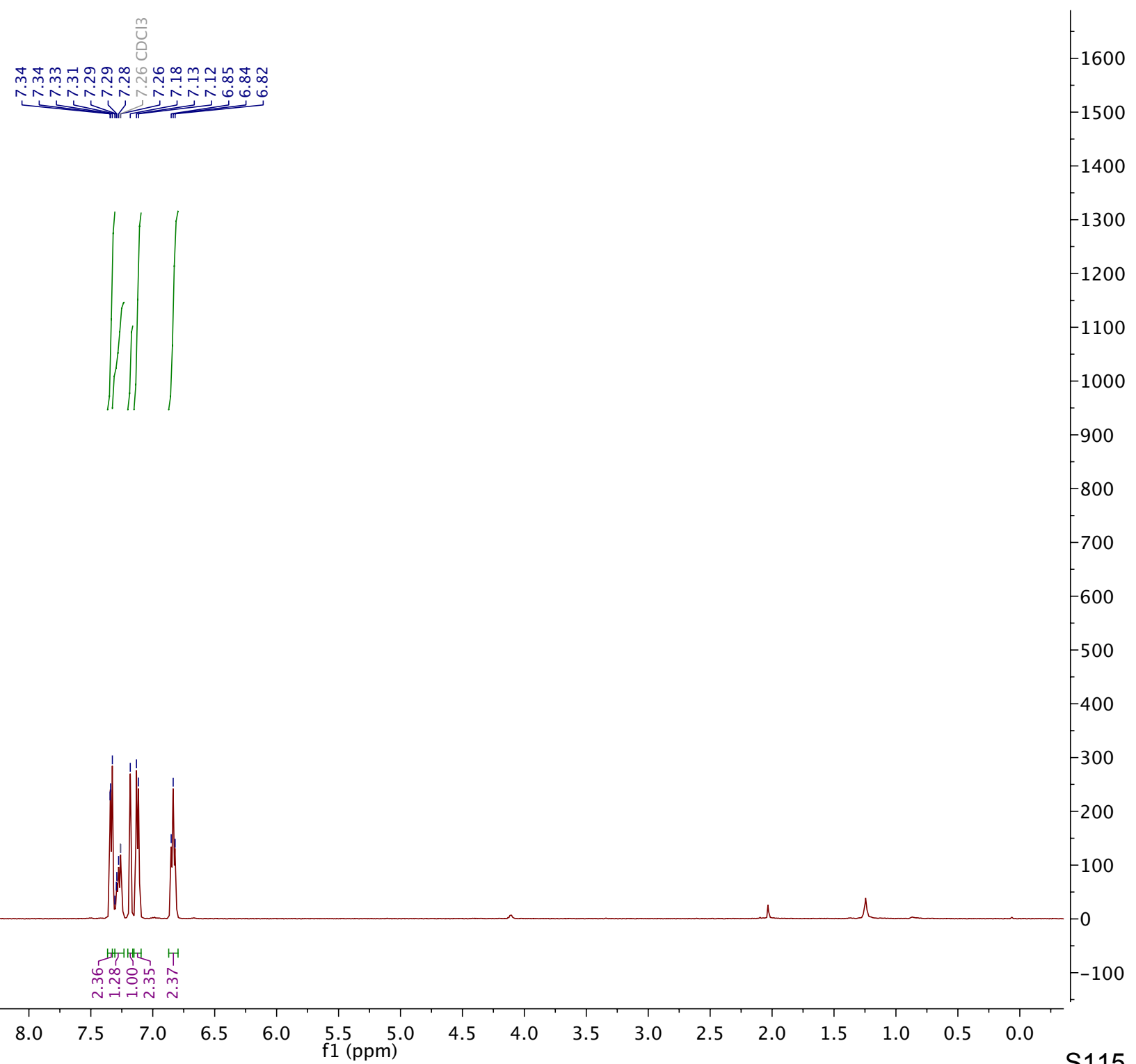


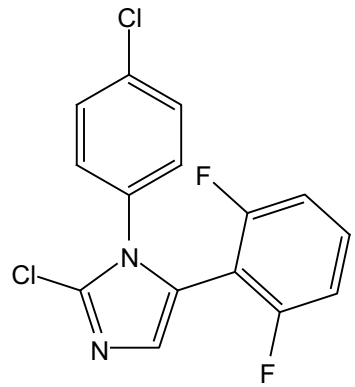
Compound 86



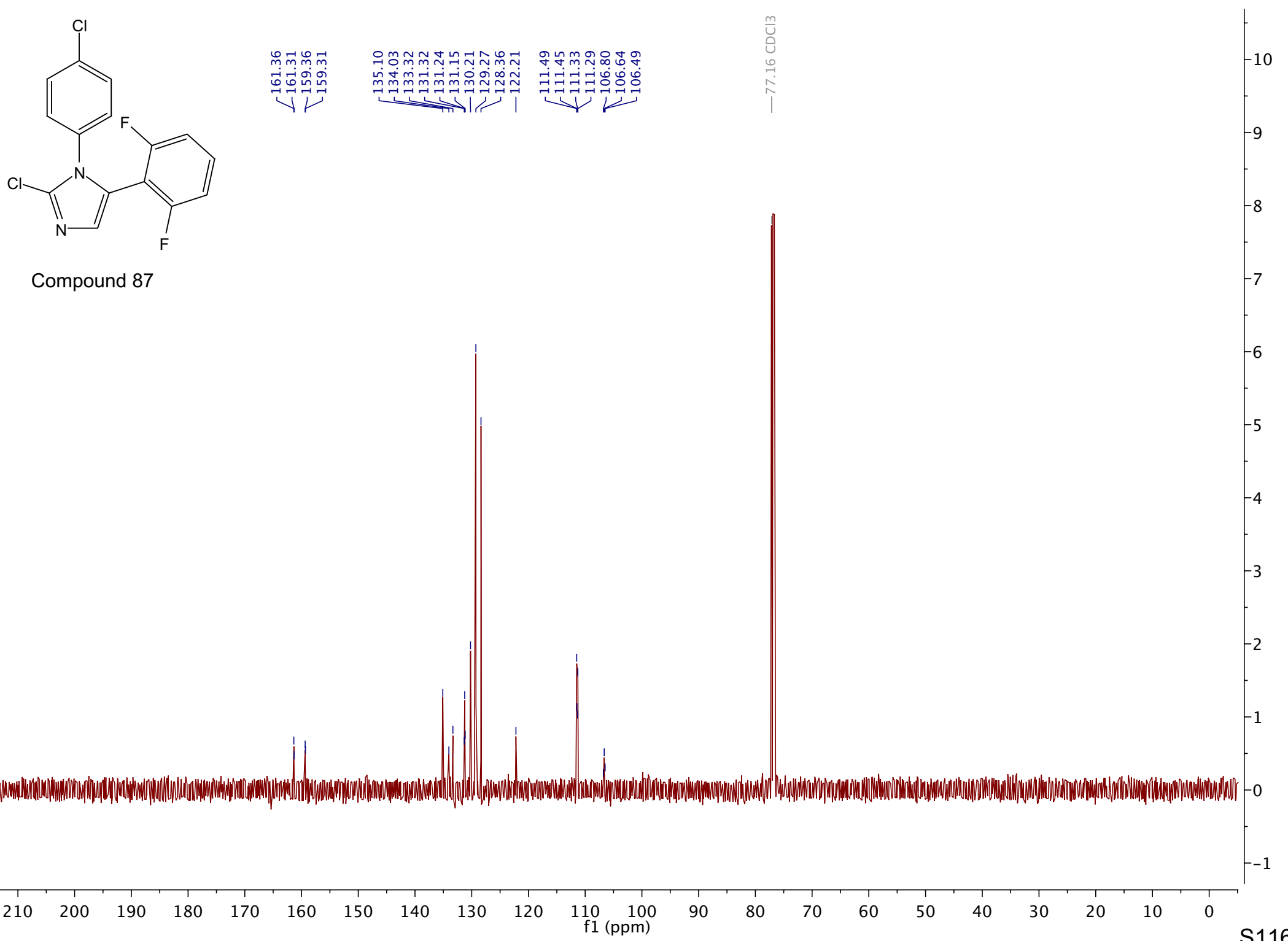


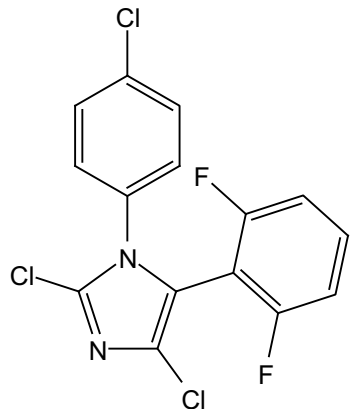
Compound 87



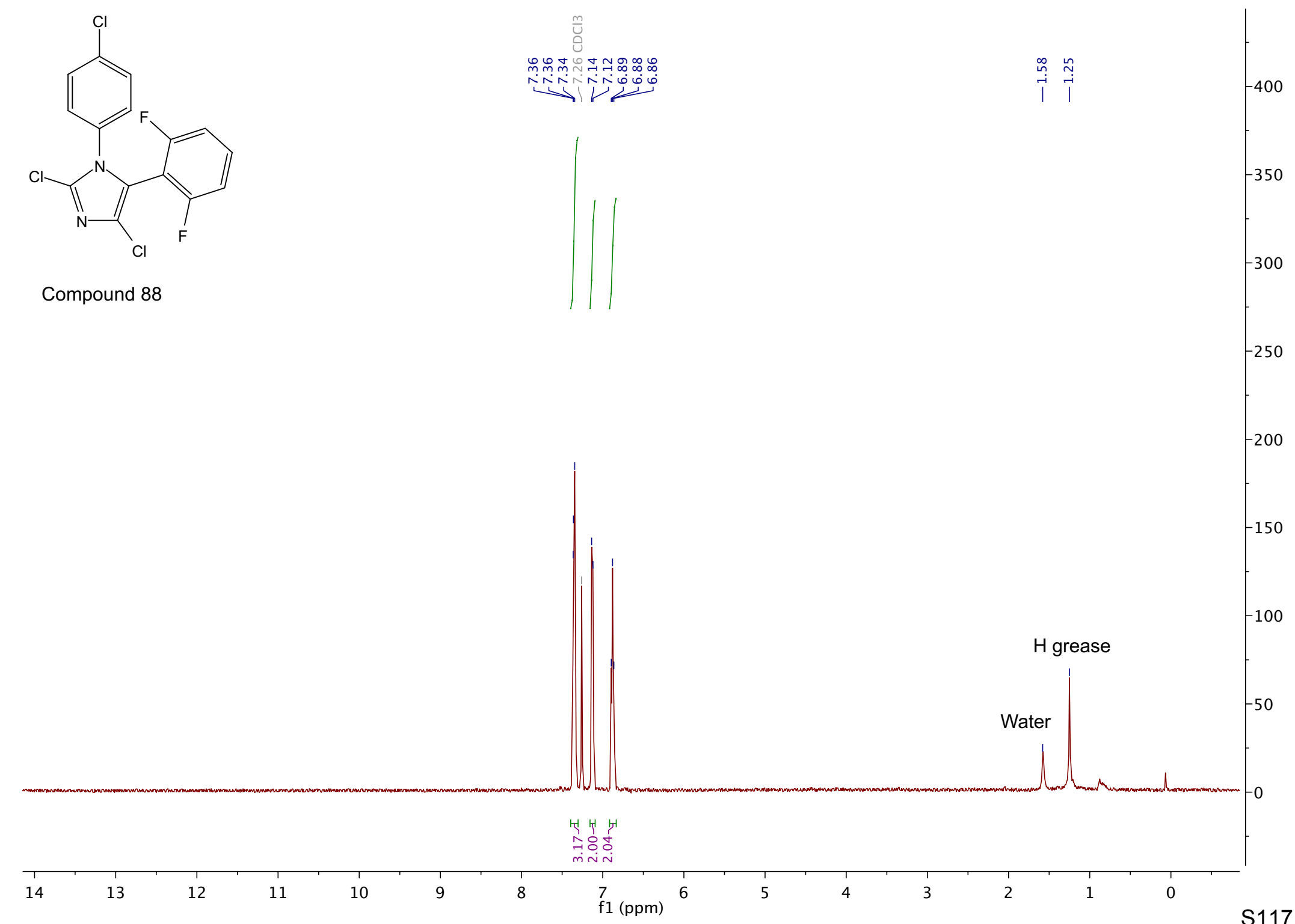


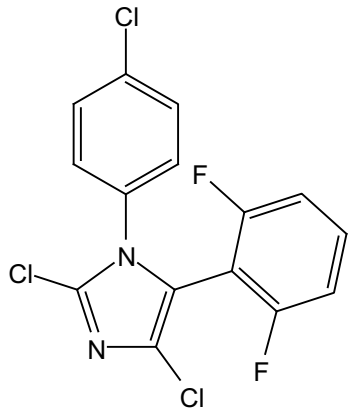
Compound 87



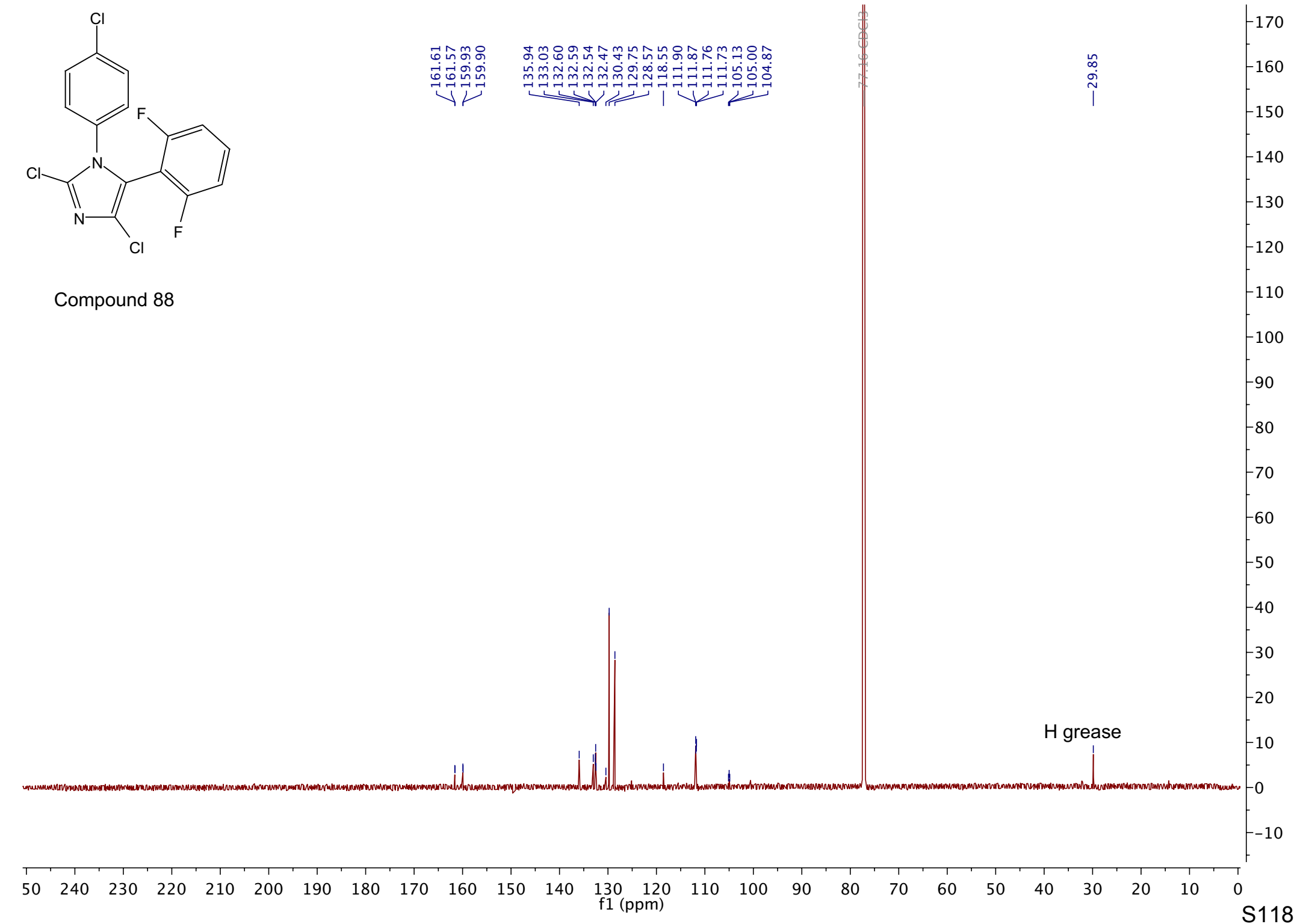


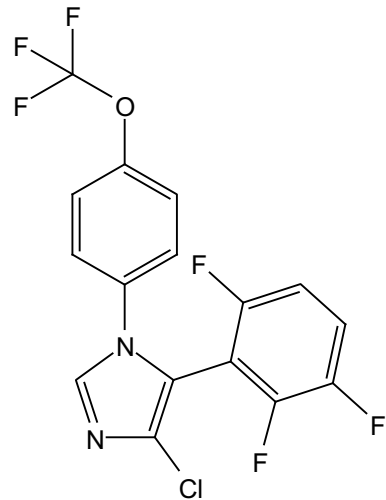
Compound 88



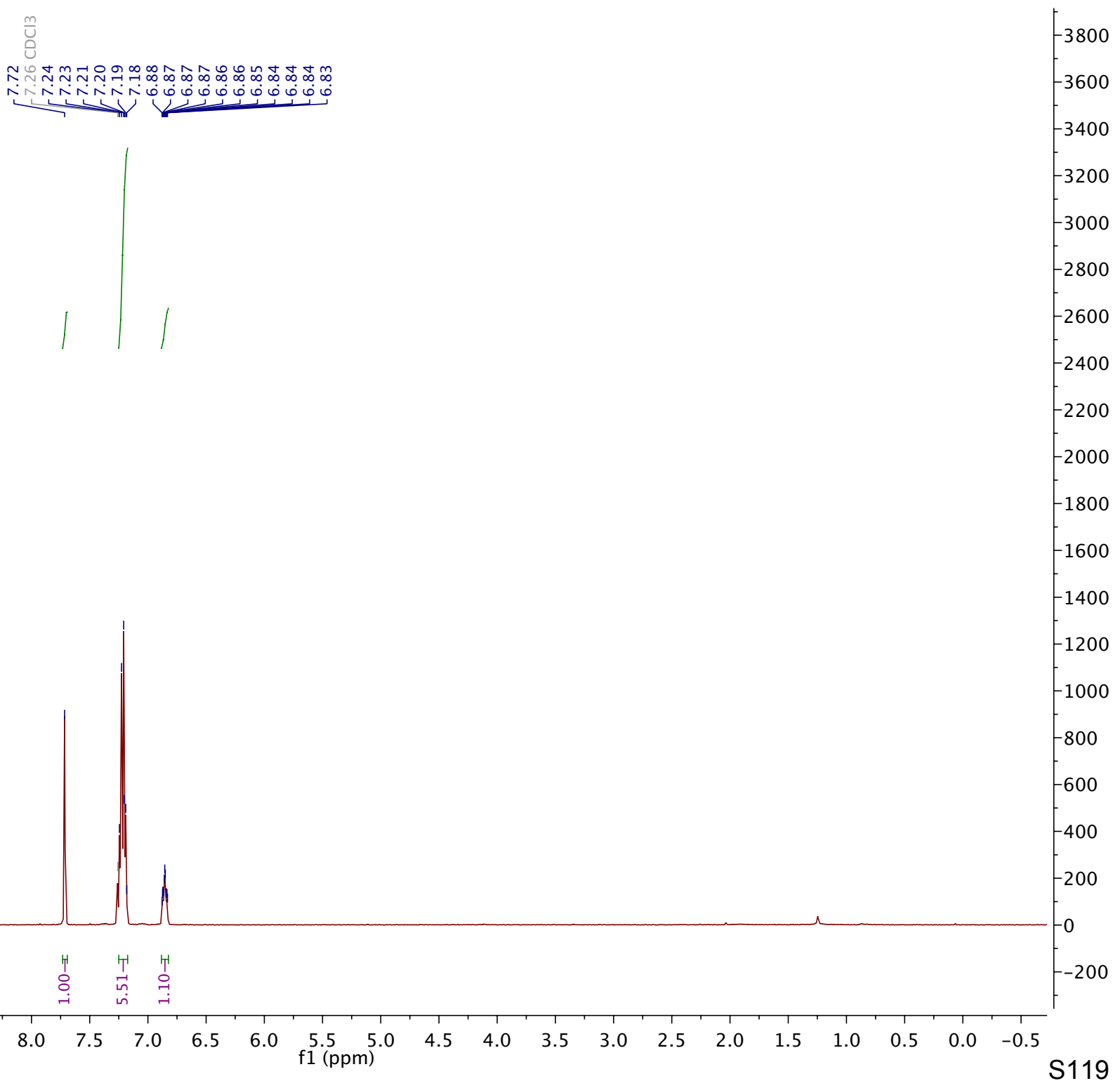


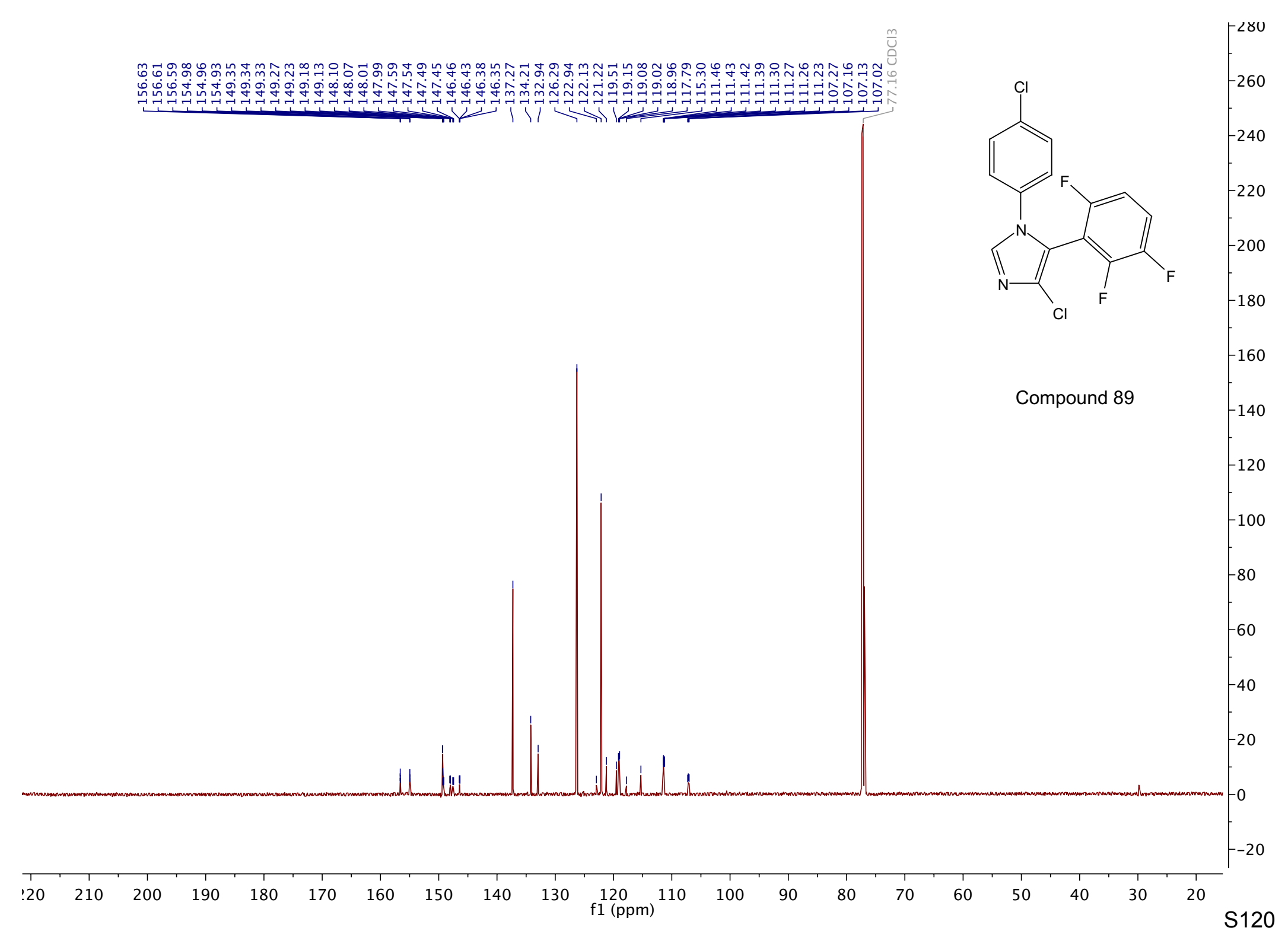
Compound 88

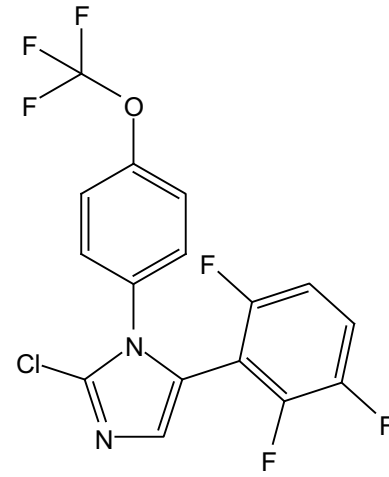




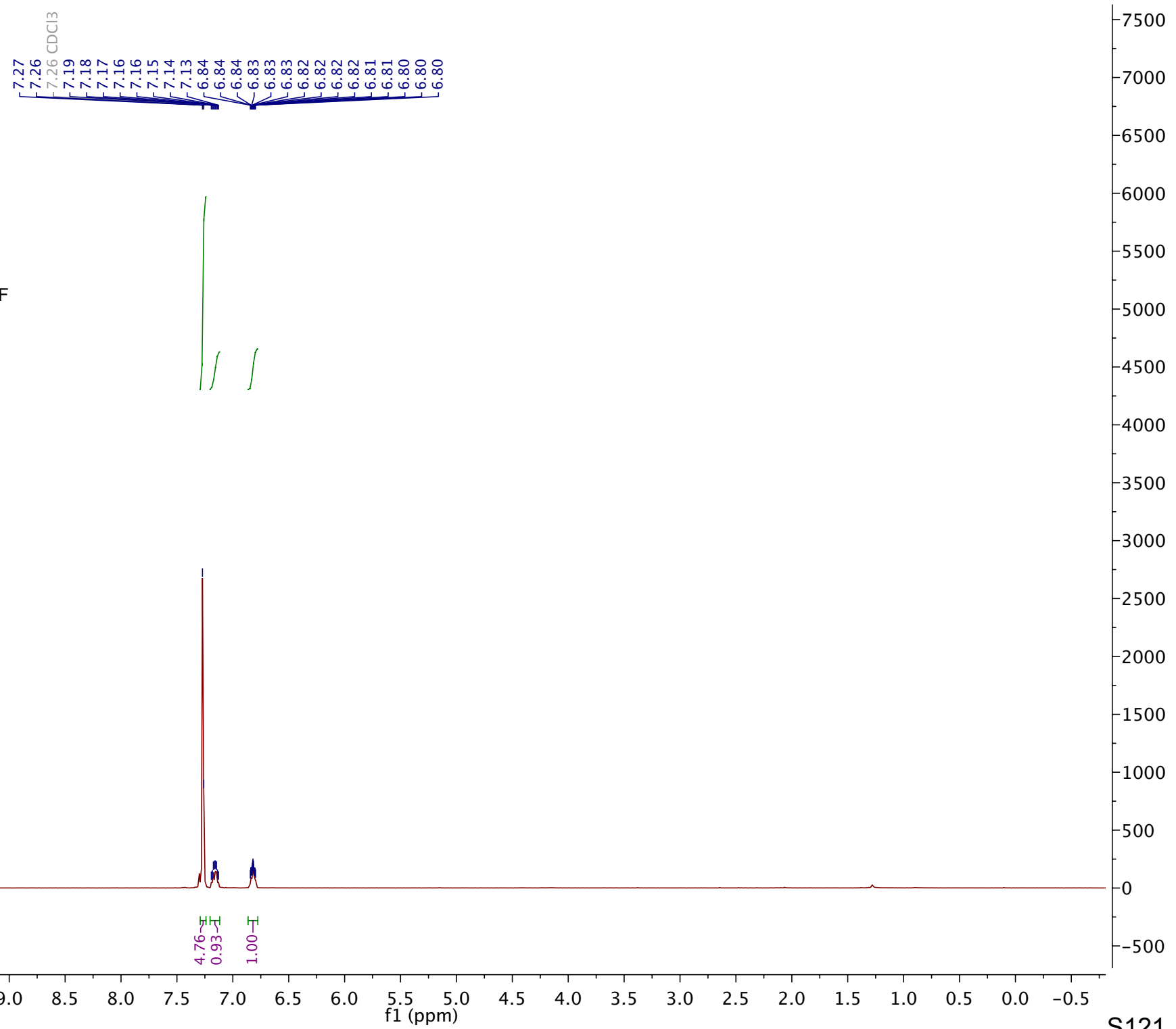
Compound 89

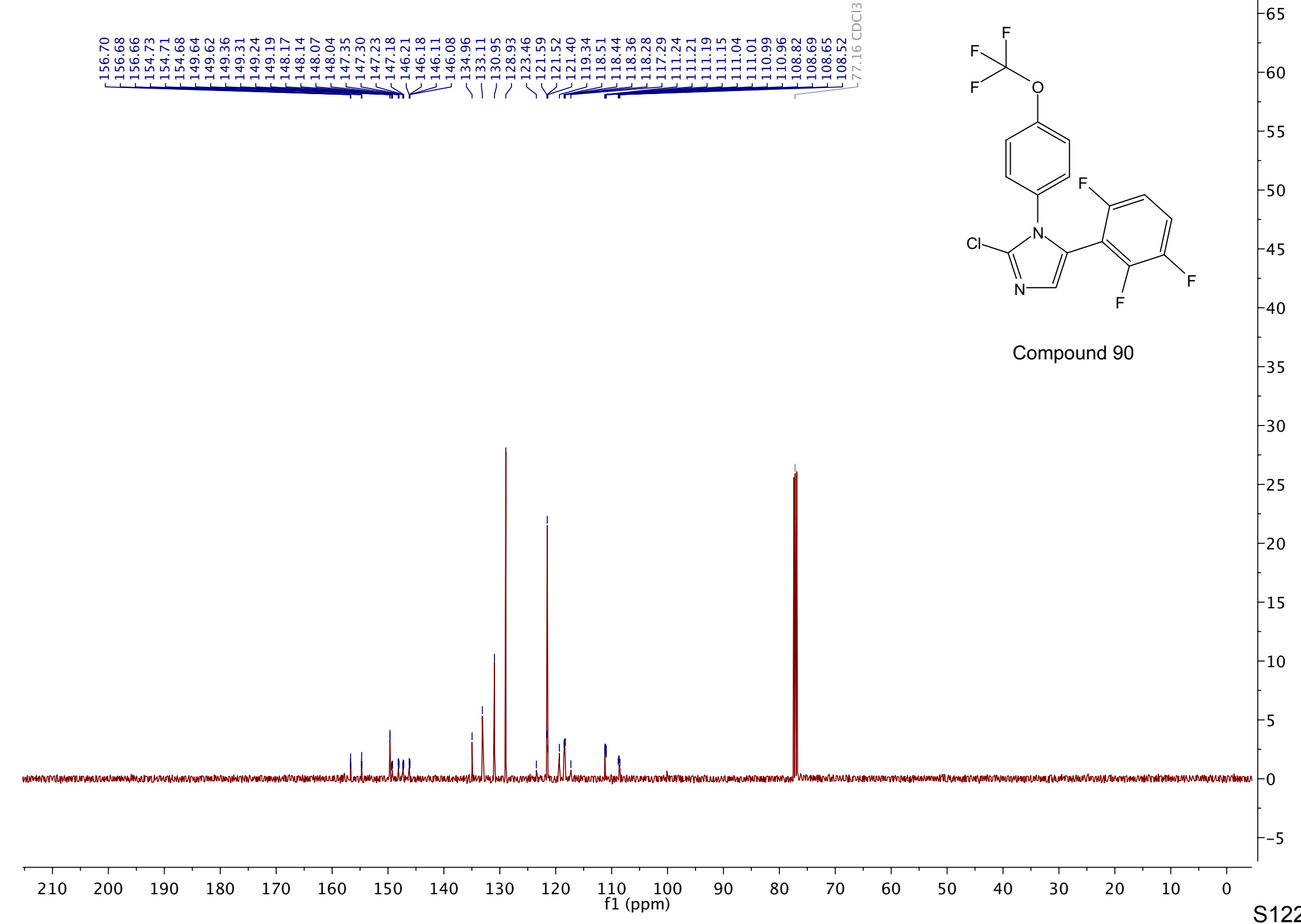
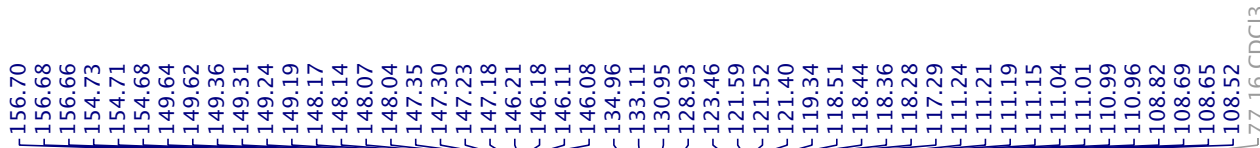


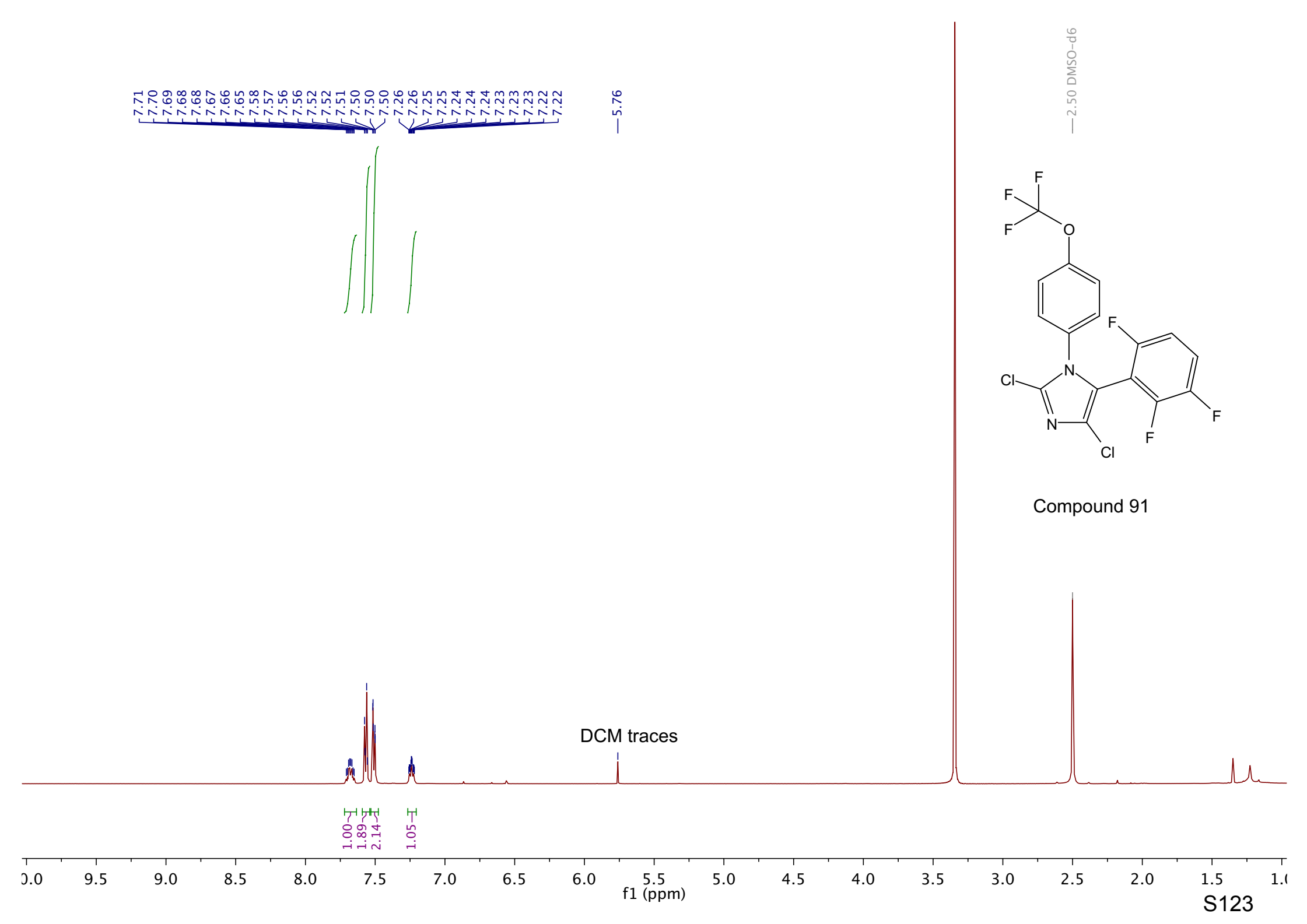


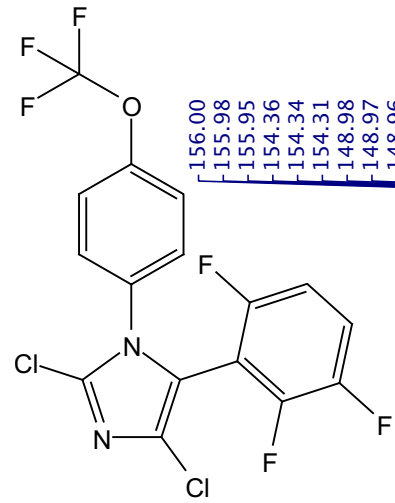


Compound 90

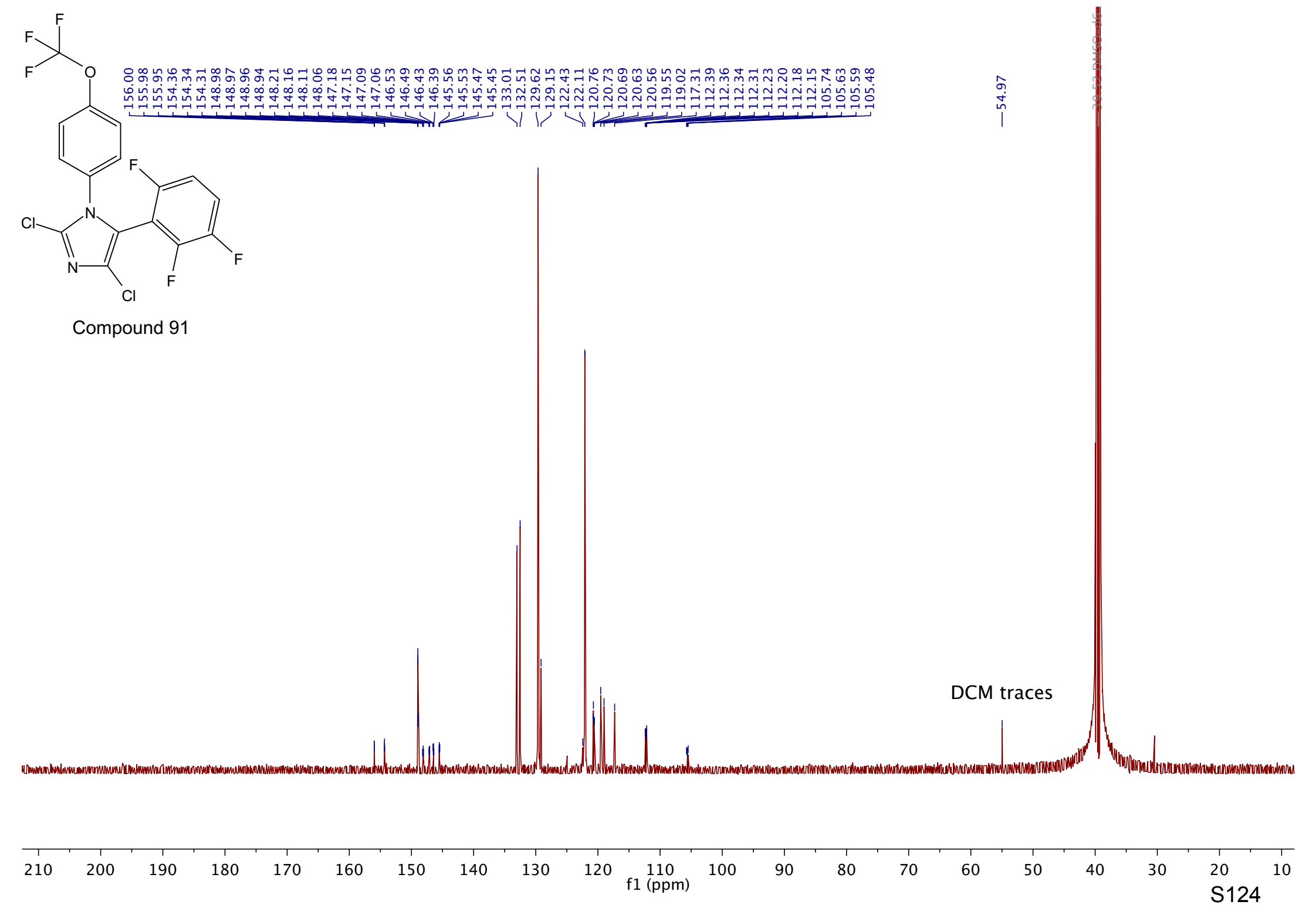


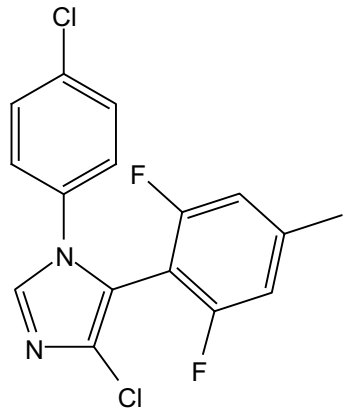




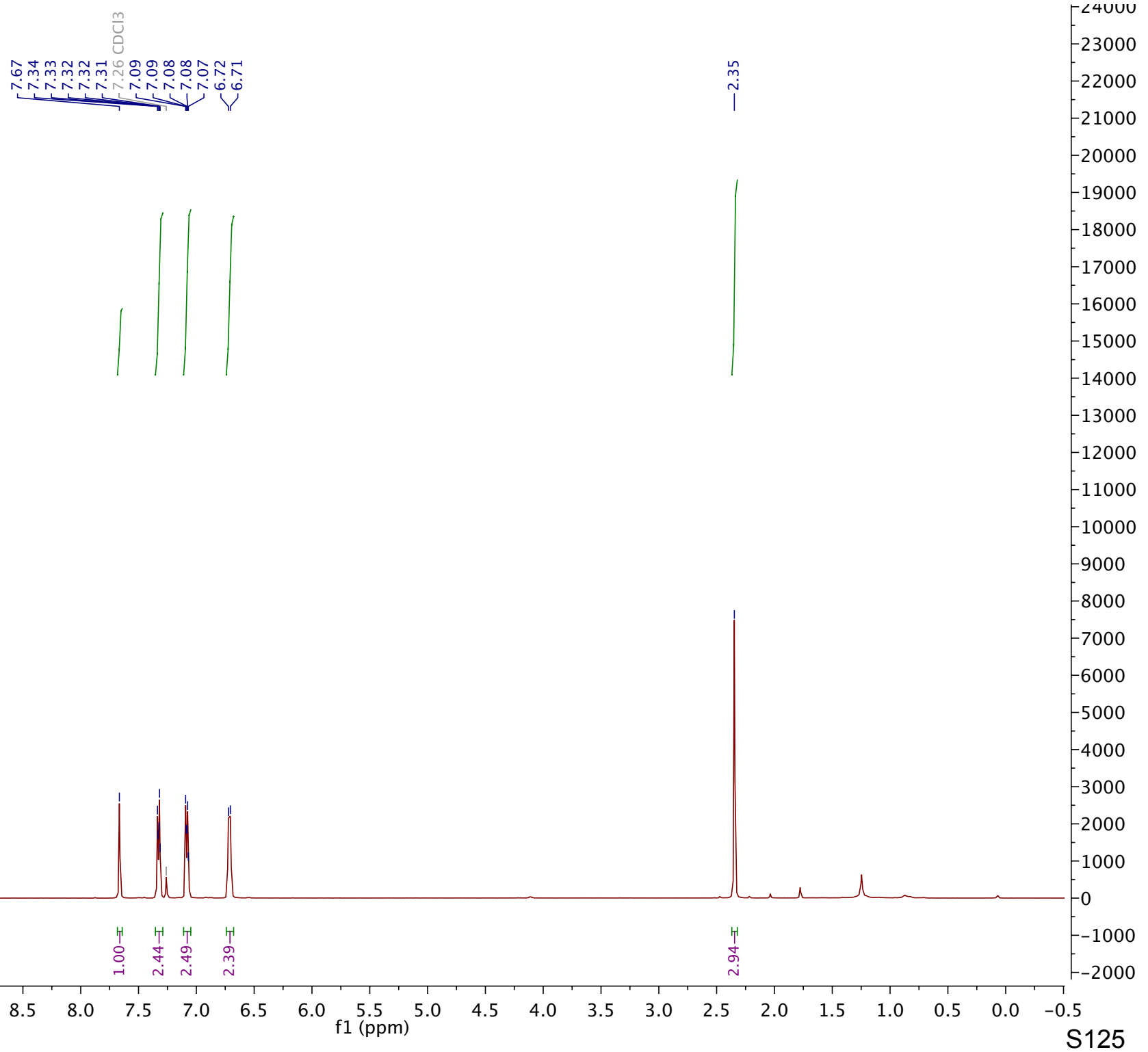


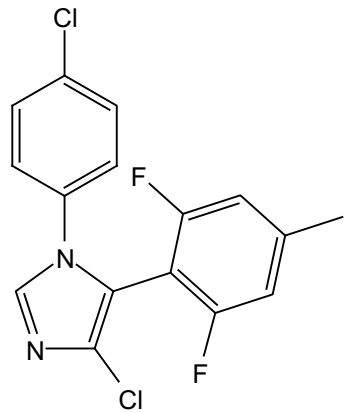
Compound 91



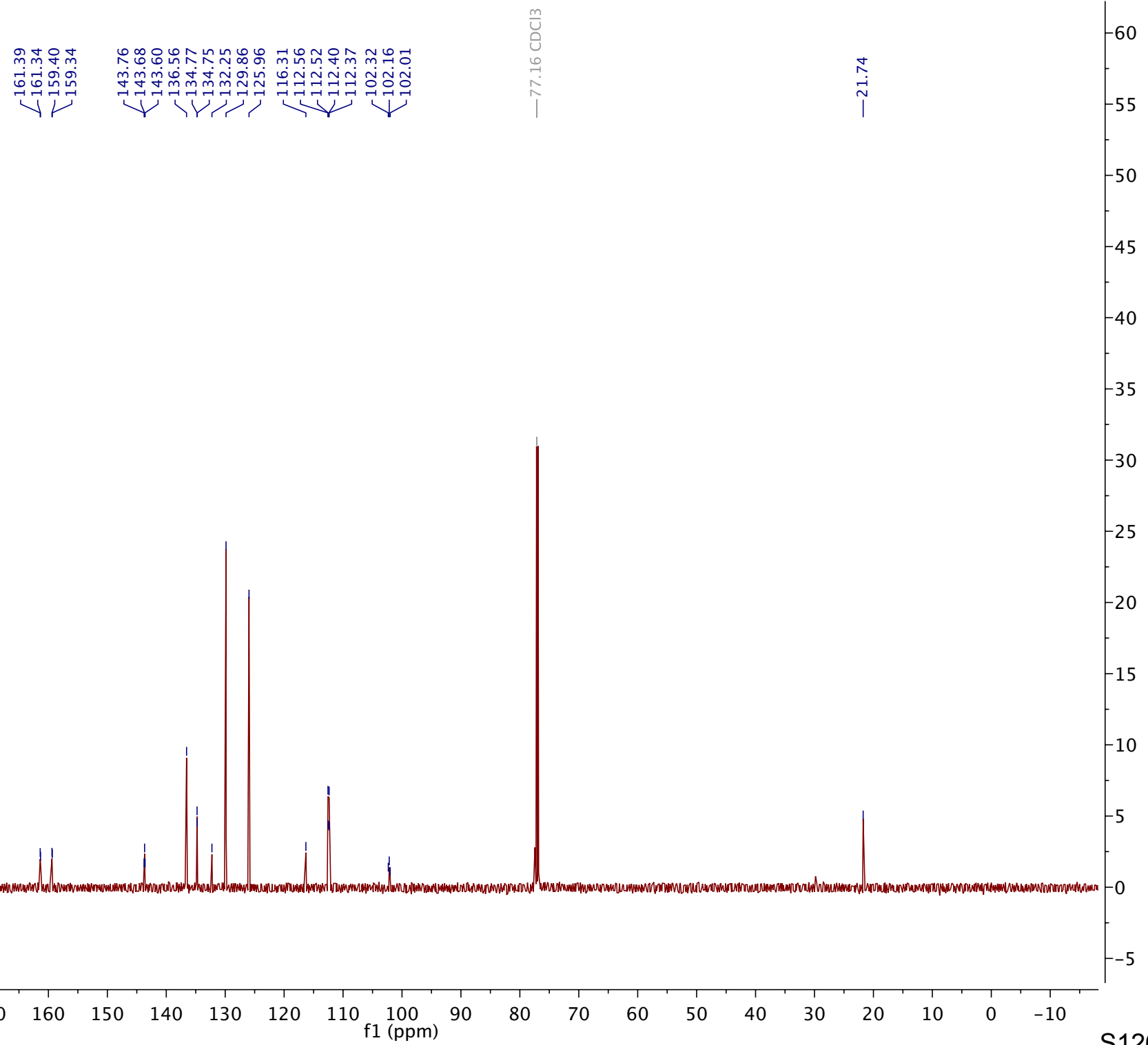


Compound 92





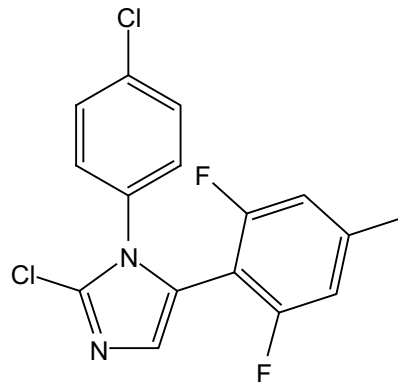
Compound 92



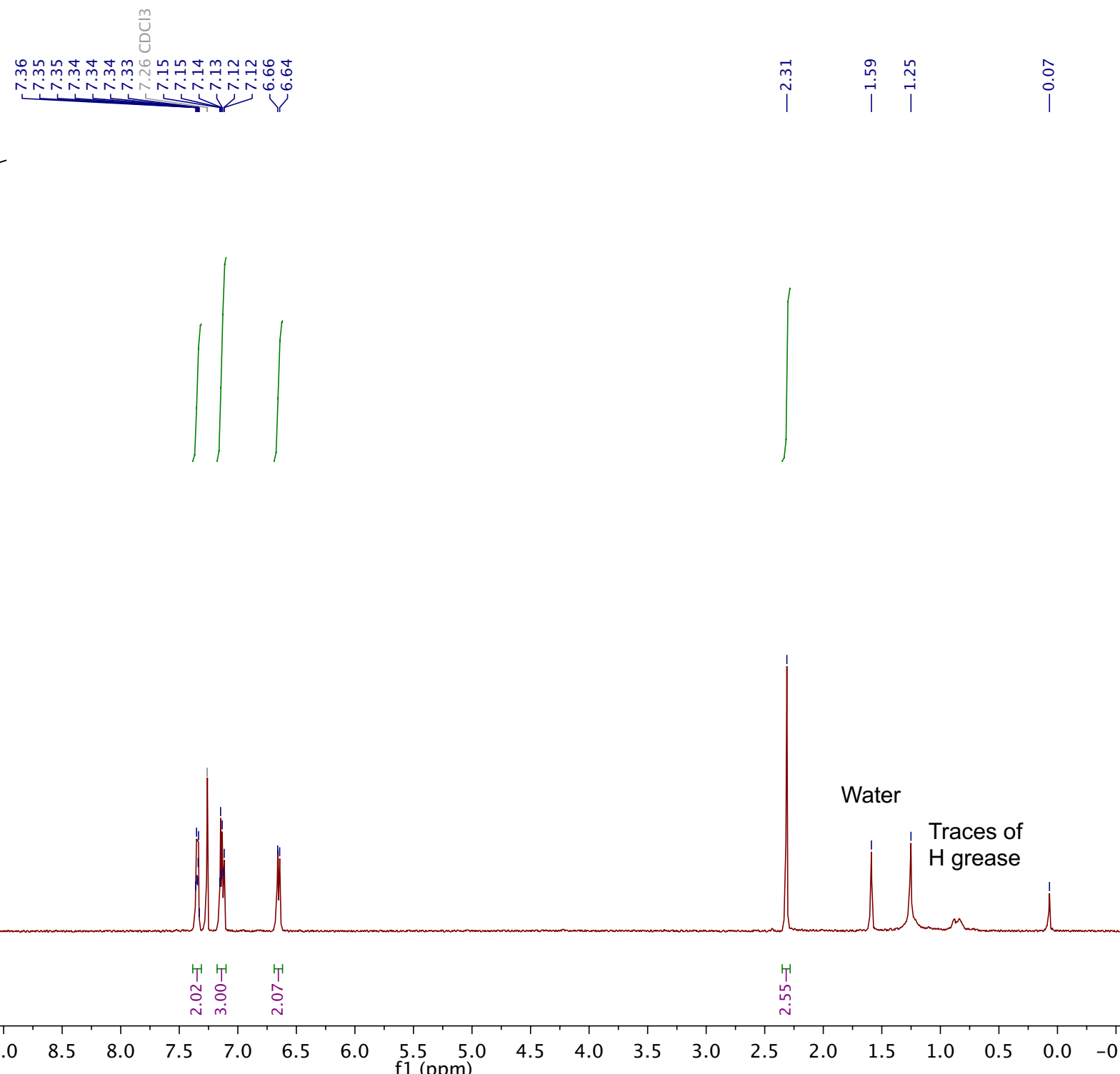
210 200 190 180 170 160 150 140 130 120 110 100 90 80 70 60 50 40 30 20 10 0 -10

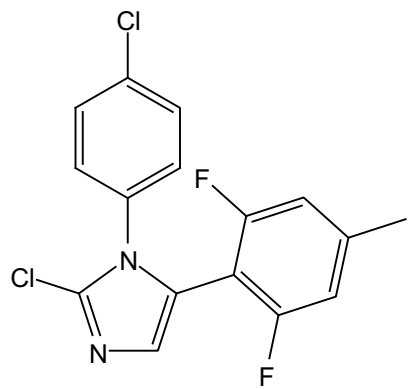
f1 (ppm)

S126



Compound 93



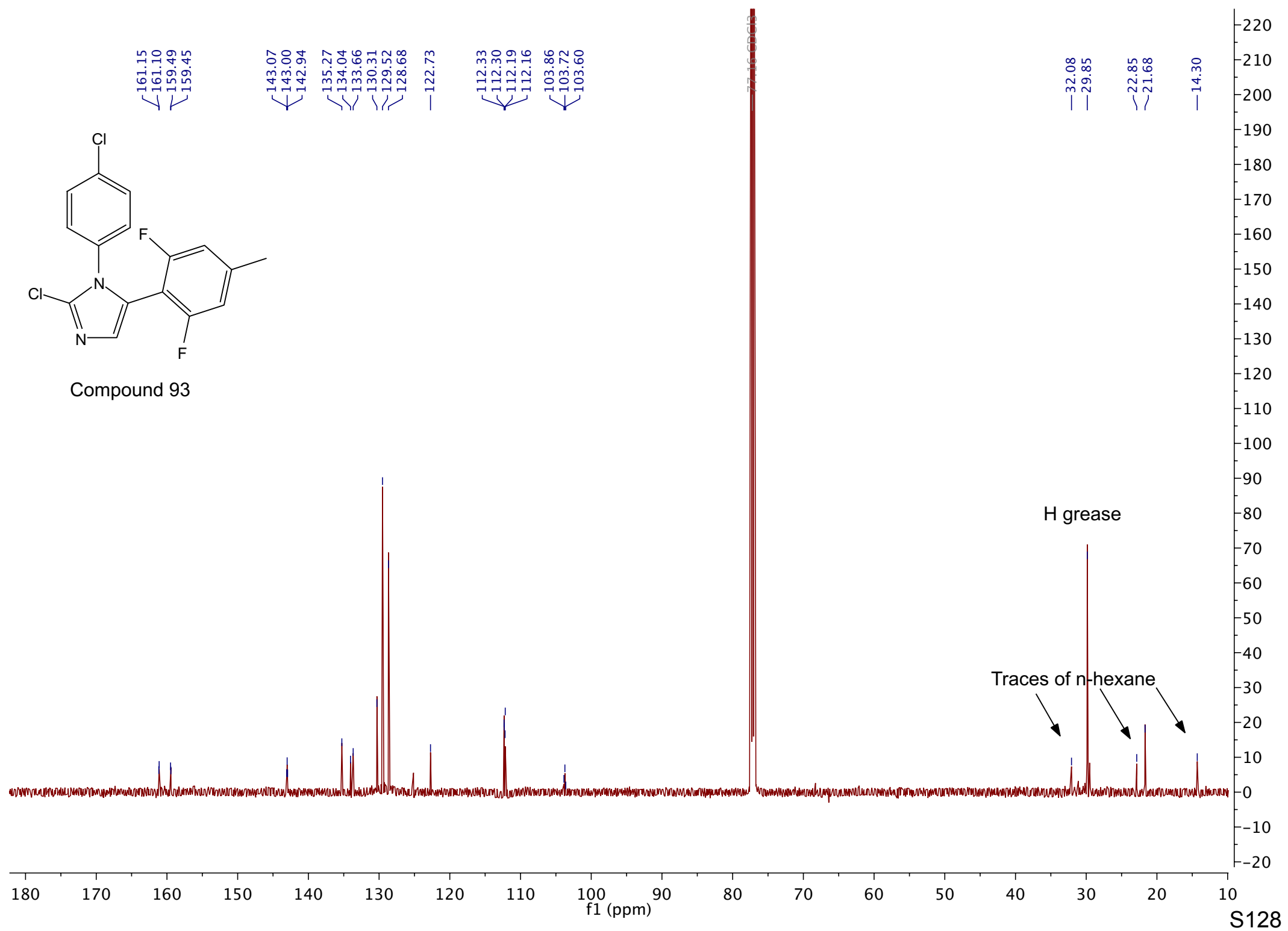


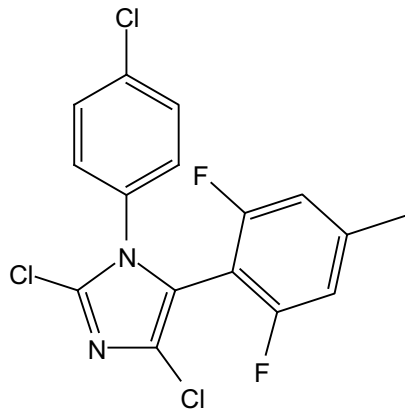
161.15
 161.10
 159.49
 159.45
 143.07
 143.00
 142.94
 135.27
 134.04
 133.66
 130.31
 129.52
 128.68
 -122.73

112.33
 112.30
 112.19
 112.16
 103.86
 103.72
 103.60

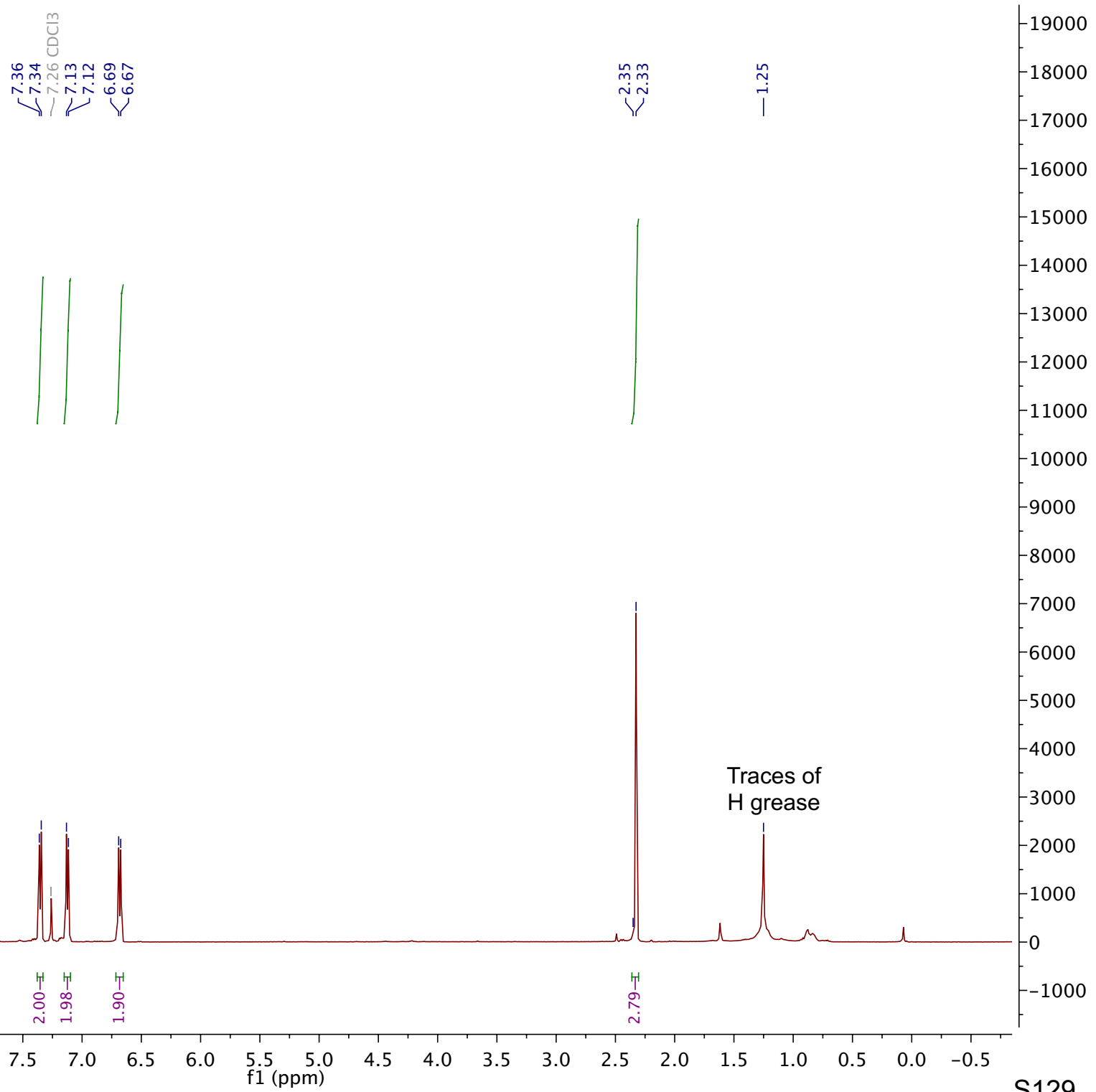
77.15 CDCl₃

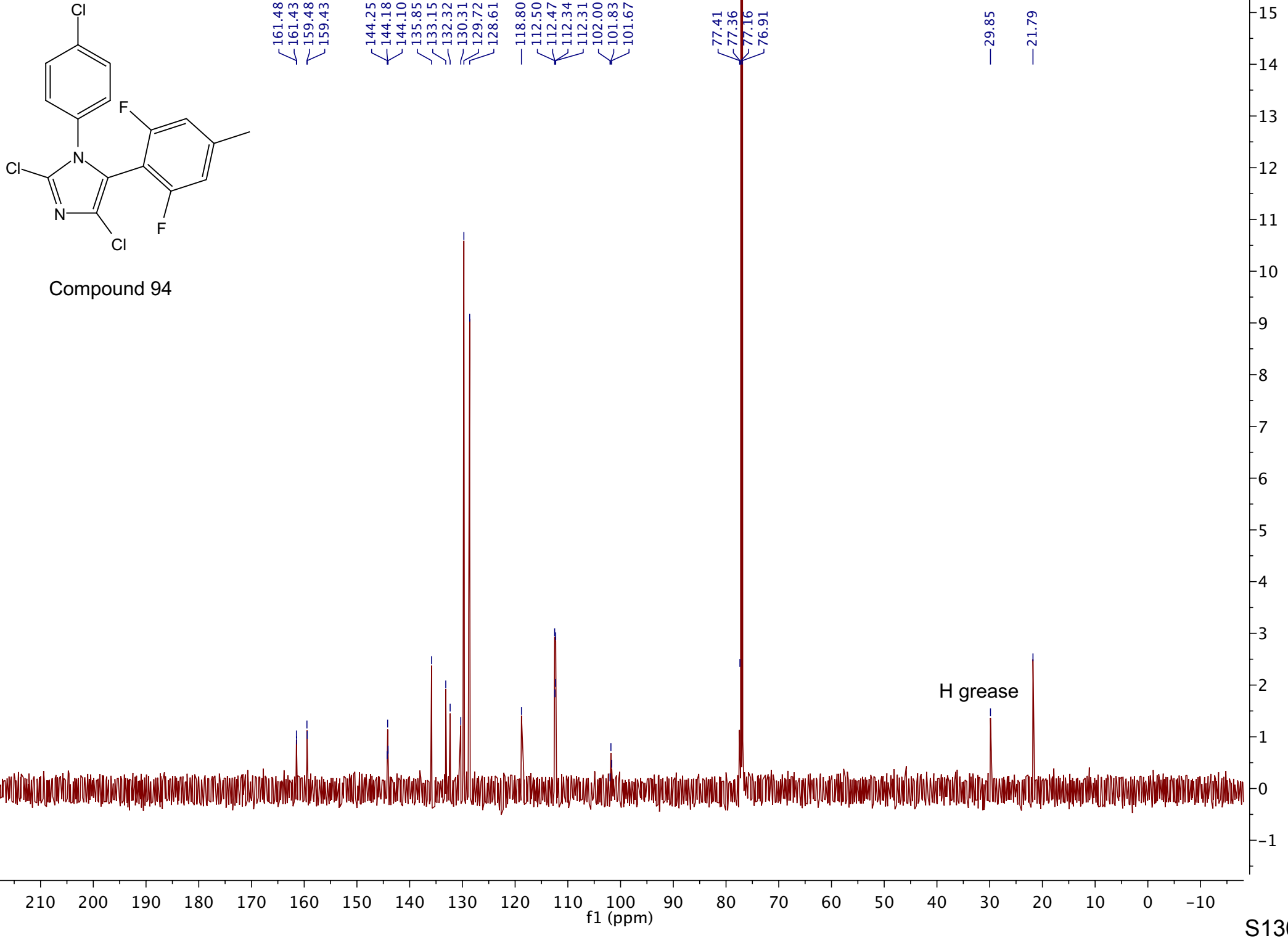
-32.08
 -29.85
 ~22.85
 ~21.68
 -14.30

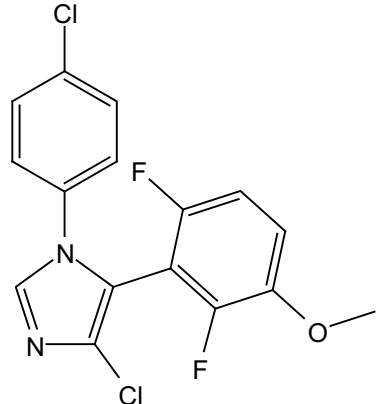




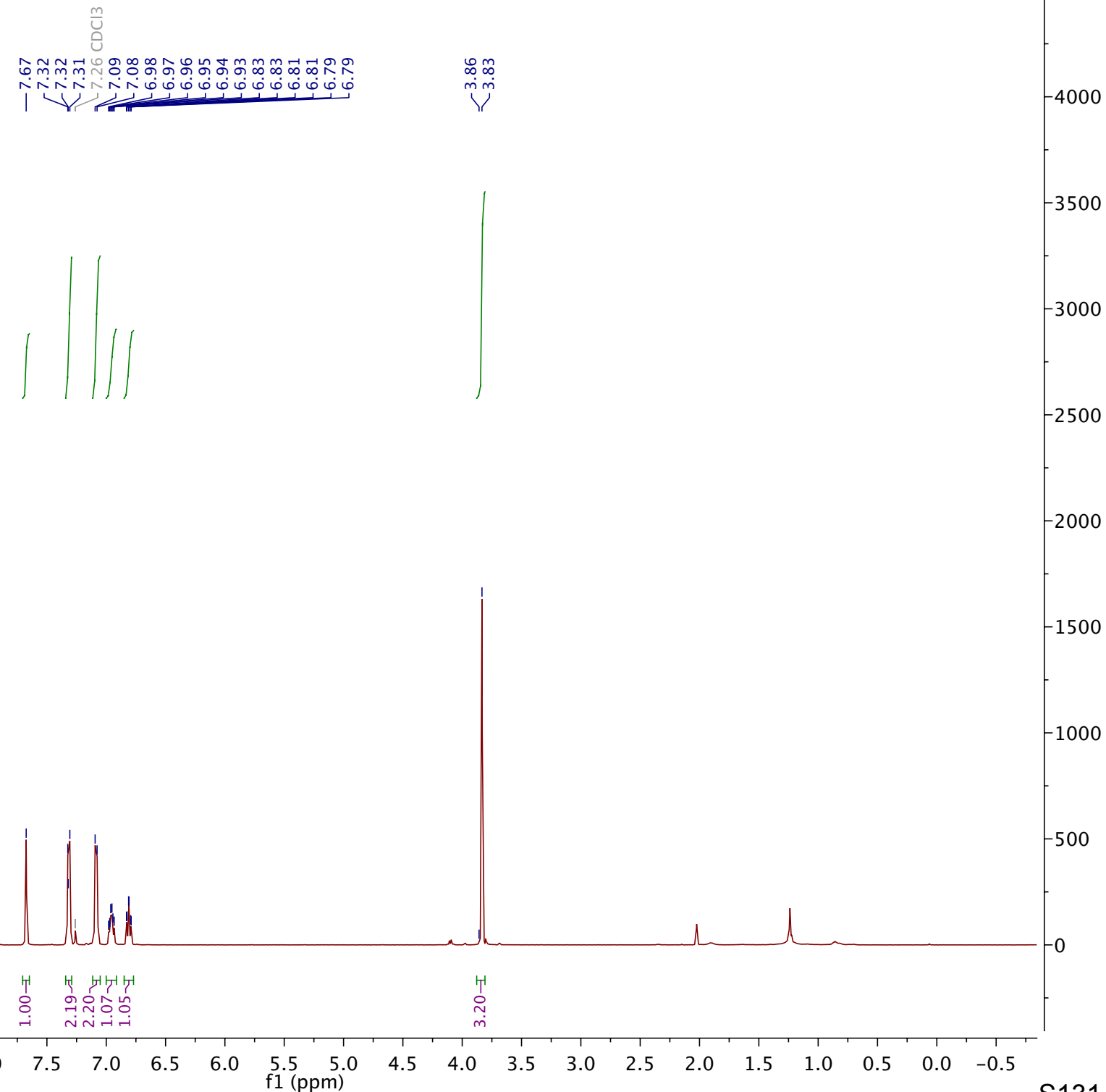
Compound 94

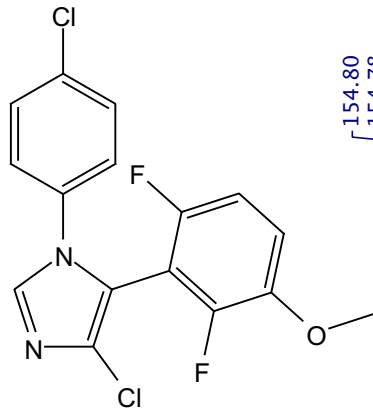




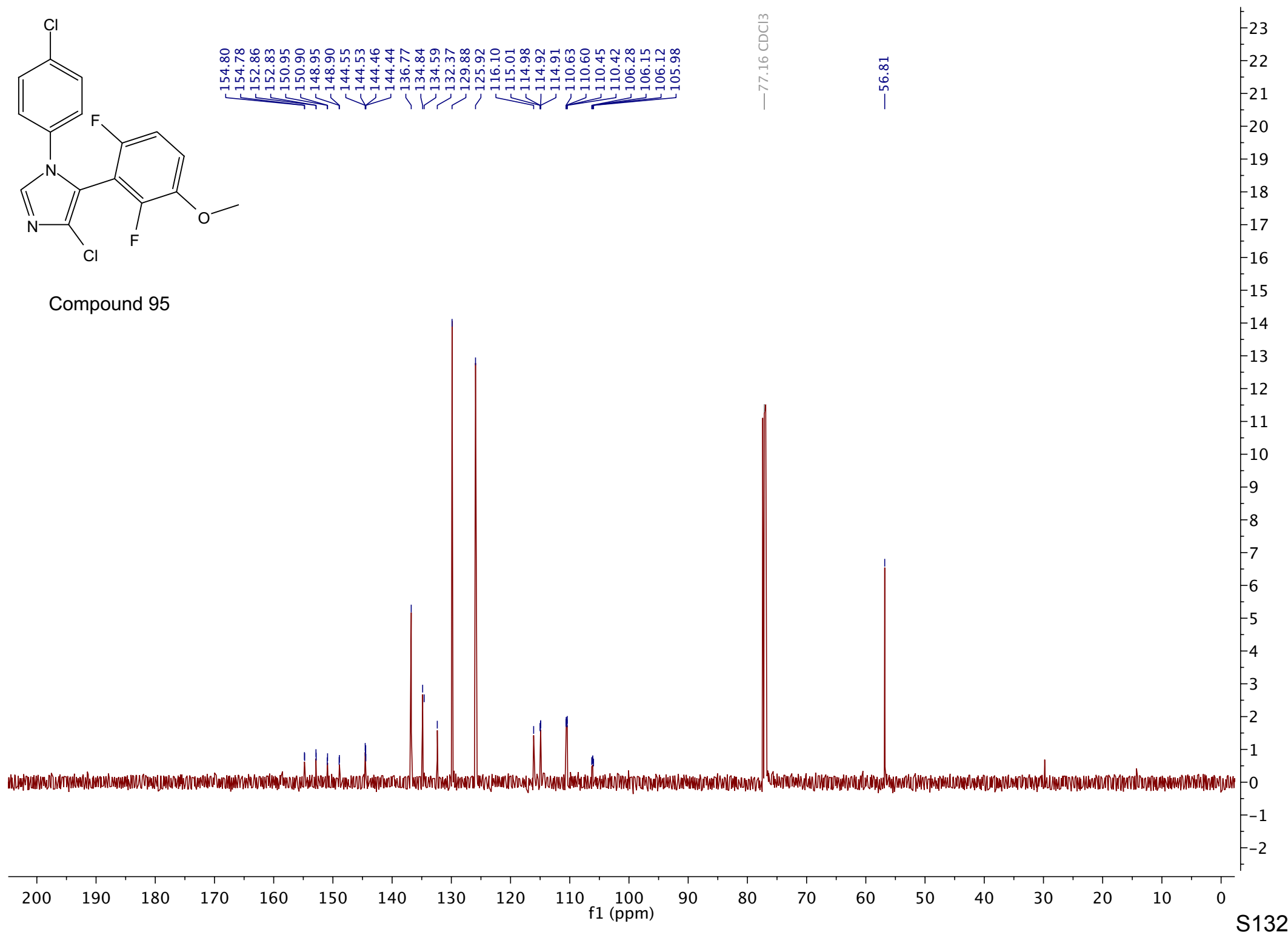


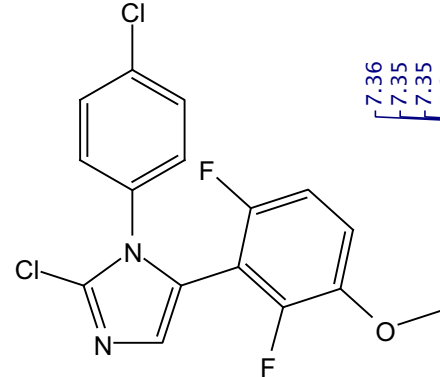
Compound 95



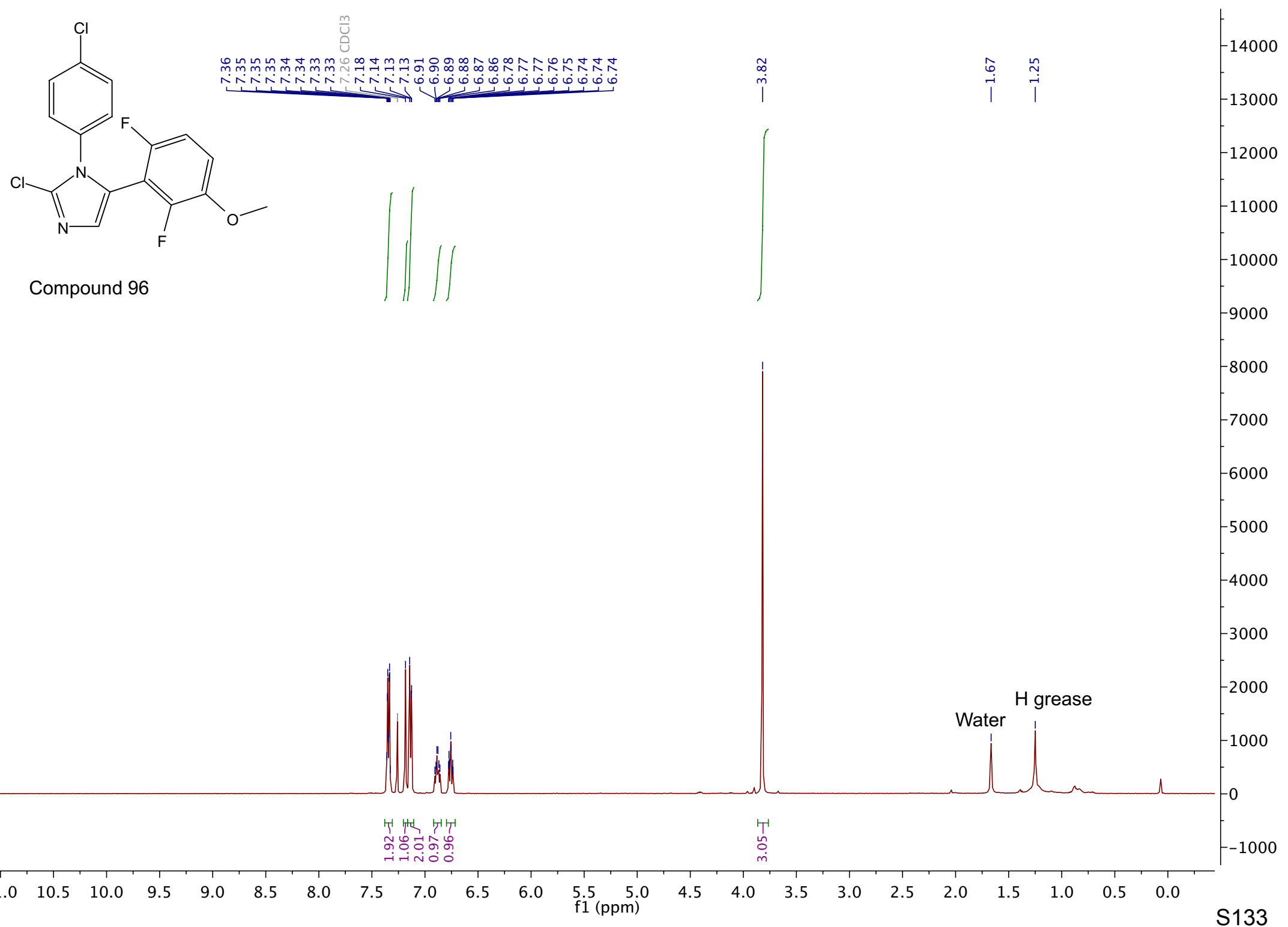


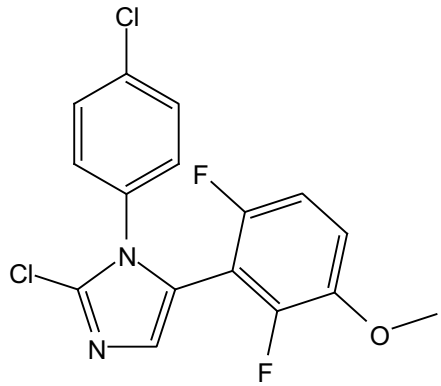
Compound 95



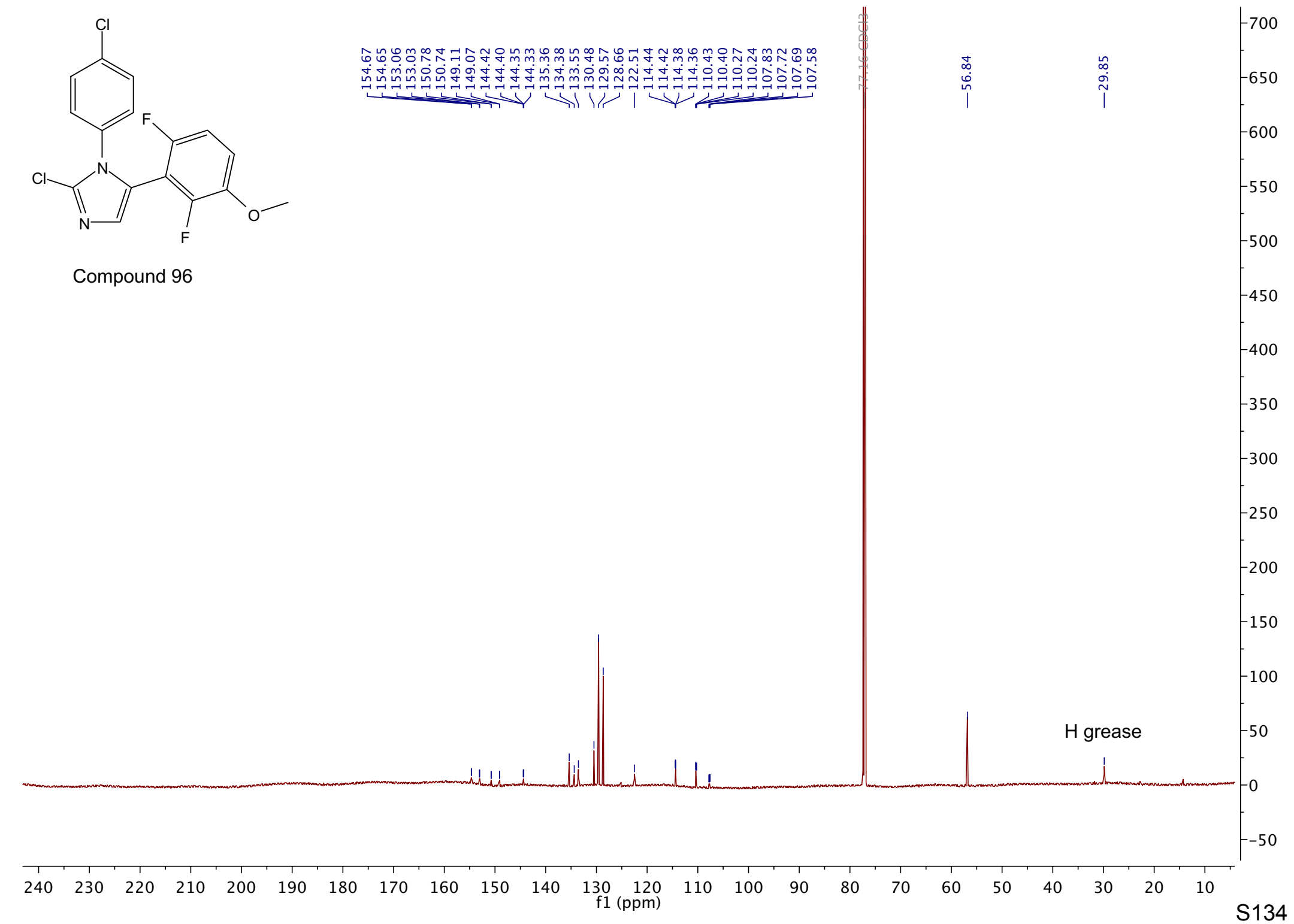


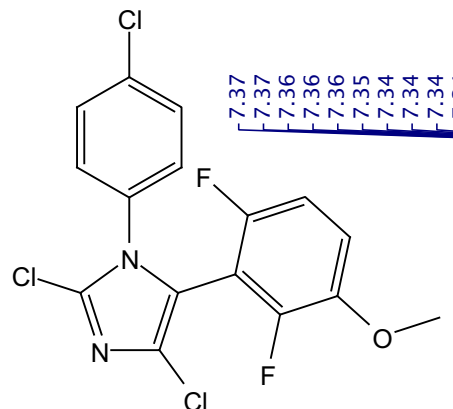
Compound 96



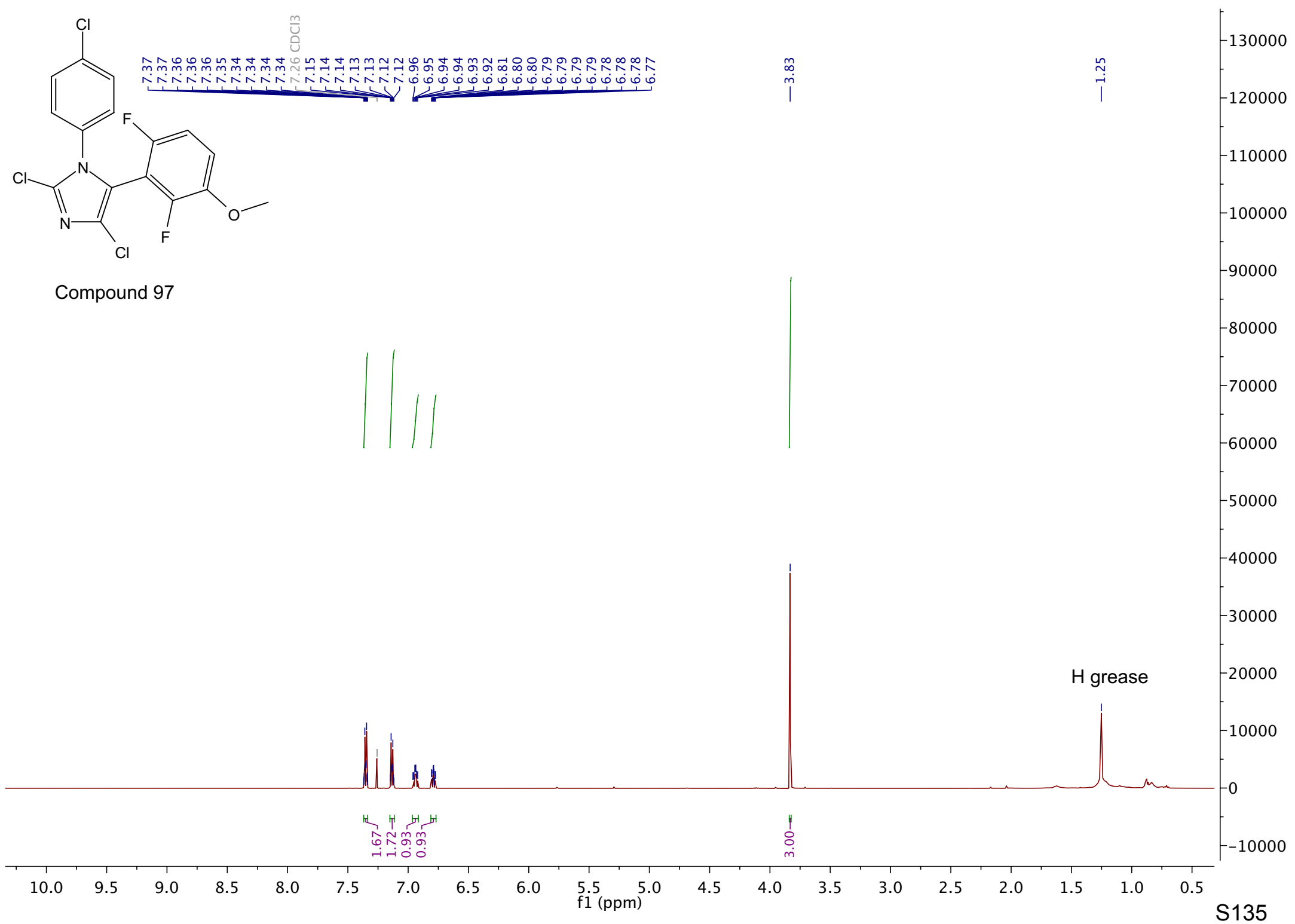


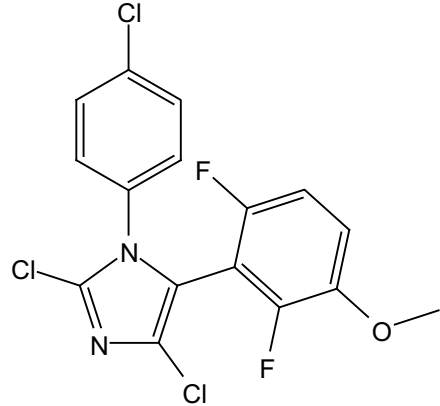
Compound 96



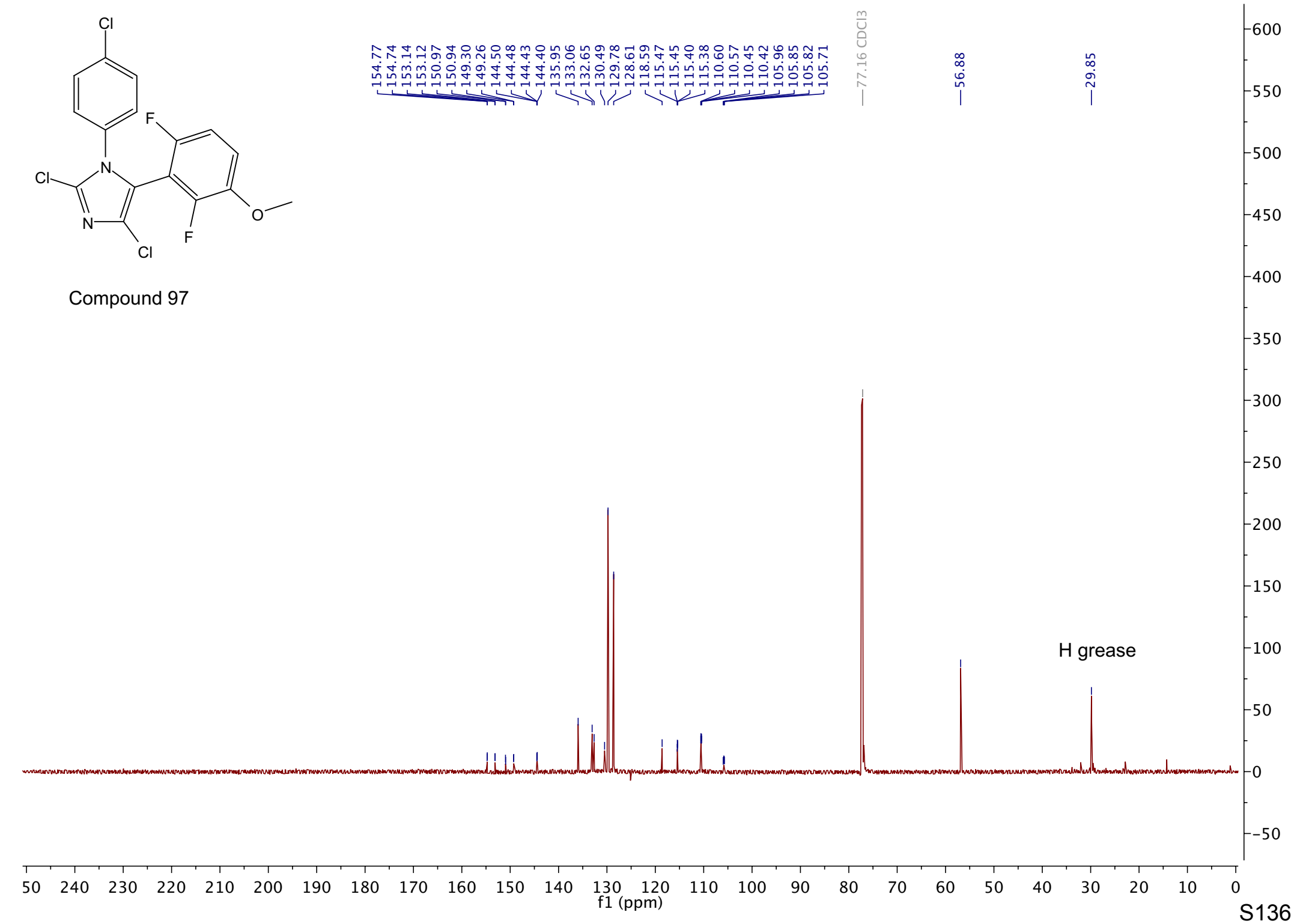


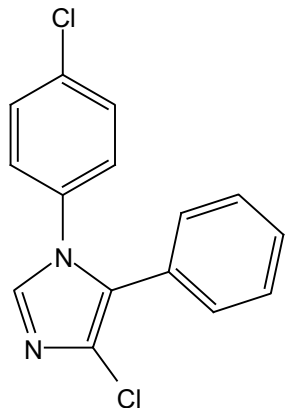
Compound 97



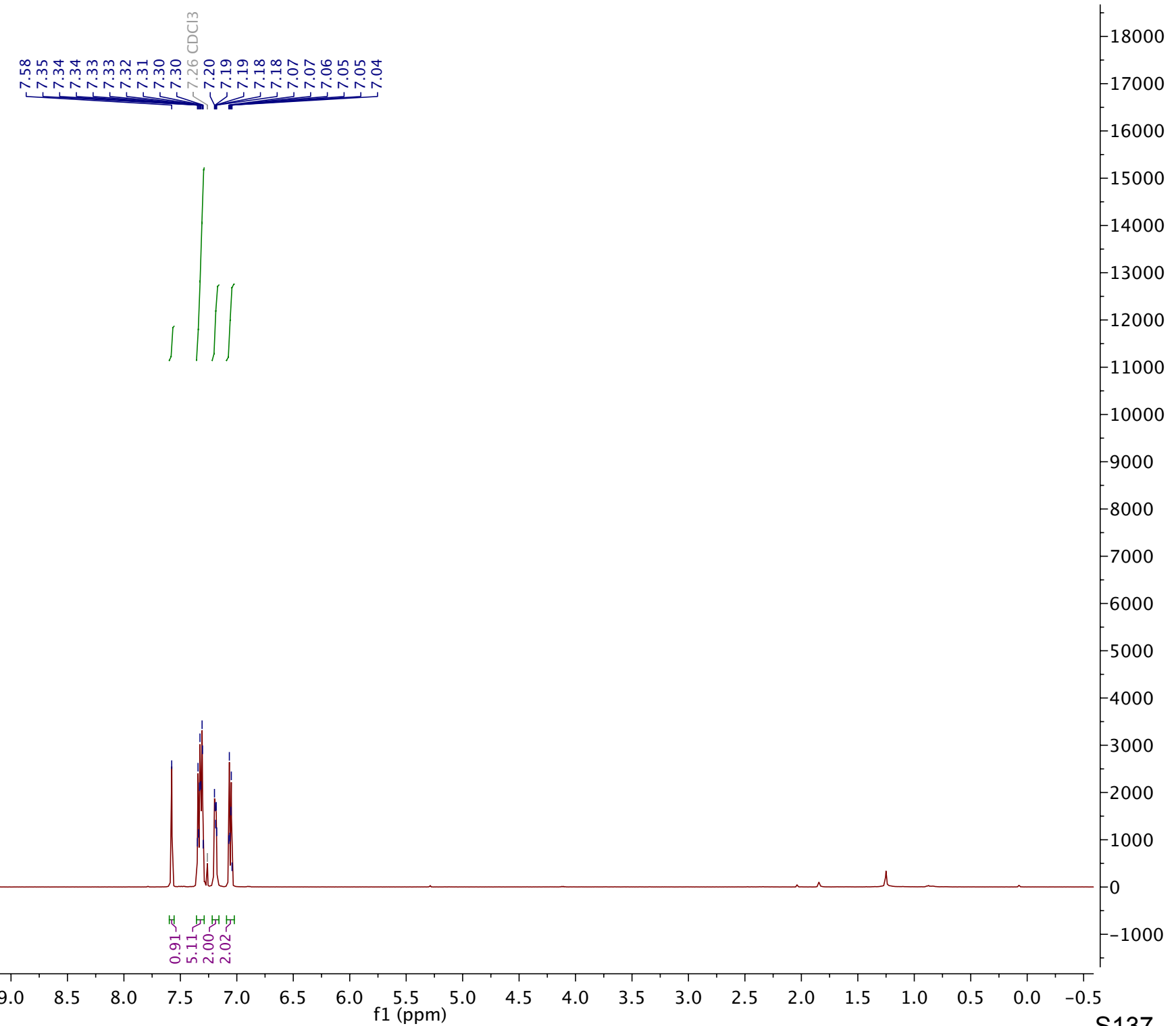


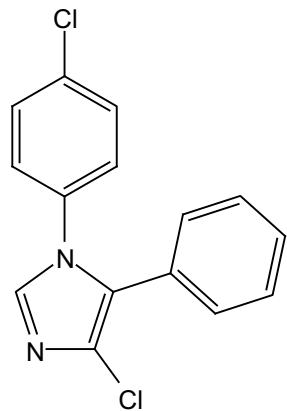
Compound 97



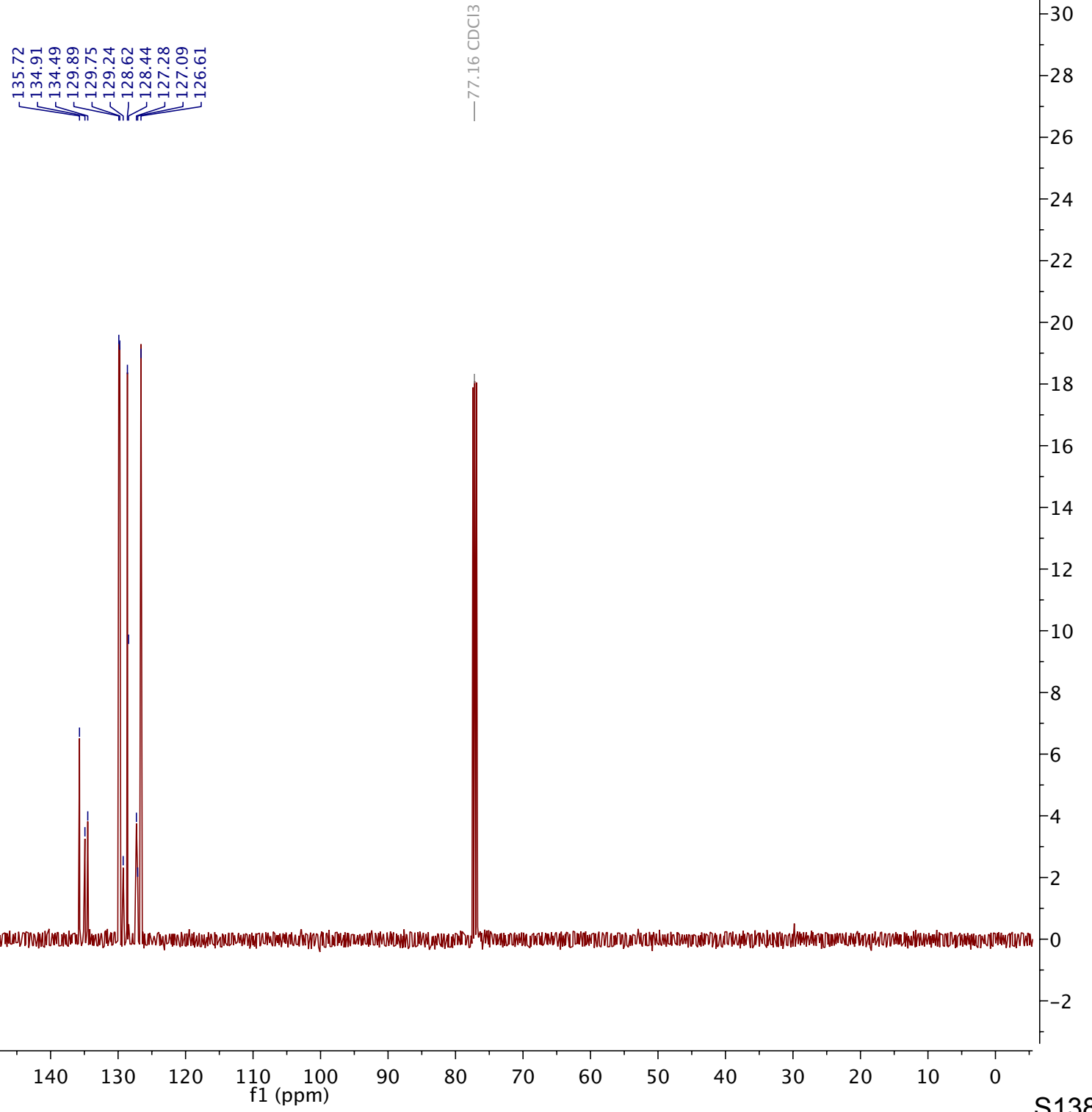


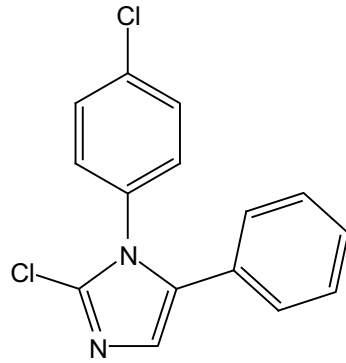
Compound 98



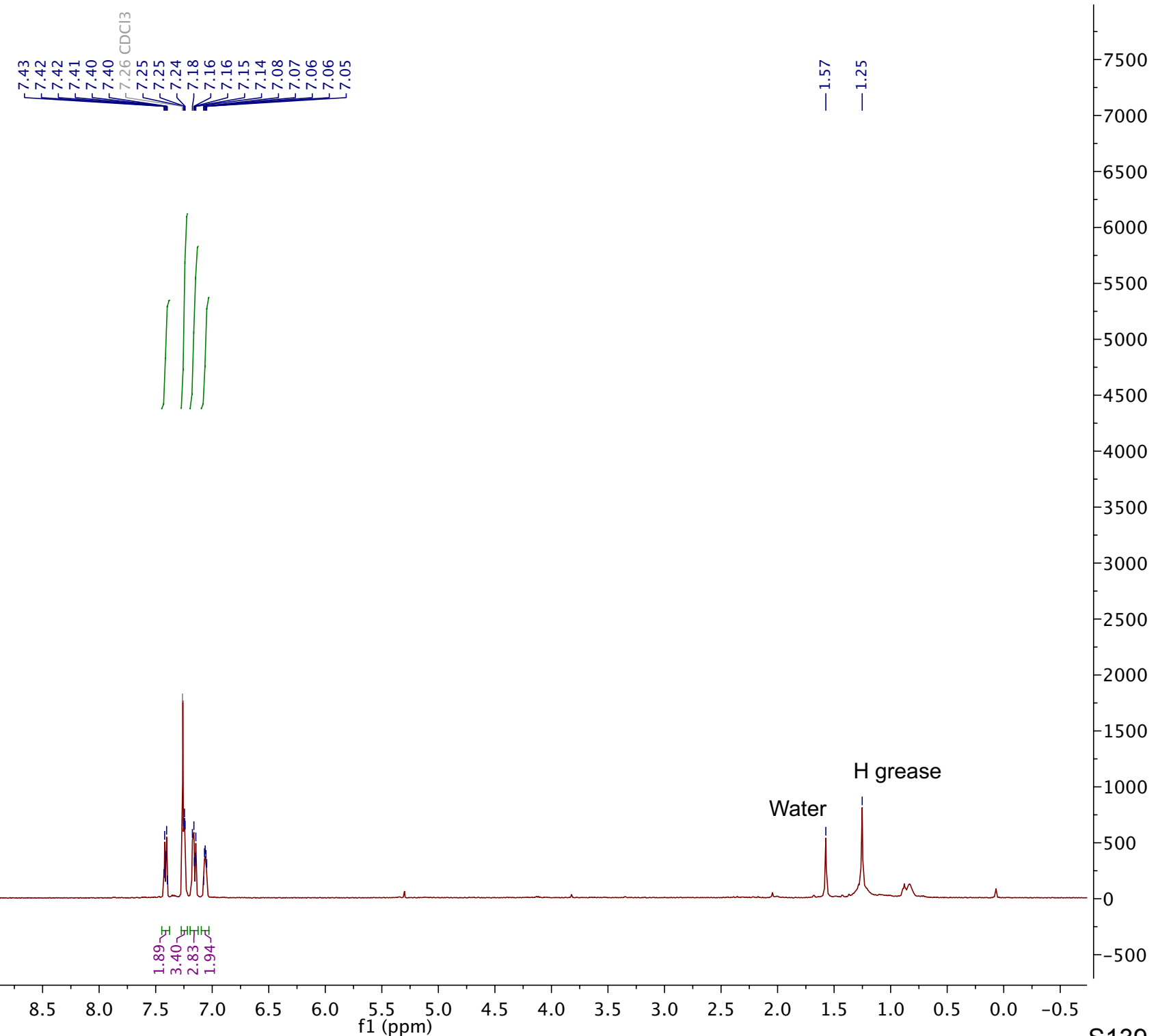


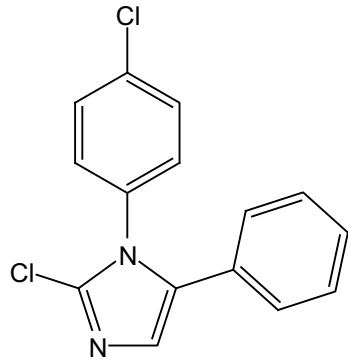
Compound 98



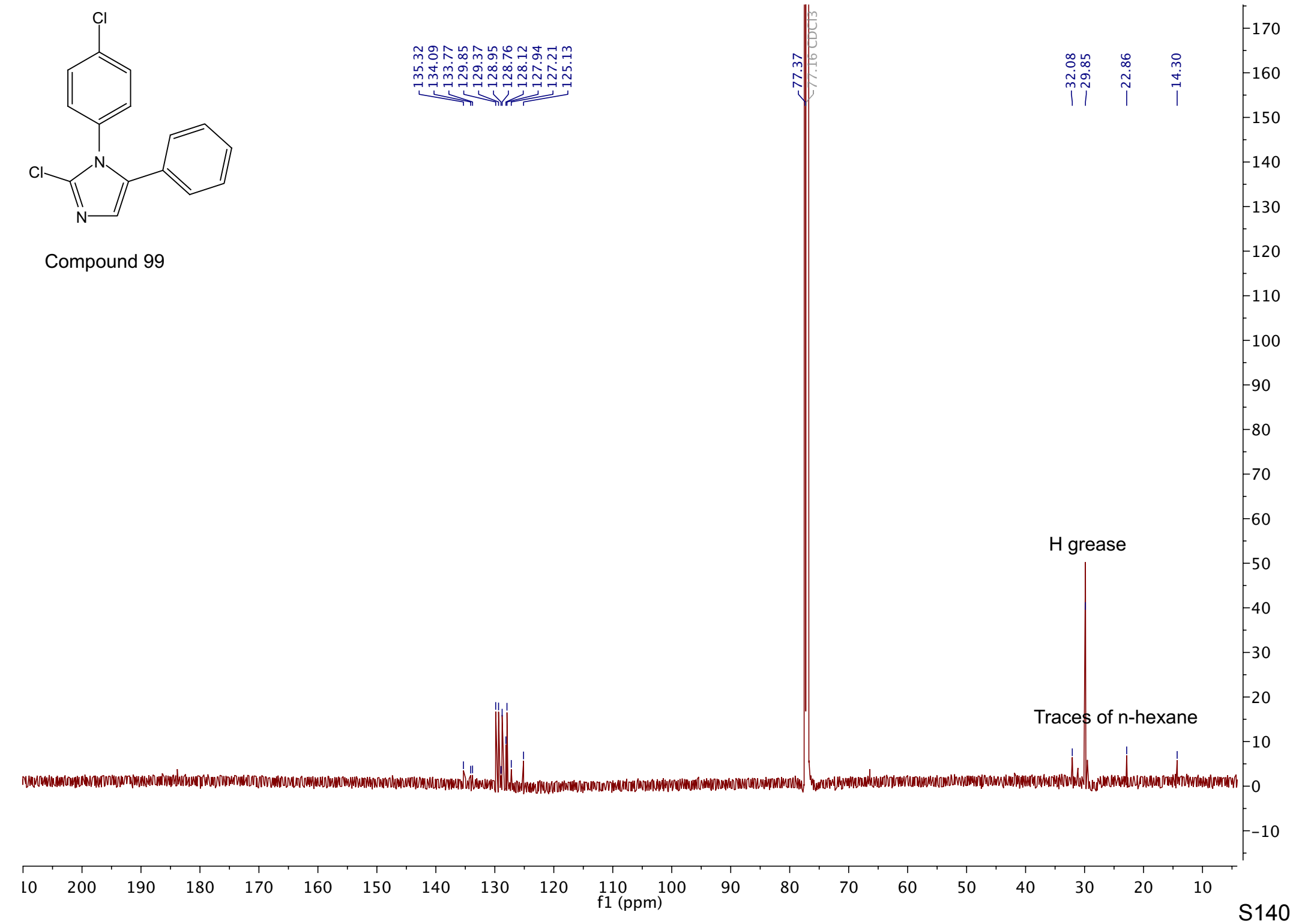


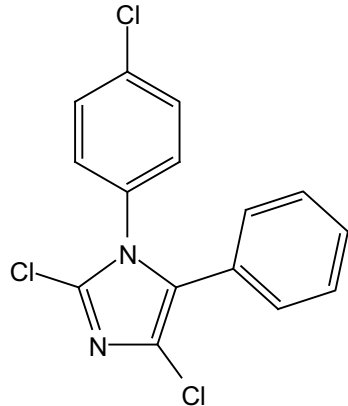
Compound 99



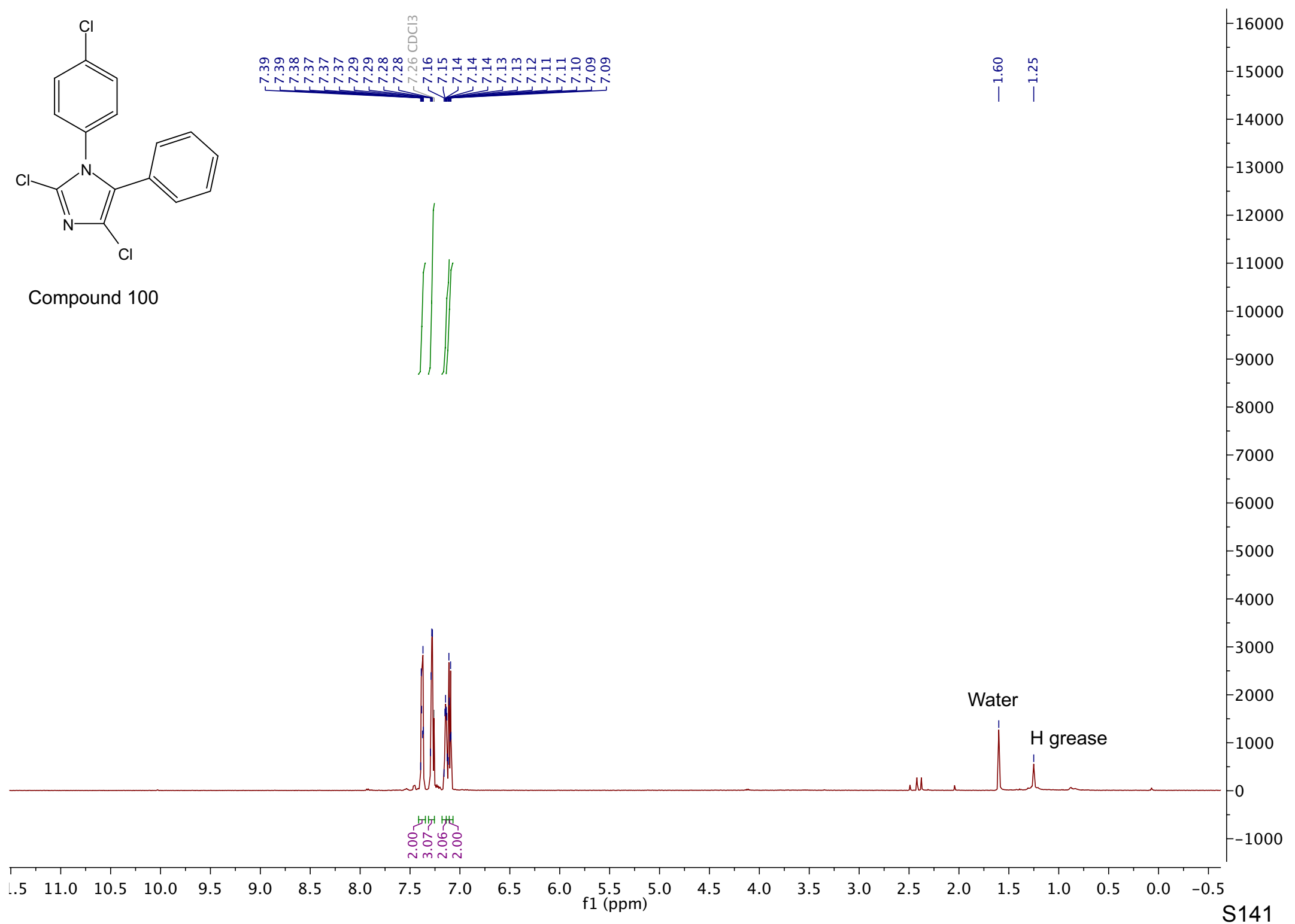


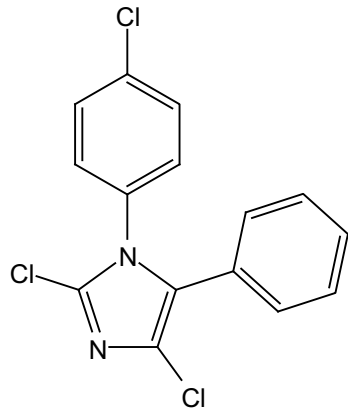
Compound 99



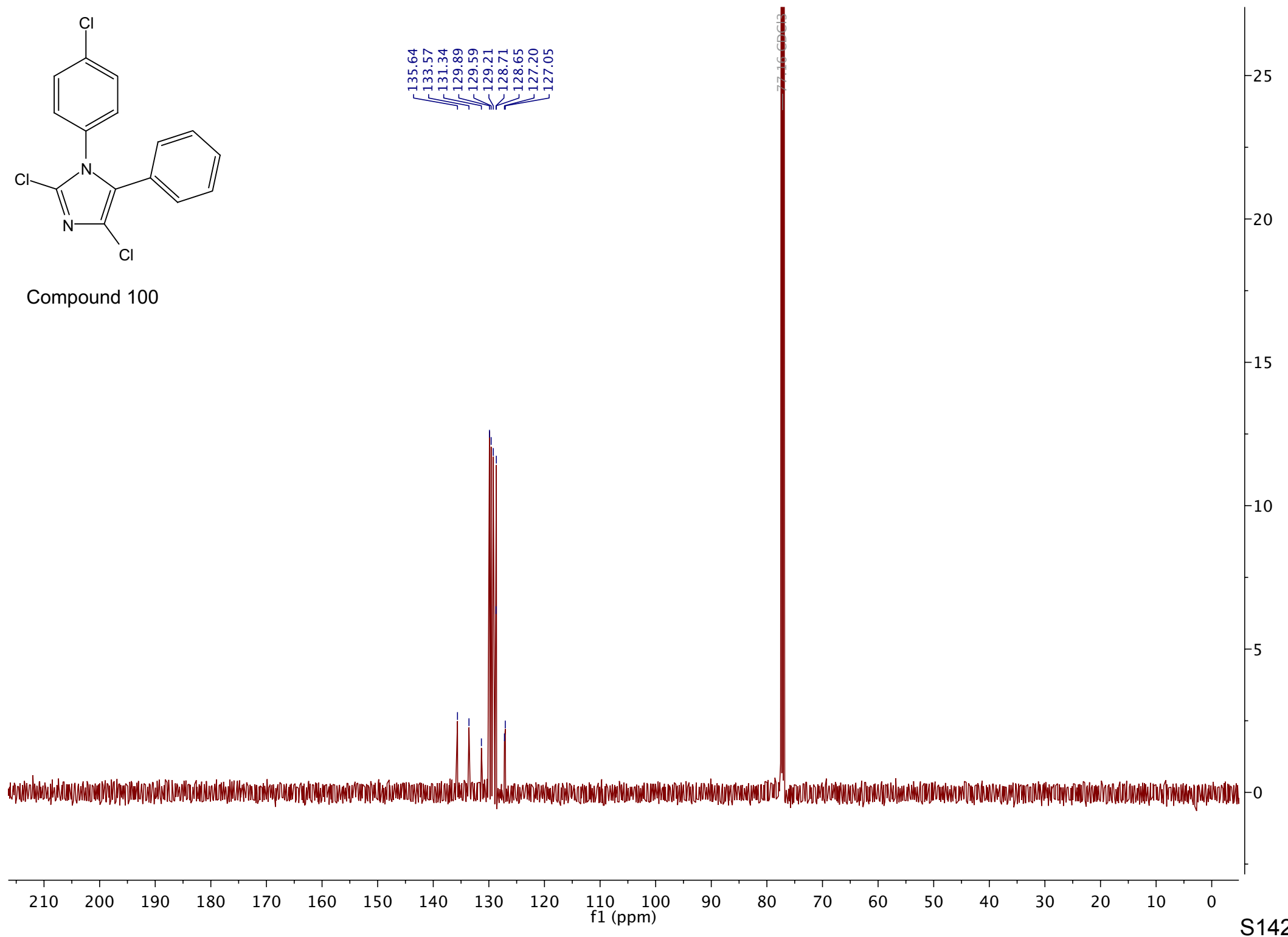


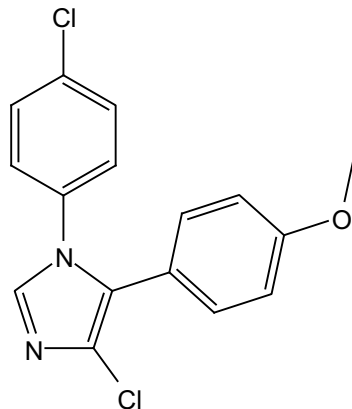
Compound 100



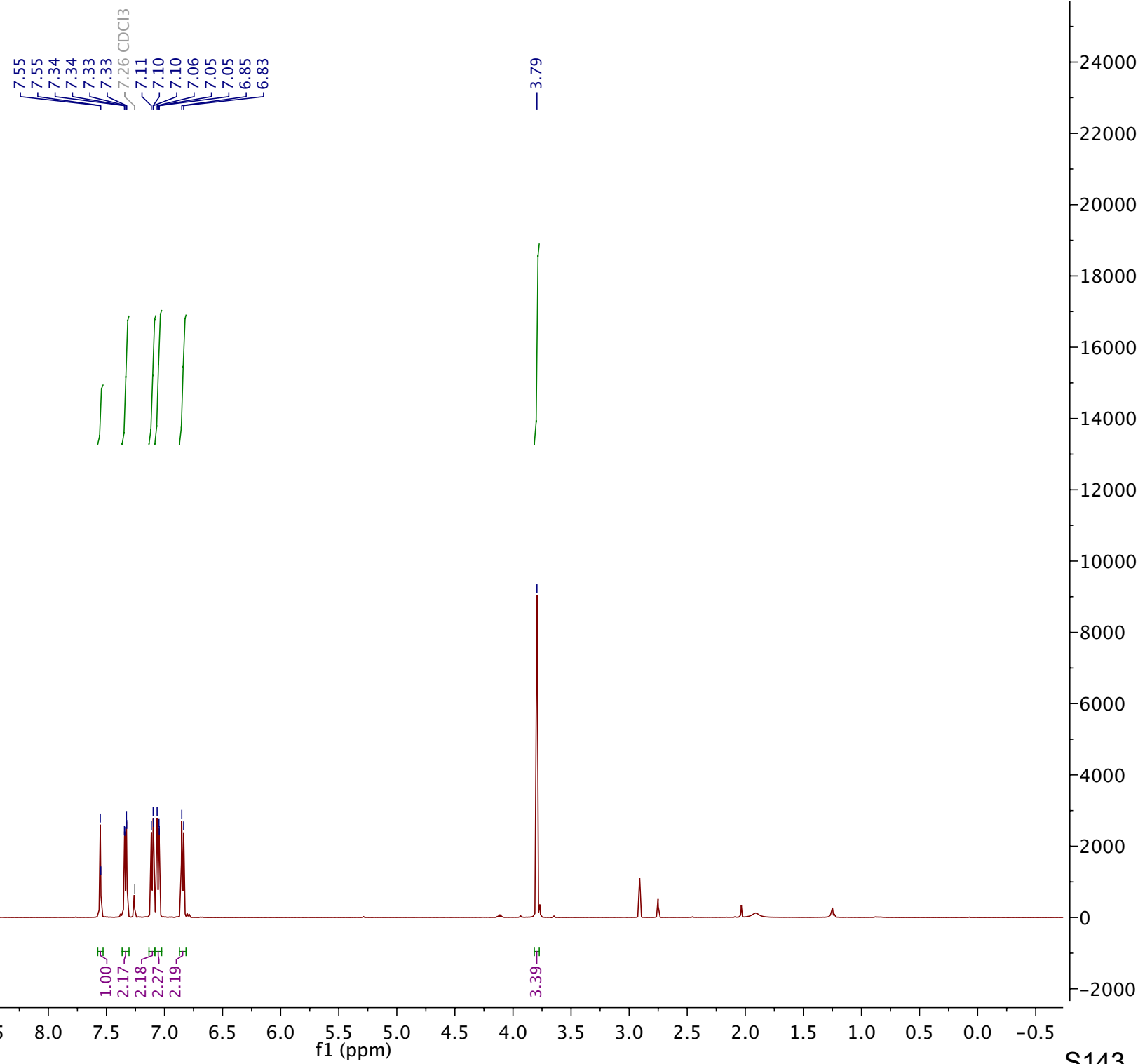


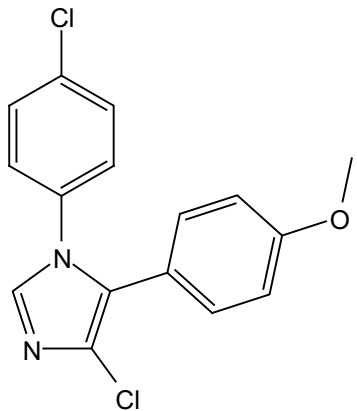
Compound 100



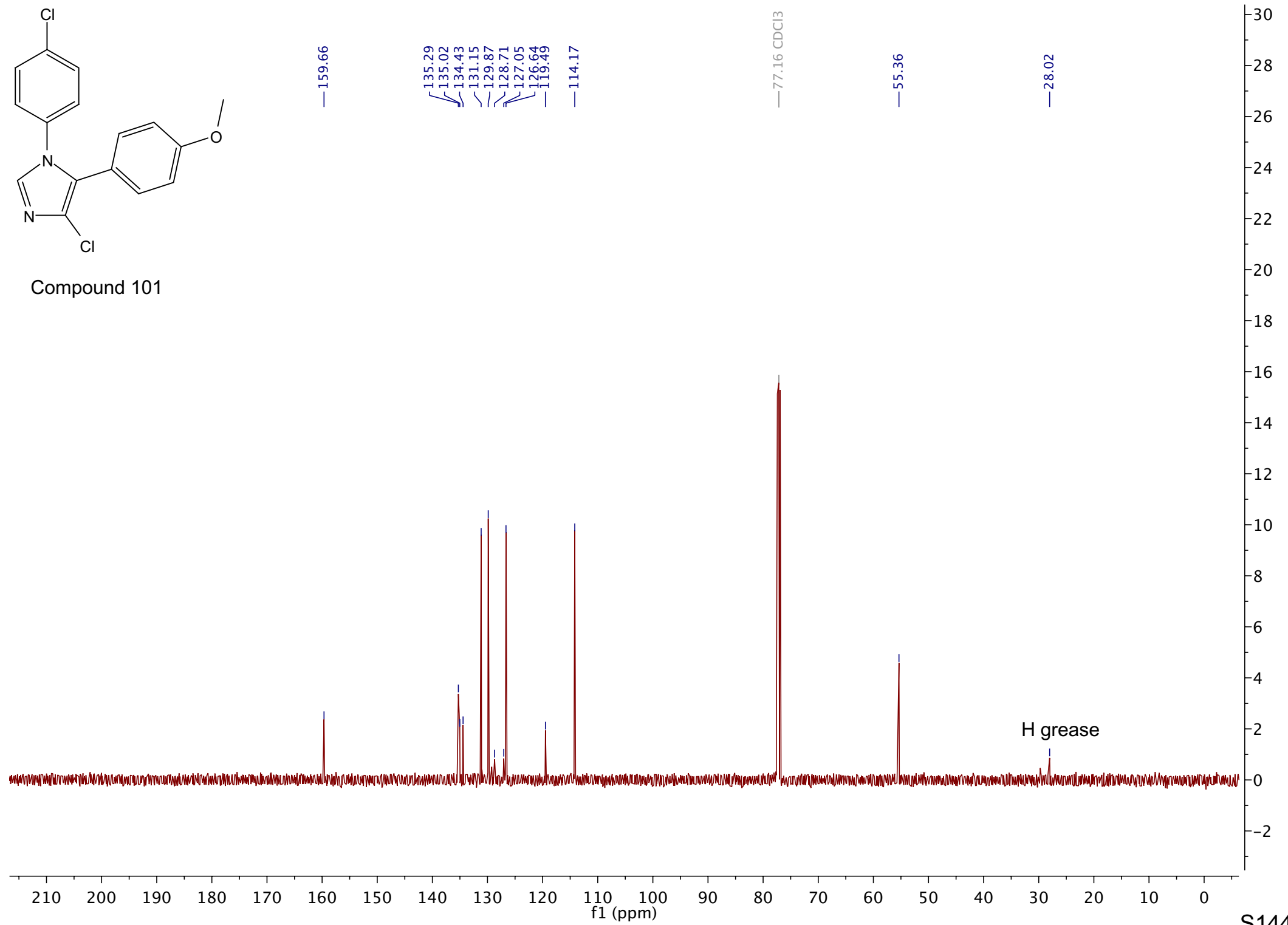


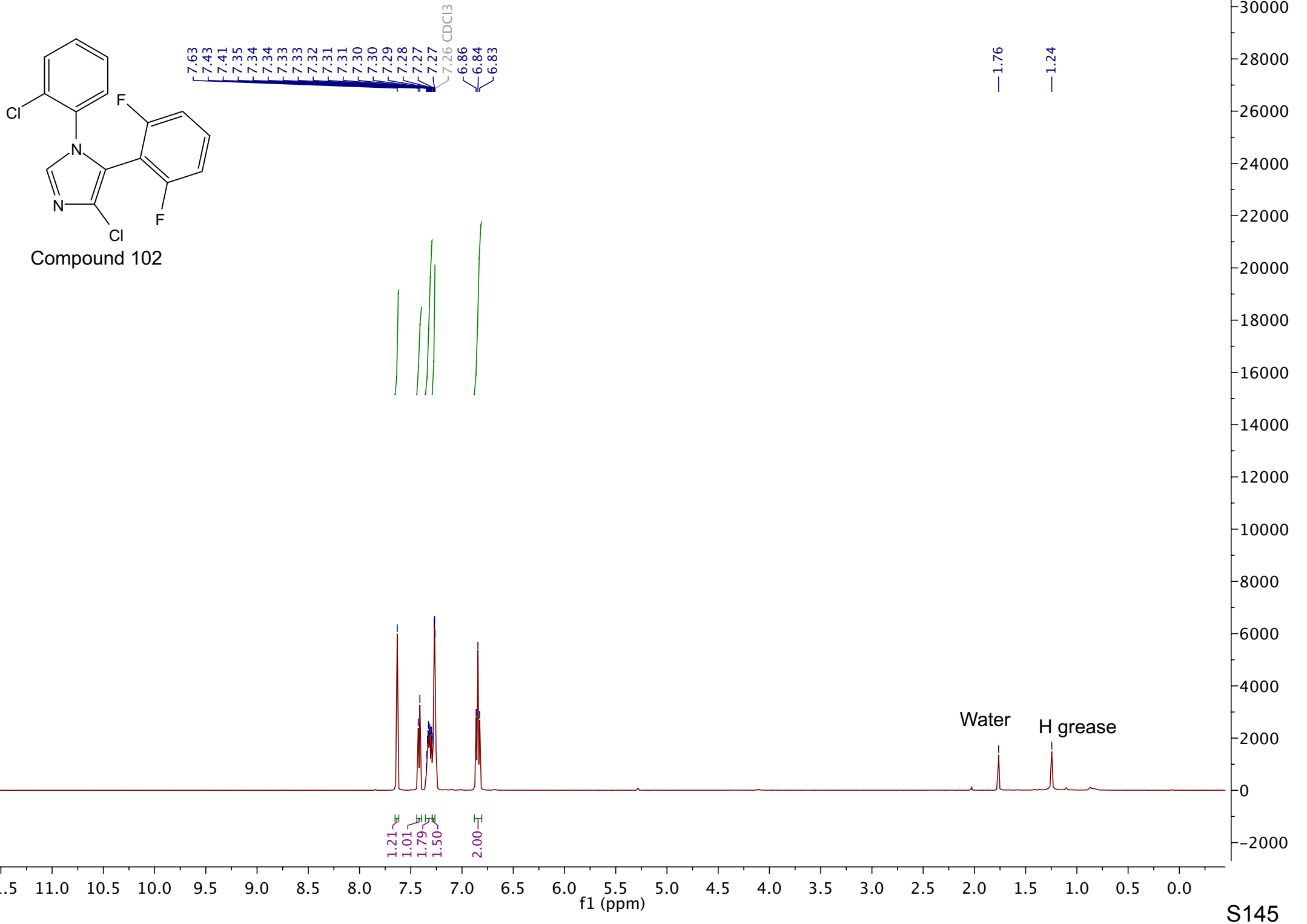
Compound 101

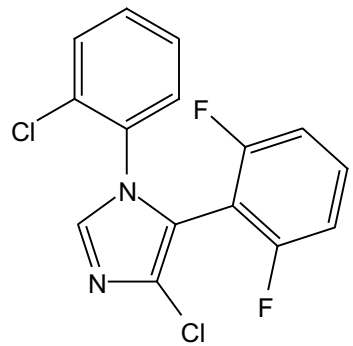




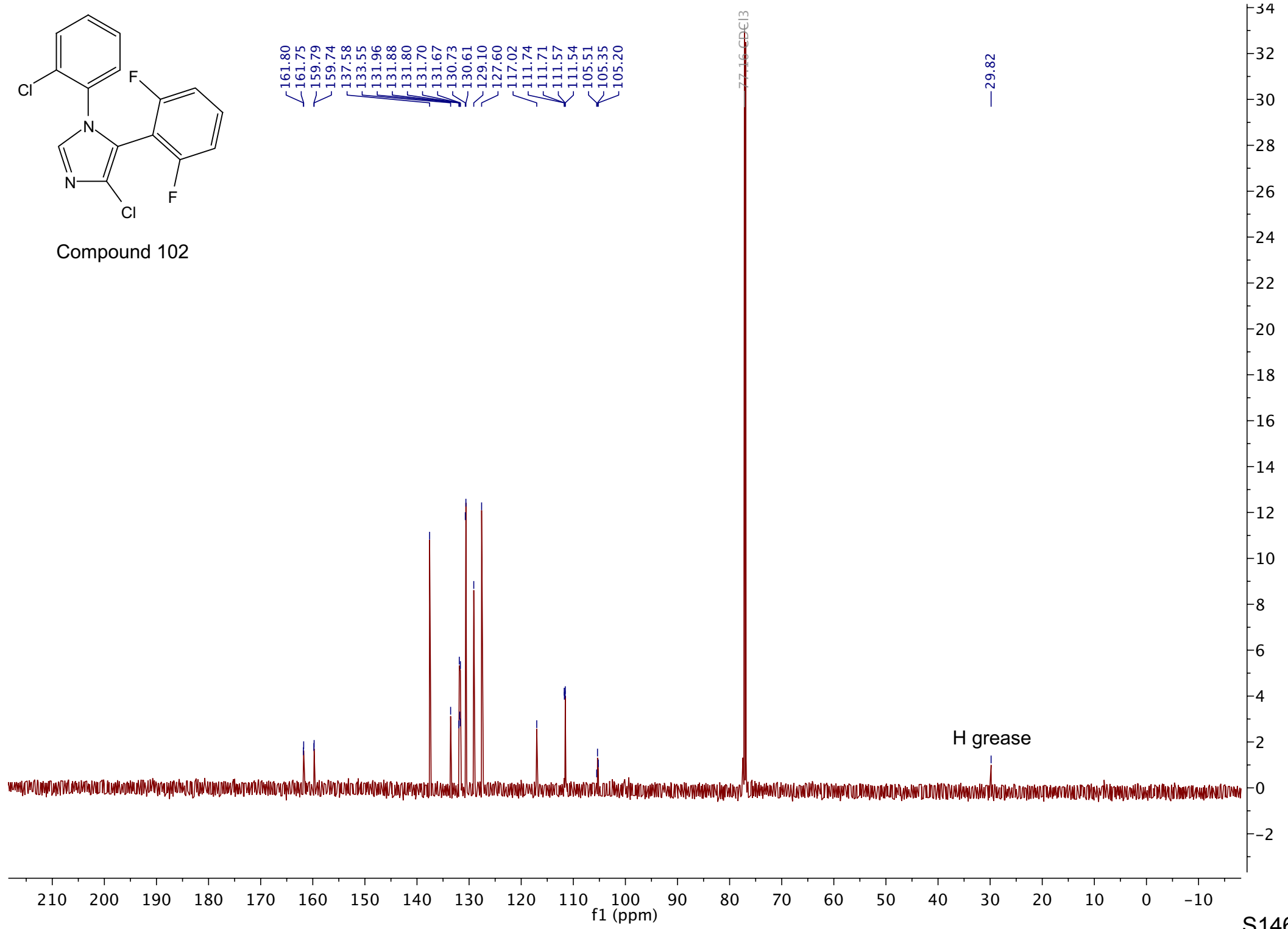
Compound 101







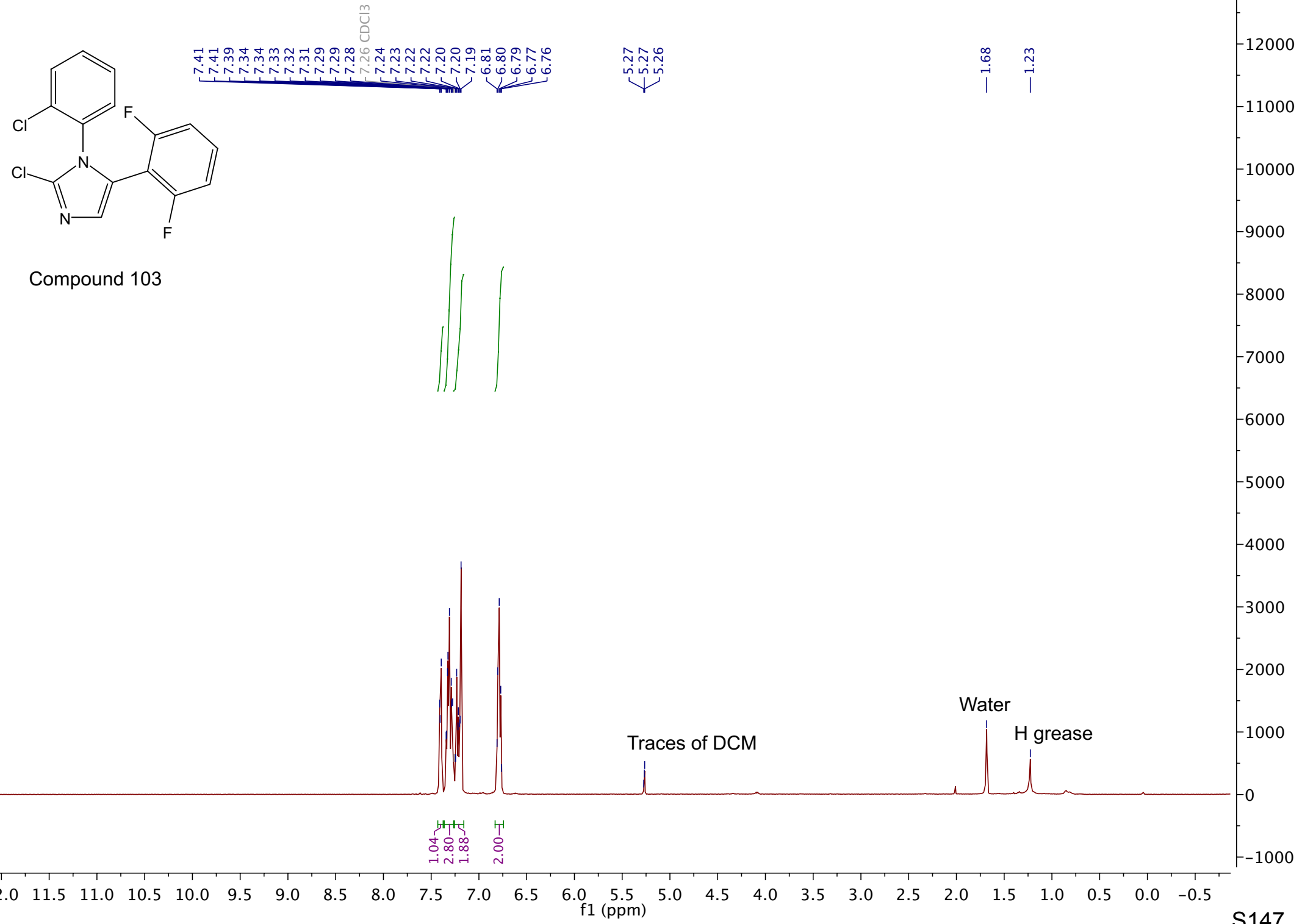
Compound 102

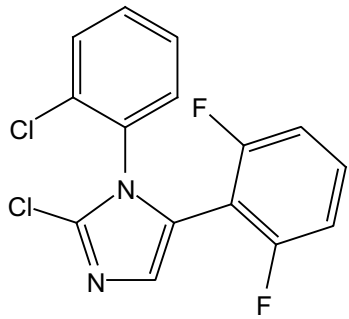


210 200 190 180 170 160 150 140 130 120 110 100 90 80 70 60 50 40 30 20 10 0 -10

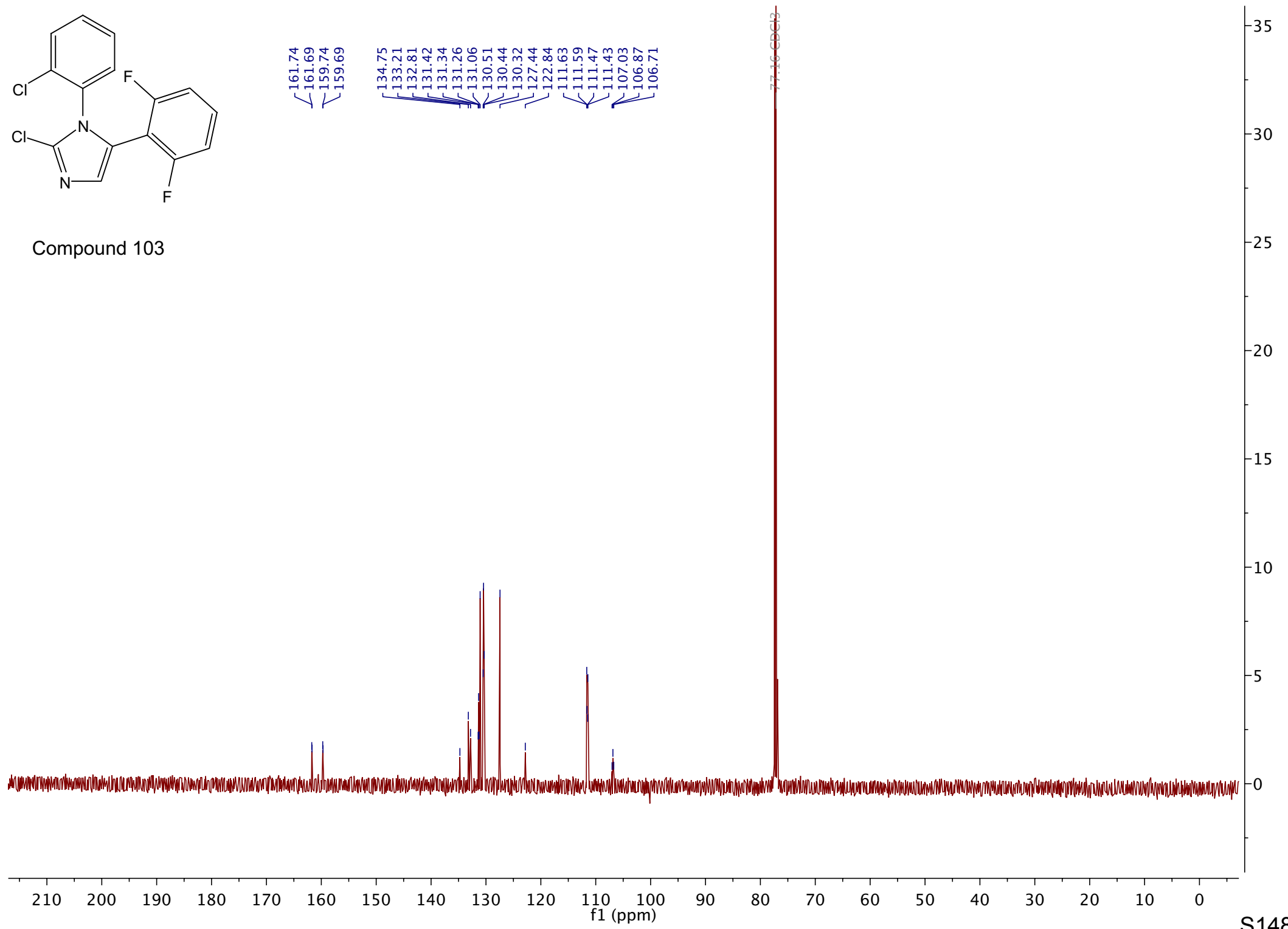
f1 (ppm)

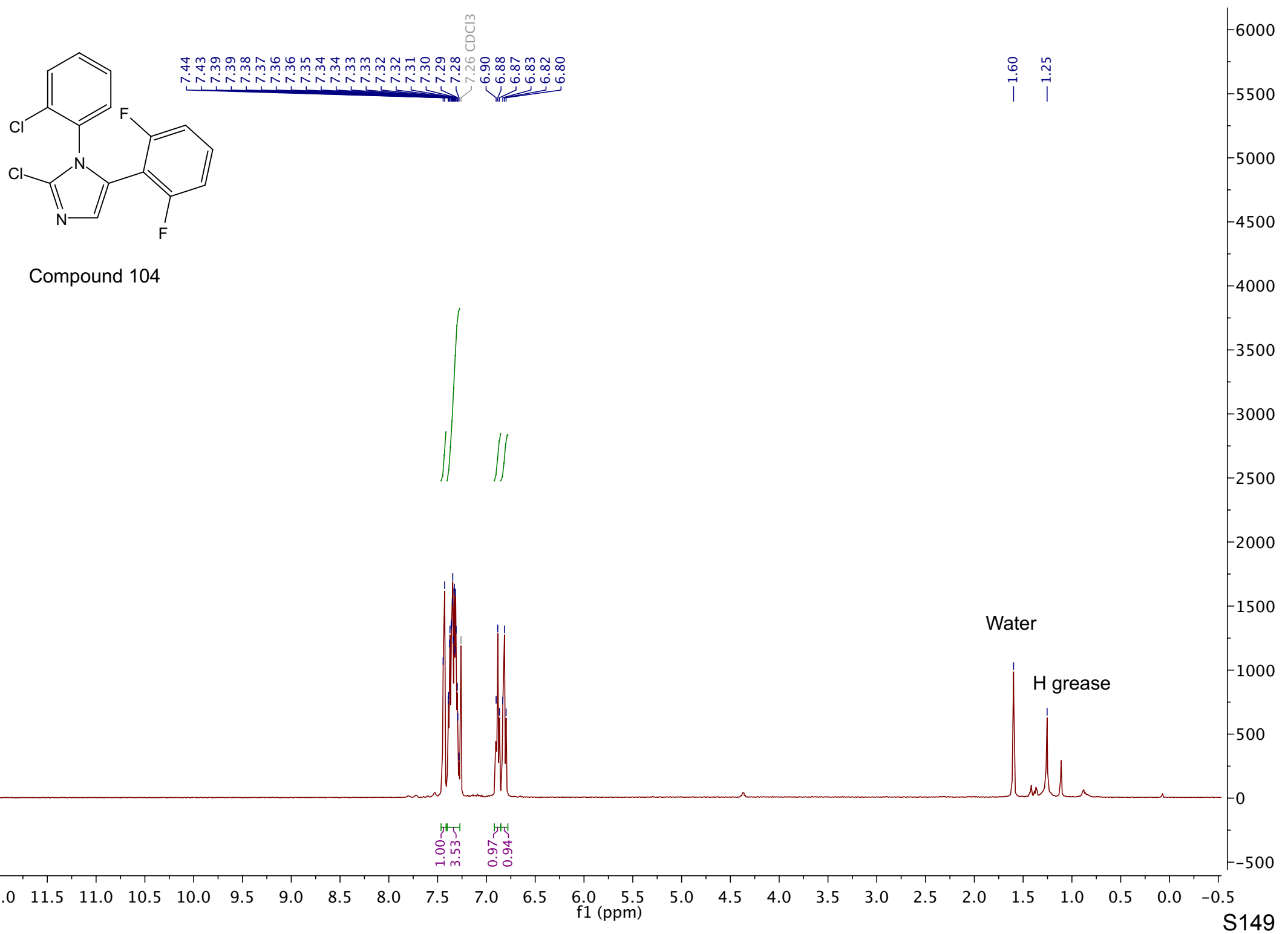
S146

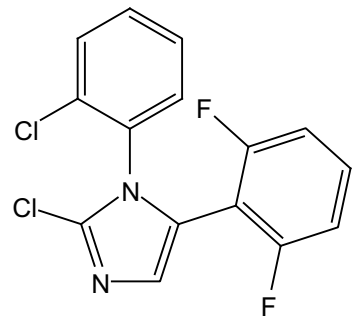




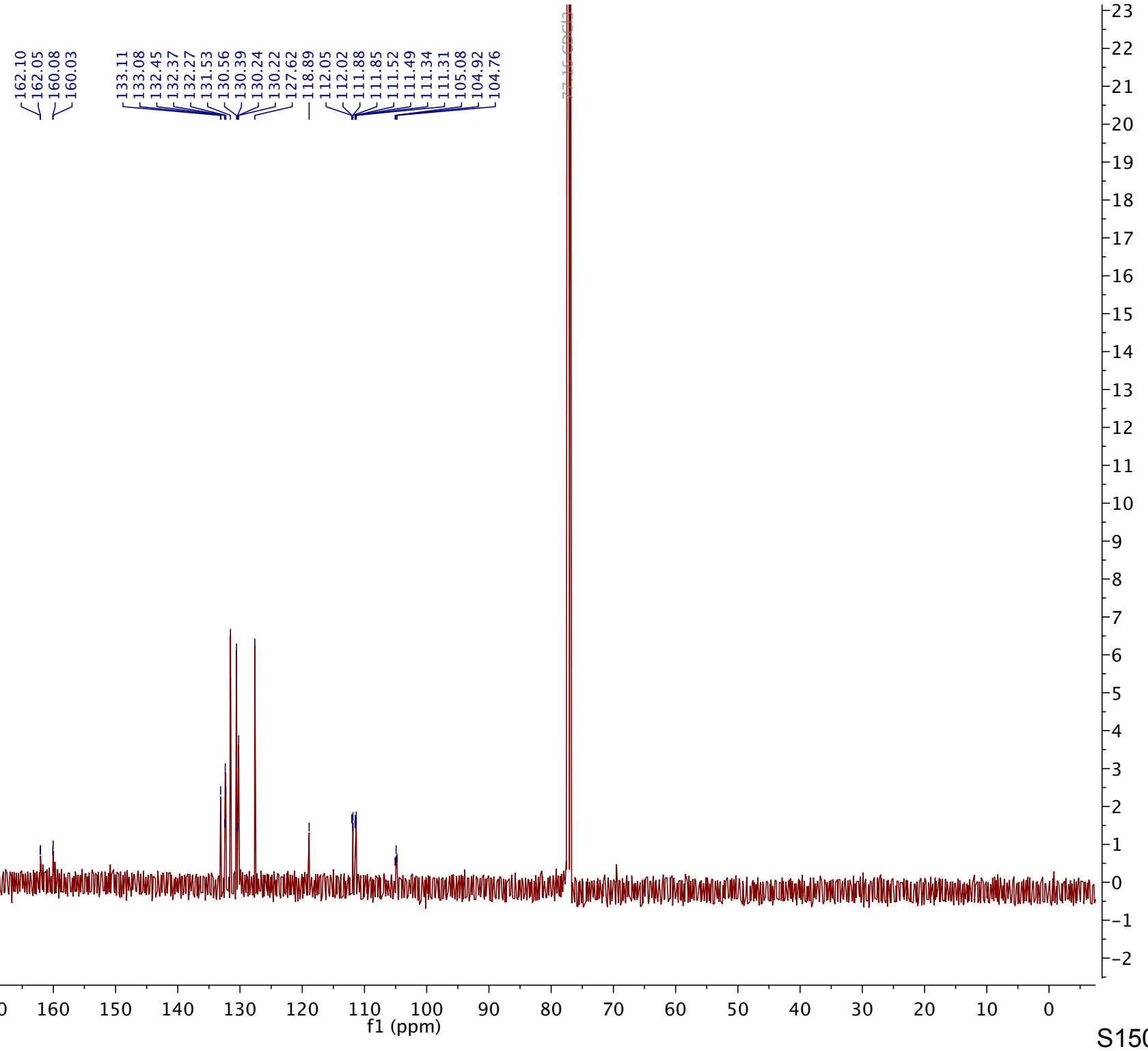
Compound 103





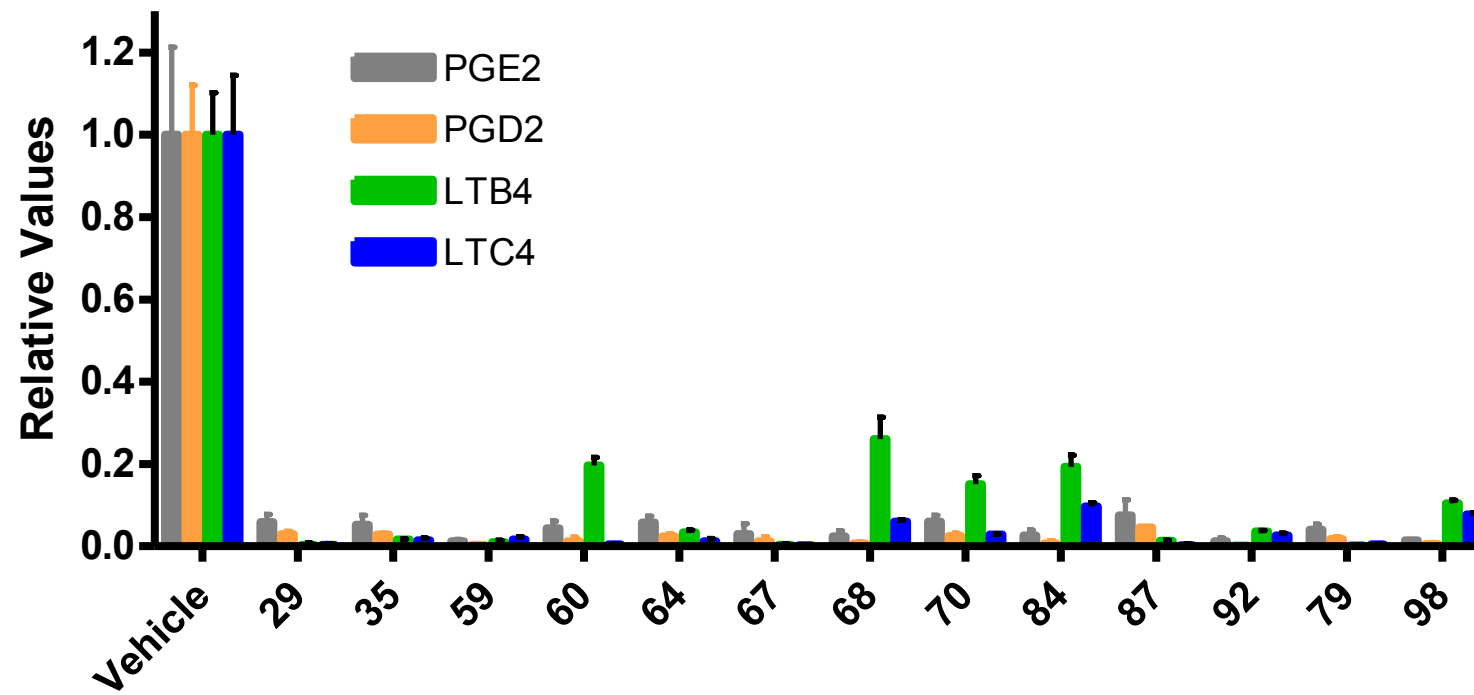


Compound 104

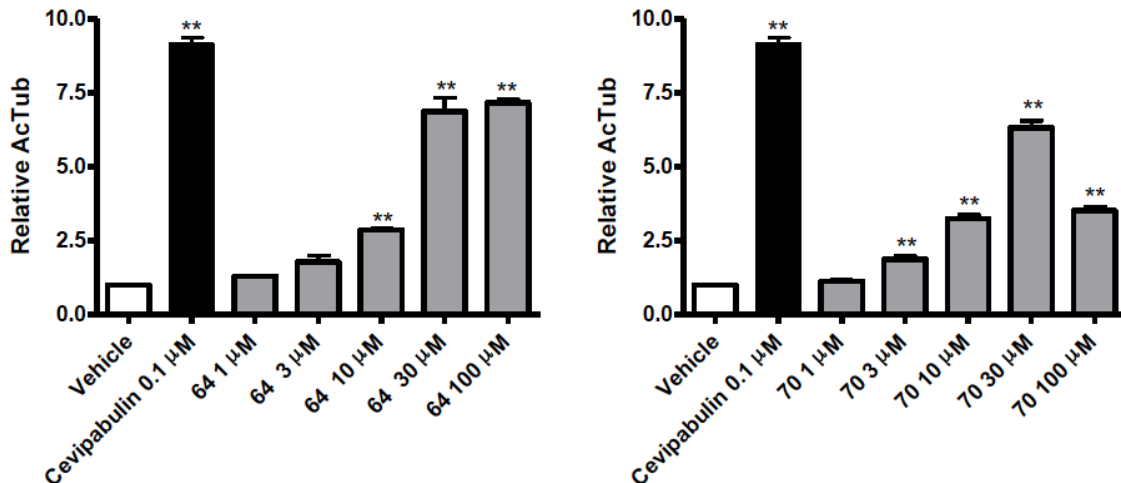


S150

Supplemental Figure 1



Analysis of Table 2 compounds for their ability to reduce multiple COX and 5-LOX products. The compounds listed in Table 2 were tested at 50 μ M in the RBL-1 assay, and COX-derived PGE2 and PGD2, as well as 5-LOX-derived LTB4 and LTC4, were assessed by LC-MS/MS. All compounds caused appreciable inhibition of all of the measured eicosanoids.



Supplemental Figure 2. Concentration response of compounds **64 and **70** in the QBI293 AcTub assay.** Compounds **64** and **70** underwent concentration-response testing in triplicate in the QBI cell acetyl tubulin (AcTub) assay from 1-100 μM and the increase in AcTub/ μg of cellular homogenate relative to vehicle-treated cells is graphed. The triazolopyrimidine, cevipabulin,¹ was tested at 0.1 μM as a positive control. Error bars represent standard error of the mean. **, p<0.01 relative to vehicle-treated cells as determined by one-way ANOVA and Dunnett's multiple comparison test.

Whereas **64** demonstrated a maximal activity that plateaued at 30 μM , a bell-shaped concentration-response was observed at high concentrations with **70**, such that a greater increase of AcTub was seen at 30 μM than 100 μM , as has been observed at lower concentrations for other imidazole and triazolopyrimidine examples (**58**, **71**, **108** in Table 1).

¹ Zhang N, et al. J. Med. Chem. 2007, 50, 319-327.